REPORT DOCUMENTATION PAGE

1. AGENCY USE ONLY (Leave blank)	2. REPORT DATE	3. REPORT TYPE AND DATES COVERED
	15-Feb-02	Final Report

4. TITLE AND SUBTITLE
Modelling Swell High Frequency Spectral and Wave Breaking

5. FUNDING NUMBERS
N00014-98-1-0070

6. AUTHOR(S)
V. E. Zakharov

7. PERFORMING ORGANIZATION NAME(S) AND ADDRESS(ES)
Department of Mathematics
617 N. Santa Rita Avenue
University of Arizona
Tucson, Arizona 85721

8. PERFORMING ORGANIZATION REPORT NUMBER

9. SPONSORING /MONITORING AGENCY NAMES(S) AND ADDRESS(ES)
Office of Naval Research, Program Officer C.L. Vincent ONR 321 CD
Ballston Centre Tower One, 800
Arlington, VA 22217-5660

10. SPONSORING/MONITORING AGENCY REPORT NUMBER

11. SUPPLEMENTARY NOTES

12a. DISTRIBUTION/AVAILABILITY STATEMENT
Approved for public release; distribution unlimited.

12b. DISTRIBUTION CODE

13. ABSTRACT (Maximum 200 words)

My long-term goal was development of a self-consistent analytical, dynamical and statistical theory of weak and strong nonlinear interactions in ocean gravity waves. The theory should be supported by the extensive numerical simulations as well as by laboratory experiments and field observations. The theory will be used as a basis for development of approximate models of Snl, which can be used in a new generation of operational models for wave forecasting. Another goal is the development of the theory of wave breaking which will make it possible to find a well-justified estimate for the rate of energy dissipation due to this process. The level of nonlinearity in an ensemble of wind-driven ocean waves is relatively small. It makes it possible to apply for its statistical description the theory of weak turbulence. In the most simple case, it is the theory of kinetic (Hasselmann's) equation for spectra of the normalized wave action. The kinetic equation has a remarkable family of exact stationary Kolmogorov-type solutions. They are governed by two parameters: fluxes of energy and momentum to the region of high wave numbers, and can be applied for description of energy spectra in the "universal" range behind the spectral peak. All Kolmogorov spectra have asymptotics $E(w) \sim w^{-4}$ after averaging in angle. The exact kinetic equation is too complicated to be used in the operational model of wave prediction. Thus, the development of its approximate models is an actual problem. The wave-breaking, which in most cases participate in the wave dynamics is a strongly nonlinear process, makes an important contribution to energy dissipation. So far, there is no reliable theory for this phenomenon. I combine in my work the analytical methods of mathematical physics with massive numerical simulation and construction of simple phenomenological models. All results are compared with laboratory experiments and field observations. The results obtained in the period of 1998 - 2001 are summarized in ten (10) articles. Five of them are published in refereed journals, another one in the Proceedings of the Sixth (6th) International Workshop on Wave Hind casting and Forecasting, three (3) others are already accepted for publication to Phys. Rev. Let. The results were also reported on six international conferences and workshops, including two (2) WISE meetings and the Twentieth (20th) International Congress of IUTAM.

14. SUBJECT TERMS	15. NUMBER OF PAGES
	115
	16. PRICE CODE

17. SECURITY CLASSIFICATION OF REPORT	18. SECURITY CLASSIFICATI	19. SECURITY CLASSIFICATION OF ABSTRACT	20. LIMITATION OF ABSTRACT
UNCLASSIFIED	UNCLASSIFIED	UNCLASSIFIED	UL

Final Report
N 00014-98-1-0070
"Modelling Swell High Frequency Spectral and Wave Breaking"

Principal Investigator: V.Zakharov
Department of Mathematics, University of Arizona, Tucson, AZ 85721
Phone: (520) 621-4841, Fax: (520) 621-8322
Email: zakharov@math.arizona.edu

Long-term goals

My long-term goal was development of a self-consistent analytical, dynamical and statistical theory of weak and strong nonlinear interactions in ocean gravity waves. The theory should be supported by the extensive numerical simulations as well as by laboratory experiments and field observations. The theory will be used as a basis for development of approximate models of Snl, which can be used in a new generation of operational models for wave forecasting. Another goal is the development of the theory of wave breaking which will make it possible to find a well-justified estimate for the rate of energy dissipation due to this process.

Objectives

The level of nonlinearity in an ensemble of wind-driven ocean waves is relatively small. It makes possible to apply for its statistical description the theory of weak turnulence. In the simpliest case, it is the theory of kinetic (Hasselmann's) equation for spectra of the normalized wave action. The kinetic equation has a remarcable family of exact stationary Kolmogorov-type

solutions. They are governed by two parameters: fluxes of energy and momentum to the region of high wave numbers, and can be applied for description of energy spectra in the "universal" range behind the spectral peak. All Kolmogorov spectra have asymptotics $E(\omega) \simeq \omega^{-4}$ after averaging in angle.

The exact kinetic equation is too complicated to be used in the operational models of wave prediction. Thus, the development of its approximate models is an actual problem.

The wave-breaking, which in most cases participate in the wave dynamics is a strongly nonlinear process, makes an important contribution to energy dissipation. So far, there is no reliable theory for this phenomenon.

Approach

I combine in my work the analytical methods of mathematical physics with massive numerical simulation and construction of simple phenomenological models. All results are compared with laboratory experiments and field observations.

Results

The results obtained in the period of 1998-2001 are summarized in ten articles. Five of them are published in refereed journals, another one in the Proceedings of the 6-th International workshop on wave hindcasting and forecasting, three others are alredy accepted for publication in refereed journals, and last one is presented for publication to Phys. Rev. Let. The results were also reported on six International conferences and workshops, including two WISE meetings and the 20th International Congress of IUTAM.

These results are described in the next chapters.

1 Theoretical foundation for the statistical description of the wind-driven surface waves

For a long time the main tool for the statistical description of wind-driven waves remains the kinetic equation for spectra of wave action, derived in 1962 by Hasselmann. Fourty years ago the work of Hasselmann was an

outstanding achievment. However, since that time the derivation of this equation was never critically revised.

I have performed this revision and found the following [1]. The Hasselmann's equations, being formally completely correct, are written not for the real spectra of wave action N_k, which can be observed in experiments. They correspond to the "renormalized", or "refined" spectrum n_k.

The difference between these two types of spectra has very clear physical origin. In the linear theory, the waves comprising a wave ensemble obey the linear dispersion relation between frequency and wave vector, $\omega = \omega(k)$. They are "free waves". In the presence of nonlinearity "slave waves" or "beatings" appear. The most important "beatings" are due to quadratic nonlinearity in dynamic equations. Their frequences and wave vectors obey the equations,

$$\begin{aligned} \omega &= \omega(k_1) \pm \omega(k_2), \\ k &= \vec{k_1} \pm \vec{k_2}, \end{aligned} \tag{1}$$

where k_1, k_2 are wave vectors of "free waves".

A real wave ensemble, described by spectrum N_k and observed in field and laboratory experiments, is a mixture of "free waves" and "slave waves" of all orders. Meanwhile, the spectrum n_k from the Hasselmann's equation is the distribution of the "free waves" only. The physical oceanography did not took this important difference into the account for almost fourty years!

The difference between n_k and N_k can be estimated as follow [1]:

$$\Delta = \frac{n_k - N_k}{n_k} \simeq \frac{\epsilon^2}{(\tanh \delta)^5}. \tag{2}$$

Here $\epsilon \simeq ka$, $\delta \simeq kh$; a is a wave amplitude, and h is a depth of the ocean. In a typical situation, $\epsilon \simeq 0.1$.

On deep water $\delta \to \infty$, $\tanh \delta \to 1$, so the difference $\Delta \simeq 10^{-2}$ is negligably small. But on shallow water the role of "slave harmonics" increases dramatically. For a moderate depth $\delta \simeq 0.5$, $\Delta \simeq 0.3$. If $\delta \simeq 0,3$, the difference $\Delta > 1$, and the weakly nonlinear approach is not applicable any more.

In future I plan to develop a numerical algorithm, making it possible to recompute n_k and N_k and *vice versa*.

2 Hasselmann's kinetic equation: constants of motion and exact solutions

Hasselmann's kinetic equation in absence of forcing reads

$$\frac{\delta N_k}{\delta t} = Snl. \tag{3}$$

It is considered that this equation preserves the standard constants of motion, i.e. wave function N, enegry E, and momentum R:

$$N = \int N_k \, dk, \tag{4}$$

$$E = \int \omega_k \, N_k \, dk, \tag{5}$$

$$\vec{R} = \int \vec{k} \, N_k \, dk.$$

In reality, only N is a real constant of motion, while E and $\vec{R}$ "leak" to the region of high wave numbers. Thus, energy and momentum are just "formal" constants of motion. The nonlinear wave interaction produces spectra governed by fluxes of energy and momentum to high wave numbers. Due to this curcumstance, four-wave interaction can arrest instability induced by wind. This question is discussed in details in article [10].

In the theory of wind-driven sea waves the exact solution of the equation

$$Snl = 0 \tag{6}$$

plays a central role. This equation is called Kolmogorov-Zakharov spectra and has the most important solution in the following form:

$$F_\omega = \frac{g^{4/3} P^{1/3}}{\omega^4} H(\frac{gM}{\omega P}, \theta) \tag{7}$$

Here F_ω is a spectrum of energy and P, M are fluxes of energy and momentum. We found [6] that for large ω

$$H(\frac{gM}{\omega P}, \theta) \simeq c_0 + \frac{c_1 gM}{\omega P} \cos\theta, \tag{8}$$

where c_0 and c_1 are first and second Kolmogorov constants. Formulae (7), (8) give the explicit expression for the spectrum in the equilibrium range. In presence of wind forcing the functions P and M are slow functions on time and frequency.

3 Numerical simulation of the Hasselmann's equation

Taking as a basis the method developed earlier by D. Resio, we (in collaboration with D. Resio and A. Pushkarev) elaborated a comfortable algorithm for numerical solution of the Hasselmann's equation in a duration-limit frame [6]. The algorithm is stable and reliable, and makes it possible to model the evolution of wave spectra for tens of hours of physical time. For a mesh as dense as 36 points in angle and 71 points in frequency it takes less then a week on a personal computer. We performed several series of numerical simulation and found that theory of weak turbulence is confirmed completely, up to details. We observed leakage of energy and momentum to high wave numbers and formation of weak-turbulent Kolmogorov spectra. We found numerically the values of Kolmogorov's constants:

$$c_0 \simeq 0.37, \quad c_1 \simeq 0.23.$$

We included into consideration the forcing, which models the influence of the wind, and obtained spectra very similiar to the ones observed in the ocean. We obtained in our experimants such characteristic phenomenon as peak enhancment and bymodality of spectra in angle. We made a comparision of our results with a few available experimental data on limited-duration frame and found a rather good coincidence.

Another set of numerical experimants performed with W. Perrie and based on more old version of Resio's code issued similiar results [2].

4 Diffusion models

The numerical simulation of the exact kinetic equation is too slow process to be used in operational models. Even the advanced algorithm of a fine enough grid runs with the rate comparable with the rate of spectral evolution in nature. To make the algorithm suitable for an operational model, its speed should be increased at least in three orders of magnitude. So far, the only way to do this is to use phenomenological models instead of exact Snl. First such model known as DIA was proposed by Hasselmann and Hasselmann in 1985. It is widely used now in WAM and SWAN operational programs. In our opinion, DIA does not give good enough results. It leads to isotropization of spectra in angles, while in reality the spectra, at least

in energy capaciting range, are narrow in angle. Moreover, DIA does not explain a peak enhancement and bymodality.

In 1999 we offered another phenomenological model[3]. This model is based on replacing the exact Snl by a second-order differential non-linear elliptic operator. This procedure turns Hasselmann's kinetic equation to a nonlinear diffusion equation. We elarorated an efficient numerical algorithm to solve this diffusion equation and found that our model is at least not worse than DIA but is four orders of magnitude faster than the exact Snl. It does not describe the peak enhancement and bimodality, but describes relatively well the angular spreading, much better than DIA does.

We consider our diffusion model as a first representative of a whole seria of more sophisticated phenomenological models, where the exact Snl is replaced by much simplier integro-differential operation. A systematic study of such models is one of our goals. We plan to use for exact solution of the kinetic equation the algorithm, which we have now in our posession, as a paragon for examination the quality of such models. A preliminary consideration of some phenomenological models shows that the peak enchancement can be reproduced easily.

5 One-dimensional dynamic models of wave turbulence

Not all the experts in the field of wind-driven sea do believe in Hasselmann's kinetic equation. Some respected scientists (M. Schassnie, M. Tulin) consider that four-wave interaction is too slow process to explain real phenomena. They note that hypothesis on phase randomness, which is a theoretical foundation of the kinetic equation is not justified well enough. However, pure theoretical justification of this hypothesis is an extremely difficult problem.

A natural way for examination of validity of the kinetic equation is direct numerical simulation of primitive dynamic equation describing wave propogation and interaction. In the ideal case it should be Navier-Stokes equation. However, as a first step, it makes sense to perform simulation of more simple one-dimensional models. The most popular model of that sort was proposed by Maida, McLaughlin and Tabak in 1998 (MMT model). Numerical experiments performed by the authors showed an essential deviation of MMT models from predictions of the weak-turbulent (WT) theory. We repeated these experiments and performed carefull analytical study of the MMT model.

We found that the deviation from the WT theory is explained by strong

influence of coherent structures - quasisolitons and wave collapses [5]. We found a modification of the MMT model where coherent structures are absent [6]; in this case the numerical experiment completely supports the weak turbulent theory. We should stress that MMT model is not "academic". For certain values of parameters ($\alpha = 1/2, \beta = 3$) it describes with a good quality strongly nonlinear gravity waves on the surface in a strictly one-dimensional case (two-dimensional, including vertical direction).

6 Direct simulation of three-dimensional wave turbulence

The most direct and persuading support of the weak turbulent theory could come from the direct numerical solution of the Navier-Stokes of the Euler equation of Hydrodynamics describing fluid with free surface. Developing such algorithm is a very difficult task. The most promising approach for solution of this problem is the use of Taylor expansion in powers of nonlinearity in the equations of potential flow and implementation of the spectral code, using the fast Fourier fransform. This program was successfully realized recently [8], on the mesh 256×256 modes. We put as an initial data the Jonswap spectrum cut at $\omega = 2\omega_p$, and observed very fast formation of spectrum ω^{-4} in high frequency domain. It is important to stress that this spectral tail was obtained in absence of wind. It is a very strong argument in support of the view-point that ω^{-4} spectrum is a result of nonlinear wave interactions only. We plan to continue these experiments using larger grids (512×512, or even 1024×1024).

7 Direct simulation of wave breaking and freak wave formation

Not all important physical phenomena can be described efficiently in a framework of the perturbative approach. Such effects as wave breaking or formation of rogue waves are essentially nonlinear. Combining a conformal mapping technique with Hamiltonian formalism, we elaborated a method which makes possible to solve efficiently exact Euler equations for 2-dimensional nonstationary potential flow of the fluid with free surface [7]. The effects of capilliarity could be included. The new method makes possible to imple-

mentate the spectral code using the fast Fourier transform. A number of harmonics could be as much as 32 000 or more. First experiments show that this method is stable and reliable and can be used systematically as a tool for study of strongly nonlinear phenomena, such as wave breaking, freak wave formation and generation of capilliary waves by gravity waves.

8 Boussinesq equation revisited

The well-known Boussinesq equation describes gravity waves of small slope on shallow water. Actually, these waves are not "weakly nonlinear". On shallow water, even if the slope is small, the "slave harmonics" could be as much important as "free harminocs". It leads to formation of solitons, which interact in a nontrival way and could be unstable. It has been known since 1973 that the Boussinesq equation can be solved exactly by the method of Inverse scattering transform.

However, this procedure never was done before. We have performed an analytical solution of the Boussinesq equation [9]. In particulary, we found an exact solution describing the scattering, merging and collapse of solitons. The results can be applied for description of real phenomena on shallow water.

List of Publications

Articles published in refereed Journals:

1. V. Zakharov, *Statistical Theory of Gravity and Capillary Waves on the Surface of a Finite-Depth Fluid*, Eur. J. Mech. B/Fluids, **18** (1999) No. 3, p. 327-344.

2. W.Perrie and V.Zakharov, *The Equilibrium Range Cascade of Wind-Generated Waves*, Eur. J. Mech. B/Fluids, **18** (1999), No. 3, p. 365-371.

3. V. Zakharov and A. Pushkarev, *Diffusion Model of Interacting Gravity Waves on the Surface of Deep Fluid*, Nonlin. Proc. Geophys., **6** (1999), p. 1-10.

4. V. Zakharov, P. Guyenne, A. Pushkarev and F. Dias, *Wave Turbulence in One-Dimensional Models*, Physica D,**152-153** (2001), p. 573-619.

5. F. Dias, P. Guyenne and V. Zakharov, *Kolmogorov Spectra of Weak Turbulence in Media with Two Types of Interacting Waves*, Phys. Let. A **291** (2001), p.139-145.

Articles accepted for publication in refereed Journals:

6. A. Pushkarev, D. Resio and V. Zakharov, *Weak Turbulent Theory of the Wind-generated Gravity Sea Waves. Part 1. Direct Cascade*, to be published in Phys. Rev.

7. V. Zakharov, A. Dyachenko and O. Vasilyev, *New Method for Numerical Simulation of a Nonstationary Potential Flow of Incompressible Fluid with a Free Surface*, to be published in Eur. J. Mech.

8. M. Onorato, A. Osborne, M. Serio, D. Resio, A. Pushkarev, V. Zakharov and C. Brandini, *Freely Decaying Weak Turbulence for Sea Surface Gravity Waves*, to be published in Phys. Rev. Let.

9. L. Bogdanov and V. Zakharov, *Boussinesq equation revised*, to be published in Physica D.

Articles published in non-refereed editions:

10. A. Pushkarev and V. Zakharov,*On conservation of the constants of motion in the models of nonlinear wave interaction*, Preprints of 6th international workshop on wave hindcasting and forecasting, Monterey, California, November 6-10, 2000, Published by Meteorological Service of Canada, p. 456–469.

List of Conferences where the results were reported

1. January, 1999. WISE meeting, Annapolis, USA.
2. June 14-20, 1999. NICOP meeting, Netherlands.
3. August 3-10, 1999. Solitons, collapses and Turbulence: Achievements, Developments and Perspectives, Chernogolovka, Russia.
4. October, 1999. Conference on Solitons and Turbulence, Tucson, Arizona, USA.
5. Workshop on Wave Modeling, Delft, Netherlands.
6. June 11-15, 2000. Invited speaker, SIAM Conference on Dispersive Wave Turbulence, South Hadley, Massachusetts, USA.
7. August 27 - September 2, 2000. Invited speaker, IUTAM, 20th international congress, Chicago, USA.
8. November 6-10, 2000. 6th international workshop on wave hindcasting and forecasting, Monterey, California, USA.
9. May 2001. WISE meeting, Orillia, Ontario, Canada.
10. August 2001. Workshop on surface waves. Cambridge, England.
11. November 2001. Conference in honor of 60th birthday of Alan Newell, Tucson, Arizona, USA.

Appendix

I. Formula, connecting observed spectrum N_k and "refined" spectrum n_k (see [6]):

$$
\begin{aligned}
n_k = N_k \; &- \; \frac{g}{2}\int \frac{|V^{(1,2)}(\vec{k},\vec{k_1},\vec{k_2})|^2}{(\omega_k-\omega_{k_1}-\omega_{k_2})^2}(N_{k_1}N_{k_2}-N_kN_{k_1}-N_kN_{k_2})\delta(\vec{k}-\vec{k_1}-\vec{k_2})dk_1dk_2 \\
&- \; \frac{g}{2}\int \frac{|V^{(1,2)}(\vec{k},\vec{k_1},\vec{k_2})|^2}{(\omega_{k_1}-\omega_k-\omega_{k_2})^2}(N_{k_1}N_{k_2}+N_kN_{k_1}-N_kN_{k_2})\delta(\vec{k_1}-\vec{k}-\vec{k_2})dk_1dk_2 \\
&- \; \frac{g}{2}\int \frac{|V^{(1,2)}(\vec{k_2},\vec{k},\vec{k_1})|^2}{(\omega_{k_2}-\omega_k+\omega_{k_1})^2}(N_{k_1}N_{k_2}+N_kN_{k_2}-N_kN_{k_1})\delta(\vec{k_2}-\vec{k}-\vec{k_1})dk_1dk_2 \\
&- \; \frac{g}{2}\int \frac{|V^{(0,3)}(\vec{k},\vec{k_1},\vec{k_2})|^2}{(\omega_k+\omega_{k_1}+\omega_{k_2})^2}(N_{k_1}N_{k_2}+N_kN_{k_1}+N_kN_{k_2})\delta(\vec{k}-\vec{k_1}-\vec{k_2})dk_1dk_2
\end{aligned}
$$

where

$$
\begin{aligned}
V^{(1,2)}(\vec{k},\vec{k_1},\vec{k_2}) = \frac{1}{4\pi\sqrt{2}}\Bigg\{ &\left(\frac{A_kB_{k_1}C_{k_2}}{B_kA_{k_1}A_{k_2}}\right)^{1/4} L^{(1)}(\vec{k_1},\vec{k_2}) - \left(\frac{B_kA_{k_1}B_{k_2}}{A_kA_{k_1}A_{k_2}}\right)^{1/4} L^{(1)}(-\vec{k},\vec{k_1}) \\
&- \left(\frac{B_kB_{k_1}A_{k_2}}{A_kA_{k_1}B_{k_2}}\right)^{1/4} L^{(1)}(-\vec{k},\vec{k_2})\Bigg\}
\end{aligned}
$$

$$
\begin{aligned}
V^{(0,3)}(\vec{k},\vec{k_1},\vec{k_2}) = \frac{1}{4\pi\sqrt{2}}\Bigg\{ &\left(\frac{A_kB_{k_1}B_{k_2}}{B_kA_{k_1}A_{k_2}}\right)^{1/4} L^{(1)}(\vec{k_1},\vec{k_2}) + \left(\frac{B_kA_{k_1}B_{k_2}}{A_kB_{k_1}A_{k_2}}\right)^{1/4} L^{(1)}(\vec{k},\vec{k_1}) \\
&+ \left(\frac{B_kB_{k_1}A_{k_2}}{A_kA_{k_1}B_{k_2}}\right)^{1/4} L^{(1)}(\vec{k},\vec{k_2})\Bigg\}
\end{aligned}
$$

$$
\begin{aligned}
L^{(1)}(\vec{k_1},\vec{k_2}) &= -(\vec{k_1},\vec{k_2}) - |k_1||k_2|\tanh k_1h \tanh k_2h \\
A_k &= k\tanh kh, \;\; B_k = g
\end{aligned}
$$

2. Results of numerical simuation of Hasselmann equation is duration-limited frame. Wind velocity $V = 10m/sec$ [6].

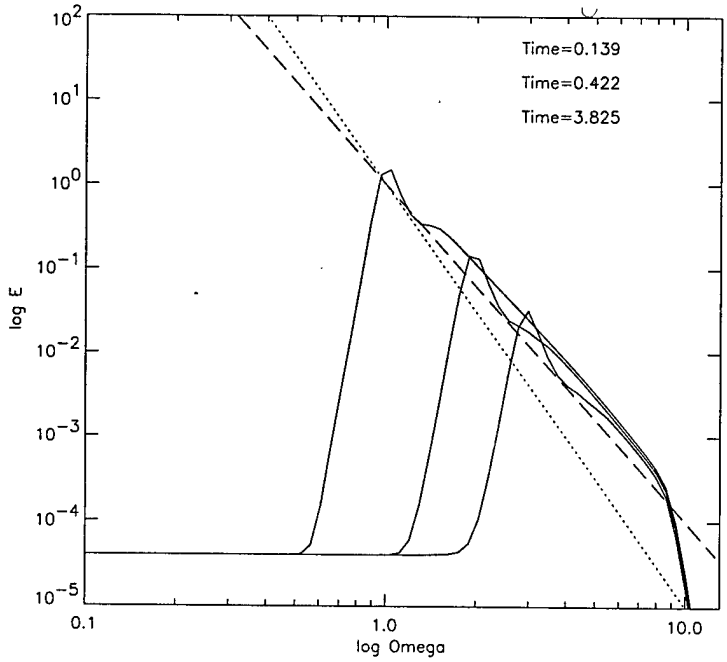

Figure 28: Logarithm of the wave energy averaged over the angle as the function of logarithm of frequency for different moments of time. Dotted line - function proportional to ω^{-5}, dashed line - function proportional to ω^{-4}.

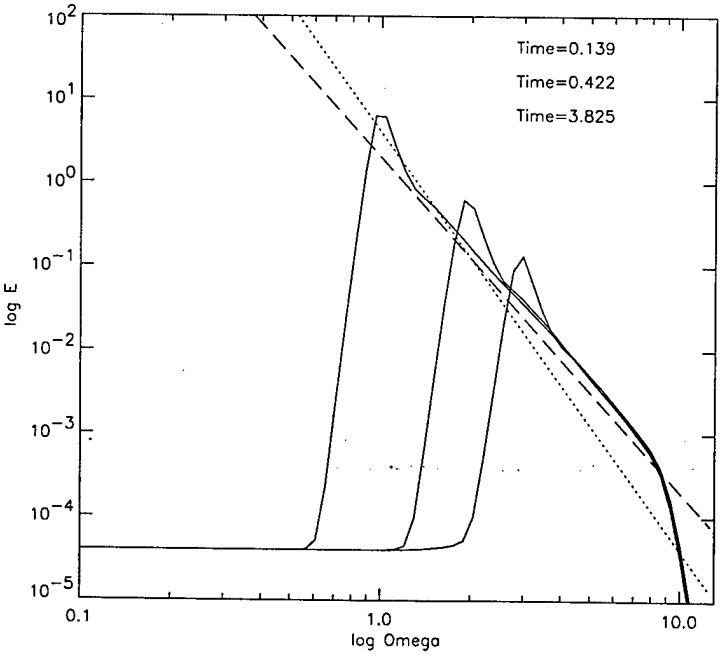

Figure 29: Logarithm of one-dimensional slices of wave energy at $\theta = 0$ as the function of logarithm of frequency for different moments of time. Dotted line - function proportional to ω^{-5}, dashed line - function proportional to ω^{-4}.

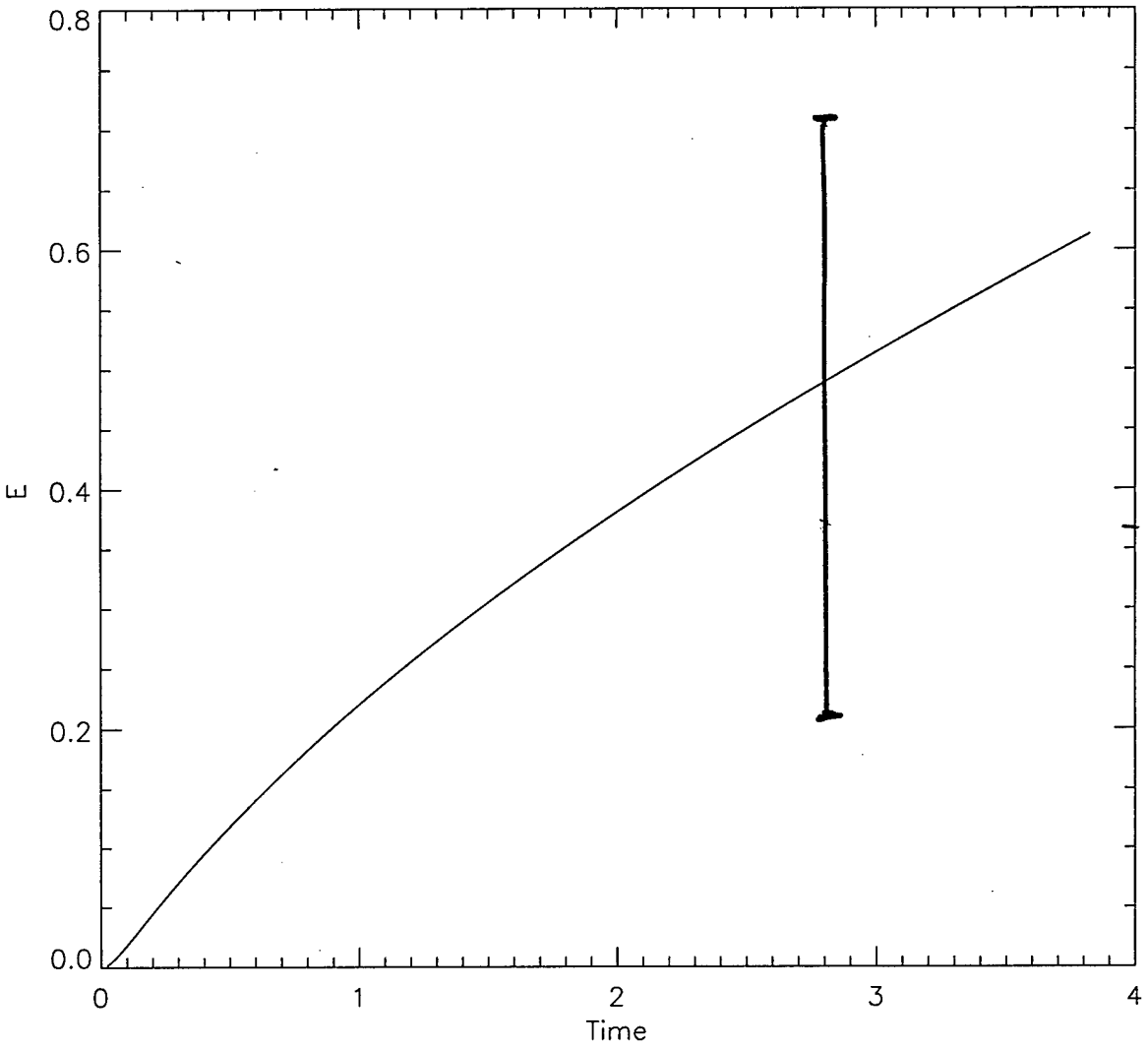

3. Comparison of numerical calculation [6] with duration-limited experimental data, taken from monograph of I.R.Young "Wind generated Ocean Waves".

4. **Oncet of wave-breaking – direct numeric solution of exact Euler equation [7].**

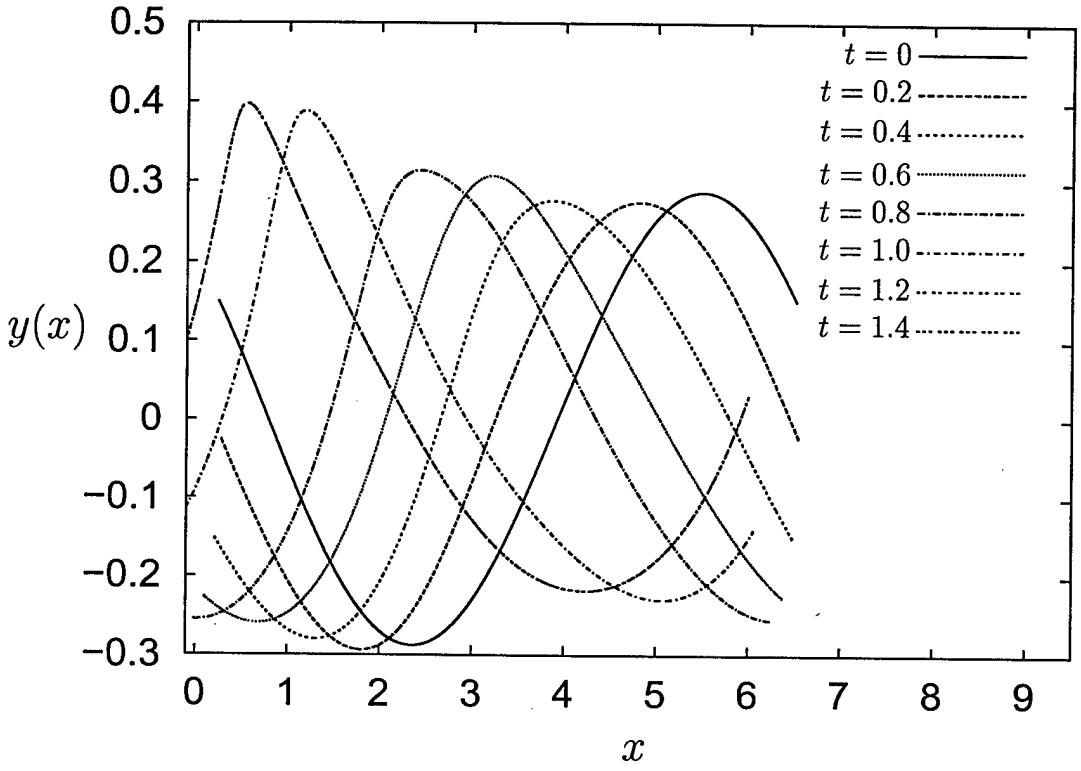

Figure 1:

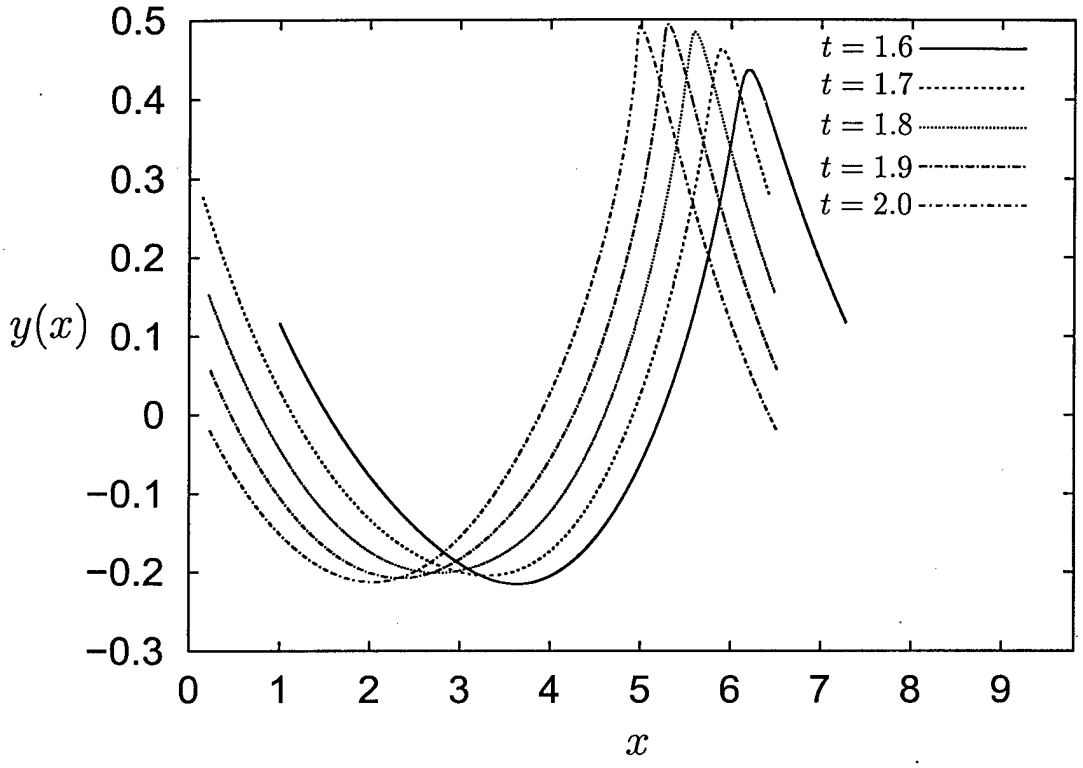

Figure 2:

5. **Formatin of freak waves as a result of mudulation instability of Stokes waves.**

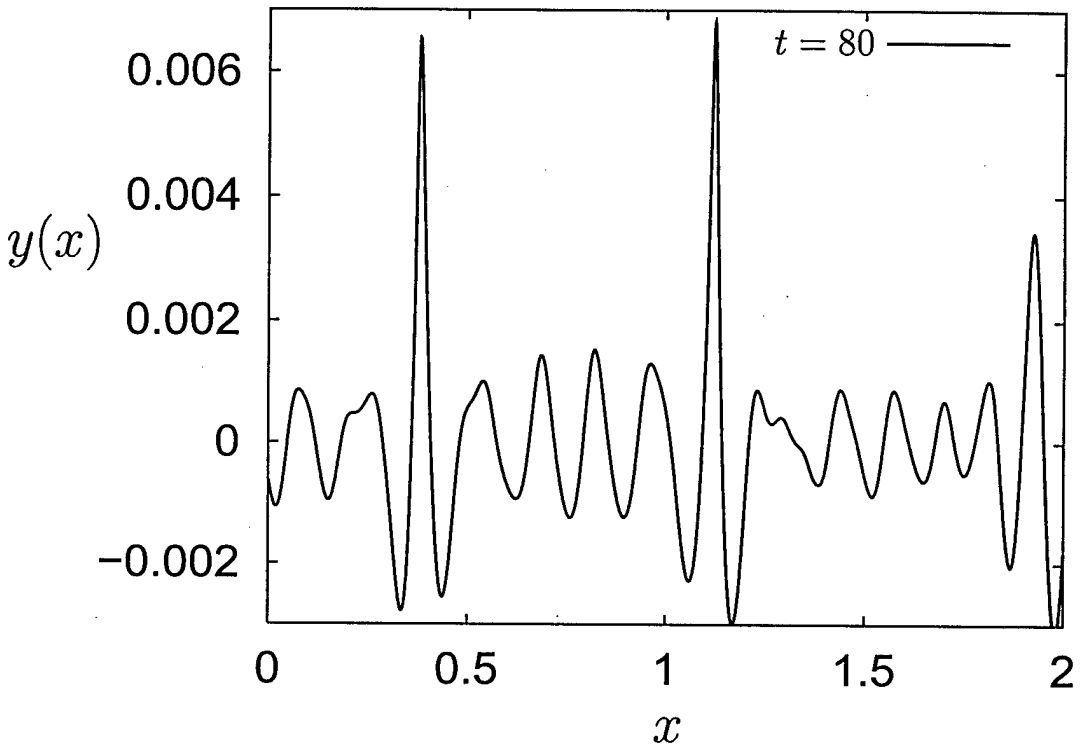

Figure 6:

6. **Diffusion approximation. Level-lines of a mature sea spectrum in polar coordinates. Wind velocity $V = 10m/sec$ [3].**

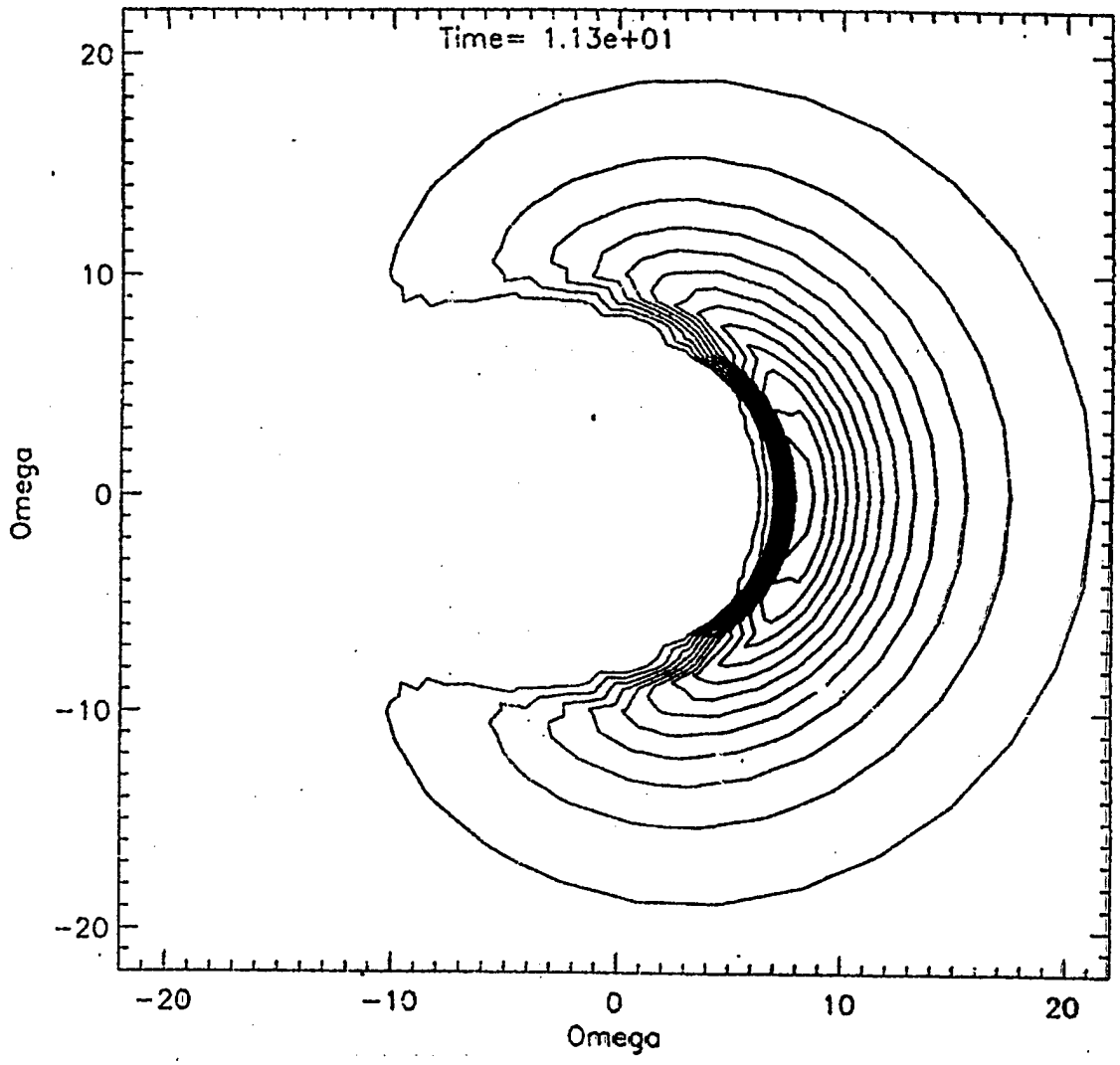

Fig. 7

7. Weak-turbulent Kolmogorov spectra in the MMT-model with 2 types of interacting waves [7].

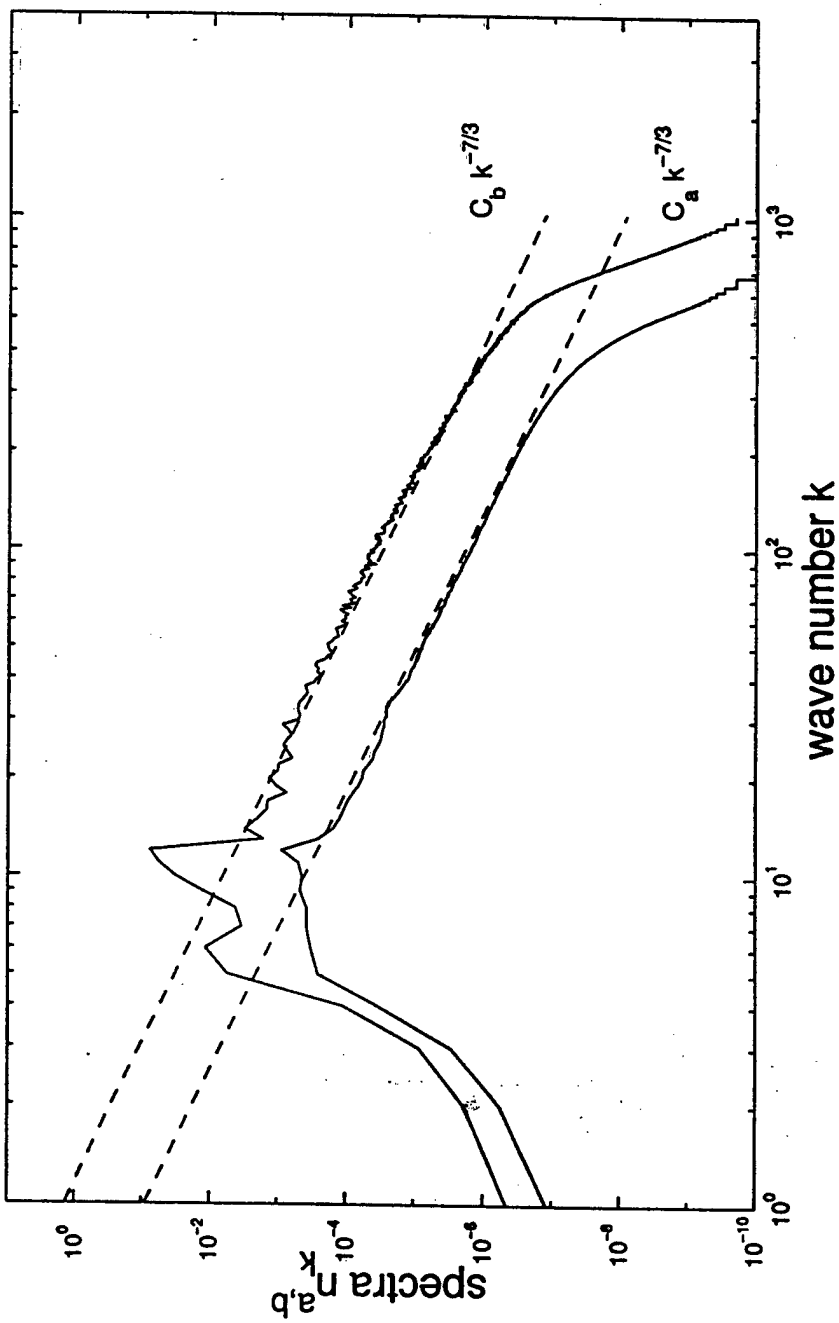

Figure 4: $s = 1/10, \alpha = 3/2, \beta = 2$. Computed spectra ($n^a_k$ for the lower one and n^b_k for the upper one) and predicted Kolmogorov spectra $C_{a,b}k^{-7/3}$ with $C_a = c_2^a P_a^{1/3}$ and $C_b = c_2^b P_b^{1/3} s^{-14/9}$ (dashed lines).

8. Formation of wave turbulence Kolmogorov spectrum $I_k \simeq k^{-2.5}$. Direct simulation of Euler equations.

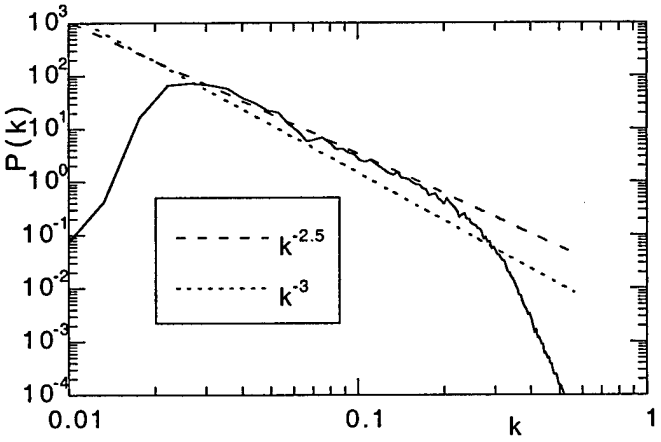

Boussinesq equation revisited

L.V.Bogdanov* and V.E.Zakharov
Landau Institute for Theoretical Physics

Abstract

Continuous spectrum and soliton solutions for Boussinesq equation are investigated using the $\bar{\partial}$-dressing method. Solitons demonstrate quite extraordinary behaviour; they may decay or form a singularity in a finite time. Formation of singularity (collaps of solitons) for Boussinesq equation was discovered several years ago. Systematic study of solitonic sector is presented.

1 Introduction

Our renewed interest to Boussinesq equation is explained mostly by unusual behaviour of soliton solutions of this equation. A common thinking about solitons in integrable system is that they are stable objects interacting trivially, changing only phase as a result of interaction. However, behaviour of solitons of Boussinesq equation destroys this stereotype. Solitons of Boussinesq equation may decay under the action of perturbation or form a singularity in a finite time. One would probably think that Boussinesq equation is itself rather unusual. Not at all, it is a typical example of dimensional reduction in the framework of KP hierarchy (KdV equation being the simplest), and it is also physically relevant equation, representing a nonlinear integrable generalization of wave equation [1]. Formation of singularity (collapse) for Boussinesq equation solitons was first observed several years ago [2] (see also [3]). In this work we perform a systematic study of solitonic sector of Boussinesq and also sum up the results concerning continuous spectrum obtained in the framework of the $\bar{\partial}$-dressing method [4, 5, 6].

*e-mail leonid@landau.ac.ru

The plan of the paper is the following. First, we sum up basic facts concerning the Boussinesq equation.

Then, we briefly review the technique of $\bar{\partial}$-dressing method [7, 8, 9, 10], restricting ourselves to the scalar case as the simplest. We would like to emphasize that most of the contents of this part is not original and is in the main described in the papers mentioned above. We concentrate on the generally less known features of the method, namely on the technique of dimensional reduction and on the characterization of continuous spectrum [4, 5, 6]. We will discuss different types of problems in the complex plane that arise in this context. We also derive determinant formula for soliton solutions.

Using the developed technique, we investigate continuous spectrum for all four versions of Boussinesq equation and obtain Carleman type problems in the complex plane and integral equations describing them.

Finally, we study behaviour of solutions defined by the determinant formula, which gives a solitonic sector for Boussinesq equation. To illustrate behaviour of soliton solutions, we will use the pictures drawn from analytical formulae by Mathematica.

2 Boussinesq equation

Boussinesq equation describes propagation of waves in weakly nonlinear and weakly dispersive media [1]. To derive Boussinesq equation for some physical model, one should start from a Lagrangian

$$L = \int dx \left(\frac{3}{4}\alpha^2 (u_t)^2 - \beta (u_x)^2 + \frac{1}{4}(u_{xx})^2 + 3(u_x)^3 \right), \tag{1}$$

where $\alpha^2, \beta \in \mathbf{R}$. Equation of motion corresponding to Lagrangian (1) is the Boussinesq equation for the function $v = u_x$

$$\left(\frac{3}{4}\alpha^2 v_{tt} - \beta v_{xx} \right) = - \left(\frac{1}{4} v_{xx} + \frac{3}{2} v^2 \right)_{xx}. \tag{2}$$

This equation describes waves moving in both directions. One-wave approximation reduces Boussinesq equation to the Korteweg-de Vries equation.

In fact there are four different cases of Boussinesq equation (2). The coefficients can be rescaled to get $\beta = \pm 1$, $\alpha^2 = \pm 1$, therefore the only choice

is the choice of the two signs. The properties of the Boussinesq equation depend essentially on this choice. The primary choice for us will be the choice of the sign of β. According to this choice, we will distinguish between the 'plus' Boussinesq equation and the 'minus' Boussinesq equation.

'Plus' Boussinesq equation reads

$$\pm\frac{3}{4}v_{tt} - v_{xx} + \frac{1}{4}v_{xxxx} + (\frac{3}{2}v^2)_{xx} = 0. \tag{3}$$

In the case of the second sign plus it is a nonlinear wave equation, having in a linear approximation monochromatic solution

$$v \simeq e^{i(\omega y + kx)},\ \omega^2 = \frac{4}{3}(k^2 + \frac{1}{4}k^4).$$

In the minus case it is a nonlinear elliptic equation.

'Minus' Boussinesq equation is

$$\pm\frac{3}{4}v_{tt} + v_{xx} + \frac{1}{4}v_{xxxx} + (\frac{3}{2}v^2)_{xx} = 0. \tag{4}$$

Dispersion law for this equation is given by the expression

$$\omega^2 = \pm\frac{4}{3}(-k^2 + \frac{1}{4}k^4).$$

For the sign plus this dispersion law is unstable for short waves and stable for long waves, for the sign minus it is stable for short waves and unstable for long waves.

So four cases of the Boussinesq equation can be characterized in the following way: wave case, elliptic case, Boussinesq equation with long-wave instability and Boussinesq equation with short-wave instability.

Boussinesq equation is integrable by the inverse problem method (see, e.g., [11]). Our interest to this equation is explained by nontrivial properties of both continuous and discrete spectrum for this equation.

Technically, Boussinesq equation is a result of dimensional reduction of KP equation taken in the moving frame. The initial KP equation in the moving frame reads

$$\frac{\partial}{\partial x}((v_t - \beta v_x) + \frac{1}{4}v_{xxx} + 3v_x v) = -\frac{3}{4}\alpha^2 v_{yy}, \tag{5}$$

where the constant α defines the choice between KPI (α = i) and KPII ($\alpha = 1$) equations, and the constant β is the velocity of the frame (we take $\beta = \pm 1$). Considering stationary solutions of (2+1)-dimensional equation (5), we get (1+1)-dimensional Boussinesq equation (2),

$$\left(\frac{3}{4}\alpha^2 v_{yy} - \beta v_{xx}\right) = -\left(\frac{1}{4}v_{xx} + \frac{3}{2}v^2\right)_{xx}, \tag{6}$$

where the role of the time variable t is played by KP variable y.

To investigate continuous spectrum, we use the $\bar{\partial}$-dressing method [7, 8, 9, 10], in which very effective apparatus to describe dimensional reductions and continuous spectrum was developed [4, 5, 6]. We get information about the structure of continuous spectrum and the problems in the complex plane corresponding to all four versions of Boussinesq equation. Geometry of the spectrum is rather interesting, the spectral data are localized on the hyperbola in the complex plane and on the segment of the real axis and small decreasing solutions are given by the Riemann problem with a shift on this curve (see another approach in [12, 13]).

Behaviour of solutions of Boussinesq equation belonging to solitonic sector is also rather unusual. The formula for the multisoliton solution of the Boussinesq equation can be obtained from the formula for the plain solitons of KP equation [11]

$$v = \frac{\partial^2}{\partial x^2}\log\det(A), \tag{7}$$
$$A_{ij} = \delta_{ij} - \frac{R_i}{\mu_i - \lambda_j},$$

here

$$R_k = ic_k \exp(i(\mu_k - \lambda_k)(x - i\alpha^{-1}(\mu_k + \lambda_k)y)),$$
$$(\lambda_k^3 \pm \lambda_k - (\mu_k^3 \pm \mu_k) = 0,\ \lambda \neq \mu \tag{8}$$

$\lambda_k \neq \mu_j$, where λ_k, μ_k are two arbitrary sets of points of the complex plane satisfying the condition (8), which characterizes stationary KP solutions in the moving reference frame (c_k , λ_k , μ_k should also satisfy some reduction conditions to get a real solution). Formula (7) can be obtained in many different ways, in our work we will derive it using the $\bar{\partial}$-dressing method.

We will treat mostly the case of the 'plus' Boussinesq equation with $\alpha = 1$. This equation has a stable 'wave sector' (i.e., in the linear limit it is a wave

equation). There are two soliton sectors for this equation: 'usual' solitons, running with the velocity limited from above, and soliton configurations, forming a singularity in a finite time. The latter may be considered as bounded states of several singular solitons.

But even 'usual' solitons demonstrate quite extraordinary behavior in this case. Slow solitons are unstable with respect to small perturbations and may decay into two solitons or two singular solitons (that means a formation of singularity in finite time). Interaction of slow solitons unavoidably leads to formation of singulatity. Rapid solitons moving in the same direction behave like it is usually expected from the system of solitons; they do not decay and their interaction does not lead to formation of singularities.

In this work we present a systematic study of solitonic sector of Boussinesq equation.

3 $\bar{\partial}$-dressing: the basic technique

The main technical tool of our work is the dressing method based on the nonlocal $\bar{\partial}$-problem [7, 8, 9, 10]. This is a powerful method of constructing (2+1)-dimensional integrable equations together with a broad class of their solutions.

Boussinesq equation may be considered as a dimensional reduction of KP equation in the moving frame. To apply $\bar{\partial}$-dressing method to Boussinesq equation, we will use the scheme of dimensional reduction for the $\bar{\partial}$-dressing method developed in [5]. It leads us to the problem with a special kind of non-locality - the $\bar{\partial}$-problem with a shift and to the Riemann problem with a shift. It appears that these *scalar nonlocal* problems are a general and natural technical tool in (1+1)-dimensional case.

The construction developed in [4] gives a simple and straightforward description of solutions belonging to continuous spectrum (i.e., small decreasing solutions) in the framework of the $\bar{\partial}$-dressing method. Continuous spectrum is characterized in terms of conditions which single out some special classes of the kernels of the general nonlocal $\bar{\partial}$-problem.

Taking into account conditions of dimensional reduction, for small decreasing solutions of (1+1)-dimensional equations we come to Carleman type problems in the complex plane.

The scheme of the dressing method uses the nonlocal $\bar{\partial}$-problem with a

special dependence of the kernel on additional (space and time) variables

$$\bar{\partial}(\psi(\mathbf{x},\lambda)-\eta(\mathbf{x},\lambda))=\hat{R}\psi(\mathbf{x},\lambda), \tag{9}$$

$$\hat{R}\psi(\mathbf{x},\lambda)=\iint \psi(\mathbf{x},\lambda)R(\lambda,\mu)\exp(\sum_i \phi_i x_i)d\mu\wedge d\bar{\mu},$$

$$\phi_i=K_i(\mu)-K_i(\lambda), 1\le i\le 3, \tag{10}$$

where $\lambda\in\mathbf{C}$, $\bar{\partial}=\partial/\partial\bar{\lambda}$, $\eta(\mathbf{x},\lambda)$ is a rational function of λ (normalization), $K_i(\lambda)$ are rational functions, the choice of which determines the equation that can be solved using the problem (9). We suppose that the kernel $R(\lambda,\mu)$ equals to zero in a neighborhood with respect to λ and to μ of the divisor of poles of functions $K_i(\lambda)$, tends to zero as $\lambda,\mu\to\infty$ and that for the chosen kernel $R(\lambda,\mu)$ problem (9) is uniquely solvable (at least for the sufficiently small $\mathbf{x}$). The solution of problem (9) normalized by η is the function

$$\psi(\mathbf{x},\lambda)=\eta(\mathbf{x},\lambda)+\varphi(\mathbf{x},\lambda),$$

where $\eta(\mathbf{x},\lambda)$ is a rational function of λ (normalization), $\varphi(\mathbf{x},\lambda)$ decreases as $\lambda\to\infty$ and is *analytic* in a neighborhood of the poles of $K_i(\lambda)$.

Problem (9) reduces to integral equation for the function φ

$$\varphi(\mathbf{x},\lambda)=\bar{\partial}^{-1}\hat{R}(\varphi(\mathbf{x},\lambda)+\eta(\mathbf{x},\lambda)), \tag{11}$$

here

$$(\bar{\partial}^{-1}\varphi)(\lambda)=(2\pi i)^{-1}\iint\frac{\varphi(\lambda')}{(\lambda'-\lambda)}d\lambda'\wedge d\bar{\lambda}'$$

$$=(2\pi i)^{-1}\lim_{\epsilon\to 0}\iint\frac{\varphi(\lambda')(\bar{\lambda}'-\bar{\lambda})}{(|\lambda'-\lambda|^2+\epsilon)}d\lambda'\wedge d\bar{\lambda}',$$

which is supposed to be uniquely solvable for given R. Solvability is guaranteed if operator $\bar{\partial}^{-1}R$ is 'small enough' (i.e., norm of this operator is less then 1 for some properly chosen space of functions).

Let us introduce $\rho(\lambda,\bar{\lambda})=\bar{\partial}\varphi$. Now

$$\psi(\mathbf{x},\lambda)=\eta+(2\pi i)^{-1}\iint\frac{\rho(\lambda')}{(\lambda'-\lambda)}d\lambda'\wedge d\bar{\lambda}'. \tag{12}$$

Substituting (12) into (11), we can get another form of the basic integral equation, resolving the nonlocal $\bar{\partial}$-problem

$$\rho(\mathbf{x},\lambda)=\hat{R}\left(\eta+\bar{\partial}^{-1}\rho\right). \tag{13}$$

The nonlocal $\bar{\partial}$-problem and its special cases ($\bar{\partial}$-problem with a shift, nonlocal Riemann problem, Riemann problem with a shift) are powerful tools for constructing integrable nonlinear equations and their solutions (see [7], [8], [9], [10])

The algebraic scheme of constructing equations is based on the following property of problem (9): if $\psi(\mathbf{x}, \lambda)$ is a solution of the problem (9), then functions

$$u(\mathbf{x})\psi,\ D_i\psi = (\partial/\partial x_i + K_i)\psi \tag{14}$$

are also solutions. Combining this property with unique solvability of problem (9), one obtains differential relations between the coefficients of expansion of functions $\psi(\mathbf{x}, \lambda)$ into powers of $(\lambda - \lambda_p)$ at the poles of $K_i(\lambda)$. Let us outline the basic steps of this scheme for KP equation that will be used in this work.

For KP equation

$$K_1(\lambda) = \mathrm{i}\lambda,\ K_2(\lambda) = \alpha^{-1}\lambda^2,\ K_3(\lambda) = \mathrm{i}\lambda^3,$$

and, respectively,

$$\begin{aligned} D_1 &= \partial/\partial x + \mathrm{i}\lambda, \\ D_2 &= \partial/\partial y + \alpha^{-1}\lambda^2, \quad (\alpha = 1; \mathrm{i}), \\ D_3 &= \partial/\partial t + \mathrm{i}\lambda^3. \end{aligned}$$

Let us introduce the solution of problem (9) normalized by 1 ($\eta = 1$),

$$\psi(\lambda, x, y, t)_{\lambda\to\infty} \to 1 + \psi_0(x, y, t)\lambda^{-1} + ...$$

The basis in the space of solutions of problem (9)) with the polynomial normalization is constituted by the set of functions $D_1^n\psi$, $0 \le n < \infty$. It follows from the unique solvability of problem (9) that ψ satisfies the relations

$$(D_3 + D_1^3 + g(x, y, t)D_1 + h(x, y, t))\psi = 0, \tag{15}$$

$$(\alpha D_2 + D_1^2 + 2v(x, y, t))\psi = 0. \tag{16}$$

The successive use of the coefficients of expansion of these relations as $\lambda \to \infty$ allows us to define the functions v, g, h

$$v = -i\frac{\partial}{\partial x}\psi_0,\ g = 3v,\ h_x = \frac{3}{2}(v_{xx} - \alpha v_y),$$

and to derive the KP equation for the first coefficient of expansion of the function ψ as $\lambda \to \infty$:

$$\frac{\partial}{\partial x}(v_t + \frac{1}{4}v_{xxx} + 3v_x v) = -\frac{3}{4}\alpha^2 v_{yy}. \tag{17}$$

3.1 Special cases of nonlocal $\bar{\partial}$-problem

In the most important cases the kernel $R(\lambda, \mu)$ is a singular function localized on some manifold in $\mathbf{C}^2$. That means that the kernel contains the δ-function localized on the corresponding manifold, or in other words that the measure of integration in the operator $\bar{\partial}^{-1}\hat{R}$ is localized on this manifold. The operator $\bar{\partial}^{-1}\hat{R}$ in this case is still well defined.

$\bar{\partial}$-problem with a shift

In a typical situation this manifold is a covering of the complex λ-plane, defined by the equation

$$f(\lambda, \bar{\lambda}, \mu, \bar{\mu}) = 0, \tag{18}$$

where f is some function in $\mathbf{C}^2$. Equation (18) defines a multi-valued shift function $\mu = \mu_i(\lambda, \bar{\lambda})$. The kernel of problem (9) in this case reads

$$R = \sum_i R_i(\lambda, \bar{\lambda})\delta(\mu - \mu_i(\lambda, \bar{\lambda})).$$

We will call this case a *$\bar{\partial}$-problem with a shift.*

Nonlocal Riemann problem

Another special case of problem (9) is a nonlocal Riemann problem. Let $\gamma = \lambda(\xi)$, $\xi \in \mathbf{R}$ be an oriented curve in a complex plane (may be not connected), and the kernel of problem (9) be concentrated on the product of couple of these curves in λ and in μ planes. In other words,

$$R(\lambda, \mu) = \delta_\gamma(\lambda) R_\gamma(\lambda, \mu)\delta_\gamma(\mu) \tag{19}$$

where $\delta_\gamma(\lambda)$ is a δ-function picking out points on γ. The solution ψ of problem (9) with the kernel (19) is rational outside γ and has boundary values ψ^+,

ψ^- on γ. After regularizing δ_γ we obtain from problem (9) with the kernel (19) a nonlocal Riemann problem

$$\psi^+ - \psi^- = \frac{1}{2}\int_\gamma (\psi^+ + \psi^-) R_\gamma(\lambda, \mu) d\mu, \tag{20}$$

the integration in (20) goes along the curve γ.

Riemann problem with a shift

A combination of these two special cases leads to the Riemann problem with a shift (or Carleman's problem). The shift function $\mu = \mu_i(\lambda)$ is defined now on the curve γ ($\lambda, \mu \in \gamma$). In this case

$$R_\gamma(\lambda, \mu) = \sum_i R^i_\gamma(\lambda) \delta_\gamma(\mu - \mu_i(\lambda))$$

and

$$\psi^+ - \psi^- = \frac{1}{2}\sum_i (\psi^+(\mu_i(\lambda)) + \psi^-(\mu_i(\lambda)) R^i_\gamma(\lambda), \tag{21}$$

where $\mu_i(\lambda)$ is a multi-valued shift function on the curve $\lambda(\xi)$. We will write problem (21) symbolically in the form

$$\Delta(\psi(\lambda(\xi))) = R_\gamma(\lambda, \mu(\lambda)) \psi(\mu(\lambda(\xi))), \tag{22}$$

where $\gamma = \lambda(\xi)$ ($\xi \in \mathbf{R}$) is a curve in the complex plane, Δ is a jump of the function across the curve, the value of the function on the curve is the half-sum of the boundary values, $\mu(\lambda)$ is the shift function (may be multi-valued).

Integral equations

In all these three cases problem (9) is equivalent to a certain integral equation which can be obtained by a proper reduction of equations (11),(13). Let us do that for a Riemann problem with a shift. Introducing

$$\rho_\gamma(\lambda) = \psi^+ - \psi^-|_{\lambda \in \gamma},$$

we can restore the function ψ in a form

$$\psi = \eta + \frac{1}{2\pi i}\int_\gamma \frac{\rho_\gamma(\lambda')}{(\lambda - \lambda')} d\lambda'.$$

Hence

$$\frac{1}{2}(\psi^+ + \psi^-)|_{\lambda\in\gamma} = \eta(\lambda) + \frac{1}{2\pi i} v.p. \int \frac{\rho_\gamma(\lambda')}{(\lambda - \lambda')} d\lambda',$$

and from equation (21) one gets

$$\rho_\gamma(\lambda) = \sum_i \left(\eta(\mu_i(\lambda)) + \frac{1}{2\pi i} v.p. \int \frac{\rho_\gamma(\lambda)}{(\mu_i(\lambda) - \lambda')} d\lambda' \right) R^i_\gamma(\lambda),\ \lambda \in \gamma. \quad (23)$$

Let the curve γ consist of n connected branches $\gamma_i = \lambda_i(\xi)$, $\xi \in \mathbf{R}$, and $\rho_i(\xi)$ be the jump of the function ψ across the corresponding branch. Then the expression for the function ψ takes the form

$$\psi = \eta + \frac{1}{2\pi i} \sum_{i=1}^{n} \int \frac{\rho_i(\xi')}{(\lambda - \lambda_i(\xi'))} \frac{d\lambda_i}{d\xi'} d\xi', \quad (24)$$

and integral equation (23) reads

$$\rho_k(\xi) = \sum_i \left(\eta(f_i(\xi)) + \frac{1}{2\pi i} \sum_{j=1}^{n} v.p. \int \frac{\rho_j(\xi')}{(\mu_i(\lambda_k(\xi)) - \lambda_j(\xi'))} \frac{d\lambda_j}{d\xi'} d\xi' \right) R^{ik}(\xi). \quad (25)$$

Thus we have obtained a system of n singular integral equations.

The δ-functional kernels

There is one important special case of nonlocal $\bar{\partial}$-problem which is exactly solvable, which corresponds to soliton solutions and discrete spectrum (in some broad sense). This is a case of δ-functional kernels

$$R(\lambda, \mu) = 2\pi i \sum_{i=1}^{N} R_i \delta(\lambda - \lambda_i)\delta(\mu - \mu_i), \quad (26)$$

where λ_i, μ_i is a set of points in the complex plane, $\lambda_i \neq \mu_j$,

$$R_k = c_k \exp((K_i(\lambda) - K_i(\mu))x_i).$$

In this case the solution of problem (9) is a rational function, and problem (9) reduces to a system of linear equations. The formula for the solution

normalized by $(\lambda-\mu)^{-1}$ is

$$\psi(\lambda,\mu)=\frac{1}{\lambda-\mu}+((A)^{-1})_{ij}\frac{R_j}{(\mu_j-\mu)(\lambda-\lambda_i)}, \qquad (27)$$
$$A_{ij}=\delta_{ij}-\frac{R_i}{\mu_i-\lambda_j},$$

here

$$R_k=c_k\exp((K_i(\mu_k)-K_i(\lambda_k))x_i),$$

or, in a more symmetric form with respect to λ and μ

$$\psi(\lambda,\mu)=\frac{1}{\lambda-\mu}+((A')^{-1})_{ij}\frac{1}{(\mu_j-\mu)(\lambda-\lambda_i)}, \qquad (28)$$
$$A'_{ij}=R_i^{-1}\delta_{ij}-\frac{1}{\mu_i-\lambda_j},$$

In the limit when a pair of poles λ_i,μ_j coincide, rational with respect to x_q factors appear in the formula for ψ. The limit $\lambda_i\to\mu_i$ for all $0<i\leq N$ corresponds to a rational with respect to x_q solution.

Expression for solution with canonic normalization ($\eta=1$) can be obtained from the formula (27),

$$\psi(\lambda,\mathbf{x})=\lim_{\mu\to\infty}-\mu\psi(\lambda,\mu,\mathbf{x})=1+\sum_j((A')^{-1})_{ij}(\lambda-\lambda_i), \qquad (29)$$

and potential

$$\psi_0(\mathbf{x})=\lim_{\lambda\to\infty}\lambda\psi(\lambda,\mathbf{x})$$

reads

$$\psi_0(\mathbf{x})=\sum_j\sum_i((A')^{-1})_{ij}. \qquad (30)$$

Introducing variable x with $K(\lambda)=i\lambda$, it is easy to check that expression (30) can be rewritten in the form

$$\psi_0(\mathbf{x})\sim-\mathrm{i}\frac{\partial}{\partial x}\log\det(A)\sim-\mathrm{i}\frac{\partial}{\partial x}\log\det(A') \qquad (31)$$

(up to a constant). Indeed,

$$-\mathrm{i}\frac{\partial}{\partial x}\log\det(A') \backsim -\mathrm{i}\frac{\partial}{\partial x}\log\det\left(c_i^{-1}\delta_{ij} - \frac{\exp(\mathrm{i}(\mu_i-\lambda_j)x)}{(\mu_i-\lambda_j)}\right)$$
$$= \sum_i\sum_j \exp(\mathrm{i}(\mu_i-\lambda_j))\left(c_p^{-1}\delta_{pq} - \frac{\exp(\mathrm{i}(\mu_p-\lambda_q)x)}{(\mu_p-\lambda_q)}\right)^{-1}_{ji}$$
$$= \sum_j\sum_i((A')^{-1})_{ij}. \qquad (32)$$

3.2 Solutions with special properties

Small decreasing solutions (continuous spectrum)

A solution given by the problem (9) in a general case is defined only locally in a vicinity of the point $\mathbf{x} = 0$, where the $\bar{\partial}$-problem is uniquely solvable. Solvability may be lost on some manifold in a space (x_1, x_2, x_3), where the solution has a singularity. To get 'good enough' solutions having no singularities and bounded (decreasing) as $|\mathbf{x}| \to \infty$ one should put some restrictions on the kernel $R(\lambda, \mu)$. These restrictions were discussed in our article [4]. The main result of this article can be formulated as follows. Let us choose a unit vector n_i ($\sum n_i^2 = 1$) defining a direction in the $\mathbf{x}$-space. The solution given by problem (9) is regular in a neighborhood of straight line $x_i = n_i\xi$ and decreasing along this line as $\xi \to \pm\infty$ if the condition

$$\mathrm{Re}\sum_{i=1}^{3} n_i(K_i(\lambda) - K_i(\mu)) = 0 \qquad (33)$$

is satisfied (this condition is in fact the condition for the kernel $R(\lambda, \mu)$, it means that we should use the kernel localized on the manifold (33)), and the kernel $R(\lambda, \mu)$ is 'small enough'.

To get a solution which is 'good enough' in a neighborhood of some plane, defined by two vectors n_i, m_i, one has to satisfy two conditions

$$\mathrm{Re}\sum_{i=1}^{3} n_i(K_i(\lambda) - K_i(\mu)) = 0,$$
$$\mathrm{Re}\sum_{i=1}^{3} m_i(K_i(\lambda) - K_i(\mu)) = 0.$$

In a generic case a pair of conditions (33) define some manifold with real dimension 2 in the space $\mathbf{C}^2$ of complex variables λ, μ.

Let us illustrate this result on the simple example of the KP equation. To obtain the small nonsingular solution decreasing in the plane (x, y) it is sufficient to use the problem (9) with the kernel localized on the manifold defined by the system of conditions (33)

$$\mathrm{Im}(\lambda - \mu) = 0, \tag{34}$$

$$\mathrm{Re}\, \alpha^{-1}(\lambda^2 - \mu^2) = 0. \tag{35}$$

If $\alpha = i$, the system (35), (34) has a solution $\lambda, \mu \in \mathbf{R}$, which defines a nonlocal Riemann problem on the real axis. So the small decreasing solutions of the KP1 equation are given by the nonlocal Riemann problem

$$\psi^+ - \psi^- = \int_\gamma (\psi^+ + \psi^-) R_\gamma(\lambda, \mu) \exp(\phi_i x_i) d\mu, \tag{36}$$

that was originally used by Manakov [14] to integrate the KP1 equation.

If $\alpha = 1$, the solution of the system (35) is $\mu = -\bar{\lambda}$. Thus the small decreasing solutions of the KP2 equation are given by the $\bar{\partial}$-problem with a conjugation

$$\bar{\partial}\psi(x, y, t, \lambda) = R(\lambda, -\bar{\lambda}) \exp(\phi_i x_i) \psi(x, y, t, -\bar{\lambda}), \tag{37}$$

and we reproduce the problem used by Ablowitz, Bar Yaacov and Fokas [15] to integrate KP2 equation.

Dimensional reduction

Solutions independent of the variable x_j can be obtained from the problem (9) with the kernel localized on the manifold

$$K_j(\lambda) - K_j(\mu) = 0. \tag{38}$$

This observation allows us to use (2+1)-dimensional dressing method for (1+1)-dimensional equations and leads us naturally to the $\bar{\partial}$-problem with a shift and, for decreasing solutions, to the Riemann problem with a shift. Let us consider this observation in more detail.

If we have (2+1)-dimensional integrable equation, defined by the functions $K_i(\lambda)$, we can descend to (1+1)-dimensional case, using the condition

(38) for some coordinate x_i in the original or rotated coordinate system. For example, y-independent KP equation gives the KdV equation

$$(v_t + \frac{1}{4}v_{xxx} + 3v_x v) = 0$$

The condition (38) in this case reads

$$\lambda^2 - \mu^2 = 0,$$

and the solutions of the KdV equation are given by the $\bar{\partial}$-problem with a shift [8]

$$\bar{\partial}\psi(\lambda) = R(\lambda, -\lambda)\exp(\phi_i x_i)\psi(-\lambda) \tag{39}$$

the shift function for this case is quite simple ($\mu = -\lambda$), and it is easy to transform problem (39) to local matrix (2×2) Riemann problem.

We may also consider the case of the t-independent KP equation, which corresponds to simplified Boussinesq equation

$$\frac{3}{4}\alpha^2 v_{yy} = -(\frac{1}{4}v_{xx} + \frac{3}{2}v^2)_{xx}, \tag{40}$$

Condition (38) in this case reads

$$\lambda^3 - \mu^3 = 0,$$

and solutions of simplified Boussinesq equation (40) are given by the $\bar{\partial}$-problem

$$\bar{\partial}\psi(\lambda) = \sum_{i=1}^{3} R_i \psi(e_i\lambda),$$

where $e_i^3 = 1$. Simplified variant of the Boussinesq equation was considered in [13]. Let us show that for decreasing solutions our approach leads us to the Riemann problem with a shift for the functions analytic in sectors (such a geometry for the local matrix Riemann problem arose in [13] from the analytical properties of the direct scattering problem). Combining the condition (38) with the condition (33)

$$\mathrm{Im}\,(\lambda - \mu) = 0,$$

we obtain

$$\begin{cases} \lambda - e_i\mu = 0 \\ \lambda - \mu = \xi,\ \xi \in \mathbf{R} \end{cases}$$

The solution of this system is

$$\begin{aligned}\lambda &= \xi(1-e_i)^{-1},\\ \mu &= -\xi(1-e_i^{-1})^{-1},\end{aligned}$$

it defines a Riemann problem with a shift on the pair of straight lines with the vectors $\exp(i\pi/6)$, $\exp(-i\pi/6)$, the shift function is $\mu = -\bar{\lambda}$. So we came to the problem for the function analytic in corresponding sectors.

For an arbitrary rational function $K_i(\lambda)$ condition (38) defines a multi-valued shift function $\mu_i(\lambda)$, and corresponding $\bar{\partial}$-problem reads

$$\bar{\partial}\psi(\lambda) = \sum_{i=1}^{n} R_i \psi(\lambda_i(\mu)). \tag{41}$$

4 Boussinesq equation via $\bar{\partial}$-dressing method

Let us consider KP equation in the moving frame equation

$$\frac{\partial}{\partial x}((v_t - \beta v_x) + \frac{1}{4}v_{xxx} + 3v_x v) = -\frac{3}{4}\alpha^2 v_{yy},\ \beta^2 = 1. \tag{42}$$

Solutions of this equation are given by problem (9) with dependence of the kernel on variables x, y, t defined by the expressions (compare (10),(14))

$$\begin{aligned}D_1 &= \partial/\partial x + i\lambda,\\ D_2 &= \partial/\partial y + \alpha^{-1}\lambda^2,\ (\alpha = 1; i),\\ D_3 &= \partial/\partial t + i\lambda^3 + i\beta\lambda.\end{aligned} \tag{43}$$

Time-independent solutions of equation (42) satisfy Boussinesq equation

$$(\frac{3}{4}\alpha^2 v_{yy} - \beta v_{xx}) = -(\frac{1}{4}v_{xx} + \frac{3}{2}v^2)_{xx}. \tag{44}$$

Such solutions are given by problem (9) ($v = -i\frac{\partial}{\partial x}\psi_0$), if the support of kernel $R(\lambda, \mu)$ belongs to the manifold defined by condition (38)

$$(\lambda^3 + \beta\lambda - \mu^3 - \beta\mu) = 0,\ \lambda \neq \mu, \tag{45}$$

or

$$\lambda^2 + \lambda\mu + \mu^2 + \beta = 0.$$

This relation defines a $\bar{\partial}$-problem with a shift

$$\bar{\partial}\psi(\lambda, x, y) = R(\lambda, \mu(\lambda)) \exp(\phi_i x_i)\psi(\mu(\lambda), x, y), \qquad (46)$$
$$\mu = \frac{1}{2}(-\lambda \pm (4\beta - 3\lambda^2)^{\frac{1}{2}}),$$

Solutions of Boussinesq equation, given by problem (46) ($v = -i\frac{\partial}{\partial x}\psi_0$), are defined locally in the neighborhood of the point $x = 0, y = 0$. We consider Boussinesq equation as a dynamical equation with respect to the variable y. To obtain small decreasing as $|x| \to \infty$ solutions, we should investigate the intersection of the manifold (38) with the manifold, defined by the condition (33) :

$$\mathrm{Im}(\lambda - \mu) = 0. \qquad (47)$$

Conditions (45), (47) define a Riemann problem with a shift (the Carleman's problem) which is a proper tool to solve Boussinesq equation. Introducing $\xi = \frac{1}{2}(\lambda - \mu)$, $\nu = -i\frac{1}{2}(\lambda + \mu)$, $\xi \in \mathbf{R}$, one can get

$$\beta + \xi^2 - 3\nu^2 = 0. \qquad (48)$$

About the reduction

Let us make a remark about the reduction. For $\alpha = 1$ $v(x, y)$ is real if the kernel of the problem (9) satisfies the condition

$$R(\lambda, \mu) = \bar{R}(-\bar{\lambda}, -\bar{\mu}), \qquad (49)$$

for $\alpha = i$ if

$$R(\lambda, \mu) = \bar{R}(\bar{\mu}, \bar{\lambda}). \qquad (50)$$

4.1 Continuous spectrum

'Plus' Boussinesq equation

One can see that the properties of Boussinesq equation depend essentially on the sign of β. Let $\beta = 1$. Corresponding equation ('plus' Boussinesq equation) has a form

$$\frac{3}{4}\alpha^2 v_{yy} - v_{xx} + \frac{1}{4}v_{xxxx} + (\frac{3}{2}v^2)_{xx} = 0. \qquad (51)$$

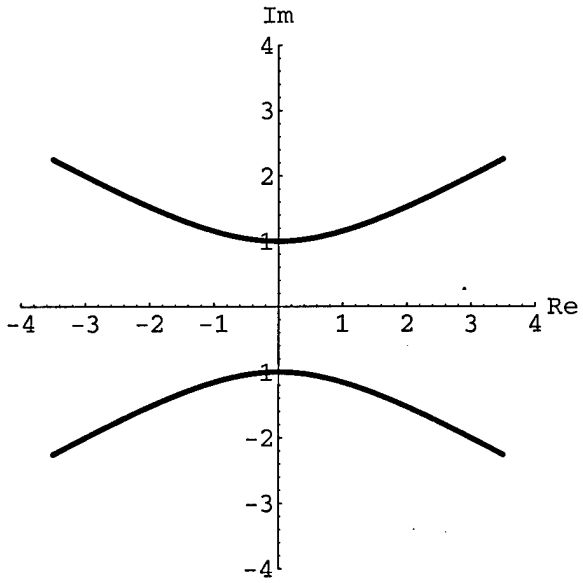

Figure 1: Localization of continuous spectrum for 'plus' Boussinesq equation

In the case $\alpha^2 = 1$ it is a nonlinear wave equation, having in a linear approximation monochromatic solution

$$v \simeq e^{i(\omega y + kx)},\ \omega^2 = \frac{4}{3}(k^2 + \frac{1}{4}k^4).$$

In the case $\alpha^2 = -1$ it is a nonlinear elliptic equation. In both cases equation (51) can be solved by the following Riemann problem with a shift

$$\begin{aligned} -3\nu^2 + \xi^2 + 1 = 0, \qquad (52) \\ \lambda = -\bar{\mu}, \\ \lambda = \xi + i\nu,\ \mu = -\xi + i\nu \end{aligned}$$

Equation (52) defines a hyperbola with the branches belonging respectively to upper and lower half-planes (Figure 1). The shift is defined as change of sign of the real part of λ. Let us introduce

$$\rho_{\pm}(\xi) = \Delta\psi\ |_{\pm},$$

jumps of the function $\psi(\lambda)$ across upper and lower branches of the hyperbola. The function ψ can be represented in a form

$$\psi = 1 + \frac{1}{2\pi \mathrm{i}} \int_{-\infty}^{\infty} \frac{\rho_+(\xi')}{(\lambda - \lambda_+(\xi'))} \frac{d\lambda_+}{d\xi'} d\xi' + \frac{1}{2\pi i} \int_{-\infty}^{\infty} \frac{\rho_-(\xi')}{(\lambda - \lambda_-(\xi'))} \frac{d\lambda_-}{d\xi'} d\xi',$$

where

$$\lambda_\pm(\xi) = \xi \pm \mathrm{i}\sqrt{\frac{1+\xi^2}{3}}.$$

Riemann problem with a shift (52) is equivalent to the system of two integral equations (25)

$$\rho_+(\xi) = \Big(1 + \frac{1}{2\pi \mathrm{i}} v.p. \int_{-\infty}^{\infty} \frac{\rho_+(\xi')}{(\lambda_+(-\xi) - \lambda_+(\xi'))} \frac{d\lambda_+}{d\xi'} d\xi' + \frac{1}{2\pi \mathrm{i}} \int_{-\infty}^{\infty} \frac{\rho_-(\xi')}{(\lambda_+(-\xi) - \lambda_-(\xi'))} \frac{d\lambda_-}{d\xi'} d\xi' \Big) R^+(\xi) e^{\frac{4\mathrm{i}}{\sqrt{3}\alpha}\xi\sqrt{1+\xi^2}y + 2\mathrm{i}\xi x},$$

$$\rho_-(\xi) = \Big(1 + \frac{1}{2\pi \mathrm{i}} v.p. \int_{-\infty}^{\infty} \frac{\rho_-(\xi')}{(\lambda_-(-\xi) - \lambda_-(\xi'))} \frac{d\lambda_-}{d\xi'} d\xi' + \frac{1}{2\pi \mathrm{i}} \int_{-\infty}^{\infty} \frac{\rho_+(\xi')}{(\lambda_-(-\xi) - \lambda_+(\xi'))} \frac{d\lambda_+}{d\xi'} d\xi \Big) R^-(\xi) e^{\frac{-4\mathrm{i}}{\sqrt{3}\alpha}\xi\sqrt{1+\xi^2}y - 2\mathrm{i}\xi x}.$$

Solution of Boussinesq equation is given by the formula

$$u = -\frac{\partial}{\partial x} \frac{1}{2\pi} \int_{-\infty}^{\infty} \left(\rho_+(\xi) \frac{d\lambda_+}{d\xi} + \rho_-(\xi) \frac{d\lambda_-}{d\xi} \right) d\xi.$$

'Minus' Boussinesq equation.

This equation,

$$\frac{3}{4}\alpha^2 v_{yy} + v_{xx} + \frac{1}{4} v_{xxxx} + (\frac{3}{2} v^2)_{xx} = 0,$$

arises after putting $\beta = -1$. The reduced $\bar{\partial}$ problem for this equation is described by the conditions

$$\lambda^2 + \lambda\mu + \mu^2 = 1 \tag{53}$$

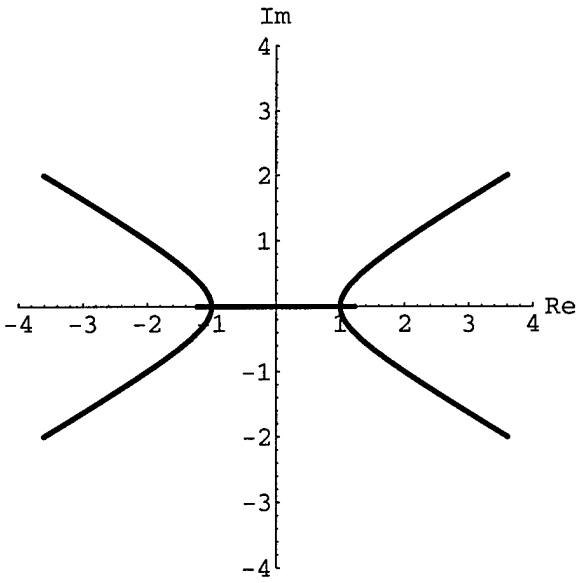

Figure 2: Localization of continuous spectrum for 'minus' Boussinesq equation

(time independence) and

$$\mathrm{Im}(\lambda - \mu) = 0 \tag{54}$$

(decreasing in x-direction). There are two possibilities to satisfy these conditions.

1. λ and μ are real ($\lambda^2 < \frac{4}{3}, \mu^2 < \frac{4}{3}$) and

$$\mu = -\frac{1}{2}\lambda \pm \sqrt{1 - \frac{3}{4}\lambda^2}. \tag{55}$$

We have a Riemann problem on the cut $-\sqrt{\frac{4}{3}} < \mathrm{Re}\lambda < \sqrt{\frac{4}{3}}$ with the twofold shift (55).

2. λ and μ are complex, $\lambda = \nu + \mathrm{i}\xi$, $\mu = -\nu + \mathrm{i}\xi$, $\xi, \nu \in \mathbf{R}$,

$$\nu^2 - 3\xi^2 = 1 \tag{56}$$

Both λ and μ belong to the hyperbola (see Figure 2). The shift as for 'plus' Boussinesq equation is reflection with respect to imaginary axis.

Let us parameterize the curves, on which the solution ψ of Riemann problem with a shift has a discontinuity, in the following way

$$\gamma_+ = \lambda_+(\xi) = \mathrm{i}\xi + \sqrt{1+3\xi^2},\ -\infty < \xi < \infty$$
$$\gamma_- = \lambda_-(\xi) = \mathrm{i}\xi - \sqrt{1+3\xi^2},\ -\infty < \xi < \infty$$
$$\gamma_0 = \lambda_0(\xi) = \xi,\ \xi^2 < \frac{4}{3}$$

and introduce the jumps $\rho_+(\xi)$, $\rho_-(\xi)$, $\rho_0(\xi)$ of the function ψ across the curves. Then the function ψ can be represented in a form

$$\psi = 1 + \frac{1}{2\pi\mathrm{i}}\int_{-\infty}^{\infty}\frac{\rho_+(\xi')}{(\lambda-\lambda_+(\xi'))}\frac{d\lambda_+}{d\xi'}d\xi'$$
$$+\frac{1}{2\pi i}\int_{-\infty}^{\infty}\frac{\rho_-(\xi')}{(\lambda-\lambda_-(\xi'))}\frac{d\lambda_-}{d\xi'}d\xi' + \frac{1}{2\pi i}\int_{-\sqrt{\frac{4}{3}}}^{\sqrt{\frac{4}{3}}}\frac{\rho_0(\xi')}{(\lambda-\xi')}d\xi'.$$

Riemann problem in this case is equivalent to the system of three integral equations

$$\rho_0(\xi) = 1$$
$$+\left(\frac{1}{2\pi\mathrm{i}}\int_{-\infty}^{\infty}\frac{\rho_+(\xi')}{(\mu_+(\xi)-\lambda_+(\xi'))}\frac{d\lambda_+}{d\xi'}d\xi' + \frac{1}{2\pi\mathrm{i}}\int_{-\infty}^{\infty}\frac{\rho_-(\xi')}{(\mu_+(\xi)-\lambda_-(\xi'))}\frac{d\lambda_-}{d\xi'}d\xi'\right.$$
$$\left.+\frac{1}{2\pi\mathrm{i}}\int_{-\sqrt{\frac{4}{3}}}^{\sqrt{\frac{4}{3}}}\frac{\rho_0(\xi')}{(\mu_+(\xi)-\xi')}d\xi'\right)R_0^+(\xi)e^{\mathrm{i}(\frac{1}{2}\xi-\sqrt{1-\frac{3}{4}\xi^2})x+\frac{1}{\alpha}(\frac{3}{2}\xi^2-\xi\sqrt{1-\frac{3}{4}\xi^2}-1)y}$$
$$+\left(\frac{1}{2\pi\mathrm{i}}\int_{-\infty}^{\infty}\frac{\rho_+(\xi')}{(\mu_-(\xi)-\lambda_+(\xi'))}\frac{d\lambda_+}{d\xi'}d\xi' + \frac{1}{2\pi\mathrm{i}}\int_{-\infty}^{\infty}\frac{\rho_-(\xi')}{(\mu_-(\xi)-\lambda_-(\xi'))}\frac{d\lambda_-}{d\xi'}d\xi'\right.$$
$$\left.+\frac{1}{2\pi\mathrm{i}}\int_{-\sqrt{\frac{4}{3}}}^{\sqrt{\frac{4}{3}}}\frac{\rho_0(\xi')}{(\mu_-(\xi)-\xi')}d\xi'\right)R_0^-(\xi)e^{\mathrm{i}(\frac{1}{2}\xi+\sqrt{1-\frac{3}{4}\xi^2})x+\frac{1}{\alpha}(\frac{3}{2}\xi^2+\xi\sqrt{1-\frac{3}{4}\xi^2}-1)y)},$$

where

$$\mu_\pm = \frac{1}{2}\xi \pm \sqrt{1-\frac{3}{4}\xi^2},$$

$$\rho_+(\xi) = 1$$
$$+\left(\frac{1}{2\pi\mathrm{i}}\int_{-\infty}^{\infty}\frac{\rho_+(\xi')}{(\lambda_-(\xi)-\lambda_+(\xi'))}\frac{d\lambda_+}{d\xi'}d\xi' + \frac{1}{2\pi\mathrm{i}}\int_{-\infty}^{\infty}\frac{\rho_-(\xi')}{(\lambda_-(\xi)-\lambda_-(\xi'))}\frac{d\lambda_-}{d\xi'}d\xi'\right.$$
$$\left.+\frac{1}{2\pi\mathrm{i}}\int_{-\sqrt{\frac{4}{3}}}^{\sqrt{\frac{4}{3}}}\frac{\rho_0(\xi')}{(\lambda_-(\xi)-\xi')}d\xi'\right)R^+(\xi)e^{2\mathrm{i}\sqrt{1-3\xi^2}x+\frac{4\mathrm{i}}{\alpha}\xi\sqrt{1-3\xi^2}y},$$

$$\rho_-(\xi) = 1$$
$$+\left(\frac{1}{2\pi \mathrm{i}}\int_{-\infty}^{\infty}\frac{\rho_+(\xi')}{(\lambda_+(\xi)-\lambda_+(\xi'))}\frac{d\lambda_+}{d\xi'}d\xi' + \frac{1}{2\pi \mathrm{i}}\int_{-\infty}^{\infty}\frac{\rho_-(\xi')}{(\lambda_+(\xi)-\lambda_-(\xi'))}\frac{d\lambda_+}{d\xi'}d\xi'\right.$$
$$\left.+\frac{1}{2\pi \mathrm{i}}\int_{-\sqrt{\frac{4}{3}}}^{\sqrt{\frac{4}{3}}}\frac{\rho_0(\xi')}{(\lambda_+(\xi)-\xi')}d\xi'\right)R^-(\xi)e^{-2\mathrm{i}\sqrt{1-3\xi^2}x-\frac{4\mathrm{i}}{\alpha}\xi\sqrt{1-3\xi^2}y}.$$

Solution of Boussinesq equation is given by the formula

$$u = -\frac{\partial}{\partial x}\frac{1}{2\pi}\left[\int_{-\infty}^{\infty}\left(\rho_+(\xi)\frac{d\lambda_+}{d\xi}+\rho_-(\xi)\frac{d\lambda_-}{d\xi}\right)d\xi + \int_{-\sqrt{\frac{4}{3}}}^{\sqrt{\frac{4}{3}}}\rho_0(\xi)\frac{d\lambda_0}{d\xi}d\xi.\right]$$

In this case the spectral data R_γ split into two parts; short-wave part of continuous spectrum is localized on the hyperbola (56), and long-wave part of the spectrum on the segment of real axis (in fact on the covering of this segment); see Figure 2. For $\alpha = 1$ hyperbola corresponds to the stable part of spectrum (exponent (10) for y is imaginary) and segment to the unstable part (exponent is real), for $\alpha = \mathrm{i}$ the situation is reversed, i.e., long-wave instability takes place for $\alpha = 1$, and short-wave instability for $\alpha = \mathrm{i}$.

4.2 Soliton solutions

Behaviour of solitons in the case of Boussinesq equation is very unusual for integrable system. We will treat mostly the case of 'plus' Boussinesq equation with $\alpha^2 = 1$. This equation has a stable 'wave sector' (i.e. in the linear limit it is a wave equation), and it may be considered as integrable nonlinear generalization of the wave equation. There are two soliton sectors for this equation: 'usual' solitons, running with the velocity limited from above, and soliton configurations, forming a singularity in a finite time. The latter may be considered as bounded states of several singular solitons.

But even 'usual' solitons demonstrate quite extraordinary behaviour in this case. They are unstable with respect to small perturbations and may decay into two solitons or two singular solitons (that means a formation of singularity).

This phenomenon was discovered by Orlov [2] several years ago, but it is not well known even in the soliton community, so we would like to investigate it here in detail in the framework of our general approach.

To study soliton solutions of the Bousinesq equation, we start from the general determinant formula (31). For KP equation in the moving frame (42) from this formula we get (see analogous expression for the KP in [11])

$$v = \frac{\partial^2}{\partial x^2} \log \det(A), \tag{57}$$
$$A_{ij} = \delta_{ij} - \frac{R_i}{\mu_i - \lambda_j},$$

where

$$R_k = -\mathrm{i}c_k \exp(i(\mu_k - \lambda_k)(x - \frac{i}{\alpha}(\mu_k + \lambda_k)y)).$$

We will use equivalent form of this formula

$$v = \frac{\partial^2}{\partial x^2} \log \det(\tilde{A}), \tag{58}$$
$$\tilde{A}_{ij} = \frac{1}{-\mathrm{i}c_i} \exp(\Phi_i)\delta_{ij} + \frac{1}{\lambda_i - \mu_j}, \tag{59}$$

where

$$\Phi_k = \mathrm{i}(\lambda_k - \mu_k)(x - \mathrm{i}(\mu_k + \lambda_k)y).$$

To get solutions for the Boussinesq equation (44), the pairs (λ_k, μ_k) should satisfy the condition of dimensional reduction (45)

$$\lambda^2 + \lambda\mu + \mu^2 + 1 = 0.$$

and $\lambda_k \neq \mu_j$. The reduction (49) is to be taken into account.

We should also put some restrictions to get from the formula (57) solutions having no singularities at least for some values of y (y is dynamical variable, 'time', in our treatment). The prescription we will use is to put the condition

$$\mathrm{Re}(\lambda_i - \mu_i) = 0. \tag{60}$$

Then the exponents containing x are real, and at $y = 0$ we can provide the absence of singularities by the choice of coefficients. This condition together with the condition (45) define a curve to which the points λ_i, μ_i should belong. This curve is identical to the curve we studied in the case of 'minus' Boussinesq equation with the interchanged real and imaginary axes (see Figure 3). So we have the curve consisting of two parts: the segment of the imaginary

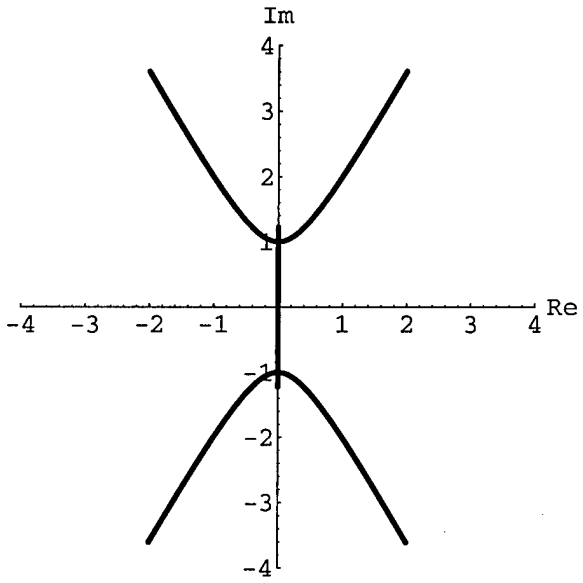

Figure 3: Localization of discrete spectrum for 'plus' Boussinesq equation

axis and hyperbola. Let us consider the simplest solutions corresponding to these parts.

First, in complete analogy with the formulae (55), (56), we introduce parameterization of the pairs of points λ_k, μ_k in the following way: for the segment of imaginary axis

$$\lambda = -\mathrm{i}\xi, \quad \mu = -\mathrm{i}\eta, \quad \eta = -\frac{1}{2}(\xi \pm \sqrt{4 - 3\xi^2}), \tag{61}$$

for pairs belonging to hyperbola $\lambda = \xi - \mathrm{i}\nu$, $\mu = \xi + \mathrm{i}\nu$, $\xi, \nu \in \mathbf{R}$,

$$\nu^2 - 3\xi^2 = 1. \tag{62}$$

Let us start with solutions corresponding to the points on the hyperbola. We should take two pairs of points on the hyperbola

$$\begin{aligned} &\lambda_1 = \xi - \mathrm{i}\sqrt{1 + 3\xi^2}, \quad \mu_1 = \xi + \mathrm{i}\sqrt{1 + 3\xi^2}, \\ &\lambda_2 = -\bar{\lambda}_1 = -\xi - \mathrm{i}\sqrt{1 + 3\xi^2}, \quad \mu_2 = -\bar{\mu}_1 = -\xi + \mathrm{i}\sqrt{1 + 3\xi^2}. \end{aligned} \tag{63}$$

to satisfy reduction condition (49)

$$R(\lambda, \mu) = \bar{R}(-\bar{\lambda}, -\bar{\mu}).$$

General formula for determinant solution (59) corresponding to two pairs of points (λ_1, μ_1), (λ_2, μ_2) is

$$\det(\tilde{A}) = \frac{(\lambda_1 - \lambda_2)(\mu_1 - \mu_2)}{(\lambda_1 - \mu_2)(\mu_1 - \lambda_2)} + \frac{\lambda_1 - \mu_1}{-ic_1}\exp(\Phi_1) + \frac{\lambda_2 - \mu_2}{-ic_2}\exp(\Phi_2)$$
$$+\frac{\lambda_1 - \mu_1}{ic_1}\exp(\Phi_1) \times \frac{\lambda_2 - \mu_2}{-ic_2}\exp(\Phi_2). \tag{64}$$

Let us take two pairs of point on the hyperbola parameterized by formulae (63) and $c_1, c_2 = c \in \mathbf{R}$. Then determinant (64) is real, and it is given by the expression

$$\det(\tilde{A}) = \frac{\xi^2}{1+4\xi^2} + \frac{2\sqrt{1+3\xi^2}}{c}\left(e^{2\sqrt{1+3\xi^2}(x-2i\xi y)} + e^{2\sqrt{1+3\xi^2}(x+2i\xi y)}\right)$$
$$+\frac{4(1+3\xi^2)}{c^2}e^{4\sqrt{1+3\xi^2}x}. \tag{65}$$

For positive c this expression has no zeroes at initial moment, so the solution is nonsingular and decreasing. But then at some moment zeroes appear in this expression, so the singularities are formed. Let us illustrate this process by several figures corresponding to some special choice of parameters $(c = -20, \quad \xi = 1)$. Figure 4 shows the lines on the plane x, y, where the determinant is equal to zero. General form of the solution is given by Figure 5. Figure 6 illustrates development of singularity for the solution (dynamics is considered with respect to y variable). Figure 7 shows the solution after creation of singularity. Then the solution behaves like two singular solitons (see Figure 8), first they go away from each other to some maximal distance, then they come close and singularity disappears (see Figure 9). The process is periodic with respect to y. Qualitatively this picture keeps for the arbitrary value of parameters. The change of c just shifts the picture. Parameter ξ defines the period of the process and the characteristic length. Maximal distance between the singularities is

$$l_{\max} = \frac{1}{\sqrt{1+3\xi^2}}\operatorname{arccosh}\left(\frac{1}{F(\xi)}\right), \tag{66}$$

time between creation and disappearance of singularities is

$$t = \frac{1}{2\xi}\arccos(F(\xi)), \tag{67}$$

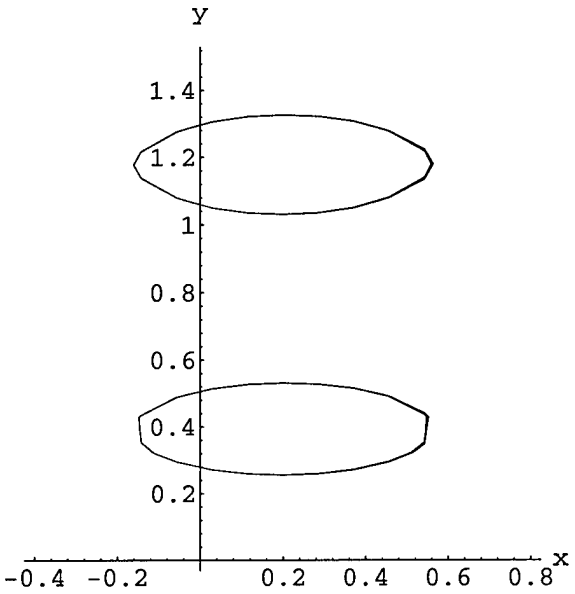

Figure 4: The curve in x, y plane where solution has a singularity

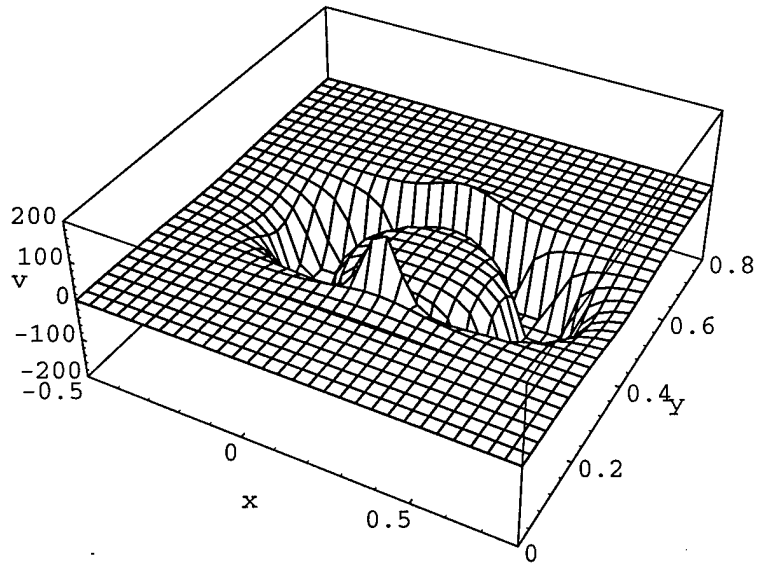

Figure 5: General form of solution in x, y plane

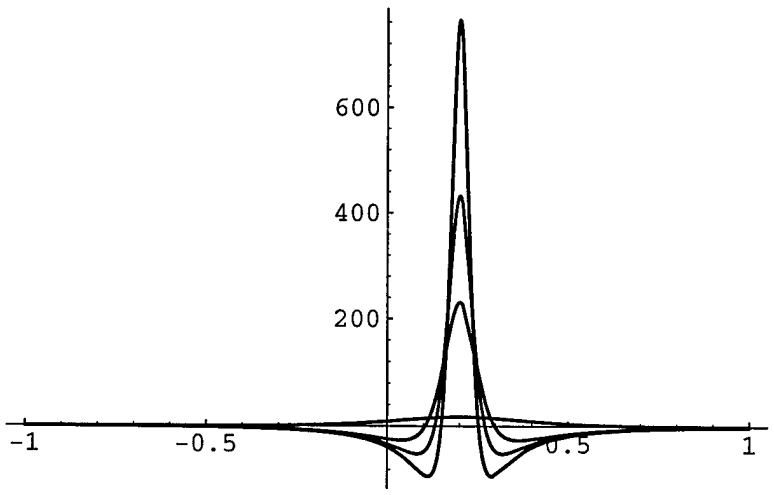

Figure 6: Development of singularity

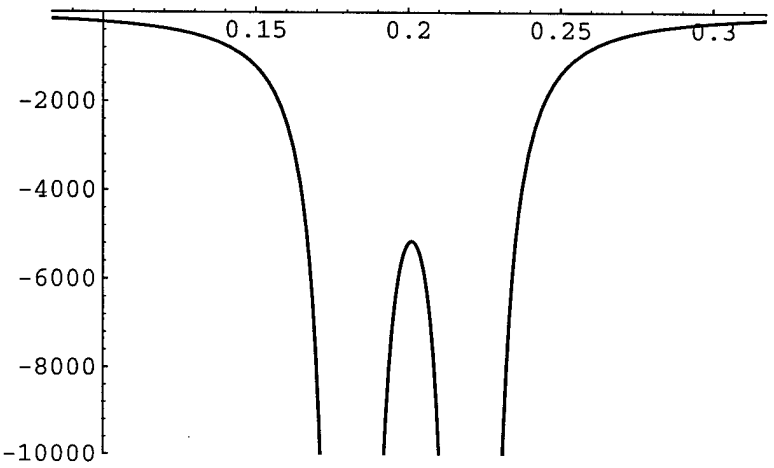

Figure 7: Singularity formed

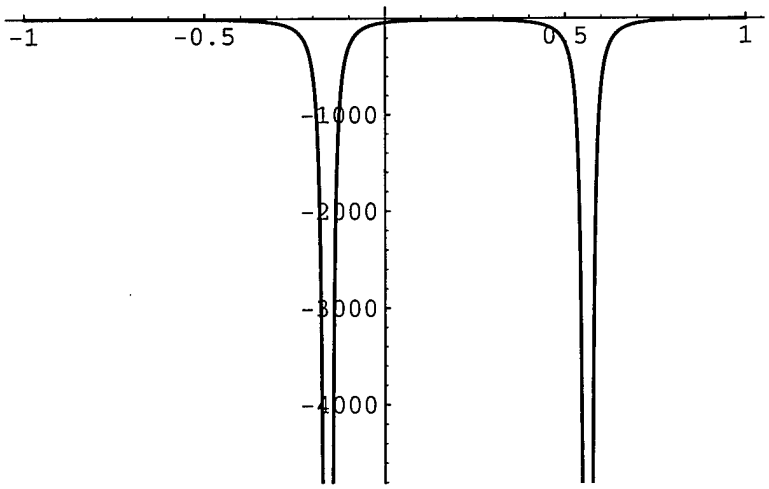

Figure 8: Two singular solitons stage of development of singularity

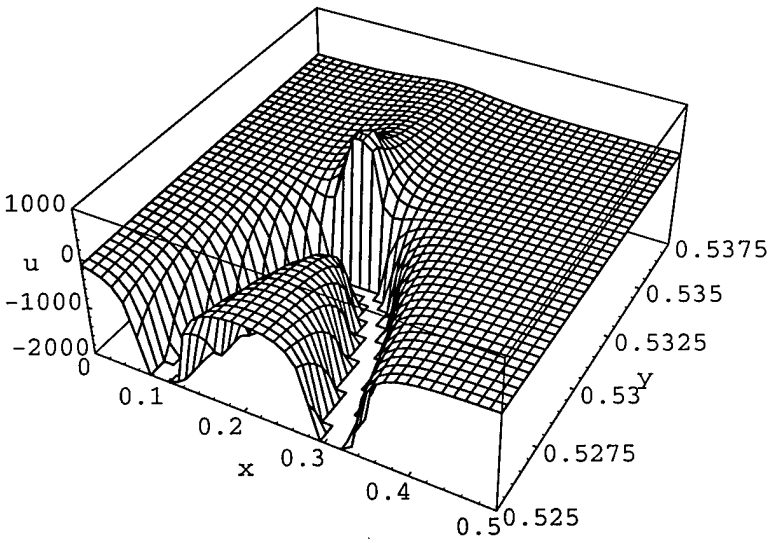

Figure 9: Disappearance of singularity

where

$$F(\xi) = 2\xi\sqrt{\frac{1}{1+4\xi^2}}. \tag{68}$$

The function $F(\xi)$ is monotone increasing function equal to zero at $\xi = 0$ with the limit 1 at infinity and -1 at minus infinity.

Dynamics of singularities becomes more complicated when we take solution corresponding to a set of several points λ_i, μ_i. The case of four pairs of points is illustrated by the Figure 10

Decay of solitons

A pair of points belonging to the segment of imaginary axis gives us a soliton solution

$$\det \tilde{A} = 1 + \frac{\lambda - \mu}{-\mathrm{i}c} \exp(\mathrm{i}(\lambda - \mu)(x - \mathrm{i}(\mu + \lambda)y)).$$

Using parameterization (63), we get the formula

$$\begin{aligned} \det \tilde{A} &= 1 + \frac{\xi - \eta}{c} \exp((\xi - \eta)(x - (\xi + \eta)y)) \\ &= 1 + \frac{3\xi \pm \sqrt{4 - 3\xi^2}}{2c} e^{\frac{1}{4}\left(3\xi \pm \sqrt{4-3\xi^2}\right)\left(2x - (\xi \mp \sqrt{4-3\xi^2})y\right)}, \end{aligned} \tag{69}$$

$$v = \frac{\partial^2}{\partial x^2} \log \cosh \frac{3\xi \pm \sqrt{4-3\xi^2}}{8}\left(2(x - x_0) - (\xi \mp \sqrt{4-3\xi^2})\, y\right). \tag{70}$$

To understand dependence of soliton on parameters ξ, η, it is useful to recall that these parameters belong to the ellipse

$$\xi^2 + \xi\eta + \eta^2 = 1. \tag{71}$$

Introducing velocity of soliton

$$v = \xi + \eta$$

and parameter defining amplitude of soliton

$$A = \xi - \eta,$$

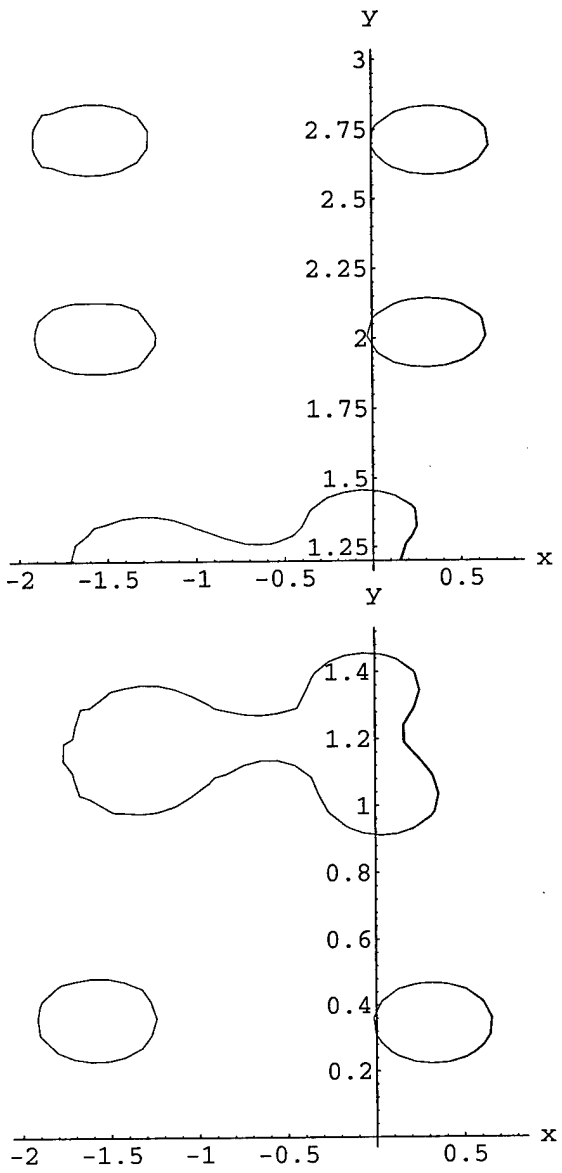

Figure 10: The curve in x, y plane where solution has a singularity, the case of four pairs of points λ_i, μ_i on the hyperbola

we rewrite the equation of this ellipse in the form

$$3v^2 + A^2 = 4.$$

Then it is easy to see that the absolute value of velocity of soliton $v = \xi + \eta$ is limited by $\sqrt{4/3}$. For $\frac{\xi-\eta}{c} > 0$ soliton is nonsingular. As $\xi - \eta \to 0$, the amplitude of soliton goes to zero, and velocity reaches its maximum $|v| \to \sqrt{4/3}$. Two points with $\xi = \eta$ belonging to the ellipse are the points of the change of sign, where (for fixed c) nonsingular soliton becomes singular and vice versa.

There are some unusual features concerning behaviour of soliton under small perturbations, which come to light when we study two-soliton solutions. General formula of two-soliton interaction (64) rewritten for the segment of imaginary axis in terms of parameters ξ, η looks like

$$\det(\tilde{A}) = \frac{(\xi_1 - \xi_2)(\eta_1 - \eta_2)}{(\xi_1 - \eta_2)(\eta_1 - \xi_2)} + \frac{\xi_1 - \eta_1}{c_1}\exp(\Phi_1) + \frac{\xi_2 - \eta_2}{c_2}\exp(\Phi_2)$$
$$+\frac{\xi_1 - \eta_1}{c_1}\exp(\Phi_1) \times \frac{\xi_2 - \eta_2}{c_2}\exp(\Phi_2), \tag{72}$$

where

$$\Phi_i = (\xi_i - \eta_i)(x - (\xi_i + \eta_i)y) = A_i(x - v_i y).$$

Considering formula (63) defining η_k through ξ_k, one remarks that there are two possible choices of η corresponding to the same ξ (and also two possible ξ corresponding to the same η). It is natural to ask a question what kind of solution we get if we consider two pairs of point with the same ξ (or the same η). The formula (72) in this case degenerates, the first term in it is equal to zero. Naively, we expect this solution to be two-soliton solution. But further study shows that this solution possesses rather unusual properties. It describes process of decay of soliton (70) (or fusion of two solitons).

Considering formula (72) with $\xi_1 = \xi_2 = \xi$, we get

$$\det(\tilde{A}) = +\frac{\xi - \eta_1}{c_1}\exp(\Phi_1) + \frac{\xi - \eta_2}{c_2}\exp(\Phi_2)$$
$$+\frac{\xi - \eta_1}{c_1}\exp(\Phi_1) \times \frac{\xi - \eta_2}{c_2}\exp(\Phi_2), \tag{73}$$

or, using explicit parameterization (63) of η_1, η_2 through ξ,

$$\det(\tilde{A}) \sim 1 + \frac{2\,c_2\,e^{1/4\left(3\xi-\sqrt{4-3\xi^2}\right)\left(-2x+\xi y+\sqrt{4-3\xi^2}y\right)}}{3\xi-\sqrt{4-3\xi^2}} + \frac{2\,c_1\,e^{1/4\left(3\xi+\sqrt{4-3\xi^2}\right)\left(-2x+\xi y-\sqrt{4-3\xi^2}y\right)}}{3\xi+\sqrt{4-3\xi^2}}, \tag{74}$$

here $c_1, c_2 \in \mathbf{R}$, and determinant is written up to exponential factor that doesn't change the solution. Experimenting with the plots drawn by Mathematica from this formula for some choice of parameters, one discovers two solitons for some (big positive) values of y, and one soliton for other (big negative) values. Analytic study of formula (74) confirms this impression.

Let us consider the simplest case of the staying soliton (soliton with velocity zero). In this case the value of parameter ξ is equal to 1, and formula (69) (with the sign +) takes the form

$$\det \tilde{A} \sim 1 + \frac{c}{2}\exp(-2x), \tag{75}$$

that corresponds to standard soliton solution with zero velocity

$$v = \cosh^{-2}(x - x_0).$$

Substituting $\xi = 1$ to the 'two-soliton' formula (74), we get

$$\det(\tilde{A}) \sim 1 + c_2\exp(y - x) + \frac{1}{2}c_1\exp(-2x). \tag{76}$$

To study asymptotic behaviour of solution corresponding to this determinant, we should take into account that solution is given by the second derivative of the logarithm of determinant (formula (57)). At $y = -\infty$ we discover only a staying soliton of the form (75)

$$v \approx \frac{\partial^2}{\partial x^2}\log(1 + \frac{1}{2}c_1\exp(-2x)),$$

which is nonsingular if c_1 is positive. Multiplying the determinant (76) by $\exp(x-y)$ (that does not change the solution), we get another representation of 'two-soliton' solution

$$v = \frac{\partial^2}{\partial x^2}\log\left(\exp(x - y) + c_2 + \frac{1}{2}c_1\exp(-x - y)\right)$$

Using this representation to study asymptotic behaviour of solution at $y = \infty$ in the arbitrary moving frame $x = \tilde{x} + vy$, we discover that for $v = \pm 1$ asymptotics is nontrivial, corresponding to two solitons moving with velocities $v = \pm 1$,

$$v \approx \frac{\partial^2}{\partial x^2} \log\left(\exp(x-y) + c_2\right) + \frac{\partial^2}{\partial x^2} \log\left(\frac{1}{2} c_1 \exp(-x-y) + c_2\right). \qquad (77)$$

As we have mentioned before, for nonsingular staying soliton c_1 is positive. If c_2 is also positive, formula (77) gives two nonsingular solitons, and negative c_2 corresponds to two singular solitons.

The initial data for the solution v corresponding to the determinant (76) may be made infinitely close to one-soliton solution by the choice of constants. In fact at $y = -\infty$ this is exactly a soliton. But then this slightly disturbed soliton solution decays! It may decay into two solitons or into two singular solitons, depending on the initial perturbation (see Figure 11,12). So staying soliton solution for the Boussinesq equation is unstable with respect to small perturbations, it may develop singularity or decay into two solitons.

A natural question to ask next is whether arbitrary soliton may decay. To answer it, we start from some general remarks concerning the decay formula (73)

$$\det(\tilde{A}) \sim 1 + \frac{c_1}{\xi - \eta_1} \exp(-\Phi_1) + \frac{c_2}{\xi - \eta_2} \exp(-\Phi_2). \qquad (78)$$

Using simple example of staying soliton, we have shown that three different solitons enter this formula. Soliton is defined by a pair of real parameters ξ, η satisfying equation (71), or, in other words, by the point of ellipse (71). The point η, ξ defines the same soliton (up to a change of constant c). Deriving formula (78), we start from two solitons having the same ξ. To understand the reason of appearance of third soliton, it is easy to show that if $\eta = \eta_1$, $\rho = \eta_2$ satisfy equation (71) with the same ξ, then the point (η, ρ) also belongs to the ellipse (71). So the formula (78)

$$\det(\tilde{A}) \sim 1 + \frac{c_1}{\xi - \eta} e^{-(\xi-\eta)(x-(\xi+\eta)y)} + \frac{c_2}{\xi - \rho} e^{-(\xi-\rho)(x-(\xi+\rho)y)} \qquad (79)$$

contains *three* solitons with the parameters (ξ, η), (ξ, ρ), (η, ρ). Thus the decay process is characterized by three real parameters ξ, η, ρ, possessing

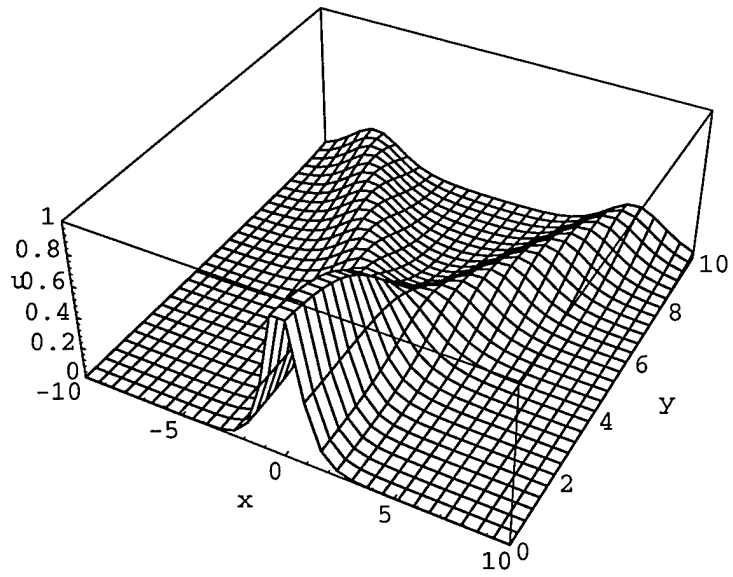

Figure 11: Decay of soliton into two solitons

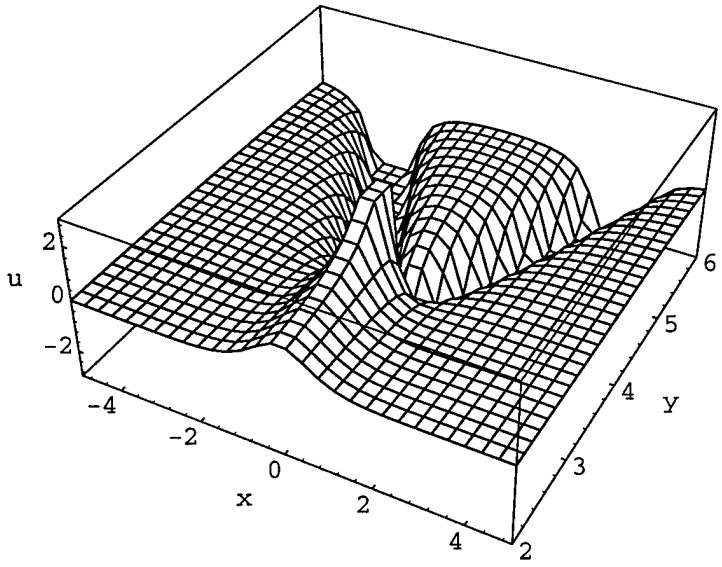

Figure 12: Decay of soliton into two singular solitons

the property that each pair of parameters defines the point of the ellipse (71). Depending on ξ (which defines η and ρ through the formula (63)), each soliton is present only at $y = \infty$ or at $y = -\infty$.

Considering formula (79) in the moving frame

$$x = \tilde{x} + (\xi + \eta)y,$$

we discover that soliton with the parameters (ξ, η) is present at

$$y = \text{sign}((\xi - \rho)(\eta - \rho))\infty.$$

Similarly, we come to the conclusion that soliton with the parameters (ξ, ρ) is present at

$$y = \text{sign}((\xi - \eta)(\rho - \eta))\infty.$$

Rewriting expression (79) in equivalent form

$$\det(\tilde{A}) \sim e^{-(\eta-\xi)(x-(\xi+\eta)y)} + \frac{c_1}{\xi - \eta} + \frac{c_2}{\xi - \rho} e^{-(\eta-\rho)(x-(\eta+\rho)y)} \qquad (80)$$

and considering the moving frame

$$x = \tilde{x} + (\eta + \rho)y,$$

we show that soliton with the parameters (η, ρ) is present at

$$y = \text{sign}((\eta - \xi)(\rho - \xi))\infty.$$

Choosing to be definite $\xi > \rho > \eta$, we discover that formula (79) describes decay of soliton with the parameters (ξ, η), i.e., the smallest and the largest of parameters ξ, ρ, η. Let us use explicit parameterization (63)

$$\eta = -\frac{1}{2}(\xi + \sqrt{4 - 3\xi^2}),$$
$$\rho = -\frac{1}{2}(\xi - \sqrt{4 - 3\xi^2}).$$

If we start from the maximal value of $\xi = \sqrt{\frac{4}{3}}$, formula (79) describes decay of soliton with the parameters (ξ, η); velocity of this soliton is

$$v = \frac{1}{2}(\xi - \sqrt{4 - 3\xi^2}).$$

As ρ comes close to ξ (at $\xi = \sqrt{\frac{1}{3}}$), velocity of the soliton (ξ, ρ) reaches maximal velocity $v = \sqrt{\frac{4}{3}}$, and velocity of decaying soliton (ξ, η) reaches the value $v = -\sqrt{\frac{1}{3}}$. At $\rho = \xi$ formula (79) degenerates, it describes one soliton with velocity $v = -\sqrt{\frac{1}{3}}$. As ξ becomes smaller then $\sqrt{\frac{1}{3}}$, ρ becomes larger then ξ, and formula (79) describes decay of soliton (ρ, η) with the velocity

$$v \doteq -\xi.$$

At $\xi = -\sqrt{\frac{1}{3}}$ ξ becomes equal to η, formula (79) degenerates once again, the velocity of decaying soliton reaches the value $\sqrt{\frac{1}{3}}$, and for $-\sqrt{\frac{1}{3}} > \xi \geq -\sqrt{\frac{4}{3}}$ it describes decay of soliton ξ, ρ with the velocity

$$v = \frac{1}{2}(\xi + \sqrt{4 - 3\xi^2}).$$

Thus the velocity of decaying soliton changes in the range

$$-\sqrt{\tfrac{1}{3}} < v_{\text{dec}} < \sqrt{\tfrac{1}{3}}.$$

There are decay processes into two solitons or two singular solitons, depending on the choice of constants c_1, c_2 in the formula (79).

There are no decay processes for the solitons with $|v| > \sqrt{\frac{1}{3}}$, so these solitons are stable. Thus we have answered our first questions, and the answer is negative, not all solitons may decay.

Interaction of solitons

Next question is about soliton systems and interaction of two solitons. It is whether singularities may appear as a result of interaction, and are there any stable soliton systems (not forming singularities as a result of interaction). First we would like to formulate two results concerning these questions.

Statement 1. Solitons moving in one direction with velocities $|v| > \sqrt{\frac{1}{3}}$ do not form singularities as a result of two-soliton interaction.

Statement 2. Two-soliton interaction of solitons with velocities $|v| < \sqrt{\frac{1}{3}}$ *necessarily* leads to formation of singularity (i.e., the result of interaction of two solitons always is two singular solitons).

The proof of both statements is based on formula (72). Interaction of two solitons is much more standard in soliton theory than decay process, so we will not consider it in detail. Using moving reference frames and considering asymptotical behaviour of solution (72) at $y = \pm infty$, it is easy to show that the character of interaction process is defined by the sign of the first term in the formula (72)

$$c = \frac{(\xi_1 - \xi_2)(\eta_1 - \eta_2)}{(\xi_1 - \eta_2)(\eta_1 - \xi_2)}. \tag{81}$$

If $c > 0$, the result of interaction is a pair of solitons, and for $c < 0$ the result is a pair of singular solitons (that means that singularity is formed in the process of interaction). The points of change of sign $\xi_1 = \xi_2$, $\eta_1 = \eta_2$, $\xi_1 = \eta_2$, $\eta_1 = \xi_2$ correspond to degeneration of formula (72) into triple (decay or fusion) process and appearance of third soliton. The results of analysis of triple soliton diagram given before show that it always contains two solitons moving in the same direction; one with velocity $|v_1| < \sqrt{\frac{1}{3}}$ (the decaying soliton), and another with velocity $|v_2| > \sqrt{\frac{1}{3}}$. Third soliton moves in the opposite direction with the velocity $|v_3| > \sqrt{\frac{1}{3}}$.

Let us take two solitons moving in the same direction with velocities $|v| > \sqrt{\frac{1}{3}}$. There are no decay diagrams containing these solitons, and expression (81) doesn't change sign when we change parameters of solitons. It is easy to check that in this case the sign is positive, and the result of interaction of two solitons is two (nonsingular) solitons, that proves Statement 1. This statement can be easily generalized to the case of N-soliton interaction, and thus the system of solitons moving in the same direction with velocities $|v| > \sqrt{\frac{1}{3}}$ doesn't form singularities and is stable with respect to decay processes. In other words, this system demonstrates a 'standard' behaviour usually associated with a system of solitons.

Similarly, considering two solitons moving in the same direction with velocities $|v| < \sqrt{\frac{1}{3}}$, we come to the conclusion that the sign of expression (81) is negative. Interaction of two solitons in this case always results in two singular solitons, i.e., in the formation of singularity, that proves Statement 2. Thus the system of solitons moving in the same direction with velocities $|v| < \sqrt{\frac{1}{3}}$ demonstrates rather extraordinary behaviour. First, the solitons are unstable under perturbation and may decay into two solitons or two

singular solitons. And second, interaction of two solitons unavoidably leads to formation of singularity in a finite time.

Acknowledgments

The work of LB was supported in part by Russian Foundation for Basic research grants 01-01-00929-a and 00-15-96007 and by INTAS grant 99-1782.

References

[1] Boussinesq J 1872 *J. Math Pures Appl.* **7** 55

[2] Orlov A Yu (1983) *Collapse of solitons in integrable models* Preprint IAiE No 221 (Novosibirsk: IAiE)

[3] Falkovich G E Spector M D and Turitsyn S K (1983) Destruction of stationary solutions and collapse in the nonlinear string equation. *Phys. Lett. A* **99** (6-7) 271-274

[4] Bogdanov L V and Zakharov V E (1992) Decreasing solutions and dispersion laws in the (2+1)-dimensional dressing method. *St. Petersburg Math. J.* **3**(3) 533-540

[5] Bogdanov L V and Zakharov V E (1994) Integrable (1+1)-dimensional systems and the Riemann problem with a shift. *Inverse Problems* **10** 817-835

[6] Bogdanov L V and Zakharov V E (1995) On some developments of the dbar-dressing method. *St. Petersburg Math. J.* **6**(3) 475-493

[7] Zakharov V E and Manakov S V (1984) Multidimensional nonlinear integrable systems and methods for constructing their solutions. *Zap. Nauchn. Sem. LOMI* **133** 77-91

[8] Zakharov V E and Manakov S V (1985) Construction of multidimensional nonlinear integrable systems and their solutions. *Funk. Anal. Ego Prilozh.* **19**(2) 11-25

[9] Bogdanov L V and Manakov S V (1988) The nonlocal $\overline{\partial}$ problem and $(2+1)$-dimensional soliton equations. *J. Phys. A.:Math. Gen.* **21**(10) L537-L544

[10] Zakharov V E 1990 On the dressing method *Inverse Methods in Action* ed P C Sabatier (Berlin: Springer)

[11] Zakharov V E Manakov S V Novicov S P and Pitaevsky L P (1984) *Theory of Solitons: the Inverse Scattering Method* (New York: Plenum Publ. Corp)

[12] Caudrey P J (1982) The inverse problem for a general $n \times n$ spectral equation. *Physica* **6D**(1) 51-66

[13] Deift P, Tomei C and Trubowitz E (1982) Inverse scattering and the Boussinesq equation. *Commun. Pure Appl. Math.* **35**(5) 567-628

[14] Manakov S V (1981) The inverse scattering transform for the time-dependent Schrödinger equation and Kadomtsev-Petviashvili equation. *Physica* **3D** 420-427

[15] Ablowitz M J Bar Yaacov D and Fokas A S (1983) On the inverse scattering transform for the Kadomtsev-Petviashvili equation. *Stud. Appl. Math.* **69** 135-143

Freely decaying weak turbulence for sea surface gravity waves

M. Onorato, A. R. Osborne, M. Serio
Dip. di Fisica Generale, Università di Torino, Via Pietro Giuria 1, 10125 Torino, Italy

D. Resio
Coastal and Hydraulics Laboratory, U.S. Army Engineer Research and Development Center, Halls Ferry Road, Vicksburg, MS 39180, USA

A. Pushkarev
Waves and Solitons LLC, 918 W. Windsong Dr., Phoenix, AZ 85045, USA

V. Zakharov
Landau Institute for Theoretical Physics, Moscow, 117334, Russia and Department of Mathematics, University of Arizona, Tucson, AZ 85721, USA

C. Brandini
La.M.M.A., Regione Toscana, Via A. Einstein 35/b 50013 Campi Bisenzio - Firenze, Italy
(January 10, 2002)

We study numerically the generation of power laws in the framework of weak turbulence theory for surface gravity waves in deep water. Starting from a random wave field, we let the system evolve numerically according to the nonlinear Euler equations for gravity waves in infinitely deep water. In agreement with the theory of Zakharov and Filonenko, we find the formation of a power spectrum characterized by a power law of the form of $|\mathbf{k}|^{-2.5}$.

PACS numbers: 47.27.-i, 92.10.Hm, 47.35.+i, 03.40.Kf

After the pioneering work by Kolmogorov [1] on the equilibrium range in the spectrum of an homogeneous and isotropic turbulent flow, there have been a number of studies on cascade processes in many other fields of classical physics such as plasma physics, magnetohydrodynamics and ocean waves. For surface gravity waves the first seminal theoretical work was done by O.M. Phillips in 1958, [2]. Using dimensional arguments, he argued that the frequency spectrum in the inertial range was of the form $F(\omega) = \alpha g^2 \omega^{-5}$, where α was supposed to be an absolute constant and g is gravity. Even though in the introduction of Phillips' paper it was stated that "a necessary condition for the equilibrium range over a certain part of the spectrum is the appreciable non-linear interactions among these wave-numbers" (from [2]), his arguments were based on the geometrical features of the free surface elevation. One of his basic assumptions was that the only variable of interest was gravity, while the friction velocity, u_*, was not supposed to be involved in the spectral relation, limiting the possibility for a correct dimensional analysis.

Some years later Zakharov and Filonenko [3] established that in infinite water the direct cascade should produce a power spectrum of the surface elevation of the form $P(|\mathbf{k}|) \sim |\mathbf{k}|^{-2.5}$ that corresponds, using the linear dispersion relation in infinite depth, to an ω^{-4} frequency power spectrum: the result was found as an exact solution of the *kinetic wave equation* (see [4]). The theory developed is known as "weak" or "wave turbulence" and has many important applications in different fields of physics such as hydrodynamics, plasma physics, nonlinear optics, solid state physics, etc. see [5]. It is called weak turbulence because it deals with resonant interactions among small-amplitude waves. Thus, contrary to fully developped turbulence, it leads to explicit analytical solutions provided some assumptions are made. The first experimental support of the theory for surface gravity waves was made by Toba [6] who was completely unaware of the paper by Zakharov and Filonenko. He reformulated the Phillips' equilibrium range law in the following way: $F(\omega) = \beta g u_* \omega^{-4}$, where β should now be an universal dimensionless constant. After the work by Toba, successive experimental observation of the ω^{-4} law have been made by a number of authors, see for example [7–10].

Even though there is a consensus on this result, it must be stressed that so far the verification of the theory has never been established from first principles and moreover the mechanisms that lead to the power law ω^{-4} are not universally recognized: geometrical aspects related to wave breaking, without invoking the nonlinear wave-wave interaction mechanism, are still retained by many oceanographers as fundamental for generating an ω^{-4} power law. Confirmation of the Zakharov-Filonenko solution to the kinetic equation has being given through numerical simulations of the kinetic wave equation itself [11] [12], solving exactly the so called S_{nl} term. Nevertheless, it must be underlined that the kinetic equation is derived from the primitive equations of motion under a number of hypotheses (see for example [13]), therefore it cannot be concluded *a priori* that power law solutions of

the kinetic equation are also shared by the fully nonlinear wave equations.

One way to verify weak turbulence theory is to perform direct numerical simulations of the primitive equations of motion. The numerical confirmation of the theory for gravity waves propagating on a surface has not been an easy task (for capillary waves see [14], for one dimensional wave turbulence see [15,16]), basically because of the intrinsic difficulties of the computation of the boundary conditions. Different numerical approaches have been used for integrating the fully nonlinear surface gravity waves equations (see [17] for a review). The numerical methods based on volume formulations show very interesting results, in particular they are capable of modeling in a quite appropriate way wave breaking. Unfortunately they have the disadvantage that they require large computational resources, and therefore are not suitable for long time numerical simulations. For irrotational and inviscid flows boundary formulations are usually preferred: only the surface is discretized reducing the dimension of computation (from three to two). The Higher-Order Spectral Methods (HOS), indeed the method used in our numerical simulations, introduced independently by West et al. [18] and by Dommermuth et al. [19], belongs to this second approach (see also the recent work byTanaka [20]). Very recently three new methods have been proposed as very promising for simulating water waves [21–23]. Results using these new approaches on turbulent cascades are still to be completed.

In this Letter we establish numerically, using a HOS method, that nonlinear interactions are sufficients for generating power laws in wave spectra; moreover we show that the Zakharov-Filonenko theory is completely consistent with the primitive equations of motion. We consider a system of random waves localized in wave number space and we show how nonlinearities "adjust" the spectrum in agreement with the Zakharov and Filonenko prediction. Numerical work in the case of a forced and dissipated system has been attempted by Willemsen [24] using what sometimes are called the "Krasitskii equations" (see also [13]). In order to avoid the effects of external forcing, we considered the case of a freely decaying wave field. If the simulations, as we will see, would show the formation of a power law, then it will have to be excluded the conjecture that this power law is caused by geometrical features related to forcing and wave breaking, since forcing is absent and wave breaking cannot be taken into account using the numerical method considered. From a physical point of view, the freely decaying case corresponds to the evolution of a swell wave field. A generic wave field is considered at time $t = 0$ and it is allowed to evolve in a natural way using a high order approximation of the Euler equations. Since numerical computation are limited by the dimension of the grid considered, an artificial dissipation is needed at high wave numbers in order to prevent accumulation of energy and a break down of the numerical code. The fluid is considered inviscid, irrotational and incompressible. Under these conditions the velocity potential $\phi(x, y, z, t)$ satisfy the Laplace's equation everywhere in the fluid. The boundary conditions are such that the vertical velocity at the bottom is zero and on the free surface the kinematic and dynamic boundary conditions are satisfied for the velocity potential $\psi(x, y, t) = \phi(x, y, \eta(x, y, t), t)$ (we assume that fluid is of infinite depth):

$$\psi_t + g\eta + \frac{1}{2}\left[\psi_x^2 + \psi_y^2 - (\phi_z|_\eta)^2(1 + \eta_x^2 + \eta_y^2)\right] = 0 \quad (1)$$

$$\eta_t + \psi_x\eta_x + \psi_y\eta_y - \phi_z|_\eta(1 + \eta_x^2 + \eta_y^2) = 0, \quad (2)$$

The major difficulty for numerical simulations of the system (1)-(2) consists in that we have to compute the derivatives of ϕ with respect to z on the surface η. This problem can be overcome if we express the velocity potential $\psi(x, y, t)$ as a Taylor expansion around $z = 0$. Inverting asymptotically the expansion one can express $\phi_z|_\eta$ as an expansion of derivatives of $\psi(x, y, t)$ that can then be computed using the Fast Fourier Transform, simplifying notably the computation. This is nothing other than a different way for formulating the HOS method. We underline that this is the same approach that has originally been used in [4] for deriving analytically the equation that is usually known as the "Zakharov equation". The order of the simulation can be decided *a priori* and depends on how many terms in the Taylor expansions are retained; in our numerical simulations we considered the expansion necessary to take into account four wave interactions so that we are consistent with the order of the "Zakharov equation".

A delicate point in our numerical simulations is related to the dissipation of energy at high wave numbers. We remark that this dissipation is completely artificial since we are dealing with a potential flow. Nevertheless we have considered the dissipation phenomenon of the wave field to be similar to the one that takes place in a turbulent flow, i.e. that is mathematically expressed by a Laplacian that operates on the velocity. As is usually done in direct numerical simulation of box turbulent flows, in order to increase the inertial range, we have used a higher order diffusive term. More explicitly on the right hand side of equation (1)-(2), we have added respectively two extra terms: $-\nu(-\nabla^2)^n\psi$ and $-\mu(-\nabla^2)^m\eta$, where ν and μ represent an artificial viscosity coefficient and ∇^2 is the horizontal Laplacian. If n and m are greater than 1 the viscosity is known as "hyperviscosity".

It has to be noted that, at first sight, one would use a very high power of the Laplacian in order to increase notably the inertial range, unfortunately very high values of m and n could bring about the "bottleneck effect" [26], i.e. an accumulation of energy at high wave numbers that could distort the power law expected [27]. In our

numerical simulations we used $\nu = \mu = 3 \times 10^4$ and $n = m = 8$. These values have been selected after some trials and errors during the development of the numerical code: because of our limitated number of grid points, smaller values of m and n, would obscure almost completely the inertial range. In our numerical simulations we did not impose any a dissipation at low wave numbers.

In order to prepare the initial wave field it is reasonable to consider a directional spectrum $S(|\mathbf{k}|, \theta) = P(|\mathbf{k}|)G(\theta)$. The directional spreading function $G(\theta)$ used here is a cosine-squared function in which only the first lobe (relative to the dominant wave direction) is considered:

$$G(\theta) = \begin{cases} \frac{1}{\sigma} cos^2\left(\frac{\pi}{2\sigma}\theta\right) & if -\sigma \leq \theta \leq \sigma \\ 0 & else \end{cases} \quad (3)$$

σ is a parameter that provides a measure of the directional spreading, i.e. as $\sigma \rightarrow 0$, the waves become increasingly unidirectional. In our numerical simulations we selected the value of $\sigma = \pi/2$. We tried to avoid the complete isotropic case in order to verify if the theory still holds for intermediate values of the spreading. At the same time the selection of a large value of σ was motivated by the fact that recently it has been found [28] that, for sufficiently narrow angle of spreading, the Benjamin-Feir instability can be responsible for the formation of freak waves. As a consequence the nonlinear energy transfer could be slightly altered and some corrections to the prediction could be necessary (this very interesting topic is now under investigation and results will be reported in a different paper). $P(|\mathbf{k}|)$ is chosen to be any localized spectrum. We have performed numerical simulations with a gaussian function or with a "chopped JONSWAP" spectrum (a JONSWAP spectrum with amplitudes equal to zero for frequencies greater than 1.5 times the peak frequency) with random phases. For the case of the gaussian function, wave numbers lower than a selected threshold have been set to zero in order to avoid extremely long large waves. The velocity potential is then computed from the initial wave field using the linear theory. Both gaussian and JONSWAP spectrum led to the same results in terms of the turbulent cascade.

Our computation is performed in dimensional units; we have selected the initial spectrum centered at 0.1 Hz, i.e. we are considering 10 seconds waves. The initial steepness computed as $\varepsilon = k_0 H_s/2$ was chosen to be around 0.15 (H_s was computed as 4 times the standard deviation of the wave field). The wave field was contained in a square grid (the resolution is 256×256) of length $L = 1417.6$ meters. The time step considered was 1/50 the dominant frequency, i.e. $\Delta t = 0.2$ seconds. We have performed our numerical simulations on a 400Mh PC. In Fig. 1 we show the evolution of the wave power spectrum for different time (t=0, 0.1, 0.5, 1 hours). We see that, as expected, the tail of the spectrum starts to grow. This process seems to be quite fast: as is shown in the figure after a few dominant wave periods some energy is already injected into high wave numbers. The process of adjusting the power law to the "correct" one becomes then very slow, especially for low wave number. This could be due to the frozen turbulent phenomenon [29], i.e. a condition in which the energy fluxes towards high wave numbers are reduced because of the discretness of the spectrum. Moreover decaying numerical simulations are very time consuming with respect forced simulations because, as time passes, energy is lost due to viscosity, thus reducing the significant wave height of the wave field and therefore the steepness. Even though it is not clear from the Log-Log representation in Fig. 1, there is a downshifting of the peak of the spectrum towards lower wave numbers; as a consequences the steepness subsequently decreases over time. The time scale of the nonlinear energy transfer becomes larger and larger. In Fig 2 we show the power spectrum of the surface elevation after 4 hours (the steepnes of the wave field is $\varepsilon \simeq 0.07$). In the same plot we show two power laws $\sim k^{-2.5}$ and $\sim k^{-3}$: the first one seems to better fit the data. In order to be completely sure that the numerical data are in agreement with the prediction of Zakharov and Filonenko, we show in Fig. 3 compensated spectra with different compensation powers: $z = 2.5$ seems to be the most plausible power law. Thus there seems to be ample evidence from our numerical simulations that the power law is in sufficiently good agreement with the value predicted that there is no need for corrections due, for example, to small scale intermittency.

After the pioneering work by Zakharov and Filonenko the kinetic wave theory has developed further, making available quantitative predictions for other physical observables such as energy fluxes, downshifting of the peak, energy dissipation etc. All this quantities will be examined and results will be reported in future papers. Other questions naturally arise from our results: in HOS simulations the order of the computation depends on how many terms are retained in the Taylor expansion; do higher order terms influence the cascade process? Our computation has been performed in a freely decaying case; could external forcing (especially if anisotropic) influence the power law? And more, what would be the influence of the water depth? These are all questions to be answered in the near future.

This work was supported by the Office of Naval Research of the United States of America (T. F. Swean, Jr.) and by the U.S. Army Engineer Research and Development Center. Consortium funds and Torino University funds (60 %) are also acknowledged. M. O. was also supported by a Research Contract from the Università di Torino.

FIG. 1. Wave spectra at different times.

FIG. 2. Wave spectrum at $t = 4$ hours. A $k^{-2.5}$ (dotted-line) and a k^{-3} (dashed-line) power law are also plotted.

FIG. 3. Compensated wave spectra for different values of the compensation power: $z = 2$ (dahsed-line) $z = 2.5$ (solid-line) and $z = 3$ (dotted-line).

[1] A. Kolmogorov, C. R. Akad. Sci. SSSR **30**, 301 (1941).
[2] O. M. Phillips, J. Fluid Mech **107**, 426 (1958).
[3] V.E. Zakharov and N. Filonenko, Soviet Phys. Dokl., **11**, 881 (1967).
[4] V. E. Zakharov, J. Appl. Mech. Tech. Phys. **9**, 190 (1968).
[5] V.E. Zakharov, G.Falkovich and V. Lvov, *Kolmogorov spectra of turbulence I* (Springer, Berlin, 1992).
[6] Y. Toba, J. Phys. Ocean., **29**, 209 (1973).
[7] K. K. Kahama, J. Phys. Ocean. **11**, 1503 (1981).
[8] G. Z. Forristall, J. Geophys. Res. **86**, 8075 (1981).
[9] M. A. Donelan, J. Hamilton and W. H. Hui, Phil. Trans. R. Soc. Lond. A **315**, 509 (1985).
[10] O.M. Phillips, J. Fluid Mech. **156**, 505, (1985).
[11] D. Resio and W. Perrie, J. Fluid. Mech **223**, 603 (1991).
[12] A. Pushkarev, D. Resio and V. Zakharov, submitted to Phys. Rev. E (2001).
[13] V. E. Zakharov, Eur. J. Mech. B-Fluid **18** 327, (1999).
[14] A. N. Pushkarev and V. E. Zakharov, Phys. Rev. Lett. **76**, 3322, (1996).
[15] D Cai, A. J. Majda, D. W. McLaughlin and E.G. Tabak, Physica D **152**, 551, (2001).
[16] V. E. Zakharov, P. Guyenne, A. N. Pushkarev and F. Dias, Physica D **152**, 573, (2001).
[17] W. T. Tsai, D.K.P. Yue, Ann. Rev. Fluid Mech. **28**, 249, (1996).
[18] B. J. West, K. A. Brueckner and R. Janda, J. Geophys. Res. **92**, 11803, (1987).
[19] D.G. Dommermuth and D.K.P. Yue, J. Fluid Mech. **184**, 267 (1987).
[20] M. Tanaka, J. Fluid Mech. **442**, 303 (2001).
[21] S. Yu. Annenkov and V.I. Shrira, J. Fluid Mech. **449**, 341 (2001).
[22] D. Clamond and J. Grue, J. Fluid Mech. **447**, 337 (2001).
[23] V. Zakharov, A. Dyachenko and O. Vasilyev, "New method for numerical simulation of a nonstationary potential flow of incompressible fluid with a free surface," submitted for pubblication (2001).
[24] J. Willemsen, Communication at the *Theoretical developments: two and three dimensional water waves*, EU-Conference, Cambridge, UK, August (2001).
[25] V.P. Krasitskii, J. Fluid Mech. **272**, 1 (1994).
[26] G. Falkovich, Phys. of Fluids **6**, 1411 (1994).
[27] D. Biskamp, E. Schwarz, A. Celani, Phys.Rev. Lett. **81**, 4855 (1998).
[28] M. Onorato, A. R. Osborne and M. Serio, to be published in Phys. of Fluids, (2002).
[29] A.N. Pushkarev and V. E. Zakharov, Physica D **135**, 98 (2000).
[30] L. E. Borgman, "Techniques for Computer Simulation of Ocean Waves", in *Topiccs in Ocean Physics, Proc. of the Int. School E. Fermi*, Eds. A. R. Osborne and P. Malanotte Rizzoli, 373 (1980).

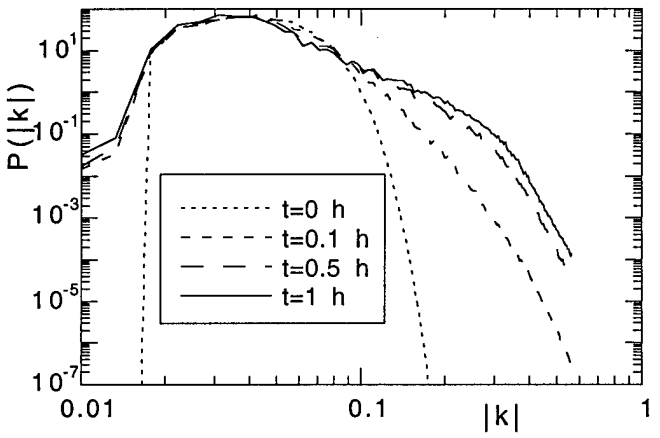
P(|k|)
10^1
10^-1
10^-3
10^-5
10^-7
0.01
0.1
1
|k|
t=0 h
t=0.1 h
t=0.5 h
t=1 h

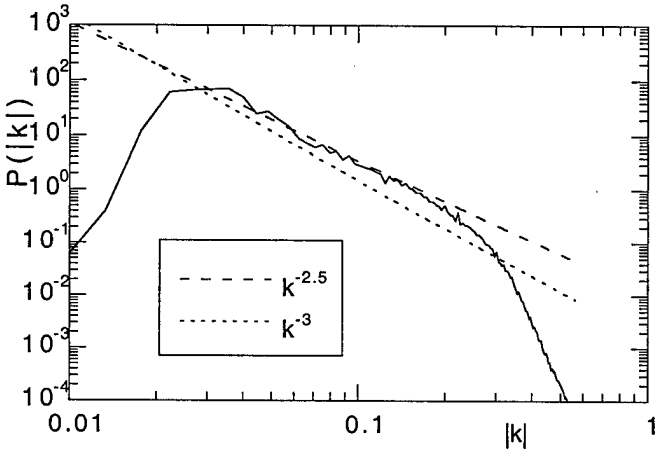
10^3
10^2
10^1
10^0
10^{-1}
10^{-2}
10^{-3}
10^{-4}
P(|k|)
0.01
0.1
1
|k|
$k^{-2.5}$
k^{-3}

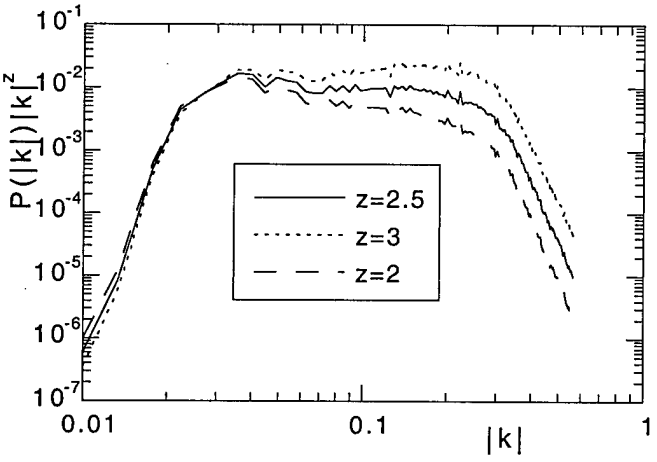
10^{-1}
10^{-2}
10^{-3}
10^{-4}
10^{-5}
10^{-6}
10^{-7}
$P(|k|)|k|^z$
0.01
0.1
1
|k|
z=2.5
z=3
z=2

New Method for Numerical Simulation of a Nonstationary Potential Flow of Incompressible Fluid with a Free Surface

Vladimir E. Zakharov[1,2,3,*], Alexander I. Dyachenko[1]
and Oleg A. Vasilyev[1]

[1] *Landau Institute for Theoretical Physics, 2 Kosygin str. Moscow, 117334, Russia*

[2] *Department of mathematics, University of Arizona, Ticson AZ 857201*

[3] *Waves and Solitons Ltd.*

[*] *e-mail:* zakharov@itp.ac.ru

short title: New Method for Numerical Simulation of a Fluid

Abstract

A new method for the numerical simulation of potential flows of a two-dimensional fluid with a free surface, based on combining a conformal mapping and a Fourier Transform is proposed. The method is efficient for studying strongly nonlinear effects in gravity waves, including wave breaking and formation of rogue waves.

1 Introduction

The problem of analytic and numeric description of a non-stationary potential flow in fluid with a free surface is one of the most fundamental in Hydrodynamics. At the moment several different approaches to the solution of this problem are elaborated. We do not plan to give in this article even a brief review of all these methods. We just mention that they can be divided, roughly speaking, into two groups. Some authors assume that nonlinearity is weak and use expansion in powers of the surface slope. In the most advanced works belonging to this direction, they use Hamiltonian formalism [1]. The most important advantage of this approach the is opportunity to implement such an efficient numerical algorithm as the fast Fourier transform. It is possible to use a very fine mesh and resolve as many as thousands or even tens of thousands of Fourier modes. The obvious disadvantage of this approach is that it is impossible to describe the most interesting physical processes such as wave breaking and formation of the freak waves. These processes are essentially nonlinear. Another group of methods uses the exact hydrodynamic equation and can in principle be applied for description of the strongly nonlinear phenomena see, for instance [2]. But these methods are usually incompatible with the Fourier formalism and allow only a relatively poor resolution (hundreds of the spectral points or the Fourier modes).

In the given article we offer a completely new method for the analytic and numeric study of a nonstationary flow of an ideal noncompressible fluid with a free surface. In our opinion, this method combines the advantages of the existing approaches, being free of their disadvantages. The basic idea of this new method is to refurmulate the exact Euler equations, describing a potential flow of a fluid with a free surface, as the "Hilbert-differential" equations with just a polynomial (cubic) nonlinearity. A new form of the exact equations makes possible to implement the Fourier method even more efficiently than in the approximate equation. As a result we can achieve a very high resolution in the description of completely nonlinear phenomena such as wave-breaking and formation of freak waves. So far we performed only first starting series of numerical experiments. This results are really impressive. For instance we clearly observed formation of freak waves as a result of development of the modulational instability of weakly-nonlinear Stokes waves.

2 Basic Equations

We study a fluid of infinite depth, occupying the area

$$-\infty < y < \eta(x,t)$$

The flow is irrotational, hence

$$V = \nabla\phi$$

The condition of incompressibility div$V = 0$ implies that the velocity potential ϕ satisfies the Laplace equation

$$\triangle\phi = 0$$

In the absence of an external pressure the boundary condition imposed on ϕ are

$$\begin{array}{rcl} \frac{\partial\phi}{\partial t} & + & \frac{1}{2}|\nabla\phi|^2 + g\eta = 0, \\ \frac{\partial\eta}{\partial t} & + & \eta_x\phi_x = \phi_y \end{array} \tag{2.1}$$

and $\frac{\partial\phi}{\partial y} = 0$ at $y \to -\infty$ The total energy of the system is

$$\mathcal{H} = \frac{1}{2}\int_{-\infty}^{\infty} dx \int_{-\infty}^{\eta(x,t)} |\nabla\phi|^2 \mathrm{d}y \ + \ \frac{g}{2}\int_{-\infty}^{\infty} \eta^2(x,t)\mathrm{d}x \tag{2.2}$$

where g is gravity acceleration. The system is hamiltonian [3, 4] and can rewritten as follows

$$\begin{array}{rcl} \frac{\partial\eta}{\partial t} & = & \frac{\delta\mathcal{H}}{\delta\psi}, \\ \frac{\partial\psi}{\partial t} & = & -\frac{\delta\mathcal{H}}{\delta\eta}. \end{array} \tag{2.3}$$

Here $\psi = \phi|_{z=\eta}$ and η are canonically conjugated variables. Let us perform the conformal mapping of the domain, filled with fluid

$$-\infty < x < \infty, \ -\infty < y < \eta(x,t)$$

to the half-plane

$$-\infty < u < -\infty, \ -\infty < v < 0$$

After the transform, the shape of surface $\eta(x,t)$ is presented in a parametric form

$$y = y(u,t), \ x = x(u,t) = u + \tilde{x}(u,t)$$

here $\tilde{x}(u,t)$ and $y(u,t)$ are related through Hilbert Transformation

$$y = \hat{H}\tilde{x}, \qquad \tilde{x} = -\hat{H}y, \qquad \hat{H}^2 = -1$$

and

$$\hat{H}(f(u)) = P.V.\frac{1}{\pi}\int_{-\infty}^{\infty} \frac{f(u')\mathrm{d}u'}{u'-u}.$$

After the conformal mapping $\phi(x,y,t) \to \phi(u,v,t)$, $\psi(x,t) \to \psi(u,t)$. It was shown [5], see also [6, 7], that $y(u,t)$ and $\psi(u,t)$ obey the following system of equations:

$$y_t = (y_u\hat{H} - x_u)\frac{\hat{H}\psi_u}{J} \tag{2.4}$$

$$\psi_t = -\frac{\psi_u^2 + \hat{H}\psi_u^2}{2J} + \hat{H}\left(\frac{\hat{H}\psi_u}{J}\right)\psi_u + \frac{\hat{H}\psi_u}{J}\hat{H}\psi_u - gy \tag{2.5}$$

$$J = x_u^2 + y_u^2 = 1 + 2\tilde{x}_u + \tilde{x}_u^2 + y_u^2. \tag{2.6}$$

Equation (2.4), (2.5) can be written in the complex form. Let $z = x + iy$, $\Phi = \psi + iH\psi$ be analytic functions in the lower half-plane. They satisfy the equation

$$z_t = iUz_u \tag{2.7}$$

$$\Phi_t = iU\Phi_u - B + ig(z - u). \tag{2.8}$$

Here U is a complex transport velocity:

$$U = \hat{P}\left(\frac{-\hat{H}\psi_u}{|z_u|^2}\right) \tag{2.9}$$

and

$$B = \hat{P}\left(\frac{|\Phi_u|^2}{|z_u|^2}\right) \tag{2.10}$$

In (2.9) and (2.10) $\hat{P}$ is the projector operator generating a function analytical in the lower half-plane $\hat{P}(f) = \frac{1}{2}\left(1 + i\hat{H}\right)f$.

It occurs [8] that equations (2.7)-(2.8) can be simplified just by changing variables. Indeed, let us introduce instead of $z(w,t)$ and $\Phi(w,t)$ another functions $R(w,t)$ and $V(w,t)$ in a following way

$$\begin{aligned} R &= \frac{1}{z_w}, \\ \Phi_w &= -iVz_w. \end{aligned} \tag{2.11}$$

(V is just $i\frac{\partial\Phi}{\partial z}$, i.e. complex velocity). Note, that because of $z(w,t)$ is a conformal mapping, its derivative exists in lower half-plane and does not have zeroes there. Thus function $R(w,t)$ is analytic in the lower half-plane and has the following boundary condition:

$$R(w,t) \to 1, \quad |w| \to \infty, \quad Im(w) \leq 0.$$

It is obvious that boundary condition for V is:

$$V(w,t) \to 0, \quad |w| \to \infty, \quad Im(w) \leq 0.$$

Then for these analytic functions equations acquire a very nice form:

$$R_t = i(UR' - U'R) \tag{2.12}$$

$$V_t = i(UV' - RB') + g(R - 1) \tag{2.13}$$

Here (see [8])

$$B = \hat{P}'(V\bar{V}), \quad U = \hat{P}(V\bar{R} + \bar{V}R).$$

Equations (2.12)-(2.13) are exact, and completely equivalent to the "traditional" system of equations for the free surface potential flow (2.1). But system (2.12)-(2.13) is much more convenient for analytical and numerical study than the "traditional" system (2.1) as well as Hamiltonian system (2.3). Indeed, one cannot express H explicitly in terms of the "natural" variables ψ and η. At the best one can present H as an infinite series in powers of η. As a result, the equations in the "natural" variables are presented by the infinite series as well. This is a great obstacle in the way of their numerical simulation. On the contrary, new motion equations (2.12)-(2.13) are just polynomial (cubic) in terms of new variables R, V. This circumstance makes it possible to implement the fast Fourier transform to the solution of new exact equations.

One can mention that all three equivalent systems of equation, describing dynamic of free surface in conformal variables (2.4)-(2.5), (2.7)-(2.8), (2.12)-(2.13) are not PDE. They are "Hilbert-differential" equations, which include together with differentiation by u

$$f \to \frac{\partial f}{\partial u} \tag{2.14}$$

the Hilbert transformation

$$f \to \hat{H} f \tag{2.15}$$

¿From an analytical viewpoint these two operations are completely different, but from a numerical viewpoint they are similar. Indeed, in terms of Fourier transform, operation (2.14) means

$$f_k \to ikf_k$$

while operation (2.15) means

$$f_k \to i\,\mathrm{sign}(k) f_k$$

¿From a computational viewpoint both these operations are of the same level of difficulty.

3 Constants of motion, forcing and dissipation

Dynamic equations describing fluids with a free surface have natural constants of motion: mass of fluid M, horizontal momentum P_x and energy H. A serious advantage of the conformal approach is an opportunity to express all of these quantities as integrals over their local densities, which can be expressed explicitly in terms of Z and Φ. Indeed, deviation of the mass of fluid from its equilibrium value can be expressed by

$$M = \int_{-\infty}^{\infty} m\,\mathrm{d}u$$

$$m = yx_u = \frac{1}{2i}\left(z\bar{z}_u - z_u\bar{z}\right) \tag{3.16}$$

$$P_x = \int_{-\infty}^{\infty} p_x \, \mathrm{d}u$$

$$p_x = \psi y_u = \frac{1}{2i}\psi\left(z_u - \bar{z}_u\right) \tag{3.17}$$

$$\mathcal{H} = \int_{-\infty}^{\infty} w \, \mathrm{d}u$$

$$w = w_T + w_U$$

where w_T is the kinetic energy density

$$w_T = -\frac{1}{2}\psi\hat{H}\psi_u = \frac{1}{8i}\left(\Phi\bar{\Phi}_u - \Phi\bar{\Phi}_u\right) \tag{3.18}$$

and w_u – the potential energy density

$$w_U = \frac{g}{2}y^2x_u = -\frac{g}{16i}\left(z - \bar{z}\right)^2\left(z_u + \bar{z}_u\right) \tag{3.19}$$

Apparently $w_T > 0$, $w_U > 0$.

Expressions of m, p and w in terms of R and V are not that elegant. One can obtain these expressions using formulae

$$z = \int \frac{\mathrm{d}u}{R}, \quad \Phi = -i\int \frac{V}{R}\,\mathrm{d}u \tag{3.20}$$

Formulae (3.16)-(3.19) can be used for the control of the numerical calculations.

In reality any system of surface waves is not conservative and such effects as viscosity and interaction with wind should be taken into account. A complete consideration of these effects is a difficult problem. In many cases one can take into take into consideration dissipative and forcing effect by the use of some phenomenological modification of the basic equations. It is convenient to perform a modification in equations (2.7)-(2.8). Equation (2.7) is just the kinematic boundary condition on the surface. It should not modified. The simplest modification of (2.8) is replacing

$$\Phi_t \to \Phi_t + \hat{\gamma}\Phi \tag{3.21}$$

Here $\hat{\gamma}$ is a pseudodifferential linear operator of convolution type.

As far as functions Φ and z are analytical in the lower half-plane, they can be presented in a form

$$\Phi(u,t) = \frac{1}{\sqrt{2\pi}}\int_0^{\infty} \Phi_k \mathrm{e}^{-iku}\mathrm{d}k$$

$$z(u,t) = \frac{1}{\sqrt{2\pi}} \int_0^\infty z_k \mathrm{e}^{-iku} \mathrm{d}k \tag{3.22}$$

Now $(\hat{\gamma}\Phi) = \gamma_k \Phi_k$ Here γ_k is a symbol of the operator $\hat{\gamma}$ in terms of Fourier transforms. The energy balance equation read

$$\frac{d\mathcal{H}}{dt} = -\frac{1}{4} \int_0^\infty k\gamma_k |\Phi_k|^2 \, \mathrm{d}k \tag{3.23}$$

Operator $\hat{\gamma}$ provides "pure dissipation" if $\gamma_k > 0$ for all $0 < k < \infty$. Otherwise it describes a coexistence of forcing in some range of scales with dissipation in the rest scales. One should take into account that special scales in the conformal variables u and in real coordinate x can be essentially different. In the linear approximation $|Z_u|^2 < 1$ and $U = i\Phi_u$. Linearization of equations (2.7)-(2.8) leads to the dispersion relation ($\Phi \simeq e^{i\omega t - iku}$)

$$\omega = \frac{i\gamma}{2} \pm \sqrt{gk - \frac{\gamma^2}{4}}, \quad 0 < k < \infty \tag{3.24}$$

It is important to stress that formula (3.23) holds not only in the linear approximation, but for waves of arbitrary large amplitude. The equivalent modification of system (2.12)-(2.13) is more complicated.

$$\begin{aligned} R_t &= i(UR' - U'R) \\ V_t &= i(UV' - RB') + g(R-1) - R\hat{\gamma}\left(\frac{V}{R}\right) \end{aligned} \tag{3.25}$$

One can see that the dissipative term in this system is essentially nonlinear.

4 Numerical algorithm

All three versions [(2.4)-(2.5), (2.7)-(3.17), (2.12)-(2.13)] of the exact equations describing free surface dynamics of fluid are convenient for numerical simulation by the use of spectral code. In the non-conservative case the equations

$$\begin{aligned} z_t &= iUz_u \\ \Phi_t + \hat{\gamma}\Phi &= iU\Phi_u - B + ig(z-u). \end{aligned} \tag{4.26}$$

are most convenient. However, in the pure conservative case one should use more simple equations (2.12)-(2.13).

Now we describe the details of the numerical simulation of these equations. We use the fourth order Runge-Kutta integration scheme to numerically solve these equations. The domain of length 2π was investigated. The actual spectral area

includes up to $N = 12288$ negative modes, whereas the total spectral area and the number of points in the real space was $2N$. This feature is a consequence of the presence of projector operator $\hat{P}$. All concerned functions are analytic in the bottom half-plane. So when we calculate projector operator we need to make nullify positive spectral modes. For this purpose we use the fast Fourier transform procedure. Empty positive spectral modes prevent aliasing - arising the parasite noise from fast Fourier transform procedure.

To keep our numerical scheme stable, we need to define time step $\Delta t < \frac{1}{N}$ because we have differential operators in equations (2.12)-(2.13). Another indispensable condition is $\Delta t < \frac{1}{F}$ where F is maximal value of right parts of equations. In our calculations we keep $\Delta t < \frac{0.5}{N}$ and $\Delta t < 0.05F$.

We check conservation of total energy H to control the accuracy of numerical calculations. In our calculations energy conserves up to 11 decimal digit after the decimal points for wave breaking and 6 decimal digits for modulational instability.

5 Preliminary results

We plan to include the effect of surface tension into the derived equation and perform massive numerical experiments embracing a vast variety of dynamical and statical problems including simulation of wave breaking, formation of freak waves, and establishment of a universal spectra of wave turbulence. In this article we present only the very preliminary results attained in framework of this program. In all cases we use Dyachenko equations (2.12)-(2.13) without any kind of dumping and forcing. In all our experiments we use the domain $0 < x < 2\pi$, $0 < u < 2\pi$ with periodic boundary conditions. The total number of harmonics was as much as 12288. We put gravity acceleration $g = 10$. In the first experiment we use the initial data in the form

$$\begin{aligned} R(u, t = 0) &= 1 + a\exp(-iu) \\ V(u, t = 0) &= -ia\sqrt{g}\exp(-iu) \end{aligned} \tag{5.27}$$

For $a \ll 1$ this initial data leads to formation of propagating wave of small amplitude

$$\begin{aligned} R(u, t = 0) &= 1 + a\exp(-iu + i\sqrt{g}t) \\ V(u, t = 0) &= -ia\sqrt{g}\exp(-iu + i\sqrt{g}t) \end{aligned} \tag{5.28}$$

However for $a \sim 1$ the propagating wave turns to break. In our experiments we put $a = 0.28$. Figures 1-2 demonstrate time evolution of the wave profile and the surface spectrum. One can see tendency to formation of singularity as well as to development of spectral "tails". Calculation was terminated when the absolute value of $R(k)$ reached the level $|R(k)| \sim 10^{-10}$ at the end of spectral interval $N = 12288$.

Second experiment demonstrates development of modulational instability and formation of freak waves. Modulational instability of Stokes waves was discovered

independently and almost simultaneously by V.E. Zakharov [3, 4] and T.B. Benjamin and J.E. Feir [9]. Nonlinear stage of this instability so far was not investigated.

A Stokes wave is characterized by its steepness $\mu = ka$, (k – wave number, a – wave amplitude). If $\mu \ll 1$ the Stokes wave is very close to a linear monochromatic propagating wave. In our experiments we put $\mu = 0.1$. That makes it possible to neglect a deviation of the Stokes wave from an exponential one and choose initial data in a form superposition of the monochromatic wave with wave number $k = -50$ and the Gaussian random noise:

$$R(u,t=0) = 0.1\exp(-50iu) + \frac{5\times10^{-5}}{\sqrt{2\pi}}\sum_{k=0}^{N}\mathrm{rand}_1(k)\exp\left(-\frac{(50-k_s)^2u^2}{800} - iku + 2\pi i\mathrm{rand}_2(k)\right)$$
$$V(u,t=0) = -i\frac{0.1}{\sqrt{5}}\exp(-50iu) -$$
$$-\frac{5\times10^{-5}i}{\sqrt{2\pi}}\sum_{k=0}^{N}\frac{\sqrt{10}}{\sqrt{k}}\mathrm{rand}_1(k)\exp\left(-\frac{(50-k_s)^2u^2}{800} - iku + 2\pi i\mathrm{rand}_2(k)\right) \tag{5.29}$$

The initial spectra of function R is shown on Fig.4 (it mark is $t = 0$), and a part of initial surface $y(x)$ is shown on Fig.5.

In our computations forcing and dumping are absent. The total energy remains constant during simulation up to $t = 90$. It means, that in this time interval the spectra don't reach the end of the spectral area and numerical results have sufficient accuracy.

The initial spectra ($t = 0$) and its evolution $t = 40$ and $t = 80$ are shown on Fig.4. We can see how smooth continuous spectra develop from single a spectral harmonic with the addition of small noise. The spectral "tail" steady propagates in the area of high wave numbers. This process can be interpreted as formation of singularities on the crests of individual waves, another words, as an onset of wave-breaking. To continue calculations beyond the moment $t = 80$ one should include dissipation into calculation.

The most impressive results of our experiments on simulation of nonlinear stage of the modulational instability is fast formation of "freak waves". Figure 5 presents the initial shape of fluid surface. One can see, that the initial random noise imposed on the monochromatic wave is very small. Figure 6 presents the shape of the surface in the end of our calculation. One can see the formation of "freak" or "rogue" waves with amplitude more than three times exceeding the initial level. Figures 7-9 displaying distribution of densities of kinetic, potential and total energy even more spectacular. One can see that the total energy density in freak waves exceeds the average level almost by two orders of magnitude.

6 Conclusions

We have developed a very efficient numerical method for the computer simulation of the dynamics of an ideal incompressible fluid with a free surface. We will show

in our next publication that the effects of dissipation and surface tension can be included in the algorithm in a very natural way. The new method makes it possible to perform massive experiments on careful study of wave-breaking, interaction of capillary waves and generation of capillary waves by gravity waves. We plan also to perform systematic study of formation of freak waves including mechanism of their appearance from a "smooth sea". As long as our mew algorithm is fast enough, we will be able soon to study the statistic of freak waves and to find PDF of their generation.

We are grateful Joint SuperComputer Center (www.jscc.ru) for disposed computational resources. This research was partially supported by INTAS-96-0413 Grant, by ONR Grant # N00014-98-1-0070, by DACA 42-00C0044, by RBRF Grant No.00-01-00929 and by the Grant of Leading scientific schools of Russia 00-15-96007.

References

[1] Craig W. and Sulem C., Numerical Simulation of Gravity Waves", Journal of Computational Physics **108**, (1993) 73-83

[2] Dold J.W. and Peregrine D.H., Water-wave modulation, "20-th International Conference on Coastal Engineering", ASCE, Taipei, **103**, (1986) 163-176.

[3] Zakharov V.E., The instability of waves in nonlinear dispersive media, Zh. Eksp. Teor. Fiz. **51**, (1956) 1107-1114, Sov. Phys. JETP, (1967) 24.4.

[4] Zakharov V.E., Stability of periodic waves of finite amplitude on the surface of a deep fluid, J. A.. Mech. Tech. Phys **27** (1968) 86-94.

Russian) 2

[5] Dyachenko A.I., Kuznetsov E.A., Spector M.D. and Zakharov V.E., Analytical description of the free surface dynamics of an ideal fluid (canonical and formalism and conformal mapping), *Phys. Lett. A,* **221** (1996) 73-79.

[6] Dyachenko A.I. and Zakharov V.E., Toward an integrable model of deep water, *Phys. Lett. A*, **221** (1996) 80-84.

[7] Zakharov V.E. and Dyachenko A.I., High-Jacobian approximation in the free surface dynamics of an ideal fluid *Physica D* **98** (1996) 652-664.

[8] Dyachenko A.I., O dynamike ideal'noy zhidkosti so svobodnoy poverhnost'uy, *Doklady Akademii Nauk. English. Doklady. Mathematics*, **63**, No. 1, (2001) 115-118.

[9] Benjamin T.B., Feir J.E., The disintegration of wave trains on deep water, Part 1. Theory, J. Fluid Mech., **27** (1967), 417

Figure captions

Figure 1. Wave breaking: the surface of the fluid $y(x)$ at the different moments of time $t = 0.2 - 1.4$. Initial amplitude $A = 0.28$.

Figure 2. Wave breaking: the surface of the fluid $y(x)$ at the moments of time $t = 1.6 - 2.0$. Initial amplitude $A = 0.28$.

Figure 3. Wave breaking: the spectra $R(k)$ of the function $R(u)$ at the different moments of time t. Initial amplitude $A = 0.28$.

Figure 4. Development of modulational instability: the spectra $R(k)$ of the function $R(u)$ at the different moments of time t.

Figure 5. Development of "freak" waves due to nonlinear interaction: the surface of a fluid for initial time moment $t = 0$.

Figure 6. Development of "freak" waves due to nonlinear interaction: the surface of a fluid for time moment $t = 80$.

Figure 7. Development of "freak" waves due to nonlinear interaction: density of kinetic $w_T(x)$ **a)** energy for time moment $t = 80$.

Figure 8. Development of "freak" waves due to nonlinear interaction: density of potential $w_U(x)$ energy for time moment $t = 80$.

Figure 9. Development of "freak" waves due to nonlinear interaction: density of total energy $w(x)$ for time moment $t = 80$.

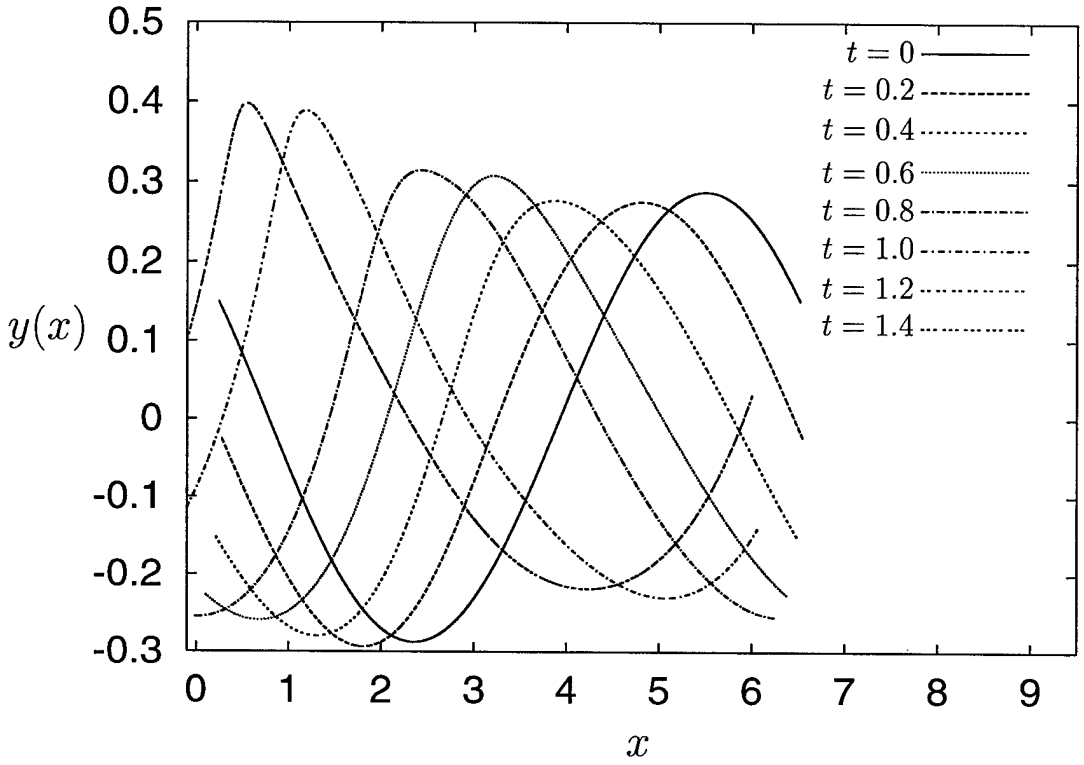
0.5
0.4
0.3
0.2
0.1
0
-0.1
-0.2
-0.3
$y(x)$
0
1
2
3
4
5
6
7
8
9
x
$t = 0$
$t = 0.2$
$t = 0.4$
$t = 0.6$
$t = 0.8$
$t = 1.0$
$t = 1.2$
$t = 1.4$

Figure 1:

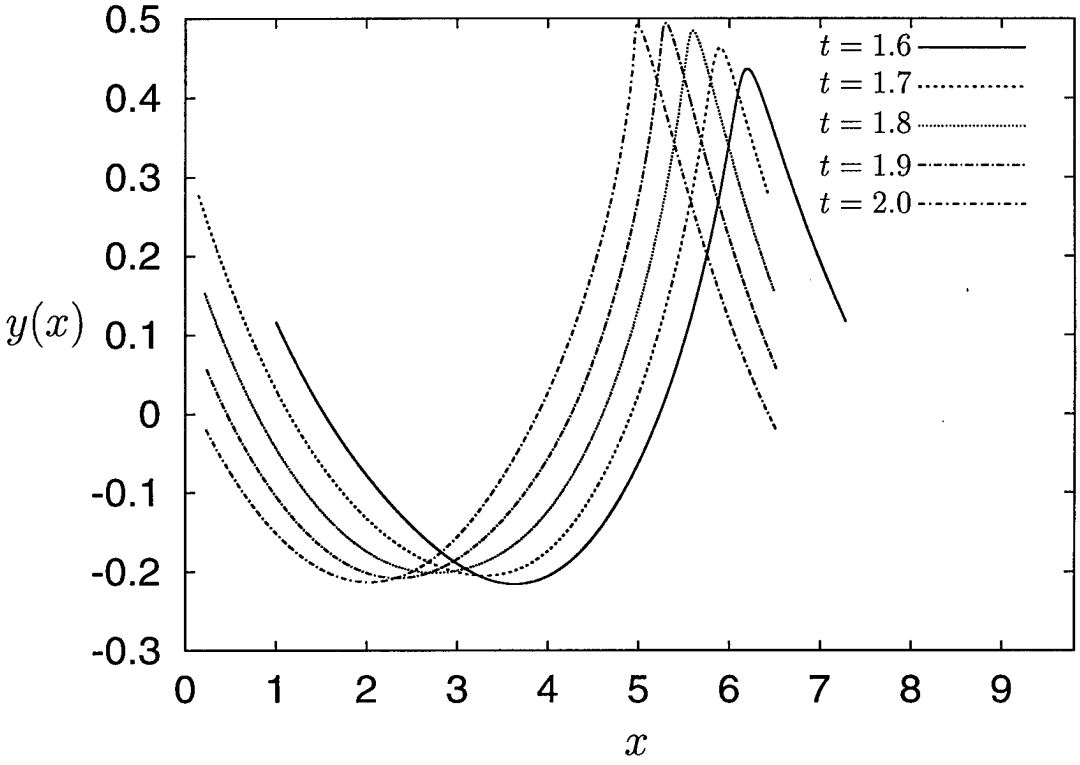

Figure 2:

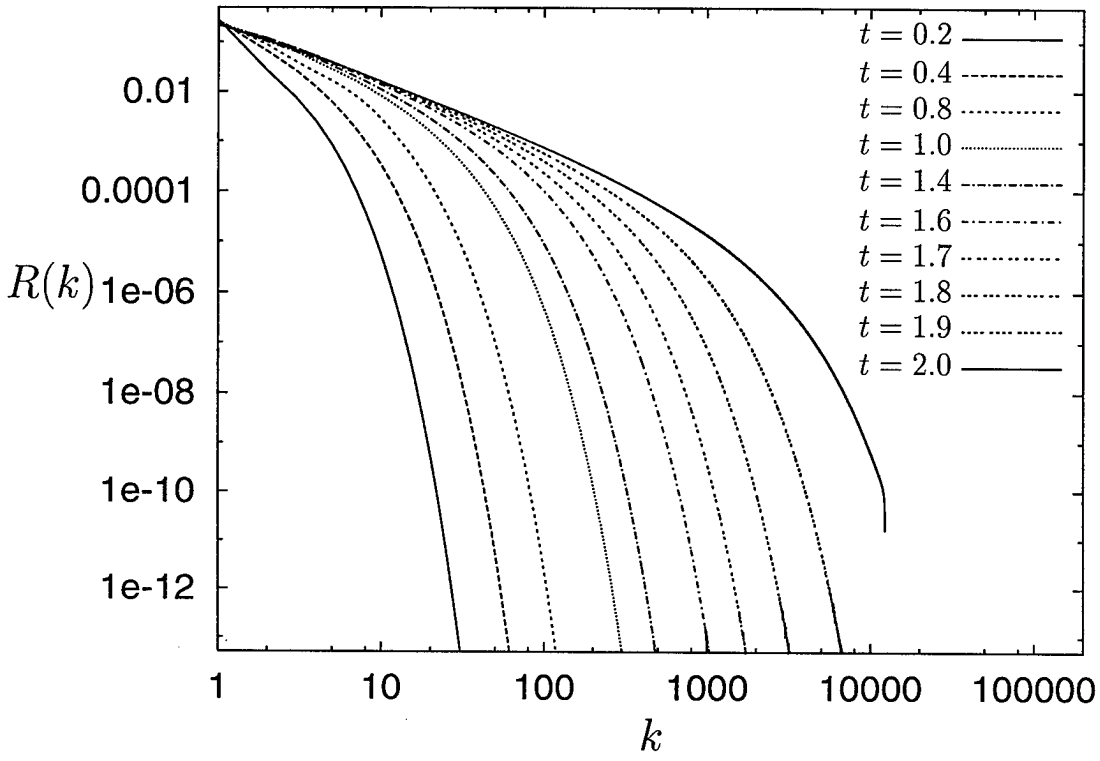
0.01
0.0001
$R(k)$ 1e-06
1e-08
1e-10
1e-12
1
10
100
1000
10000
100000
k
$t = 0.2$
$t = 0.4$
$t = 0.8$
$t = 1.0$
$t = 1.4$
$t = 1.6$
$t = 1.7$
$t = 1.8$
$t = 1.9$
$t = 2.0$

Figure 3:

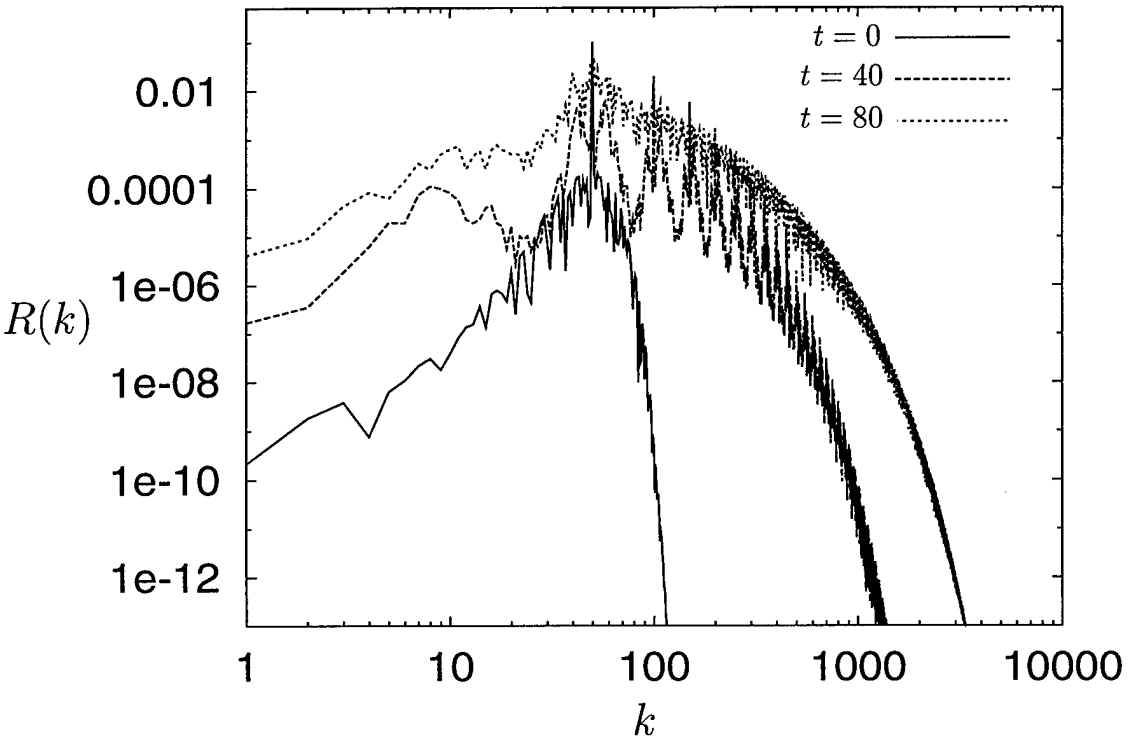

Figure 4:

function

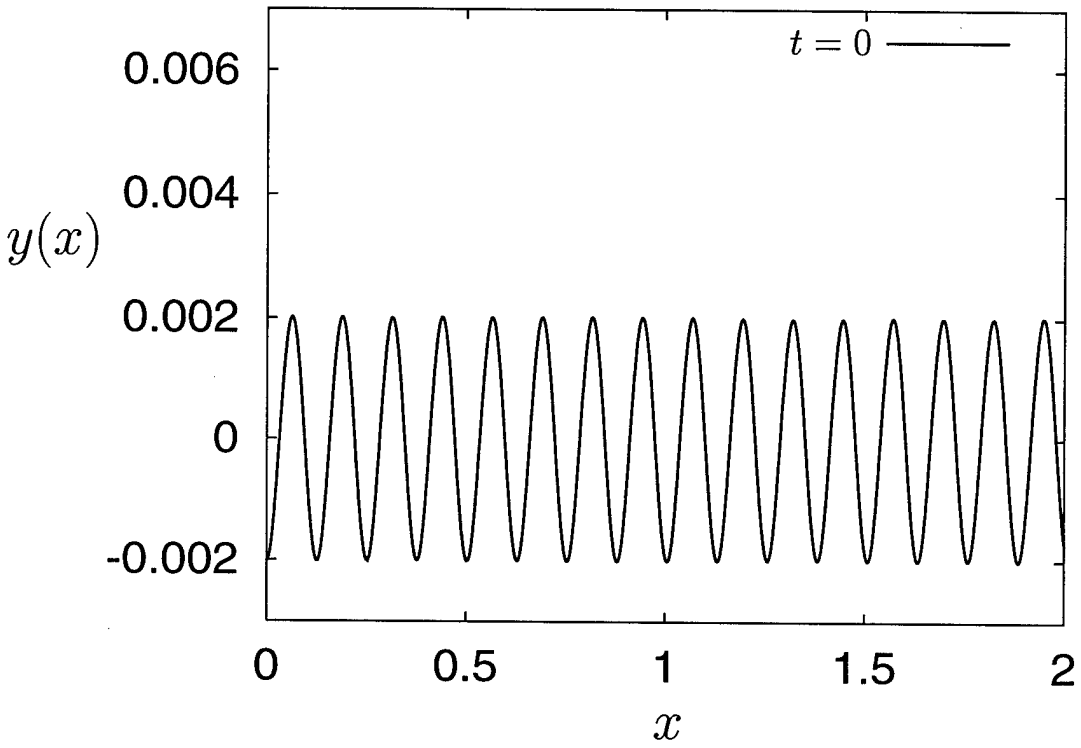

Figure 5:

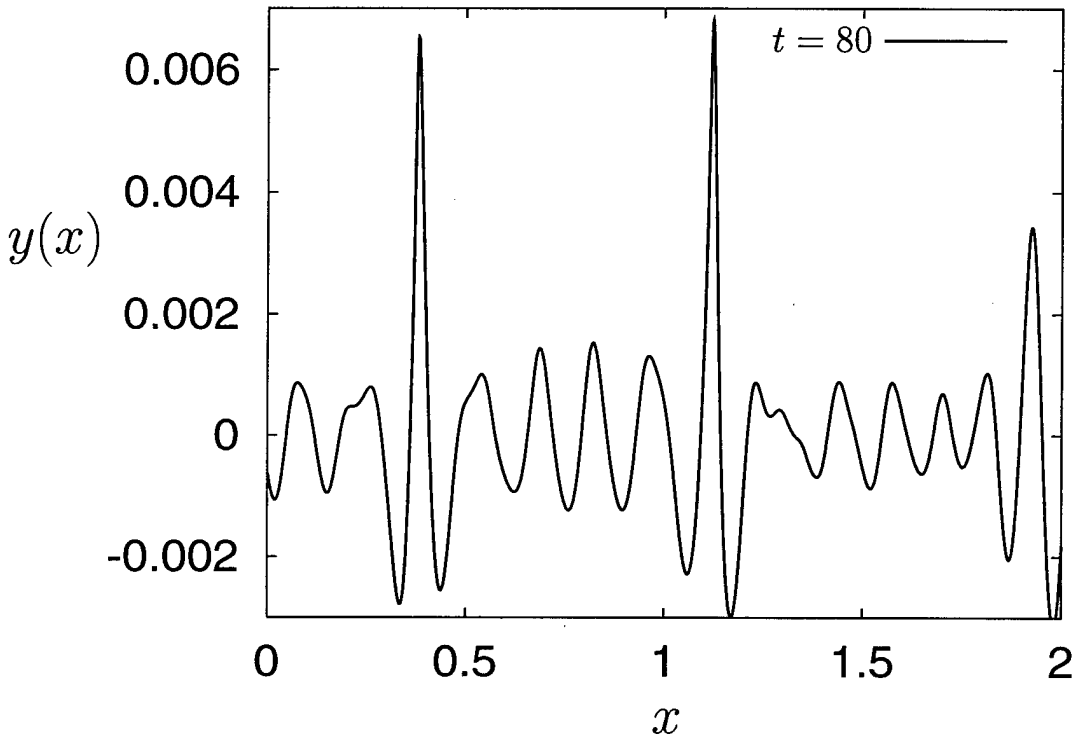

Figure 6:

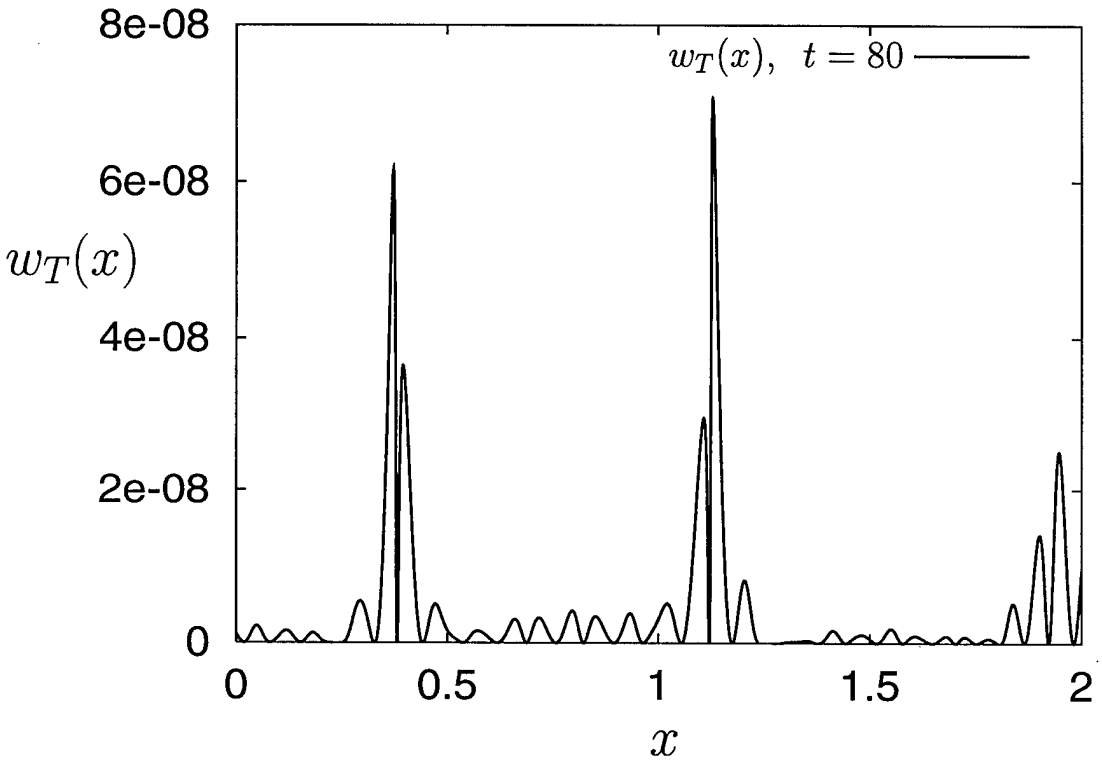

Figure 7:

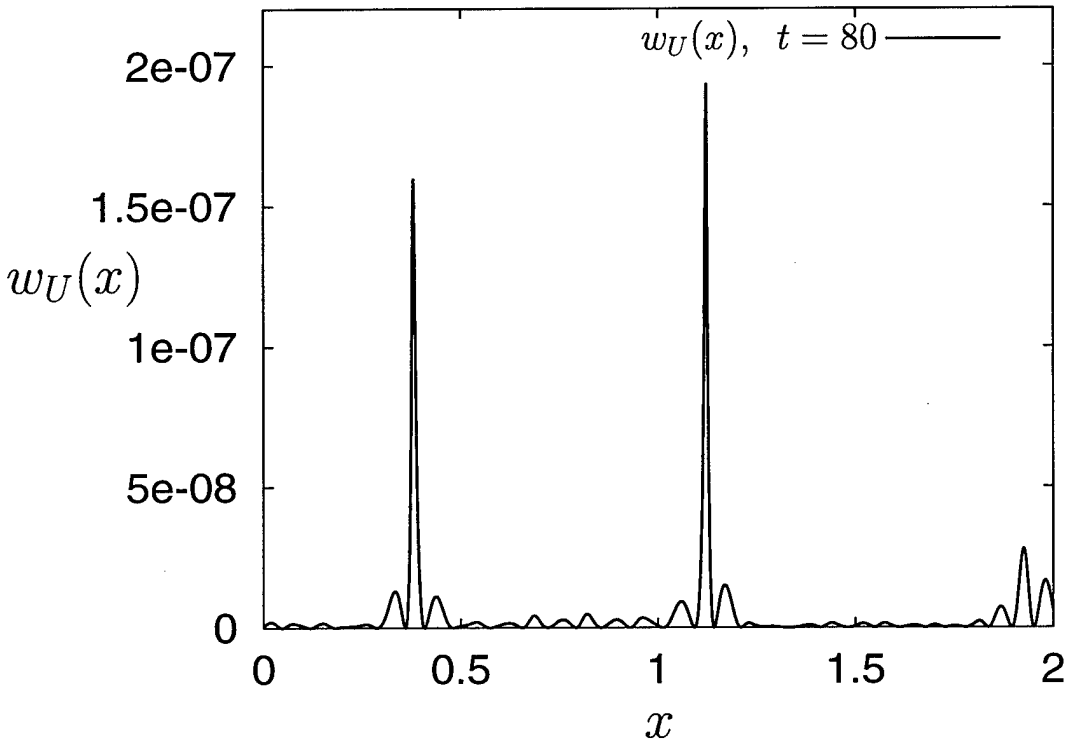

Figure 8:

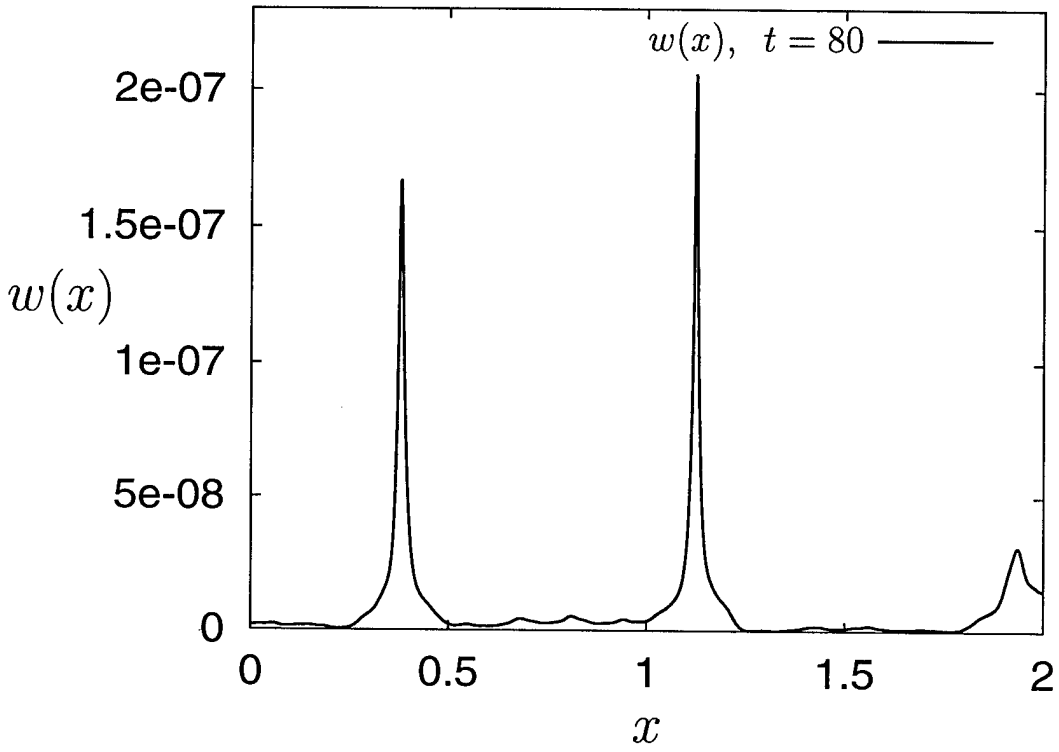

Figure 9:

On conservation of the constants of motion in the models of nonlinear wave interaction.

A.Pushkarev, V.Zakharov

1. Introduction

One of the central problem of the development of the operational models for sea-wave prediction is an adequate description of nonlinear wave interaction. So far, the most solidly justified approach to this description is the use of the kinetic equation for the spectral density of wave action first derived by K.Hasselmann in 1962. Since this time, several codes for numerical simulation of nonlinear wave interaction were developed (Webb 1978, Masuda 1980, Hasselmann and Hasselmann 1981, Resio and Perrie 1991, Polnikov 1994, Lavrenov 1998, Komatsu and Masuda 1996, Van Vledder 1999, etc).

Nonlinear wave interaction is described by a complicated nonlinear integral operator and its numerical simulation is a tricky problem. All existing algorithms for its simulation are cumbersome and time consuming. So far, they are too slow to be directly used in practical operational models of wave prediction. Therefore, the development of faster approximate models of the nonlinear wave interaction is a very urgent problem.

The mostly common approximate model is DIA (Discrete Interaction Approximation), known also as the WAM method. Hasselmann and Hasselmann offered it in 1985. In this model, the integral operator in S_{nl} is replaced by a sum consisting of few discrete terms. Zakharov and Pushkarev proposed quite another approximate model, based on the use of the nonlinear diffusion operator in 1999.

To estimate the quality of an approximate model one should compare its prediction with the results of numerical simulation in the framework of the "exact" kinetic equation. To make this comparison reliable on should be sure that the " exact" model is good enough to be a paragon for such test. Actually, the real criteria for examination of quality of such models are absent.

Different schemes for numerical solution of the Hasselmann kinetic equation give qualitatively similar, but quantitatively slightly different results, and there was no so far a standard way for estimation of their reliability. This circumstances makes the problem of construction of fast approximate models of nonlinear wave interaction difficult and uneasy. One cannot believe in an approximate model if one cannot compare it with a real good standard for calibration.

Meanwhile there is a natural way for examination of numerical method for solution of the wave kinetic equation. This is the control of conservation of the basic constants of motion - wave action, energy, and two components of momentum. Similar approach is widely used in applied mathematics in the case when physical situation is described by conservative ordinary or partial differential equations.

In the case of nonlinear wave interaction, the situation is more complicated. It is described by not differential, but by the integral operator, which is non-local in the k-space. Any scheme of numerical integration of the kinetic equation operates in some finite domain of this space, always bounded in frequency and sometimes limited in angle. Integrals of motion, contained in any bounded domain are not conserved; the non-linear wave interaction carries them out of the domain. Due to non-locality of the S_{nl} operator, this leakage cannot be interpreted just as a flux through a boundary of the domain. The loss of the motion constants from finite domains is not a mathematical abstraction. Its is a real and a very strong physical effect. In many cases, the transport of motion constants is the major mechanism defining shape of spectra. For instance, a typical asymptotic behavior of energy spectrum at large frequency $\mathrm{E}_f \propto f^{-4}$ is the result of constant transport of wave energy to the large frequency region.

In this article, we propose a modified method of calculation of conservation of the motion constant in finite domain making possible to take into consideration the leakage outside a domain. We call it "clean

test", which allows accurate estimation of the quality of any algorithms for numerical solution of the wave kinetic equation.

2. Are the constants of motion really conserved?

In the absence of pumping from the wind and dissipation the Hasselmann equation reads:

$$\frac{\partial n}{\partial t} = S_{nl} \tag{2.1}$$

$$S_{nl} = \int |T_{kk_1k_2k_3}|^2 \, \delta(k + k_1 - k_2 - k_3)\delta(\omega_k + \omega_{k_1} + \omega_{k_2} + \omega_{k_3}) \times (n_{k_1} n_{k_2} n_{k_3} + n_k n_{k_2} n_{k_3} - n_k n_{k_1} n_{k_2} - n_k n_{k_1} n_{k_3}) dk_1 dk_2 dk_3 \tag{2.2}$$

It is considered that equation preserves the following constants of motion

$$N = \int n d\vec{k} \text{ - Wave action} \tag{2.3}$$

$$E = \int \omega_k n_k d\vec{k} \text{ - Energy} \tag{2.4}$$

$$\vec{M} = \int \vec{k} n_k d\vec{k} \text{ - Momentum} \tag{2.5}$$

Are these constants really constant? To prove conservation of these integrals, one must prove validity of following identities:

$$\frac{\partial N}{\partial t} = \int S_{nl} d\vec{k} = 0 \tag{2.6}$$

$$\frac{\partial E}{\partial t} = \int \omega_k S_{nl} d\vec{k} = 0 \tag{2.7}$$

$$\frac{\partial \vec{M}}{\partial t} = \int \vec{k} S_{nl} d\vec{k} = 0 \tag{2.8}$$

These identities are trivial if one can change the order of integration by different k_i. If this operation is possible, one can transform, for instance, the expression (2.7) to the form

$$\int \omega_k S_{nl} dk = \int (\omega_k + \omega_{k_1} + \omega_{k_2} + \omega_{k_3}) \delta(k + k_1 - k_2 - k_3) \delta(\omega_k + \omega_{k_1} + \omega_{k_2} + \omega_{k_3}) n_{k_1} n_{k_2} n_{k_3} dk_1 dk_2 dk_3 \tag{2.9}$$

As it is known from the classical calculus, the operator of change of the integration order in improper integrals is allowed if the integrand decays fast enough at infinity. Let us consider this question in detail.

In equation (2.2), as well as in formulae (2.3)-(2.9), the integration is going on the infinite domain. In reality, both in experiment and in computer modeling the domain of integration is finite. Thus to check the identities (2.6)-2.8) we should first consider a finite domain. This is a quite nontrivial procedure. Suppose that the domain of integration is finite

$$|k| < p \tag{2.10}$$

One can denote

$$n_k^p = \begin{cases} n_k, |k| < p \\ 0, |k| > p \end{cases} \tag{2.11}$$

By plugging n_k^p instead of n_k into S_{nl} one get by definition $S_{nl} \to S_{nl}^{(p)}$. Apparently integrand in $S_{nl}^{(p)}$ has bounded support and change of order of integration is permitted at any value of p. Hence

$$\begin{aligned} \int S_{nl}^{(p)} dk &= \int_{|k|<p} S_{nl}^{(p)} dk + \int_{|k|>p} S_{nl}^{(p)} dk = 0 \\ \int \omega_k S_{nl}^{(p)} dk &= \int_{|k|<p} \omega_k S_{nl}^{(p)} dk + \int_{|k|>p} \omega_k S_{nl}^{(p)} dk = 0 \\ \int \vec{k} S_{nl}^{(p)} dk &= \int_{|k|<p} \vec{k} \omega_k S_{nl}^{(p)} dk + \int_{|k|>p} \vec{k} S_{nl}^{(p)} dk = 0 \end{aligned} \tag{2.12}$$

Let us denote

$$N^p = \int_{|k|<p} n dk, \quad E^p = \int_{|k|<p} \omega_k n_k dk, \quad \vec{M}^p = \int_{|k|<p} \vec{k} n_k dk$$

Now one can find balance of the motion constants in the domain $|k| < p$

$$\begin{aligned} \frac{\partial N^{(p)}}{\partial t} &= \frac{\partial}{\partial t} \int_{|k|<p} n_k dk = \int_{|k|<p} S_{nl}^{(p)} dk = -\int_{|k|>p} S_{nl}^{(p)} dk = -Q(p) \\ \frac{\partial E^{(p)}}{\partial t} &= \frac{\partial}{\partial t} \int_{|k|<p} \omega_k n_k dk = \int_{|k|<p} \omega_k S_{nl}^{(p)} dk = -\int_{|k|>p} \omega_k S_{nl}^{(p)} dk = -P(p) \\ \frac{\partial \vec{M}^{(p)}}{\partial t} &= \frac{\partial}{\partial t} \int_{|k|<p} \vec{k} n_k dk = \int_{|k|<p} \vec{k} S_{nl}^{(p)} dk = -\int_{|k|>p} \vec{k} S_{nl}^{(p)} dk = -\vec{K}(p) \end{aligned} \tag{2.13}$$

Last integrals in (2.13) can be calculated by the use of identity (2.11). In (2.13) Q, P and $\vec{K}$ are the values of the "losses" of the constants of motion. One can present S_{nl} in the following form

$$S_{nl}(k) = \dot{F}_k - \gamma_k n_k \tag{2.14}$$

$$\begin{aligned} F_k = \int |T_{kk_1k_2k_3}|^2 \delta(\omega_k + \omega_{k_1} + \omega_{k_2} + \omega_{k_3}) \delta(\vec{k} + \vec{k}_1 + \vec{k}_2 + \vec{k}_3) \times \\ n_{k_1} n_{k_2} n_{k_3} dk_1 dk_2 dk_3 \end{aligned} \tag{2.15}$$

$$\begin{aligned} \gamma_k = \int |T_{kk_1k_2k_3}|^2 \delta(\omega_k + \omega_{k_1} + \omega_{k_2} + \omega_{k_3}) \delta(\vec{k} + \vec{k}_1 + \vec{k}_2 + \vec{k}_3) \times \\ (n_{k_1} n_{k_2} + n_{k_1} n_{k_3} - n_{k_2} n_{k_3}) dk_1 dk_2 dk_3 \end{aligned} \tag{2.16}$$

By definition

$$S_{nl}^{p}(k) = F_k^{(p)} - \gamma_k^{(p)} n_k^p \tag{2.17}$$

$$F_k^{(p)} = \int\limits_{|k_1|<p,|k_2|<p,|k_3|<p} |T_{kk_1k_2k_3}|^2 \delta(\omega_k + \omega_{k_1} + \omega_{k_2} + \omega_{k_3}) \delta(\vec{k} + \vec{k}_1 + \vec{k}_2 + \vec{k}_3) \times n_{k_1} n_{k_2} n_{k_3} dk_1 dk_2 dk_3 \tag{2.18}$$

$$\gamma_k^{(p)} = \int\limits_{|k_1|<p,|k_2|<p,|k_3|<p} |T_{kk_1k_2k_3}|^2 \delta(\omega_k + \omega_{k_1} + \omega_{k_2} + \omega_{k_3}) \delta(\vec{k} + \vec{k}_1 + \vec{k}_2 + \vec{k}_3) \times (n_{k_1} n_{k_2} + n_{k_1} n_{k_3} - n_{k_2} n_{k_3}) dk_1 dk_2 dk_3 \tag{2.19}$$

One should mention that $S_{nl}^{p}(k) \neq 0$ at $|k \rhd p$. As far as $n_k^p = 0$ at $|k \rhd p$, one has:

$$S_{nl}(k) = F_k^p, \; |k \rhd p \tag{2.20}$$

Formula (2.20) is extremely important. It expresses the following clear physical fact: the income term F_k^p is nonzero far beyond the domain of $|k \lhd p$ where the wave spectrum is concentrated. Meanwhile $F_k^p \neq 0$ only in a finite domain. Indeed, vector $\vec{k}$ satisfies the conditions

$$\vec{k} = \vec{k}_2 + \vec{k}_3 - \vec{k}_1 \tag{2.22}$$

$$\omega_k = \omega_{k_2} + \omega_{k_3} - \omega_{k_1} \tag{2.23}$$

and $|k_1 \lhd p, |k_2 \lhd p, |k_3 \lhd p$.

Conditions (2.22), (2.23) can be satisfied only for

$$|k \lhd p_{\max} \tag{2.24}$$

Here $p_{\max} = f(p)$ - some upper limit depending on a shape of ω_k. One can get some apriori estimate for $p_{\max}$. From (2.22) one can get

$$p_{\max} < 3p \tag{2.25}$$

From (2.23) one obtains

$$\omega_{p_{\max}} < 2\omega_p \tag{2.26}$$

More accurate estimate for $p_{\max}$ is defined by ω_k and depends on the depth. On the infinite depth $\omega_k = \sqrt{gk}$ and $p_{\max}$ is achieved if

$$\vec{k}_2 = \vec{k}_3,\ \vec{k}_1 = -\frac{1}{4}\vec{k}_2,\ |\vec{k}_2| = p \tag{2.27}$$

In this case

$$p_{\max} = \frac{9}{4}p \tag{2.28}$$

$$\omega_{p_{\max}} = \frac{3}{2}\omega_p \tag{2.29}$$

Introducing polar coordinates in $\vec{k}$ -pane, we have the following expressions for losses (rates of leakage) of the constants of motion from the domain $|k| > p$

$$\begin{aligned} Q(p) &= \int_p^{p_{\max}} pdp \int_0^{2\pi} F^p(p,\theta)d\theta \\ P(p) &= \int_p^{p_{\max}} p\omega_p dp \int_0^{2\pi} F^p(p,\theta)d\theta \\ K_x(p) &= \int_p^{p_{\max}} p^2 dp \int_0^{2\pi} F^p(p,\theta)\cos\theta d\theta \\ K_y(p) &= \int_p^{p_{\max}} p^2 dp \int_0^{2\pi} F^p(p,\theta)\sin\theta d\theta \end{aligned} \tag{2.30}$$

3. Clean test for integrals conservation

Now we can answer the question about real conservation of the integrals. If the domain is finite, they are never preserved. It is obvious from (2.30) that in all cases

$$Q(p) > 0,\ P(p) > 0 \tag{3.1}$$

Thus, wave action and energy always leak out of the domain $|k| < p$. In most cases, wave spectrum is concentrated in the right half-plane $-\frac{\pi}{2} < \theta < \frac{\pi}{2}$, $\cos\theta > 0$. In this situation $K_x(p) > 0$, the sign of $K_y(p)$ can be arbitrary.

Suppose again that

$$n_k = 0,\ |k| > p \tag{3.2}$$

We showed that

$$\frac{\partial n}{\partial t} = S_{nl}^{(p)}(k) = F^{(p)}(k) > 0 \tag{3.3}$$

if $|k| < p_{\max}$.

Hence, from physical viewpoint condition (3.2) is artificial. If it is satisfied in the initial moment of time, it will be immediately violated. In the close moment of time δt

$$n = n_0 + S_{nl}^p(k) \cdot \delta t \tag{3.4}$$

n becomes positive in the whole domain $|k| < p_{\max}$.

Anyway, the consideration we performed is useful. It can be used as a foundation for a "clean" test for all codes for numerical solution of the kinetic wave equation.

If condition (3.2) is satisfied

$$\frac{\partial n}{\partial t} = 0 \quad \text{if } |k| > p_{\max} \tag{3.5}$$

Hence

$$\begin{aligned}
&\frac{\partial}{\partial t} \int_{|k|<p_{\max}} S_{nl}^p dk \Big|_{t=0} = 0 \\
&\frac{\partial}{\partial t} \int_{|k|<p_{\max}} \omega_k S_{nl}^p dk \Big|_{t=0} = 0 \\
&\frac{\partial}{\partial t} \int_{|k|<p_{\max}} \vec{k} S_{nl}^p dk \Big|_{t=0} = 0
\end{aligned} \tag{3.6}$$

Conditions (3.6) can be rewritten in polar coordinates as

$$\begin{aligned}
&\frac{\partial}{\partial t} \int_0^{p_{\max}} p dp \int_0^{2\pi} S_{nl}^{(p)} d\theta \Big|_{t=0} = 0 \\
&\frac{\partial}{\partial t} \int_0^{p_{\max}} \omega_p p dp \int_0^{2\pi} S_{nl}^{(p)} d\theta \Big|_{t=0} = 0 \\
&\frac{\partial}{\partial t} \int_0^{p_{\max}} p^2 dp \int_0^{2\pi} S_{nl}^{(p)} \cos\theta d\theta \Big|_{t=0} = 0 \\
&\frac{\partial}{\partial t} \int_0^{p_{\max}} p^2 dp \int_0^{2\pi} S_{nl}^{(p)} \sin\theta d\theta \Big|_{t=0} = 0
\end{aligned} \tag{3.7}$$

Condition (3.7) can be relatively easily checked for any numerical code used for solution of the kinetic equation. To check the quality of the code one should put the initial data $n_k > 0$ at $|k| < p_{\max}$. Expansion of the integration domain is the price to be paid for nonlocality of the four-wave interactions.

Relations (2.13) can be generalized to the case when there is the interaction with wind and damping. Now kinetic equation (2.1)-(2.2) reads

$$\frac{\partial n}{\partial t} = S_{nl} + \beta_k n_k \tag{3.9}$$

where β_k is growth-rate of the instability or the damping depending on the sign. Equations (2.6)-(2.8) now should be replaced by the following relations:

$$\begin{aligned} \frac{\partial N}{\partial t} &= \int \beta_k n_k dk \\ \frac{\partial E}{\partial t} &= \int \omega_k \beta_k n_k dk \\ \frac{\partial \vec{M}}{\partial t} &= \int \vec{k} \beta_k n_k dk \end{aligned} \tag{3.10}$$

Relations (3.10) are formal and for a finite domain should be deciphered in a proper way. To do that one can assume

$$\beta_k = -A\,,\ A \to \infty\,,\ |k \rhd p$$

In the domain $|k \rhd p$ one can neglect the time derivative $\frac{\partial n}{\partial t}$ and put

$$S_{nl} - \beta_k n_k = F_k^p - (\gamma_k + A) n_k = 0$$

As far as $\gamma_k << A$, one can consider approximately ($|k \rhd 1$)

$$n_k = \frac{F_k^{(p)}}{A} \tag{3.11}$$

By plugging (3.11) into (3.10) one notice that the value of A is cancelled from the equations, taking the form

$$\begin{aligned} \frac{\partial N^p}{\partial t} &= -\int_{|k|<p} \beta_k n_k dk - Q \\ \frac{\partial E^p}{\partial t} &= -\int_{|k|<p} \omega_k \beta_k n_k dk - P \\ \frac{\partial \vec{M}}{\partial t} &= -\int_{|k|<p} \vec{k} \beta_k n_k dk - \vec{K} \end{aligned} \tag{3.12}$$

Equations (3.12) are the balance equations which also could be used to control numerical codes. One should either specially program the calculation of the losses $Q, P, \vec{K}$ or extend the integration domain to $|k \models p_{\max}$.

4. Estimates for integral losses.

Suppose that spectral density of wave action $n(k)$ has the maximum at $k \approx k_0$ and $p >> k_0$. Let us estimate in this limit the losses Q, P and $\vec{K}$. Integrals (2.30) consist of two parts. One part is given by integration in a small domain $p' \cong p + \delta p$, $\delta p \leq k_0$. In this domain, integration by k_1, k_2 is performed over the vicinity of the spectral maximum k_0. Thus

$$\begin{aligned} Q &= Q^{(1)} + Q^{(2)} \\ P &= P^{(1)} + P^{(2)} \\ \vec{K} &= \vec{K}^{(1)} + \vec{K}^{(2)} \end{aligned} \tag{4.1}$$

Here

$$\begin{aligned} Q^{(1)} &\cong \frac{n(p)n^2(k_0)}{\omega(k_0)} \cdot \left|T_{p,k_0,p,k_0}\right|^2 k_0^6 \\ P^{(1)} &\cong \frac{\omega(p)}{\omega(k_0)} n(p)n^2(k_0) \cdot \left|T_{p,k_0,p,k_0}\right|^2 k_0^6 \\ K^{(1)} &\cong \frac{p}{\omega(k_0)} n(p)n^2(k) \cdot \left|T_{p,k_0,p,k_0}\right|^2 k_0^6 \end{aligned} \tag{4.2}$$

Other part of contribution in (4.1) is given by integration in the domain $p' \cong p$. In this case, all wave vectors in (2.18) have the same order of magnitude. Hence

$$\begin{aligned} Q^{(2)} &\cong \frac{n^3(p)}{\omega(p)} \cdot \left|T_{p,p,p,p}\right|^3 p^6 \\ P^{(2)} &\cong n^3(p)\left|T_{p,p,p,p}\right|^3 p^6 \\ K^{(2)} &\cong \frac{p}{\omega(p)} n^3(p) \cdot \left|T_{p,p,p,p}\right|^2 p^6 \end{aligned} \tag{4.3}$$

We consider now the case of deep fluid. In this case $\omega(p) \cong g^{1/2} p^{1/2}$

$$\begin{aligned} T(p,p,p,p) &\cong p^3 \\ T(p,k_0,p,k_0) &\cong k_0^2 p \end{aligned} \qquad k_0 << p \tag{4.4}$$

We will consider that $n(k)$ is a powerlike function

$$n(k) \cong k^{-s} \tag{4.5}$$

Comparing $Q^{(1)}$ and $Q^{(2)}$ one see that for the case $S > 19/4$ $\quad Q^{(1)} << Q^{(2)}$. The same is correct for other constants of motion. Finally, one obtains

$$\begin{aligned} Q &\cong p^{23/2-3s} \\ P &\cong p^{12-3s} \\ K &\cong p^{25/2-3s} \end{aligned} \tag{4.6}$$

Now we can answer the question about real conservation of the motion constants. All motion constants conserve if

$$n(k) < Ck^{-25/6} \text{ at } k \to \infty \tag{4.7}$$

5. Kolmogorov spectra and their experimental confirmation.

It is known since 1966 (Zakharov, Filonenko) that the stationary equation

$$S_{nl} = 0 \tag{5.1}$$

has isotropic powerlike solutions

$$n_k^{(1)} = C_1 k^{-23/6} \tag{5.2}$$

$$n_k^{(2)} = C_2 k^{-4} \tag{5.3}$$

The physical meaning of this solution becomes clear after plugging (5.2) into (4.6). For $s = 23/6$ $\quad Q$ is the constant while P and K grow in time. Hence, (5.2) is a Kolmogorov spectrum, corresponding to constant flux of wave action from large to small wavenumbers. For such type of asymptotic neither N, E or $\overrightarrow{M}$ are "real" constants of motion.

If $s = 4$ $\quad Q \cong p^{-1/2}$. In this case $Q \to 0$ at $p \to \infty$, and wave action is "a real" constant of motion. Meanwhile, in this case $P = const$. Hence, (5.3) is a Kolmogorov spectrum describing permanent leakage of energy to large wavenumbers. In terms of spectral density of energy spectra (5.2)-(5.3) read

$$E_\omega^{(1)} = a_1 Q^{1/3} \omega^{-11/3} \tag{5.4}$$

$$E_\omega^{(2)} = a_2 P^{1/3} \omega^{-4} \tag{5.5}$$

Here a_1, a_2 are unknown Kolmogorov constants. One can formulate a conjecture that a general physically relevant solution equation

$$n_k = p^{1/3} k^{-4} F\left(\frac{Q}{P}(gk)^{1/2}, \frac{K}{P}(gk)^{-1/2}\right) \tag{5.6}$$

where F is an unknown function of two variables. It can be found explicitly in heuristic "diffusive" model of S_{nl} (Zakharov, Pushkarev 1999).

The spectrum ω^{-4} has the long history. Zakharov and Filonenko found it analytically as a well-hidden exact solution of equation (5.1) in 1966. Both authors lived in the USSR and were not allowed to travel abroad and report their results on international conferences. That was one reason why the paper of Zakharov and Filonenko, published in the leading Russian scientific journal (Doklady Academii Nauk) was almost not noticed.

There was another reason too. In 1958, O.Phillips offered that the spectrum of wind-driven waves is defined completely by wave breaking and has a universal form

$$\varepsilon_\omega \approx \alpha g^2 \omega^{-5} \tag{5.7}$$

Here α is the dimensionless "Phillips constant".

The very idea of Phillips was seminal and productive. A we understand now, situations when spectra of wave turbulence are defined completely by local singularities is rather common (see, for instance, Zakharov, Dias, Pushkarev, Guyenne 2000).

According to original idea of Phillips, spectrum (5.7) is automatically established at $\omega > \omega_0$, where ω_0 is a characteristic frequency of the spectral maximum. All spectral dynamics is just evolution $\omega_0 = \omega_0(t) \to 0$ at $t \to \infty$. In spite of its elegance and simplicity, the initial conjecture of Phillips is not confirmed by experiments. By definition

$$\int_0^\infty \varepsilon_\omega d\omega = \langle \eta^2 \rangle = H^2 \tag{5.8}$$

By integration of (5.7) one obtain

$$H^2 \cong \frac{\alpha g^2}{4\omega^4} \cong \frac{\alpha g^2}{4(2\pi)^4} T^4$$

or

$$H \propto T^2 \tag{5.9}$$

Here $T = 2\pi/\omega_0$ - characteristic period of energy containing waves.

Relation (5.9) can be checked experimentally. It was Yoshiaki Toba who did it. In 1972-73, he published a set of articles, summarizing his long-time experiments on the wind-wave channel in Sendai University. He found that, instead of (5.9), another relation holds:

$$H \propto T^{3/2} \tag{5.10}$$

Moreover, the Phillips constant, supposed to be universal and not depending on the wind velocity, happened to be proportional to the " friction velocity" u_*, characterizing the momentum transfer from air to sea. These facts can be naturally explained if one assume that instead of (5.7), the spectrum has a form

$$\varepsilon_\omega = \beta g u_* \omega^{-4} \tag{5.11}$$

Here β is another dimensionless constant (Toba's constant). Toba made careful measurements of the spectrum tale and found that formula (5.9) describes the spectral asymptotic very well. He found experimentally that the value of β is:

$$\beta = 6.2 \cdot 10^{-2} \tag{5.12}$$

We must stress that Toba was completely unaware about the paper of Zakharov and Filonenko.

After pioneering works of Toba experimental confirmation of ω^{-4} spectrum are mounted. Just a list of authors who observed this asymptotic is impressive: among them Kawai at al. 1977, Kahma 1981, Forristall 1981, Battjes at al 1986, Donelan, Hamilton and Hui 1985, Donelan and Pierson 1987. In 1985 O.Phillips, summarizing all experimental data, criticized his early theory (which, in our opinion, is still a sample of outstanding scientific intuition) and agreed that ω^{-4} is a reality.

Another approach for confirmation of the ω^{-4} spectrum is the numerical experiment. Several groups (see Masuda and Komatsu 1980, 1996; Resio and Perrie 1991; Polnikov 1994, 2000) observed a universal effect. If the initial data in equation (2.1)-(2.2) decay like ω^{-5}, very soon its asymptotic behavior changes to ω^{-4}.

In this connection, we would like to mention especially works of the group of D.Resio. They did not only follow formation of the ω^{-4} spectrum, but also calculated fluxes of energy at $k \to \infty$ and checked that for ω^{-4} the flux is constant in ω.

In conclusion, one can say that the spectrum ω^{-4} is definitely confirmed now by both many experiments as well as many numerical simulation arguments. The spectrum $\omega^{-11/3}$ also is confirmed quite well, but this point is beyond the scope of this article.

5. Why ω^{-4} not ω^{-5}?

The battle between ω^{-4} and ω^{-5} could look strange for a person outside of a narrow community of S_{nl} experts. Nevertheless, this argument makes a serious sense. It is enough to compare the value of the energy loss P in (4.6) for both spectra. For $\varepsilon_\omega \cong \omega^{-4}$ and $s = 4$, P is the constant. . For $\varepsilon_\omega \cong \omega^{-5}$ $s = 9/4$, $P \cong p^{-3/2} \to 0$ at $p \to \infty$.

Another words, for $\varepsilon_\omega \cong \omega^{-5}$ the energy in the wave ensemble is conserved, while in the case $\varepsilon_\omega \cong \omega^{-4}$ it leaks out with a constant rate. This is a very critical difference. Just an elementary analysis of the observational data contradicts the idea that both wave action and energy are conserved. Indeed, all experiments show that the spectral maximum moves in the process of "maturing " to the low wave numbers. At the same time, the spectrum in the asymptotic area $\omega >> \omega_0$ stays almost constant. As far as quanta of waves loose their energy, moving from high to low frequency region, the outlined facts are compatible with the fact of permanent loss of wave energy, existence of the constant flux of energy to high ω and, as a result, to the ω^{-4} asymptotic at $\omega \to \infty$.

Summarizing the facts, one can say that the asymptotic $\varepsilon_\omega \cong \omega^{-5}$ in the weak turbulent regime is a contradiction to the energy conservation law.

Said Aristotle: "You are friend Plato, but the truth is more valuable". We can say
" You are a friend Dr.... but the conservation of energy is more important".

Acknowledgments.

The authors are grateful for the support of US ARMY under the grant DACA 39-99-C-0018 and ONR, under the grant N00014-98-1-0439.

We would like to express our special gratitude to Dr. Donald Resio for numerous discussions.

References

Dias F., Guyenne P., Pushkarev A.N., Zakharov V.E. Wave turbulence in one-dimensional models, Preprint N2000-4, Centre de Mathematiques et del leur Applications, E.N.S.de CACHAN, pp.1-48, 2000

Battjes J.A., Stive M.J. Calibration and verification of a dissipation model for random breaking waves. J.Geophys.Res., 90(C5), pp.9159-9167, 1986.

Donelan M.A., Hamilton J. and Hui W.H. Directional spectra of wind-generated waves, Phil.Trans.Roy.Soc. London, A315, pp.509-562, 1985.

Forristall J.Z. Measurements of a saturated range in ocean wave spectra, J.Geophys.Res., 86, pp.8075-8084, 1981.

Hansen C., Katsaros K.B., Kitaigorodskii S.A., Larsen S.E. The dissipation range of wind-wave spectra observed on a lake, Journ. Phys.Oceanogr., 20, pp.1264-1277, 1990.

Hashimoto N., Tsukuya H. and Nakagawa Y. Numerical computations of the nonlinear energy transfer of gravity-wave spectra in finite water depth, Coastal Engineering Journal, 40, N1, pp.23-40, 1998.

Hasselmann, K. On the nonlinear energy transfer in a gravity wave spectrum. Part 1, J.Fl.Mech., 12 , pp.481-500, 1962.

Hasselmann, K. On the nonlinear energy transfer in a gravity-wave spectrum. Part 2., J.Fl.Mech., 15, pp.273-281, 1963.

Hasselmann S., Hasselmann K., Komen J., Janssen P., Ewing J. and Cardone V. The WAM model – a third generation ocean wave prediction model. J.Phys.Oceanogr., 18, pp. 1775-1810, 1958.

Hasselmann S. and Hasselmann K. , A symmetrical method of computing the nonlinear transfer in a gravity wave spectrum. Hamburger Geophys. Einzelschrifte., Hamburg, p.52-172, 1981.

Hasselmann S., Hasselmann K. and Bartnett T. Computation and parameterization of the nonlinear transfer in a gravity wave spectrum. Part II. J.Phys.Oceanogr., 15, pp.1378-1391, 1985.

Kahma K.K. A study of the growth of the wave spectrum with fetch, J.Phys.Oceanogr., 11, pp.1503-1515, 1981.

Kawai S., Okada K. and Toba Y. Field data support of three-second power law and $gu_*\sigma^{-4}$ spectral form for growing wind waves., J.Oceanog.Soc.Japan, 33, pp.137-150, 1977.

Kitaigorodskii S.A. On the theory of equilibrium range in the spectrum of wind-generated gravity waves, J.Phys.Oceanogr., 13, N5, pp.816-827, 1983.

Kitaigorodskii S.A. The equilibrium ranges in wind-wave spectra in wave dynamics and radio probing of the ocean surface, Ed. by O.M. Phyllips and K.Hasselmann. Plenum Press Corp., pp.9-40, 1986.

Komatsu K. and Masuda A. A new scheme of Nonlinear Energy Transfer among wind waves: RiAM method – algorithm and performance, Journal of Oceanography, 32, pp.509-537, 1996.

Lavrenov I.V. Mathematical modeling of wind waves in spatially inhomogeneous ocean, Gidrometeoizdat, Sankt-Petersburg, 1998.

Masuda A., Nonlinear energy transfer between wind waves. J.Phys.Oceanogr., 23, pp.1249-1258, 1980.

Phillips O.M. The equilibrium range in the spectrum of wind-generated waves. J.Fl.Mech., 4, pp. 426-434, 1958.

Phillips O.M. Spectral and statistical properties of the equilibrium range in wind-generated gravity waves. J.Fl.Mech., 156, pp. 505-531, 1985.

Polnikov V. Numerical modeling of the constant flux spectra for surface gravity waves in the case of angular anysotropy, Wave Motion, 1008, pp.1-12, 2000.

Polnikov V. Numerical modeling of the flux energy formation for surface gravity waves, J.Fl.Mech., 278, pp.289-291, 1994.

Resio D.T. and Perrie W.A. Implication of an f^{-4} equilibrium range for wind-generated waves. J.Phys.Oceanogr., 2, pp.193-204, 1989.

Resio D. and Perrie W. A numerical study of nonlinear energy fluxes due to wave-wave interactions. Part I. Methodology and basic results, J.Fl.Mech., 223, pp.603-629, 1991.

Tracy B.A. and Resio D.T. Theory and calculation of the nonlinear transfer between sea wave in deep water wave information studies. Report of US Army Engineer Waterway Experimental Station, Vicksburg, MS, 1982.

Toba Y. Local Balance in the air-sea boundary processes. I, J.Oceanog.Soc.Japan, 28, pp.109-120, 1972.

Toba Y. Local balance in the air-sea boundary processes. II, J.Oceanog.Soc.Japan, 29, pp.70-75, 1973.

Toba Y. Local balance in the air-sea boundary processes. III. On the spectrum of wind waves. J.Oceanog.Soc.Japan, 29, pp.209-220, 1973.

Zakharov V.E., Lvov V.S. and Falkovich J. Kolmogorov spectra of wave turbulence, Springer-Verlag, 1992.

Zakharov V.E. and Filonenko N.N. The energy spectrum for stochastic oscillation of a fluid surface, Doklady Akademii Nauk, 170, pp.1292-1295, 1966.

Zakharov V.E. and Zaslavskii M.M. The kinetic equation and Kolmogorov spectra in the weak-turbulence theory of wind waves, Izv.Atm.Ocean.Phys., 18, pp.747-753, 1982.

Zakharov V.E., Pushkarev A.N. Diffusion model of interacting gravity waves on the surface of deep fluid, Nonlin.Proc.Geophys., 6, pp.1-10, 1999.

Van Vledder G., Private communication

Webb D.J. Non-linear transfer between sea waves. Deep Sea Research, 25, pp.279-298, 1978.

Weak turbulent theory of the wind-generated gravity sea waves I. Direct Cascade

A. Pushkarev[1], D. Resio[2] and V. Zakharov[1,3,4]

February 12, 2002

[1] Waves and Solitons LLC, 918 W. Windsong Dr., Phoenix, AZ 85045, USA
[2] Coastal and Hydraulics Laboratory, U.S. Army Engineer Research and Development Center, Halls Ferry Road, Vicksburg, MS 39180, USA
[3] Landau Institute for Theoretical Physics, Moscow, 117334, Russia
[4] Department of Mathematics, University of Arizona, Tucson, AZ 85721, USA

PACS codes: **92.10.H, 05.45, 92.10.L, 42.65.H,K**

Abstract

We performed numerical simulation of the kinetic equation describing behavior of an ensemble of random-phase, spatially homogeneous gravity waves on the surface of the infinitely deep ocean. Results of simulation support the theory of Weak Turbulence not only in its basic points, but also in many details.

The Weak Turbulent theory predicts that the main physical processes taking place in the wave ensemble are down-shift of spectral peak and "leakage" of energy and momentum to the region of very small scales where they are lost due to local dissipative processes. Also, spectrum of energy right behind the spectral peak should be close to the weak-turbulent Kolmogorov spectrum which is the exact solution of the stationary kinetic (Hasselmann) equation. In a general case, this solution is anisotropic and is defined by two parameters - fluxes of energy and momentum to high wave numbers. Even in the anisotropic case the solution in the high wave number region is almost proportional to the universal form ω^{-4}. This result should be robust with respect to change of the parameters of forcing and damping.

In all our numerical experiments, the ω^{-4} Kolmogorov spectrum appears in very early stages and persists in both stationary and non-stationary stages of spectral development. A very important aspect of the simulations conducted here was the development of a quasi-stationary wave spectrum under wind forcing, in absence of any dissipation mechanism in the spectral peak region. This equilibrium is achieved in the spectral range behind the spectral peak due to compensation of wind forcing and leakage of energy and momentum to high wave numbers due to nonlinear four wave interaction. Numerical simulation demonstrate slowing down of the shift of the spectral peak and formation of the bimodal angular distribution of energy in the agreement with field and laboratory experimental data. More detailed comparison with the experiment can be done after developing of an upgraded code making possible to model a spatially inhomogeneous ocean.

1 Introduction

The phenomenon of wind-generated gravity waves on the sea surface is a very interesting object not only for oceanographers, naval architects and coastal engineers. It is also a subject of fundamental interest for the physicists. The ocean waves is the most conspicuous natural example of weakly nonlinear waves in a strongly dispersing media.

Indeed, on a deep water the dispersion relation is $\omega = \sqrt{gk}$, thus the dispersion is very strong. The level of nonlinearity could be measured by the characteristic steepness, $\mu = ka$ (k is an average wave number and a is a wave amplitude). Numerous observational data show that typically, $\mu \simeq 0.1$ (see, for instance [1]). Even in the

condition of a strong storm, μ rarely exceeds this limit. Meanwhile, the critical steepness of the Stokes waves is $\mu \simeq 0.45$. Thus, the level of nonlinearity of the ocean waves is small or at least moderate. This statement is very much enhanced by the predictions of the weakly nonlinear statistical theory. According to this theory a characteristic time of evolution of the wave spectrum is

$$\tau \simeq \frac{1}{\omega \mu^4}.$$

Even for $\mu \simeq 0.1$ this time is equal 10^4 wave periods.

The weakly nonlinear statistical ensemble of surface gravity waves can be described by the theory of weak turbulence. This theory is quite universal and is applicable to a very broad scope of physical phenomena, including waves in plasmas, waves in liquid super-fluid Helium, a Rossby waves, and acoustic waves. The references can be found in the monograph [2]. And this list is far from being complete.

The theory of weak turbulence is far advanced analytically. In this theory the evolution of basic correlation functions is described in terms of kinetic equations for the wave action. These kinetic equations are nothing but standard kinetic equations for bosons, traditionally used in statistical physics since twenties. The new point is the following: we deal now not with thermodynamically equilibrium solutions, which are not relevant for description of a real wave turbulence, but focus our interest on Kolmogorov-type solutions. These solutions carry a finite amount of constants of motion (energy, momentum, wave numbers) from the region in k-space, where they are generated, to the region where they are accumulated or absorbed by some kind of dissipation mechanism. In the theory of weak turbulence we study these equations in the limit of very high occupation numbers, where the equations become homogeneous with respect to the distribution function (quadratic, cubic, etc). As a result, in most physical situations the Kolmogorov-type solutions are power-like functions.

The analytical theory of weak turbulent Kolmogorov solutions has been studied in details, but the experimental and the numerical justifications of this theory cannot be considered as being sufficient. There is only one physical situation, the capillary wave turbulence, where the weak-turbulent theory is strongly supported by the experiment and the numerical simulation [3], [4], [5].

It is extremely challenging and attractive to apply the theory of weak turbulence to such a great natural laboratory as the world ocean. In this article we make a step in this direction. We present here our numerical experiments on solution of the Hasselmann's kinetic equation for gravity waves on a deep sea. We show that these experiments completely confirm the prediction of the wave turbulent theory. First of all, they confirm the fundamental role of the universal Kolmogorov spectrum $\varepsilon_\omega \simeq \omega^{-4}$, which was found by Zakharov and Filonenko in 1966 [6]. They make it possible to explain in a natural way a lot of experimental data accumulated in the physical oceanography for decades.

2 General consideration

Let $\eta(\vec{r},t)$ is a surface elevation, $\psi(\vec{r},t)$ is a potential on the surface. We assume that density of the fluid $\rho = 1$. The complex amplitude of propagating waves is given by formula:

$$a_k = \frac{1}{\sqrt{2}}\left[\left(\frac{g}{k}\right)^{1/4}\eta_k - i\left(\frac{k}{g}\right)^{1/4}\psi_k\right] \tag{2.1}$$

In the pair of correlation functions,

$$< a_k a^*_{k'} >= g N_k \delta_{k-k'},$$

N_k is a spectral density of the wave action. This definition of wave action is common in oceanography. It has dimension $N_k \sim L^4 T$. The Hamiltonian describing the motion of fluid is a functional that includes terms of all orders in expansion on a_k, a^*_k. One can perform the canonical transformation to new variables b_k, excluding the cubic terms in the Hamiltonian. For new variables b_k we have

$$< b_k b^*_{k'} >= g n_k \delta_{k-k'}. \tag{2.2}$$

The complex amplitude a_k is expressed through b_k as the power series, as well as N_k through n_k. Their cumbersome coefficients are presented in the Appendix I (see also [35]. The details of calculation can be found in Appendix III. The difference between N_k and n_k on a deep water is of the order μ^2, and can be neglected. In shallow water this difference is much more important.

If the nonlinearity is weak, the fluid is described by the Hamiltonian

$$H = \int \omega_k b_k b^*_k dk + \frac{1}{4}\int T_{kk_1k_2k_3} b^*_k b^*_{k_1} b_{k_2} b_{k_3} \delta_{k+k_1-k_2-k_3} dk dk_1 dk_2 dk_3. \tag{2.3}$$

Here T is a homogeneous function of third order,

$$T(\epsilon k, \epsilon k_1, \epsilon k_2, \epsilon k_3) = \epsilon^3 T(k, k_1, k_2, k_3).$$

The explicit formula for $T_{kk_1k_2k_3}$ is in the Appendix II.

The kinetic equation for n_k reads

$$\frac{\partial n_k}{\partial t} = S_{nl} + \gamma(k) n_k. \tag{2.4}$$

This equation was derived by K.Hasselmann in 1962 [7],[8], and broadly applied in oceanography. Hasselmann erroneously considered that equation (2.4) is written for N_k, and this view is shared until now by most oceanographers. While the difference between n_k and N_k is relatively small for deep water, it becomes significant for shallow water.

In (2.4)

$$\begin{aligned} S_{nl} &= 2\pi g^2 \int_{|k_2|<|k_3|} |T_{kk_1k_2k_3}|^2 (n_{k_1} n_{k_2} n_{k_3} + n_k n_{k_2} n_{k_3} - n_k n_{k_1} n_{k_2} - n_k n_{k_1} n_{k_3}) \times \\ &\delta(\omega_k + \omega_{k_1} - \omega_{k_2} - \omega_{k_3}) \delta(\vec{k} + \vec{k_1} - \vec{k_2} - \vec{k_3}) dk_1 dk_2 dk_3. \end{aligned} \tag{2.5}$$

The function γ_k describes the active forcing by the wind and the damping due to the wave breaking. Due to complexity of these processes, this function should be found from the experiments. For large and moderate scales γ_k is dominated by the interaction with wind. Due to the large difference between air and water densities, γ_k is small and is of order

$$\frac{\gamma_k}{\omega_k} \simeq \epsilon \sim \frac{\rho_{air}}{\rho_{water}}. \tag{2.6}$$

From (2.4) one obtains $\mu \simeq \epsilon^{1/4}$, in accordance with experimental data. For the rate of the spectrum evolution one has

$$\omega\tau \simeq \frac{1}{\epsilon} \sim 10^3. \tag{2.7}$$

Applicability of the weak turbulent theory in a final degree comes from the small value of ϵ.

Hereafter the polar coordinates $\omega = \sqrt{gk}, \theta$ in k-plane are used. The wind velocity V defines the characteristic frequency $\omega_0 = g/V$. Even for a very weak wind, $V \simeq 1 - 2m/sec$, the characteristic frequency is by the order of magnitude less than the frequency $\omega_c \simeq 30Hz$, where the effects of capillarity become important. For $\omega < \omega_0$, γ is negative, small and unknown. It is defined by friction between sea surface and turbulent air boundary layer. For $\omega > \omega_0$, γ is positive due to Cherenkov-type excitation of waves by the wind. According to Donelan [9], one can put

$$\gamma(\omega, \theta) = \begin{cases} 0.2\epsilon(\frac{\omega}{\omega_0} - 1)^2 \omega \cos\theta & \cos\theta > 0, \ \omega > \omega_0 \\ 0 & otherwise \end{cases} \tag{2.8}$$

This expression can be trusted up to ω equal $5 \div 6\omega_0$. For higher frequencies experimental data are scarce, and the expression for $\gamma(\omega, \theta)$ is not clearly known.

If the wind is weak enough, $U < 5m/sec$, a wave breaking is absent, the sea surface is smooth, and $\gamma > 0$ at least up to $\omega \simeq \omega_{cap}$. For stronger winds, the effects of micro-scale and macro-scale (white capping) wave breaking make $\gamma < 0$ in the high enough frequency region (see [10]). In both cases there is an effective sink of wave energy in small scales. In the absence of wind velocity, this sink is realized either by excitation of capillary waves and their viscous dissipation, or by the wave breaking.

Existence of this sink leads to a conjecture that real physics of wind-driven waves on the sea surface can be compared with the physics of turbulence in the incompressible fluid at high Reynolds numbers. It is considered that kinetic equation (2.4), if $\gamma = 0$ has constants of motion. In the isotropic case case they are

$$E = \int \omega_k n_k dk \tag{2.9}$$

and a wave action

$$N = \int n_k dk \tag{2.10}$$

In the general case it also should preserve momentum

$$\vec{R} = \int \vec{k} n_k dk \tag{2.11}$$

In reality neither energy nor momentum are constants of motion. They "leak" to the region of high wave numbers (similar situation takes place in turbulence of incompressible fluid). Only wave action is the true constant of motion. Other conservation laws (of energy and momentum) are just formal. The problem of non-conservation of formal motion constants is discussed in details in the article of Pushkarev and Zakharov [15].

"Leakage" of energy to high wave numbers is clearly demonstrated practically by all numerical experiments of the Hasselmann equation, since pioneering works of Hasselmann and Hasselmann [16]. In a typical case angle-averaged S_{nl}

$$f(\omega) = \frac{1}{2\pi} \int_0^{2\pi} S_{nl} d\theta$$

is a "two-lobe" function. It has only one zero at $\omega = \omega_p$ and $f(\omega) > 0$ for $0 < \omega < \omega_p$ while $f(\omega) < 0$ for $\omega > \omega_p$. Preservation of both wave action and energy means that $f(\omega)$ satisfies simultaneously two conditions:

$$\int_0^{\infty} \omega^3 f(\omega) d\omega = 0 \tag{2.12}$$

$$\int_0^{\infty} \omega^4 f(\omega) d\omega = 0 \tag{2.13}$$

Apparently it is impossible if $f(\omega)$ is a "two-lobe" function. Integral (2.13) must be negative. We denote

$$\int_0^{\infty} \omega^4 f(\omega) d\omega = -\frac{g^2}{P} \tag{2.14}$$

Here P is the flux of energy to high wave-numbers. Inevitable presence of the flux lead us to the theory of Kolmogorov style.

In the Kolmogorov theory of turbulence the spectra are governed by fluxes of the constants of motion. Due to the presence of two constants of motion even in the isotropic case, the turbulence of gravity waves is qualitatively similar to turbulence of two-dimensional incompressible fluid, which is governed by fluxes of energy and enstrophy.

We should stress here the fundamental difference between weak (wave) and strong (hydrodynamic) turbulence. In the theory of turbulence Kolmogorov spectra are just a plausible hypothesis, which is not supported properly by rigorous arguments. In the theory of weak turbulence, Kolmogorov spectra appear as exact solution of equation

$$S_{nl} = 0 \tag{2.15}$$

For gravity waves on the surface of a fluid the most important Kolmogorov spectrum, describing the direct cascade of energy to high frequencies has a form

$$\varepsilon_\omega \simeq P^{1/3} \omega^{-4} \tag{2.16}$$

In 1966 Zakharov and Filonenko found that spectrum (2.16) satisfies equation (2.15). In 1972 spectra with this form were experimentally observed by Toba [11], who was not aware about the work of Zakharov and Filonenko. The interpretation of spectrum (2.16) as a Kolmogorov spectrum was published first in 1982 by Zakharov and Zaslavskii [12] and than propagated by Kitaigorodskii [13].

3 Weak turbulent Kolmogorov spectra

In this chapter we summarize the basic facts on weakly turbulent Kolmogorov spectra. We discuss solutions of the equation (2.15) and present these facts without detail analytical justification. This justification is referred to Appendix III in the brief form.

Naively, one can think that this equation has thermodynamic solutions of the form

$$n_k = \frac{T}{\omega_k + C} \tag{3.1}$$

In fact, in the considered case of gravity waves these solutions do not exist because of divergence of the integral (2.5) at large wave numbers. Let us call a function n_k "allowed" if the integrals in the operator $S_{nl}[n_k]$ are converged for both $k \to \infty$ and $k \to 0$.

To determine the class of allowed functions one put $k_1 \to \infty$, $k_3 \to \infty$. From the conditions

$$\vec{k} + \vec{k_1} = \vec{k_2} + \vec{k_3} \tag{3.2}$$

$$\omega_k + \omega_{k_1} = \omega_{k_2} + \omega_{k_3} \tag{3.3}$$

one can see that at $\vec{k_1} \to \infty$, $\vec{k_3} \to \infty$, k_2 remains finite ($|k_2| \sim |k|$).

The contribution $S_{nl}^{(1)}$ to the integral (2.5) comes from integration over large k_1, and can be written approximately as follows:

$$S_{nl}^{(1)} \simeq 2\pi g^2 n_k \int |T_{kk_1}|^2 n_{k_2} \delta(\omega_k - \omega_{k_2}) \left(\vec{k} - \vec{k_2}, \frac{\partial n}{\partial \vec{k_1}}\right) d\vec{k_1} d\vec{k_2} \tag{3.4}$$

$$T_{kk_1} = T_{kk_1,kk_2} \tag{3.5}$$

As far as (see Appendix II) $|T_{kk_1}|^2 \simeq k_1^2 k^4$ at $k_1 >> k$, integral (3.4) converges if

$$n_k < \frac{C}{k^3} \tag{3.6}$$

at $k \to \infty$. Thermodynamic solutions do not satisfy the condition (3.6).

Let $k_1 \to 0$. Due to (3.2) $k_2 \to 0$ as well. The contribution $S_{nl}^{(2)}$ provided by integration over small k_1,k_2 reads

$$\begin{aligned} S_{nl}^{(2)} \simeq\ & 2\pi g^2 \int n_{k_1} n_{k_2} \{|T_{k,k_1,k_2,k+k_1-k_2}|^2 (n_{k+k_1-k_2} - n_k) \delta(\omega_k + \omega_{k_1} - \omega_{k+k_1-k_2} - \omega_{k_2}) \\ +\ & |T_{k,k_2,k_1,k+k_2-k_1}|^2 (n_{k-k_1+k_2} - n_k) \delta(\omega_k + \omega_{k_2} - \omega_{k-k_1+k_2} - \omega_{k_1})\} dk_1 dk_2 \end{aligned} \tag{3.7}$$

The integrand should be expanded in Taylor series over k_1, k_2. First term of expansion vanishes due to the symmetry. In the second approximation kinetic equation transforms to the diffusion equation

$$\frac{\partial n}{\partial t} = div D(k) \nabla n \tag{3.8}$$

$$D(k) = \frac{\pi}{2} g^2 \int |T_{kk_1}|^2 n_k n_{k_1} (k_1 - k_2)^2 \delta(\omega_{k_1} - \omega_{k_2}) dk_1 k_2 \tag{3.9}$$

Suppose that $n_k \simeq k^{-s}$. Integral (3.9) converges if $s < \frac{19}{4}$. Thus n_k must satisfy the condition

$$n_k < \frac{C}{k^{19/4}}, \quad k \to 0 \tag{3.10}$$

Conditions (3.6), (3.10) define the class of allowed functions. In particular, the power-like function $n_k = k^{-x}$ is allowed if :

$$3 < x < \frac{19}{4} \tag{3.11}$$

Let us formulate the central results of the theory of weak turbulence:

Suppose that an ensemble of weakly-nonlinear waves in the space of dimension d is described by kinetic equation (2.4). Suppose that the following conditions are satisfied:

1. Equation (2.4) is invariant with respect to rotations in d-dimensional k-space. This condition implies that the dispersion law depends only on modulus of k: $\omega = \omega(|k|)$.
2. There is no characteristic length in the system. It implies that ω is a power-like function, while T is a homogeneous function of its arguments $\omega = |k|^\alpha$:

$$T(\epsilon k, \epsilon k_1, \epsilon k_2, \epsilon k_3) = \epsilon^\beta T(k, k_1, k_2, k_3) \tag{3.12}$$

In this case equation (2.15) has no more than four power-like solutions :

$$n_k = k^{-x_i}, \quad i = 1, ..., 4 \tag{3.13}$$

$$x_1 = \frac{2\beta}{3} + d, \quad x_2 = \frac{2\beta - \alpha}{3} + d, \quad x_3 = \alpha, \quad x_4 = 0 \tag{3.14}$$

The solutions are

$$n_1 \sim |k|^{-\frac{2\beta}{3} - d} \tag{3.15}$$

$$n_2 \sim |k|^{-\frac{2\beta - \alpha}{3} - d} \tag{3.16}$$

$$n_3 \sim \frac{T}{k^\alpha} \tag{3.17}$$

$$n_4 \sim \lambda = const, \quad \lambda = \lim_{\substack{T \to \infty \\ \mu \to \infty}} \frac{T}{\mu} \tag{3.18}$$

To find a real amount of power-like solutions, one should determine the class of functions, allowed by the S_{nl}. If this class does not include power-like functions, neither of solutions (3.15)-(3.18) is relevant for description of a real physical simulation. Suppose that power-like functions $n_k = k^{-x}$ are allowed if

$$s_1 < x < s_2 \tag{3.19}$$

The power-like solution $n_k \simeq k^{-x_i}$ is physically relevant if x_i belongs to this interval

$$s_1 < x_i < s_2 \tag{3.20}$$

In the case of gravity waves on deep water the conditions (3.6)-(3.10) are obviously satisfied and $\alpha = 1/2$, $\beta = 3$. Hence

$$x_1 = 4\ , \quad x_2 = \frac{23}{6}, \quad x_3 = \frac{1}{2}, \quad x_4 = 0 \tag{3.21}$$

According to (3.6), (3.10) $s_1 = 3$, $s_2 = \frac{19}{4}$. Thus $s_1 < x_1 < s_2$, $s_1 < x_2 < s_2$, while $x_3 < s_1$, $x_4 < s_1$ and only solutions can be used for description of real physical situations. These solutions are weak-turbulent Kolmogorov spectra. We define spectral density of energy by relation

$$\varepsilon_\omega d\omega = \omega(k) n(k) d\vec{k} = \frac{2\omega^4}{g^2} n(\omega, \theta) d\omega d\theta \tag{3.22}$$

In terms of energy density Kolmogorov spectra read :

$$\varepsilon_\omega^{(1)} = C_0 g^{4/3} P^{1/3} \omega^{-4} \tag{3.23}$$

$$\varepsilon_\omega^{(2)} = q_0 g^{4/3} Q^{1/3} \omega^{-11/3} \tag{3.24}$$

In (3.23)-(3.24), P is the energy flux to high wave-numbers, Q is the wave action flux to small wave numbers. C_0 and q_0 are dimensionless Kolmogorov constants.

According to (3.22)

$$n_k^{(1)} = \frac{C_0}{2g^{2/3}} P^{1/3} k^{-4} \tag{3.25}$$

$$n_k^{(2)} = \frac{q_0}{2g^{1/2}} Q^{1/3} k^{-23/6} \tag{3.26}$$

From (2.1) one obtains

$$\eta_k = \frac{1}{\sqrt{2}} \left(\frac{k}{g}\right)^{1/4} (a_k + a_{-k}^*) \tag{3.27}$$

Hence

$$I_k = < |\eta_k|^2 > = \frac{1}{2} (gk)^{1/2} (N_k + N_{-k}) \tag{3.28}$$

Here $I_k = I_{-k}$ is the spatial spectrum. For deep water one can neglect the difference between N_k and n_k and put according to (3.25), (3.26), (3.28)

$$I_k^{(1)} = \frac{C_0}{2}\frac{g^{3/2}P^{1/3}}{k^{7/2}} \tag{3.29}$$

$$I_k^{(2)} = \frac{q_0}{2}\frac{g^{3/2}Q^{1/3}}{k^{10/3}} \tag{3.30}$$

Power-like isotropic Kolmogorov spectra are not unique solutions of the equation (2.15). One has to expect that this equation has also anisotropic power-like Kolmogorov spectrum

$$\varepsilon_\omega^{(3)} = M^{1/3} f(\theta)\omega^{-13/3} g^{5/3} \tag{3.31}$$

Here M is the flux of momentum along the x-axis to the high-frequency region. In (3.31) $f(\theta)$ is an unknown function of angle with respect to real axis which cannot be found analytically in a general case. It can be done for special "diffusion" model (see Zakharov and Pushkarev [14]).

Moreover, from the symmetry consideration one has

$$f(-\theta) = -f(\theta) \tag{3.32}$$

hence his function is not positively defined and cannot be a model of any real spectrum.

More general Kolmogorov-type solutions are governed by more than one flux of motion constants. Even in the isotropic case a general solution of (2.15) must have a form

$$\varepsilon_\omega = \frac{g^{4/3}P^{1/3}}{\omega^4} F\left(\frac{\omega Q}{P}\right) \tag{3.33}$$

where $F(\xi)$ - some unknown positive function, satisfying the conditions $\xi = \frac{\omega Q}{P}$. Here P is the flux of energy originated by sources concentrated at $k \to \infty$, Q is the flux of wave action, coming from infinity.

Then:

$$F(0) = C_0 \tag{3.34}$$

$$F(\xi) \to q_0 \xi^{1/3}, \quad \xi \to \infty \tag{3.35}$$

Spectrum (3.33) describes the situation when there is the source of energy P in small frequencies and source of wave action Q in high frequencies.

The most general Kolmogorov solution of equation

$$S_{nl} = 0$$

has the form

$$\varepsilon_\omega = \frac{g^{4/3}P^{1/3}}{\omega^4} G\left(\frac{\omega Q}{P}, \frac{gM}{\omega P}, \theta\right) \tag{3.36}$$

Here G is some function of three variables to be found numerically by solution of the system of nonlinear integral equations imposed on Fourier component of angular-frequency spectrum (see Appendix III). We plan to undertake a full-scale numerical experiment for definition of this function. Some particular properties of this function, however, can be found analytically.

General Kolmogorov spectrum (3.36) appears in the case when one has sources of energy and momentum P, M at small wave-numbers together with the source of wave action Q at high wave-numbers. In the situation we are discussing (direct cascade) there is no flux of wave action from infinity, and $Q = 0$. In this case one has

$$\varepsilon_\omega = \frac{g^{4/3}P^{1/3}}{\omega^4} H\left(\frac{gM}{\omega P}, \theta\right) \tag{3.37}$$

Let us introduce dimensionless parameter $\xi = \frac{gM}{\omega P}$. For completely isotropic spectrum $M = 0$, hence $\xi = 0$. One can say that value of ξ characterizes a degree of anisotropy. For small values of ξ function H can be expanded in Taylor series

$$H = H_0(\theta) + H_1(\theta)\xi + ... \tag{3.38}$$

Apparently, $H_0(\theta) = C_0$ does not depend on θ. This is just the Kolmogorov constant, introduced in (3.23). One can prove that $H_1(\theta) = C_1 \cos\theta$ [2].

The constants C_0, C_1 can be called the first and and the second Kolmogorov constants. We established that for small ξ

$$\varepsilon_\omega = \frac{g^{4/3}P^{1/3}}{\omega^4}\left(C_0 + C_1\frac{M}{\omega P}\cos\theta + ...\right) \tag{3.39}$$

This case is realized at any values of M, P if $\omega \to \infty$. Hence the spectrum (3.36) becomes completely isotropic at large values of ω.

One can determine $H(\xi,\theta)$ at very large values of ξ. In this "extremally" anisotropic case the spectrum is governed by a single parameter M and its dependence of the flux of energy P should be dropped out. It means that in this limit $H(\xi,\theta) \to \xi^{1/3}f(\theta)$ at $\xi \to \infty$ and formula (3.37) goes to the formula (3.31).

In reality the simple formula (3.39) gives a reasonable approximation to observed spectra. Banner [1] found, by analysis of the experimental data that the averaged by angles spectrum behave like ω^{-4}, while the one-dimensional slice at $\theta = 0$ goes to zero faster. Banner assumes that its behavior obeys the Phillips law ω^{-5}. Another words, according to Banner

$$\frac{\varepsilon_\omega(0)}{<\varepsilon_\omega>} \simeq \frac{1}{\omega} \tag{3.40}$$

According to our formula (3.39)

$$\frac{\varepsilon_\omega(0)}{<\varepsilon_\omega>} \simeq C_0 + \frac{C_1 M}{P\omega} \tag{3.41}$$

This is the decreasing function of ω as well and our results coincide with Banner's results at least on a qualitative level. However, the difference due to presence of constant C_0 in our formula (3.41) is very essential. C_0 is the Kolmogorov constant, which certainly cannot be zero.

4 Matching with sources and non-stationary behavior

Now we discuss under what conditions weak-turbulent Kolmogorov spectra can be realized in a physical situation. We will discuss only the "direct cascade", which is described in a general anisotropic case by the spectrum (3.37). First and foremost condition for realization of this spectrum is an efficient sink in the high-frequency domain. For surface waves this sink is provided by generation of capillary waves or wave breaking. In the framework of the model (2.4) the sink is described by $\gamma(k) < 0$ at $|k| > k_d$, $\gamma(k) \to -\infty$ if $|k| \to \infty$.

Like in the Kolmogorov theory of turbulence in incompressible fluid, a detailed shape of $\gamma(k)$ is not important. Damping coefficient $\gamma(k)$ just must absorb fluxes of energy and momentum coming from small frequency region. In the conditions of full absorption

$$P = -\int\limits_{|k|>k_d} \gamma(k)\omega(k)n(k)dk \tag{4.1}$$

$$M = -\int\limits_{|k|>k_d} \gamma(k)kn(k)dk \tag{4.2}$$

The ideal conditions for realization of Kolmogorov spectrum (3.37) takes place if the region of instability, where $\gamma(k) > 0$, is localized in the domain

$$k_0 < k < k_1 \tag{4.3}$$

and $k_1 << k_d$. To provide absorption of the inverse cascade which is forming at $k < k_0$, one should have damping at $k < k_0$. Thus $\gamma(k) < 0$ at $k < k_0$.

In this situation one can expect formation of a stationary spectrum, obeying the equation

$$S_{nl} + \gamma(k)n_k = 0 \tag{4.4}$$

A shape of the spectrum in the region $0 < k < k_1$ can not be predicted from the general principles. But in the "window of transparency"

$$k_1 < k < k_d \tag{4.5}$$

one expects the appearance of a Kolmogorov spectrum (3.37), defined by the fluxes P, M.

By integrating (4.4) one has

$$P = \int\limits_{|k|<k_1} \omega_k\gamma_k n_k dk \tag{4.6}$$

$$P = -\int\limits_{|k|<k_1} \omega_k S_{nl} dk \tag{4.7}$$

In a similar way

$$M = \int\limits_{|k|<k_1} \gamma_k k \cos\theta n_k dk \tag{4.8}$$

$$M = -\int\limits_{|k|<k_1} k \cos\theta S_{nl} dk \tag{4.9}$$

Thus we have three different ways for calculation of the fluxes P, M.

We want to point out that localization of instability in small wave number is the sufficient, but not the necessary condition for forming Kolmogorov spectrum of the inverse cascade. The income of energy ε^+ is defined by formula

$$\varepsilon_k^+ = \gamma(k)\omega(k)n(k) \tag{4.10}$$

includes product of $\gamma(k)$ and $n(k)$. Even if $\gamma(k)$ grows at large k, the product $\gamma(k)\omega(k)n(k)$ could be concentrated at small k.

Let us suppose that there is no damping in small k. In this case no stationary state can be established. In the region $k < k_0$ one will observe formation of the inverse cascade, propagating like a front toward $k \to 0$. Meanwhile, in $k \geq k_0$ a stationary state will be reached in a finite time. Formulae (4.1)-(4.2) as well as (4.7)-(4.9) remain valid, while formulae (4.6) and (4.8) are not correct anymore.

Propagation of the inverse cascade front is described by self-similar solution of equation

$$\frac{\partial n}{\partial t} = S_{nl} \tag{4.11}$$

It has the following self-similar solution

$$n = t^\alpha U\left(kt^\beta\right) \tag{4.12}$$

where α and β are connected by relation

$$2\alpha + 1 = \frac{19}{2}\beta \tag{4.13}$$

To determine α, β one should use some additional information about the solution. In the case of inverse cascade this information can be extracted from the fact that there is no flux of wave action to high frequencies if $k_1 << k_d$. All gained wave action is deposited to the wave ensemble. Assuming that in the instability region $k \sim k_0$ the stationary state is reached, one has

$$N = \int n_k dk \sim t \tag{4.14}$$

Hence

$$\alpha - 2\beta = 1, \quad \beta = \frac{6}{11}, \quad \alpha = \frac{23}{11} \tag{4.15}$$

Solution (4.12) takes a form

$$n = t^{23/11} U\left(kt^{6/11}\right) \tag{4.16}$$

and the front propagates to small k according to the law

$$k_f \sim t^{-6/11} \tag{4.17}$$

The region $k \sim 0$ has "infinite capacity" and can absorb infinite amount of wave energy.

At $k \simeq k_1$ solution (4.12) should be matched with the Kolmogorov spectrum (3.37) with some fluxes P, M which are formed in the instability region.

Another important self-similar solution describes the evolution of "swell" or water waves in the absence of any type of sources. In this case wave action is preserved, while energy and momentum leak to $k \to \infty$. Preservation of N implies

$$\alpha = 2\beta, \quad \beta = \frac{2}{11}, \quad \alpha = \frac{4}{11} \tag{4.18}$$

Self-similar solution has the form

$$n = t^{4/11} U\left(kt^{2/11}\right) \tag{4.19}$$

It describes down-shift of wave maximum

$$k_m \simeq t^{-2/11} \tag{4.20}$$

Total energy and momentum of solution (4.19) decreases as

$$\varepsilon \simeq t^{-1/11}, \quad M \simeq t^{-2/11} \tag{4.21}$$

Finally we discuss a self-similar solution describing formation of direct cascade Kolmogorov spectrum. An additional constrain on α, β can be found from the assumption that at small k Kolmogorov spectrum is already established. In this area n does not depend on time, and $U \simeq \xi^{-4} \sim 1/k^4$. It might happen only if

$$\alpha = 4\beta, \quad \alpha = \frac{2}{3}, \quad \beta = \frac{8}{3} \tag{4.22}$$

Corresponding solution has a form

$$n = (t_0 - t)^{\frac{8}{3}} U\left(k(t_0 - t)^{\frac{2}{3}}\right) \tag{4.23}$$

Formula (4.23) describes propagation of the "shock" wave to the high-frequency region. A trajectory of the shock

$$k_M \simeq \frac{1}{(t - t_0)^{2/3}} \tag{4.24}$$

This shock is self-accelerating. It reaches infinity in a finite time and Kolmogorov spectrum ω^{-4} is established in the explosive way.

Finally, let us perform an elementary derivation of the Kolmogorov spectrum ω^{-4}. To do this, we return back to the stationary equation (4.4). Let k_s be some wave number inside the interval of transparency $k_1 < k_s < k_d$. Multiplying (4.4) by ω_k and integrating by the domain $|k| < k_s$, one find for the local value of energy flux

$$P(k_s) = \int_{|k|<k_s} \omega_k S_{nl} dk \tag{4.25}$$

The other hand, $\gamma_k = 0$ if $k_1 < k < k_d$. Hence, P is defined by formulae (4.6)-(4.7).

Let us assume that

$$n_k = C_0 P^{1/3} k^{-x}, \quad 3 < x < 19/4 \tag{4.26}$$

Plugging (4.26) into (4.25) and taking into account convergence of the operator S_{nl} on this class of allowed functions, one find from dimension consideration

$$P(k_s) = P C_0^3 \lambda k_s^{12-3x} \tag{4.27}$$

As far as the flux $P(k_s)$ does not depend on k_s, one find

$$x = 4 \tag{4.28}$$

$$C_0 = \lambda^{-\frac{1}{3}} \neq 0 \tag{4.29}$$

Comparing with (3.22) one can see that we obtained again Zakharov-Filonenko spectrum $\varepsilon \simeq \omega^4$. Due to convergence of S_{nl}, λ is finite and $C_0 \neq 0$.

Note that for the Phillips spectrum $\varepsilon_\omega \simeq \omega^{-5}$ gives $\lambda = 9/2$. In this case

$$P(k_s) \simeq k_s^{-3/2} \tag{4.30}$$

$$\tag{4.31}$$

and $P(k_s) \to 0$ at $k_s \to \infty$.

Another words, Phillips asymptotic means that energy is preserved and there is no leakage of energy to small scales. This point is in contradiction with the Kolmogorov picture of weak turbulence. We would like to make clear that the Phillips asymptotic ω^{-5} never can be obtained as the solution of the Hasselmann's equation.

Anyway, experimentalists systematically observe ω^{-5} tails in spectra of gravity waves, both in laboratory and in the ocean (Forrestall [26], Kitaigorodski [13]). On our opinion, these tails appear in the conditions when local steepness is close to critical and the kinetic Hasselmann's equation in this case is not applicable, because the level of nonlinearity is very high.

Our slogan is :

"Hasselmann equation and ω^{-5} spectrum are incompatible things".

5 Numerical simulation

Numerical integration of kinetic equation for gravity waves on deep water (Hasselmann equation) was the subject of considerable efforts for last three decades. The "ultimate goal" of the effort – creation of the operational wave model for wave forecast based on direct solution of the Hasselmann equation, happened to be extremely difficult computational problem due to mathematical complexity of S_{nl} term, which require calculation of three-dimensional integral at every advance in time.

Historically, numerical methods of integration of kinetic equation for gravity waves exist in two "flavors". First one is associated with works of Hasselmann and Hasselmann [16], Dungey and Hui [17], Masuda [18]-[19], Lavrenov [20], Polnikov [21] and is based on transformation of 6-fold into 3-fold integrals using δ-functions . Such transformation leads to the appearance of integrable singularities, which creates additional difficulties in calculations of S_{nl} term.

All numerical experiments show that angle-averaged S_{nl} is "two-lobe" function and consequently support the Kolmogorov scenario of wave turbulence. In some experiments (Masuda [18],[19]; Polnikov [21]) the Kolmogorov asymptotic ω^{-4} was observed.

Second type of models developed in works of Webb [22] and Resio and Perrie [23] uses direct calculation of resonant quadruplet contribution into S_{nl} integral based on the following property: given fixed two vectors $\vec{k}$, $\vec{k_1}$, another two $\vec{k_2}$, $\vec{k_3}$ are uniquely defined by the point "moving" along the resonant curve - locus.

Numerical simulation in current work was performed with the help of modified version of second type algorithm. Calculations were made on grid 71x36 points in the frequency-angle domain $[\omega, \theta]$ with exponential distribution of points in frequency domain and uniform distribution of points in the angle direction.

We performed two series of experiments. In the first one we put in equation (2.4) an "artificial" driving and damping, which provide relatively broad "window of transparency". We assumed that damping is isotropic while instability can be either isotropic or anisotropic. These experiments are pure "academic". Their results cannot be applied to physical oceanography directly. They are designed to examine applicability of the weak turbulent theory and to validate a fundamental importance of weak turbulent Kolmogorov spectra. In these experiments we made calculation of the first and the second Kolmogorov constants.

Second series of experiments is modeling of the realistic case where equation (2.4) is supplied with wind-driven instability.

All cases of simulation started from uniformly distributed low level noise. Having in mind an application to real wind-driven sea waves we calibrate time of evolution in hours. Criterion for stop of the calculations was reaching of stationary or asymptotic regimes. Simulation was performed on Compaq Presario 1700 notebook computer featuring 850 Pentium III CPU with 256 Mb of RAM. Typical time of calculations varied between several dozens hours and several days.

5.1 Isotropic case

In the isotropic case

$$\gamma(\omega,\theta) = \begin{cases} C_1 \exp\left(-\left(\frac{\omega-\omega_0}{0.19}\right)^4\right) & if \;\; 0.63 < \omega < 1.26 \\ -C_2(\omega - 0.63)^2 & if \;\; \omega < 0.63 \\ -C_3\,(\omega - 5.65)^2 & if \;\; \omega > 5.65 \end{cases} \tag{5.1}$$

where C_i, $i = 1, 2, 3$ are positive constants. Coefficient C_1 at (5.1) is defined from the condition of the smallness of the growth rate with respect to the corresponding local frequency. Negative components of (5.1) are high and low frequency damping terms, the only purpose of which is to absorb direct (energy) and inverse (wave action) cascades. Constants C_2 and C_3 as well as the frequencies $\omega = 0.63$ and $\omega = 5.65$ are defined experimentally from the conditions of the effectiveness of the fluxes absorption and maximization of the inertial (forcing/damping rates free) interval with respect to ω.

Fig.1 show evolution of wave action as a functions of time. The picture indicates that there are three main stages associated with system evolution: instability development, saturation at $t = 3.7$ hours, and final evolution into the stationary state. Energy demonstrates similar behavior.

Fig.2 shows logarithm of energy distribution against logarithm of frequency at different moments of time. One can see formation of ω^4 asymptotic at finite moment of time. We interpret this fact as a vigorous support of the weak-turbulent theory. We should stress that ω^{-4} asymptotic is very robust. Actually it appears in all our experiments.

According to the predictions of *Section 4*, formation of the ω^{-4} asymptotic is going by the explosive way. Energy spectra taken in four moments of time, closed to the moment of explosion are shown in Fig.3.

Next two figures display Kolmogorov flux of energy as a function of time measured by two different ways, by formula (4.1) (see Fig.5) and (4.6) (see Fig.4).

On the first stage energy grows exponentially until the "shock wave" in k-space reaches the Kolmogorov asymptotic. Then dissipation in high wave numbers explodes and the level of energy falls down and reaches its stationary asymptotic value.

Fig.6 presents the function

$$\frac{\omega^4}{2\pi P^{1/3} g^{4/3}} \int_0^{2\pi} \varepsilon(\omega, \theta) d\theta \tag{5.2}$$

which gives for the first Kolmogorov constant

$$0.35 < C_0 < 0.45 \tag{5.3}$$

Fig.6 shows that in the stationary state the spectrum has two different components - the Kolmogorov tail ω^{-4} and the sharp peak concentrated near the frequency $\omega \simeq 0.6$, corresponding to the lower edge of the instability region. Similar coexistence of "peak" and "tail" components is typical for wind-driven wave spectra, observed in the real ocean. In the standard JONSWAP spectrum a special parameter, determining peakedness is provided (see also Donelan, Hamilton and Hui [9]).

5.2 Anisotropic case

In the anisotropic case

$$\gamma(\omega, \theta) = \begin{cases} D_1 \exp\left(-\left(\frac{\omega-\omega_0}{0.19}\right)^4 - \left(\frac{\theta}{\pi/4}\right)^8\right) & if \ 0.63 < \omega < 1.26 \\ -D_2(\omega - 0.63)^2 & if \ \omega < 0.63 \\ -D_3\,(\omega - 5.65)^2 & if \ \omega > 5.65 \end{cases} \tag{5.4}$$

where D_i, $i = 1, 2, 3$ are positive constants, selected similarly to isotropic case. Fig.7 shows distribution of damping and instability defined by (5.4).

This numerical simulation was motivated by the following reasons:

1. We want to be assured that weak-turbulent Kolmogorov spectra are realized not only in isotropic case. We would like to be completely sure that they play the same key role for essentially anisotropic spectra as well.
2. We planned to check once more the value of the first Kolmogorov constant C_0 and be sure that it is the same as in the isotropic case.
3. We want to trace the difference between the angle-averaged spectrum and its slice at $\theta = 0$. We want also to find the value of the second Kolmogorov constant C_1.

The experiment shows that the stationary state is established similarly to the isotropic case. Typical saturation time for given forcing and damping is $t \simeq 0.68$ hour.

Fig.8-10 display line-levels of energy distribution at different moments of time. One can see that stationary picture is bimodal and has double spike. Similar double spike picture is typical for experimental results [24], [25].

Fig.11 demonstrate set of angle averaged energy distribution taken in different moments of time. They are very close to ω^{-4} law. Fig.12 presents one-dimensional slices at $\theta = 0$ for the energy distribution at the same times. Fig.13 presents ratio of one-dimensional slices of spectra to angle averaged spectra. One can see that one-dimensional spectra decay at $\omega \to \infty$ faster, than averaged energy spectrum, in accordance with Banner's observations [1]. We cannot identify, however, one-dimensional spectra with Phillips spectrum ω^{-5}. Their decay is more slow and not uniform in ω.

In the anisotropic case we also saw explosive formation of spectra tails, similar to the isotropic case. Fig.14 shows the energy spectrum development at four close equidistant time moments. As in the isotropic case one can notice that Kolmogorov spectrum establishment happens strongly non-uniformly in space and time and looks like the "shock" propagation, in accordance with (4.16).

Fig.15 shows the function $\frac{\omega^4}{P^{1/3}} \int_0^{2\pi} \varepsilon \cos\theta d\theta$. If the formula (3.39) is correct, this plot should be proportional to ω^{-1}. It easy to see that correspondence is quite good.

Fig.16 presents the function

$$\frac{\omega^4}{2\pi P^{1/3} g^{4/3}} \int_0^{2\pi} \varepsilon(\omega,\theta) d\theta \tag{5.5}$$

which gives the value of first Kolmogorov constant in anisotropic case

$$0.33 < C_0 < 0.37 \tag{5.6}$$

Fig.17 presents the function

$$\frac{P^{2/3}\omega^5}{\pi M g^{7/3}} \int_0^{2\pi} \varepsilon(\omega,\theta)\cos\theta d\theta \tag{5.7}$$

which gives the value of second Kolmogorov constant

$$0.18 < C_1 < 0.27 \tag{5.8}$$

Fig.16-17 show that in the anisotropic case we have again a combination of the spectral peak and the Kolmogorov-type tail.

5.3 Wind forcing case

In this chapter we present the results of modeling of the situation which is close to reality in maximum degree. We studied the surface waves excited by the wind in the angle-frequency domain $0 < \theta < 2\pi$ and $\omega_{min} < \omega < \omega_{max}$ where $\omega_{min} = 0.06$ and $\omega_{max} = 12.56$. Initial conditions is the noise in energy space $\varepsilon_\omega = 4 \cdot 10^{-5}$. Wind forcing and sink of energy at large ω are defined in accordance with (2.8) as:

$$\gamma(\omega,\theta) = \begin{cases} 2\cdot 10^{-4}(\frac{\omega}{\omega_0}-1)^2\omega\cos\theta & if\ \cos\theta > 0\ and\ \omega_0 < \omega < \omega_1 \\ -C(\omega-\omega_1)^2 & if\ \omega_1 < \omega < \omega_{max} \\ 0 & otherwise \end{cases} \tag{5.9}$$

where $\omega_0 = 0.94$ (corresponds to wind velocity $U \simeq 10.4 m/sec$) and $\omega_1 = 8.48$. High-frequency damping is used to simulate infinite-capacity phase volume at high wave numbers. Constant C and frequency ω_1 are defined experimentally from the condition of the effectiveness of the energy flux absorption at high frequencies. As in the reality, we did not provide any damping at small wave-numbers. Fig.18 shows distribution of damping and instability defined by (5.9).

We started our calculation from low-level noise and stopped them, when sea was close to its "mature state". As far as we know, nobody has performed similar experiments before.

The main purpose of our experiments is to prove that the weak-turbulent four-wave interaction of gravity waves is a powerful enough mechanism to stabilize the wind-driven instability at relatively low level $ka \simeq 0.1 \div 0.2$ and to provide fast enough down-shift of the peak of spectral density. This viewpoint is far from being widely accepted. Some authors (M.Stiassnie [44]) consider that the random phase four-wave interaction is too weak process to explain the rate of spectral evolution observed in real ocean. Many authors traditionally believe that stationary spectra could appear only as a result of saturation of the instability by wave-breaking.

To argue with these point, we deliberately did not include the effects of wave-breaking in our consideration. We will show that the income of energy and momentum from wind is mostly compensated by Kolmogorov fluxes of these constants of motion. Income of wave action cannot be stabilized, thus a whole process is non-stationary. But at large times all spectral grows is concentrated in very small wave numbers, while at finite wave numbers it reaches a quasi-stationary state, which slowly changes in time. We should stress that on the current stage of our work we cannot perform detailed comparison of our theory with experiments, because in the most real cases spectra are non-uniform in space. They depend essentially on "fetch" (distance from the shore) and are "fetch-limited". Experimental data, pertaining to the spatially-uniform ocean ("duration limited fetch") are scarce and note quite accurate. Some of this data are reviewed in the recent monograph of J.Young [45].

We performed comparison of our results with this data and found quite good coincidence. Anyway, we plan to perform the full-scale comparison of our numerical results with field and laboratory experiments as soon as we will have in our possession a numerical algorithm for modeling of non-stationary limiting fetch situation. Then we will consider more carefully possible role of wave-breaking in he balance of energy in the wind-driven sea.

In our experiments wind velocity was $10.4 m/sec$. The total duration of running was about $4h$ of physical time. We discuss below the results of these experiments. First of all, one can see that four-wave interaction is a

very powerful and fast mechanism of the instability saturation. Fig.19 presents total wave action as a function of time. After few minutes of exponential growth, described by linear theory, wave action stabilizes and turns into linear function of time.

Total energy H and significant wave height a_s defined by standard formula

$$a_s = 4\sqrt{H} \tag{5.10}$$

grow more slowly (Fig.20,21):

$$H(t) \simeq t^{0.79} \tag{5.11}$$

$$a_s(t) \simeq t^{0.39} \tag{5.12}$$

In the end of experiment a_s reaches the value $a_s \simeq 3m$.

Four-wave interaction provide efficient down-shift. Average frequency $< \omega >$ decays approximately as

$$< \omega > \simeq t^{-0.27} \tag{5.13}$$

and reaches the value $< \omega > \simeq 1.2Hz$, see Fig.22.

Dependence of the average slope on time $\mu =< ka >$ is presented on Fig.23. Here $a = \sqrt{2H}$ is a characteristic amplitude of the wave. One can see that in the initial stage of evolution a reaches its maximum value $\mu = 0.27$ and decreases slowly to $\mu = 0.15$. Fig.24, 25 demonstrate comparison of our calculations with experimental results presented in the book of J.Young [45].

One should stress that physical time of numerical experiment ($4h$) is moderate and even in the end of our calculations waves are relatively young. Recently we performed more long calculations and can pre-announce some new results. After $10h$ of physical time average frequency $< \omega >$ down-shifts to $0.6Hz$, while slope decreases down to $\mu \simeq 0.1$, in accordance with estimates obtained from analysis of experimental data.

Fig.26 presents level-lines of the spectral density at the end of calculations. The spectral peak is narrow in angle and is concentrated inside the range $< \delta\theta >< 30^0$. The spectral tail is more broad. Fig.27 presents evolution of averaged spectra in logarithmic scale. It is clear that spectral tail is close to ω^{-4}. On the Fig.28 "compensated" spectra $\omega^4 \varepsilon_\omega$ are plotted in natural scale. Fig.29 presents one-dimensional slices of wave energy in different moment of time. Fig.30 presents ratio of one-dimensional spectra to averaged spectrum in natural scale. One can see that one-dimensional spectra decay faster than average in accordance with Banner's observation.

Pictures Fig.31-33 demonstrate contribution of different terms in equation

$$\frac{\partial n}{\partial t} = S_{nl} + \gamma_k n_k \tag{5.14}$$

in three different moments of time. One can see that in area of spectral maximum $\frac{\partial n}{\partial t}$ is almost equal to S_{nl} and forcing terms are small even in the initial stage of the process. On the contrary, in the area of spectral tail, time derivative of action is very small, and instability term $\gamma_k n_k$ is compensated by nonlinear interaction term S_{nl}. In this case the spectrum is quasi-stationary. These figures clearly demonstrate that S_{nl} alone arrests the growth of instability on the very low level. To make this fact more conspisious, we present the same picture in natural scales on Fig.34-36, performing zoom on the vertical axis.

Fig.37-39 present fluxes of action, energy and momentum

$$Q(\Omega) = \frac{2}{g^2} \int_0^{2\pi} \gamma n \omega^3 d\omega d\theta \tag{5.15}$$

$$P(\Omega) = \frac{2}{g^2} \int_0^{2\pi} \gamma n \omega^4 d\omega d\theta \tag{5.16}$$

$$M(\Omega) = \frac{2}{g^3} \int_0^{2\pi} \gamma n \omega^5 \cos\theta d\omega d\theta \tag{5.17}$$

as the functions of current frequency Ω.

All three fluxes reach their maximum values at the end of the range of instability. Thus $Q_{max}, P_{max}, M_{max}$ are total income of motion constants from the wind per unit of time. Apparently, $Q_\infty, P_\infty, M_\infty$ taken at the

end of damping region can be identified with time derivatives of total action, energy and momentum. One can see that at the end of calculation

$$\frac{Q_\infty}{Q_{max}} \simeq 0.80 \tag{5.18}$$

$$\frac{P_\infty}{P_{max}} \simeq 0.45 \tag{5.19}$$

$$\frac{M_\infty}{M_{max}} \simeq 0.29 \tag{5.20}$$

Weak turbulent theory predicts that at $t \to \infty$ ratios $\frac{P_\infty}{P_{max}} \to 0$, $\frac{M_\infty}{M_{max}} \to 0$, while $\frac{Q_\infty}{Q_{max}} \to \lambda < 1$, where λ is some constant.

Another words, for very developed sea waves almost all energy and momentum are transferred from air to sea are carried by Kolmogorov fluxes to high frequency region. Our calculation clearly demonstrate this tendency.

6 Conclusions

The method presented here for numerical solution of Hasselmann's kinetic equation for gravity waves makes it possible to solve this equation in a broad domain that covers more than two decades in frequency. This algorithm makes it possible to perform $10^4 \div 10^5$ time steps without accumulating significant error or developing any instabilities. Results based on the numerical simulations conducted here support the theory of Kolmogorov spectra for weak turbulence not only in its basic points but also in many details. Some key conclusions from our investigation are as follows:

1. In accordance with weak-turbulence theory, we found that energy and momentum of the wave ensemble are not preserved. Both of these quantities are "leaked" to the region of very small scales where it is assumed that they are lost due to local dissipative processes (wave breaking, generation of capillary waves, etc.). This leakage is an important part of the formation of the universal Kolmogorov spectrum.
2. Directionally integrated energies in the equilibrium range are proportional to ω^{-4}. This result is very persistent; and in all numerical experiments, the ω^{-4} Kolmogorov spectrum appears in very early stages of the simulation and persists in both stationary and non-stationary stages of spectral development.
3. A very important aspect of the simulations conducted here was the development of a quasi-stationary wave spectrum under wind forcing, without the need for a dissipation mechanism in the spectral peak region. Previous investigations (for example Komen et al. [37] and Banner and Young [38]) have been unable to achieve this result and consequently concluded that wave breaking in the spectral peak region must be an important component in developing fully-developed seas. Our results suggest that primary wave dissipation region is most likely located only in the high-frequency tail of the spectrum.
4. Fluxes of momentum and energy through the equilibrium range (Kolmogorov region) of the wave spectrum are observed to produce a bimodal angular distribution of energy at high frequencies. This is consistent with observations of sea waves in nature (Hwang [24]).

It should be recognized here that our results are consistent with several previous empirical investigations. First of all, behavior of integral characteristics of wave ensemble (average energy and mean frequency) is in accordance with experimental data on limited duration observations. Laboratory data from the classic study of Toba [11], clearly showed that wave spectra at laboratory scales contain characteristic ω^{-4} equilibrium ranges, rather than the ω^{-5} form initially hypothesized by Phillips [39] and adopted into many early spectral parameterizations of ocean spectra (Pierson and Moskowitz [40] and Hasselmann et al. [41]). More recent studies, including Mitsuyasu et al. [42], Forristall [26], Donelan et al. [9] and Battjes et al. [31], have all shown that the equilibrium range in deep-water ocean waves follows an ω^{-4} form. Resio et al. [43] have shown that the infinite-depth form for the equilibrium form is $k^{-5/2}$, which is also consistent with the Kolmogorov spectrum and asymptotically approaches ω^{-4} form in deep water.

The findings here are quite robust and hopefully will be applied to the practical problems. Present wave prediction models are based on fairly crude parameterizations of the nonlinear energy transfers. In large part due to inaccuracies in these parameterizations, these models have had to include strong dissipation in the spectral peak region to inhibit wave growth as full development is approached. Possibly because of the dominance of the dissipative term in the energy balance near full development, these models consistently under-predict wave heights in larger storms. Results from this study could be used to reformulate the complete energy balance

equation for wave generation, propagation and decay which could lead to substantially improved predictions in the near future.

The research presented in this paper was conducted under the U.S. Army Corps of Engineers, RDT&E program, grant DACA 42-00-C0044, ONR grant N00014-98-1-0070 and NSF grant N... . The Chief of Engineers has granted permission for publication. This support is gratefully acknowledged.

The authors are grateful to I.Lavrenov for valuable comments.

7 Appendix I

Presented formulae are valid for any depth. They are taken from the article [35]. Variables ψ, ω are canonical. They obey the Hamiltonian equations

$$\begin{aligned}\frac{\partial \eta}{\partial t} &= -\frac{\delta H}{\delta \Psi}\\ \frac{\partial \Psi}{\partial t} &= \frac{\delta H}{\delta \eta}\end{aligned}$$

H is the total energy of fluid. It is presented by the series in powers of characteristic slope ka in terms of Fourier transforms:

$$\begin{aligned}H &= H_0 + H_1 + H_2 + ...\\ H_0 &= \frac{1}{2}\int \left[A_k|\Psi_k|^2 + B_k|\eta_k|^2\right] dk, \quad A_k = k\tanh(kh), \quad B_k = g\\ H_1 &= \frac{1}{2(2\pi)}\int L^{(1)}(\vec{k_1},\vec{k_2})\Psi_{k_1}\Psi_{k_2}\delta(\vec{k_1}+\vec{k_2}+\vec{k_3})dk_1dk_2dk_3\\ H_2 &= \frac{1}{2(2\pi)^2}\int L^{(2)}(\vec{k_1},\vec{k_2},\vec{k_3},\vec{k_4})\Psi_{k_1}\Psi_{k_2}\eta_{k_3}\eta_{k_4}\delta(\vec{k_1}+\vec{k_2}+\vec{k_3}+\vec{k_4})dk_1dk_2dk_3dk_4\end{aligned}$$

where

$$L^{(1)}(\vec{k_1},\vec{k_2}) = -(\vec{k_1}\vec{k_2}) - |k_1||k_2|\tanh k_1h\tanh k_2h$$

and

$$\begin{aligned}L^{(2)}(\vec{k_1},\vec{k_2},\vec{k_3},\vec{k_4}) &= \frac{1}{4}|k_1||k_2|\tanh k_1h\tanh k_1h\\ &\cdot \left[\frac{-2|k_1|}{\tanh k_1h} + \frac{-2|k_2|}{\tanh k_2h} + |\vec{k_1}+\vec{k_3}|\tanh|\vec{k_1}+\vec{k_3}|h\right.\\ &+ \left.|\vec{k_2}+\vec{k_3}|\tanh|\vec{k_2}+\vec{k_3}|h + |\vec{k_1}+\vec{k_4}|\tanh|\vec{k_1}+\vec{k_4}|h + |\vec{k_2}+\vec{k_4}|\tanh|\vec{k_2}+\vec{k_4}|h\right]\\ &= \frac{1}{4}A_1A_2\left[-\frac{2k_1^2}{A_1} - \frac{2k_2^2}{A_2} + A_{1+3} + A_{2+3} + A_{1+4} + A_{2+4}\right]\end{aligned}$$

Cubical terms in Hamiltonian are excluded by canonical transformation. The Hamiltonian is given by the infinite series

$$a_k = a_k^{(0)} + a_k^{(1)} + a_k^{(2)} + ...$$

where

$$\begin{aligned}a_k^{(0)} &= b_k\\ a_k^{(1)} &= \int \Gamma^{(1)}(\vec{k},\vec{k_1},\vec{k_2})b_{k_1}b_{k_2}\delta(\vec{k}-\vec{k_1}-\vec{k_2})dk_1dk_2\\ &- 2\int \Gamma^{(1)}(\vec{k_2},\vec{k},\vec{k_1})b^*_{k_1}b_{k_2}\delta(\vec{k}+\vec{k_1}-\vec{k_2})dk_1dk_2\\ &+ \int \Gamma^{(2)}(\vec{k},\vec{k_1},\vec{k_2})b^*_{k_1}b^*_{k_2}\delta(\vec{k}+\vec{k_1}+\vec{k_2})dk_1dk_2\\ a_k^{(2)} &= \int B(\vec{k},\vec{k_1},\vec{k_2},\vec{k_3})b^*_{k_1}b_{k_2}b_{k_3}\delta(\vec{k}-\vec{k_1}-\vec{k_2}-\vec{k_3})dk_1dk_2dk_3 + ...\\ \Gamma^{(1)}(\vec{k},\vec{k_1},\vec{k_2}) &= -\frac{1}{2}\frac{V^{(1,2)}(\vec{k},\vec{k_1},\vec{k_2})}{\omega_k - \omega_{k_1} - \omega_{k_2}}\\ \Gamma^{(2)}(\vec{k},\vec{k_1},\vec{k_2}) &= -\frac{1}{2}\frac{V^{(0,3)}(\vec{k},\vec{k_1},\vec{k_2})}{\omega_k - \omega_{k_1} - \omega_{k_2}}\\ B(\vec{k},\vec{k_1},\vec{k_2},\vec{k_3}) &= \Gamma^{(1)}(\vec{k_1},\vec{k_2},\vec{k_1}-\vec{k_2})\Gamma^{(1)}(\vec{k_3},\vec{k},\vec{k_3}-\vec{k}) + \Gamma^{(1)}(\vec{k_1},\vec{k_3},\vec{k}-\vec{k_3})\Gamma^{(1)}(\vec{k_2},\vec{k},\vec{k_2}-\vec{k})\\ &- \Gamma^{(1)}(\vec{k},\vec{k_2},\vec{k}-\vec{k_2})\Gamma^{(1)}(\vec{k_3},\vec{k_1},\vec{k_3}-\vec{k_1}) - \Gamma^{(1)}(\vec{k_1},\vec{k_3},\vec{k_1}-\vec{k_3})\Gamma^{(1)}(\vec{k_2},\vec{k_1},\vec{k_2}-\vec{k_1})\\ &- \Gamma^{(1)}(\vec{k}+\vec{k_1},\vec{k},\vec{k_1})\Gamma^{(1)}(\vec{k_2}+\vec{k_3},\vec{k},\vec{k_1}) + \Gamma^{(2)}(-\vec{k}-\vec{k_1},\vec{k},\vec{k_1})\Gamma^{(2)}(-\vec{k_2}-\vec{k_3},\vec{k_2},\vec{k_3})\end{aligned}$$

Then

$$
\begin{aligned}
n_k = N_k \quad &+ \quad \frac{g}{2}\int \frac{|V^{(1,2)}(\vec{k},\vec{k_1},\vec{k_2})|^2}{(\omega_k-\omega_{k_1}-\omega_{k_2})^2}(N_{k_1}N_{k_2}-N_kN_{k_1}-N_kN_{k_2})\delta(\vec{k}-\vec{k_1}-\vec{k_2})dk_1dk_2 \\
&+ \quad \frac{g}{2}\int \frac{|V^{(1,2)}(\vec{k},\vec{k_1},\vec{k_2})|^2}{(\omega_{k_1}-\omega_k-\omega_{k_2})^2}(N_{k_1}N_{k_2}+N_kN_{k_1}-N_kN_{k_2})\delta(\vec{k_1}-\vec{k}-\vec{k_2})dk_1dk_2 \\
&+ \quad \frac{g}{2}\int \frac{|V^{(1,2)}(\vec{k_2},\vec{k},\vec{k_1})|^2}{(\omega_{k_2}-\omega_k+\omega_{k_1})^2}(N_{k_1}N_{k_2}+N_kN_{k_2}-N_kN_{k_1})\delta(\vec{k_2}-\vec{k}-\vec{k_1})dk_1dk_2 \\
&+ \quad \frac{g}{2}\int \frac{|V^{(0,3)}(\vec{k},\vec{k_1},\vec{k_2})|^2}{(\omega_k-\omega_{k_1}+\omega_{k_2})^2}(N_{k_1}N_{k_2}+N_kN_{k_1}+N_kN_{k_2})\delta(\vec{k}-\vec{k_1}-\vec{k_2})dk_1dk_2
\end{aligned}
$$

where

$$
\begin{aligned}
V^{(1,2)}(\vec{k},\vec{k_1},\vec{k_2}) = \frac{1}{4\pi\sqrt{2}}\Bigg\{&\left(\frac{A_kB_{k_1}C_{k_2}}{B_kA_{k_1}A_{k_2}}\right)^{1/4}L^{(1)}(\vec{k_1},\vec{k_2}) - \left(\frac{B_kA_{k_1}B_{k_2}}{A_kA_{k_1}A_{k_2}}\right)^{1/4}L^{(1)}(-\vec{k},\vec{k_1}) \\
&- \left(\frac{B_kB_{k_1}A_{k_2}}{A_kA_{k_1}B_{k_2}}\right)^{1/4}L^{(1)}(-\vec{k},\vec{k_2})\Bigg\}
\end{aligned}
$$

$$
\begin{aligned}
V^{(0,3)}(\vec{k},\vec{k_1},\vec{k_2}) = \frac{1}{4\pi\sqrt{2}}\Bigg\{&\left(\frac{A_kB_{k_1}B_{k_2}}{B_kA_{k_1}A_{k_2}}\right)^{1/4}L^{(1)}(\vec{k_1},\vec{k_2}) + \left(\frac{B_kA_{k_1}B_{k_2}}{A_kB_{k_1}A_{k_2}}\right)^{1/4}L^{(1)}(\vec{k},\vec{k_1}) \\
&+ \left(\frac{B_kB_{k_1}A_{k_2}}{A_kA_{k_1}B_{k_2}}\right)^{1/4}L^{(1)}(\vec{k},\vec{k_2})\Bigg\}
\end{aligned}
$$

8 Appendix II

The coefficient of four-wave interaction for pure gravity waves on deep water was calculated by many authors since Hasselmann (1962). We present here relatively compact expression for this coefficient (see [35]):

$$
\begin{aligned}
T_{1234} &= \frac{1}{2}\left(\tilde{T}_{1234}+\tilde{T}_{2134}\right) \\
\tilde{T}_{1234} &= -\frac{1}{16\pi^2}\frac{1}{(k_1k_2k_3k_4)^{1/4}}\{-12k_1k_2k_3k_4 \\
&- 2(\omega_1+\omega_2)^2\left[\omega_3\omega_4\left((\vec{k_1}\cdot\vec{k_2})-k_1k_2\right)+\omega_1\omega_2\left((\vec{k_3}\vec{k_4})-k_3k_4\right)\right]\frac{1}{g^2} \\
&- 2(\omega_1-\omega_3)^2\left[\omega_2\omega_4\left((\vec{k_1}\vec{k_3})+k_1k_3\right)+\omega_1\omega_3\left((\vec{k_2}\vec{k_4})+k_2k_4\right)\right]\frac{1}{g^2} \\
&- 2(\omega_1-\omega_4)^2\left[\omega_2\omega_3\left((\vec{k_1}\vec{k_4})+k_1k_4\right)+\omega_1\omega_4\left((\vec{k_2}\vec{k_3})+k_2k_3\right)\right]\frac{1}{g^2} \\
&+ \left[(\vec{k_1}\cdot\vec{k_2})+k_1k_2\right]\left[(\vec{k_3}\cdot\vec{k_4})+k_3k_4\right]+\left[-(\vec{k_1}\cdot\vec{k_3})+k_1k_3\right]\left[-(\vec{k_2}\cdot\vec{k_4})+k_2k_4\right] \\
&+ \left[-(\vec{k_1}\cdot\vec{k_4})+k_1k_4\right]\left[-(\vec{k_2}\cdot\vec{k_3})+k_2k_3\right] \\
&+ 4(\omega_1+\omega_2)^2\frac{[(\vec{k_1}\cdot\vec{k_2})-k_1k_2][(\vec{k_2}\cdot\vec{k_3})-k_2k_3]}{\omega_{1+2}^2-(\omega_1+\omega_2)^2} \\
&+ 4(\omega_1-\omega_3)^2\frac{[(\vec{k_1}\cdot\vec{k_3})+k_1k_3][(\vec{k_2}\cdot\vec{k_4})+k_2k_4]}{\omega_{1-3}^2-(\omega_1-\omega_3)^2} \\
&+ 4(\omega_1-\omega_4)^2\frac{[(\vec{k_1}\cdot\vec{k_4})+k_1k_4][(\vec{k_2}\cdot\vec{k_3})+k_2k_3]}{\omega_{1-4}^2-(\omega_1-\omega_4)^2}\Bigg\}
\end{aligned}
$$

Here $\omega_i = \sqrt{g|k_i|}$.

For coinciding wave vectors $T_{12,12} = T_{12}$:

$$T_{12} = -\frac{1}{8\pi^2}\frac{1}{(k_1k_2)^{1/2}}\left\{3k_1^2k_2^2 + (\vec{k_1}\vec{k_2})^2 - 4\omega_1\omega_2(\vec{k_1}\cdot\vec{k_2})(k_1+k_2)\frac{1}{g^2}\right.$$
$$\left. + \; 2\frac{(\omega_1+\omega_2)^2\left[\vec{k_1}\cdot\vec{k_2} - k_1k_2\right]^2}{\omega_{1+2}^2 - (\omega_1+\omega_2)^2} + 2\frac{(\omega_1-\omega_2)^2\left[\vec{k_1}\vec{k_2} + k_1k_2\right]^2}{\omega_{1-2}^2 - (\omega_1-\omega_2)^2}\right\} \tag{8.1}$$

In the one-dimensional case the formula (8.1) becomes remarkably simple (see [36]):

$$T_{12} = \frac{1}{2\pi^2}\begin{cases} k_1^2k_2 & k_1 < k_2 \\ k_1k_2^2 & k_1 > k_2 \end{cases}$$

In a general case T_{12} has the asymptotic

$$T_{12} \simeq \frac{1}{2\pi^2}k_1k_2^2\cos\theta$$

at $k_1 >> k_2$.

9 Appendix III

To determine the equation, describing the general Kolmogorov solution (3.36) one defines the following function:

$$F(\omega,\theta) = 4\pi\int_0^\infty d\omega_1\int_0^{\omega_3} d\omega_2\int_\omega^\infty d\omega_3\int_0^{2\pi} d\theta_1\int_0^{2\pi} d\theta_2\int_0^{2\pi} d\theta_3\delta(\omega+\omega_1-\omega_2-\omega_3) \tag{9.1}$$
$$\delta(\omega\cos\theta+\omega_1\cos\theta_1-\omega_2\cos\theta_2-\omega_3\cos\theta_3)\delta(\omega\sin\theta+\omega_1\sin\theta_1-\omega_2\sin\theta_2-\omega_3\sin\theta_3)$$
$$\left[\omega^3N_{\omega_1}N_{\omega_2}N_{\omega_3} + \omega_1^3N_\omega N_{\omega_2}N_{\omega_3} - \omega_2^3N_\omega N_{\omega_1}N_{\omega_3} - \omega_3^3N_\omega N_{\omega_1}N_{\omega_2}\right]\cdot|T_{\omega\omega_1\omega_2\omega_3,\theta\theta_1\theta_2\theta_3}|^2$$

$$N(\omega,\theta) = \frac{2\omega^3}{g}n(\omega,\theta) \tag{9.2}$$

$$N(\omega,\theta)d\omega d\theta = n_k dk \tag{9.3}$$

and find its Fourier coefficients

$$F_n(\omega) = \int_0^{2\pi} F_n(\omega,\theta)\cos n\theta d\theta \tag{9.4}$$

A general Kolmogorov spectrum is defined by the following system of equations:

$$P + \omega Q = \int_0^\omega(\omega-\omega_1)F_0(\omega_1)d\omega_1 \tag{9.5}$$

$$M = \frac{1}{g}\int_0^\omega\omega_1^2F_1(\omega_1)d\omega_1 \tag{9.6}$$

$$F_n(\omega) = 0 \quad if \quad n \geq 2 \tag{9.7}$$

Now $\varepsilon_\omega(\theta) = \omega N_\omega(\theta)$. One can present N in a form of the Fourier series

$$N(\omega,\theta) = \frac{1}{2\pi}\sum N_n(\omega)\cos n\theta \tag{9.8}$$

and turn (9.5)-(9.7) into an infinite system of nonlinear integral equations imposed on $N_n(\omega)$.

References

[1] M.L. Banner, J. Phys. Oceanogr. **20**, 7 (1990).

[2] V.E. Zakharov, G.Falkovich and V. Lvov, *Kolmogorov spectra of turbulence I* (Springer, Berlin, 1992).

[3] A.N. Pushkarev and V.E. Zakharov, Phys. Rev. Lett. **76**, (1996)

[4] A.N. Pushkarev and V.E. Zakharov V.E., Physica D **145**, (2000)

[5] V.E. Zakharov, N.N. Filonenko, J. Appl. Mech. Tech. Phys., **4**, (1967).

[6] Zakharov, V.E., N.N Filonenko, Dokl. Acad. Nauk SSSR **170**, 6 (1966).

[7] K. Hasselmann, J. Fluid Mech. **12**, (1962)

[8] K. Hasselmann, J. Fluid Mech. **15**, (1963)

[9] M.A. Donelan, J. Hamilton, and W.H. Hui, Phil. Trans. R. Soc. Lond. **A315**, (1985).

[10] A. Newell and V.E. Zakharov, Phys. Rev. Lett. **69**, (1992).

[11] Y. Toba, J. Oceanogr. Soc. Japan **29**, (1973).

[12] V.E. Zakharov and M.M. Zaslavsky, Izv. Atm. Ocean. Phys. **18**, 9 (1982).

[13] S.A. Kitaigorodskii, J. Phys. Oceanogr. **13**, (1983).

[14] V.E. Zakharov and A.N. Pushkarev, Nonlin. Proc. Geophys., **6**, pp.1-10, (1999).

[15] A.N. Pushkarev and V.E. Zakharov, in *Preprints of 6th International Workshop on Wav Hindcasting and Forecasting*, Monterey, California (2000).

[16] S. Hasselmann and K. Hasselmann, J. Phys. Oceanogr. **15** (1985).

[17] J. C. Dungey and W. H. Hui, Proc. R. Soc. **A368**, (1985).

[18] A. Masuda, J. Phys. Oceanogr. **10**, 12 (1980).

[19] A. Masuda, in *Waves Dynamics and Radio Probing of the Ocean Surface*, edited by Phyllips O.M. and Hasselmann K. (Plenum Press, New-York, 1986).

[20] I. V. Lavrenov, *Mathematical modeling of wind waves at non-uniform ocean* (Gidrometeoizdat, St.Petersburg, 1998).

[21] V. G. Polnikov, Wave motion **33**, (2001).

[22] D. J. Webb, Deep-Sea Res. **25**, (1978).

[23] D. Resio and W. Perrie, J. Fluid. Mech. **223**, (1991).

[24] P. A. Hwang *et al.*, J. Phys. Oceanogr. **30**, (2000).

[25] I. R. Young, L.A. Verhagen and M.L. Banner, J. Geophys. Res. **100**, (1995).

[26] G.Z. Forristall, J. Geophys. Res. **86**, (1981).

[27] K. K. Kahma, J. Phys. Oceanogr. **11**, (1981).

[28] S. Kawai, K. Okuda and Toba Y., J. Oceanogr. Soc. Japan **33**, (1977).

[29] H. Mitsuyasu *et al.*, J. Phys. Oceanogr. **10**, (1998).

[30] O.M. Phillips, J. Fluid Mech. **156**, (1985).

[31] J.A. Battjes *et al.*, J. Phys. Oceanogr. **17**, (1987).

[32] I. R. Young, Appl. Ocean Res. **16**, (1994).

[33] W. Perrie and V. Zakharov, Eur. J. Mech. B/Fluids **18**, 3 (1999).

[34] D. T. Resio and W. A. Perrie, J. Phys. Oceanogr. **19**, (1989).

[35] V. E. Zakharov, Eur. J. Mech. B/Fluids **18**, 3 (1999).

[36] V. E. Zakharov, in *Inverse and direct cascade in a wind-driven surface wave turbulence and wave-breaking*, proceedings of the IUTAM symposium, Sydney, Australia (Springer-Verlag, 1992)

[37] G. J. Komen, S. Hasselmann and K. Hasselmann, J. Phys. Oceanogr., **14**, 8 (1984).

[38] M. L. Banner, I. R. Young, J. Phys. Ocenogr. **24**, 7 (1994).

[39] O. M. Phillips, J. Fluid Mech **107**, (1958).

[40] W. J. Pierson and L. A. Moskowitz, J. Geophys. Res. **69**, (1964).

[41] K. Hasselmann *et al.*, Dtsch. Hydrogh. Z. Suppl. A **8**, 12 (1973).

[42] H. Mitsuyasu *et al.*, J. Phys. Oceanogr. **10**, (1980).

[43] D. Resio, J. H. Pihl, B. A. Tracy, and C. L. Vincent, J. Geophys. Res. **106**, C4 (2001).

[44] M. Stiassnie

[45] I.R.Young, *Wind Generated Ocean Waves* (ELSEVIER, 1999).

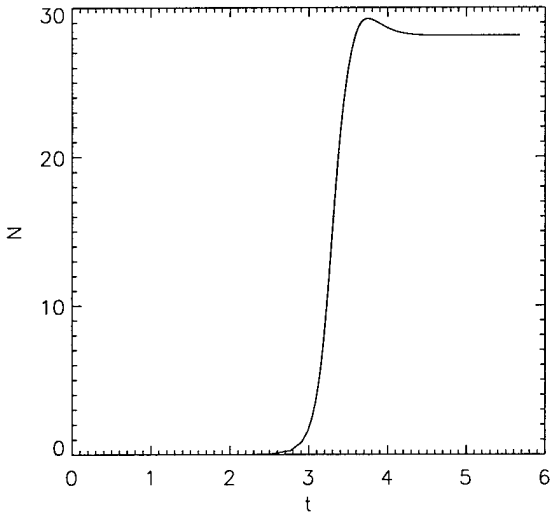

Figure 1: Total wave action as the function of time (hours)

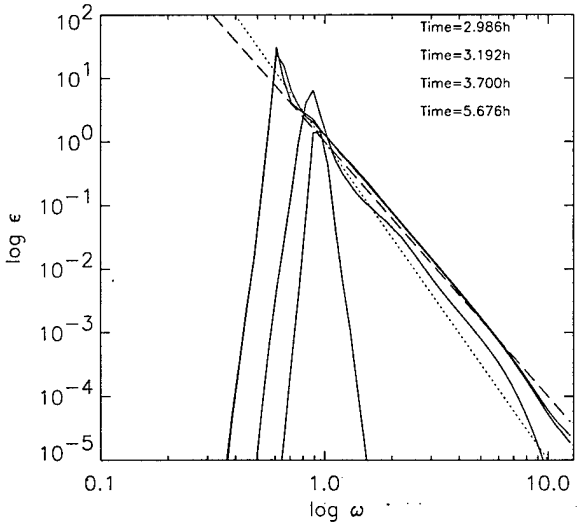

Figure 2: Logarithm of the wave energy averaged over the angle as the function of logarithm of frequency for different moments of time. Dotted line - function proportional to ω^{-5}, dashed line - function proportional to ω^{-4}.

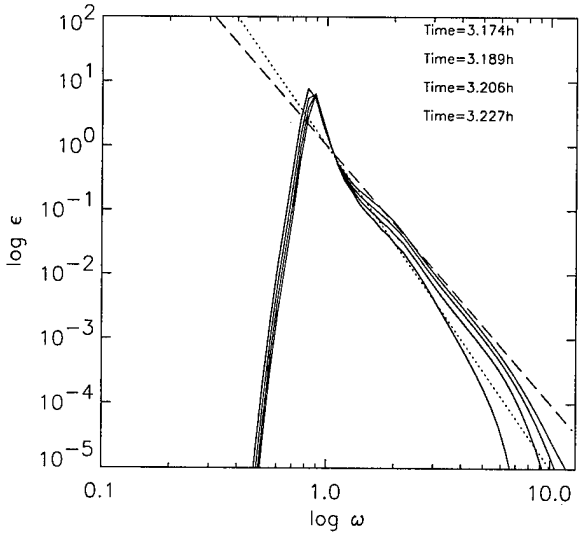

Figure 3: Dynamics of the "shock" propagation for different equidistant moments of time: logarithm of the wave energy at zero angle versus logarithm of ω. Dotted line - function proportional to ω^{-5}, dashed line - function proportional to ω^{-4}.

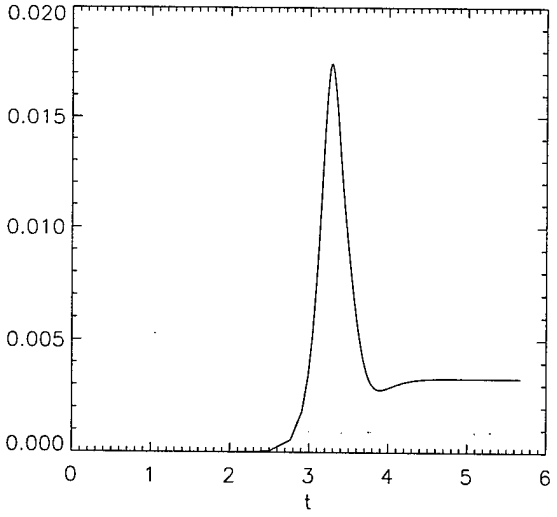

Figure 4: Energy flux P as a function of time

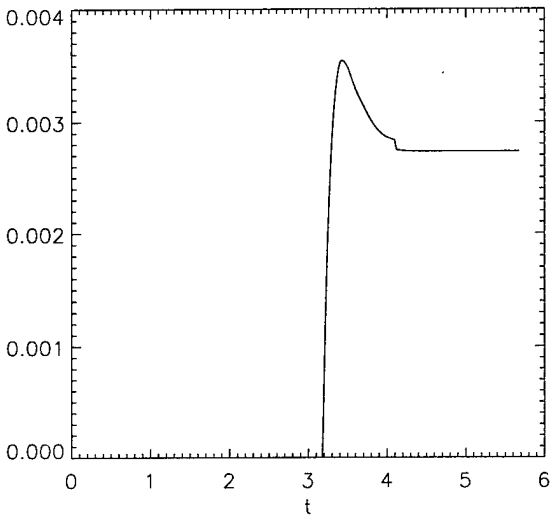

Figure 5: Energy absorption as a function of time

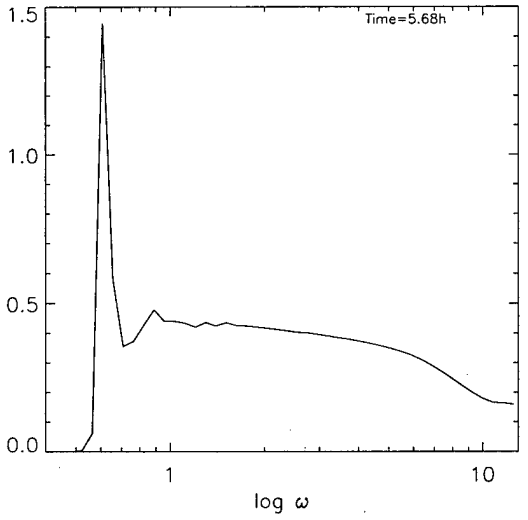

Figure 6: Function $\frac{\omega^4}{2\pi P^{1/3} g^{4/3}} \int_0^{2\pi} \varepsilon(\omega, \theta) d\theta$ as a function of $\log \omega$

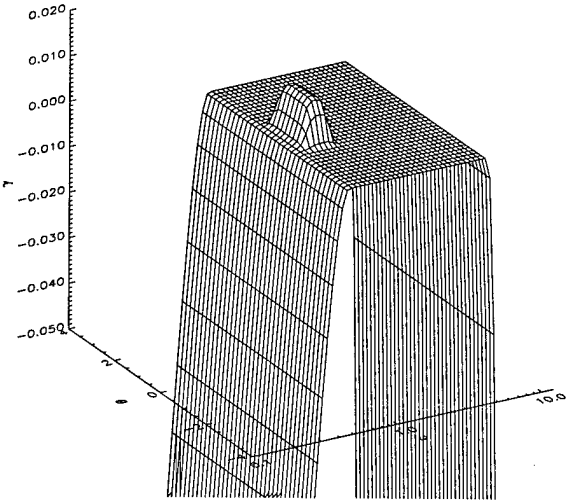

Figure 7: Linear growth rate as the function of frequency and angle.

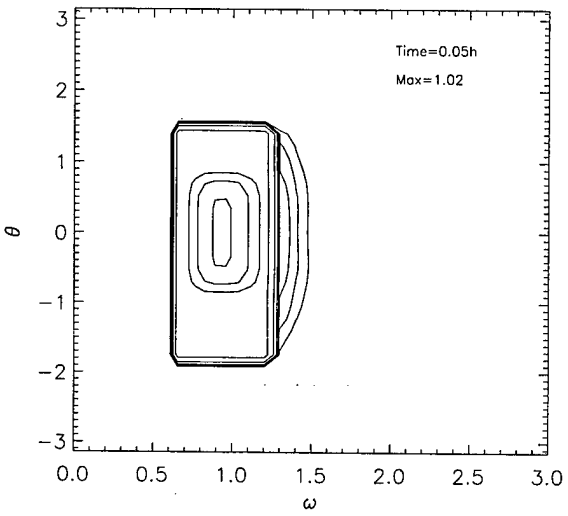

Figure 8: Levels of constant energy density as the function of frequency and angle. Levels positioned as $Max/2^{n-1}$, where Max is the maximum of the distribution and $n = 1, ...10$ are contour number starting from the highest contour.

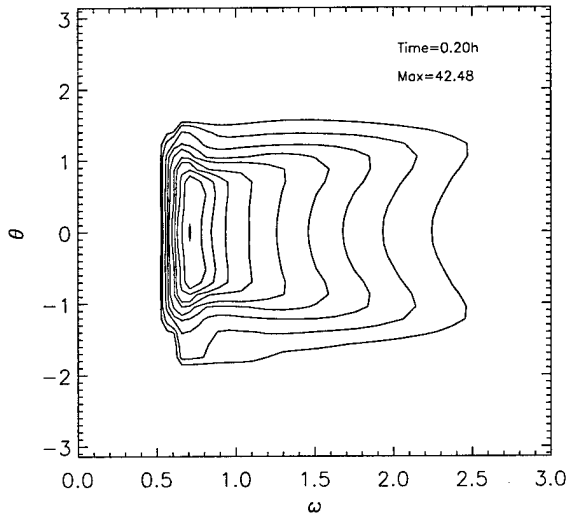

Figure 9: Same as Fig.8, for different time.

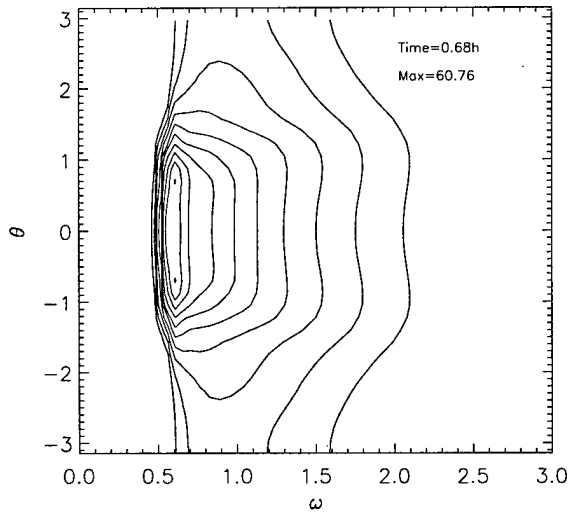

Figure 10: Same as Fig.8, for different time.

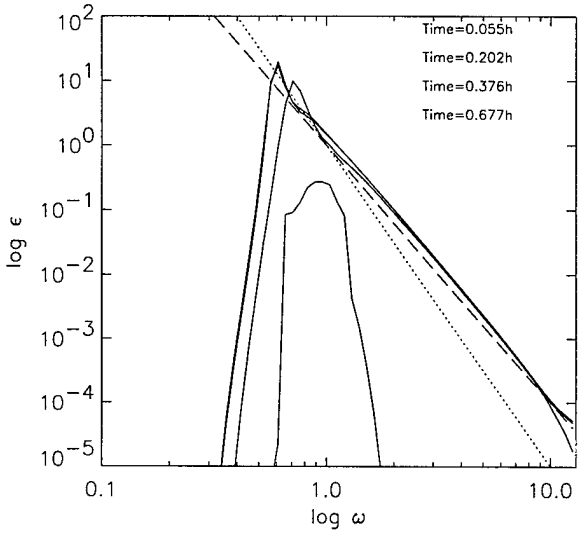

Figure 11: Logarithm of the wave energy averaged over the angle as the function of logarithm of frequency for different moments of time. Dotted line - function proportional to ω^{-5}, dashed line - function proportional to ω^{-4}.

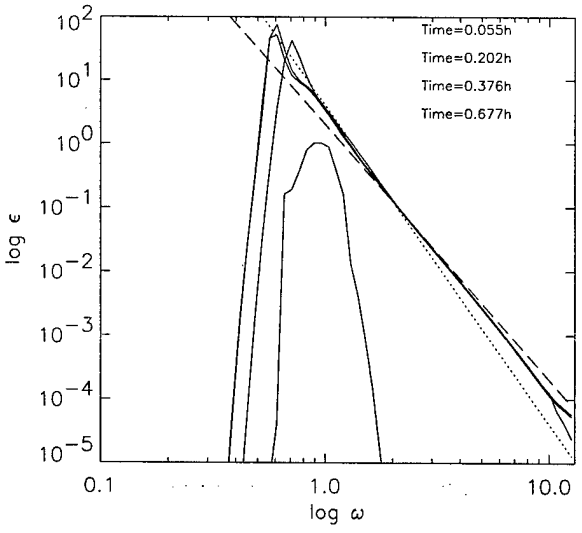

Figure 12: Logarithm of one-dimensional slices of wave energy at $\theta = 0$ as the function of logarithm of frequency for different moments of time. Dotted line - function proportional to ω^{-5}, dashed line - function proportional to ω^{-4}.

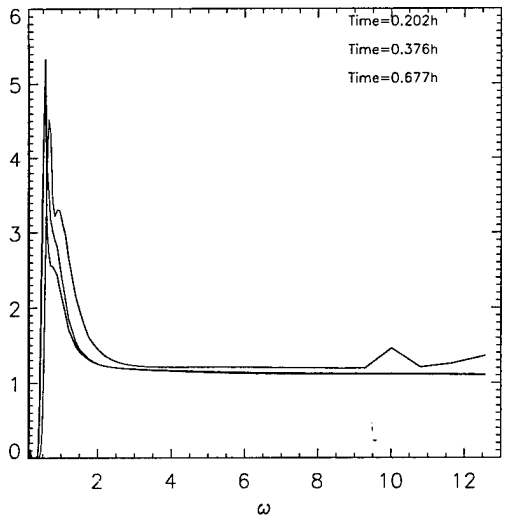

Figure 13: Ratio of one-dimensional slice of wave energy at $\theta = 0$ to angle averaged spectrum as the function of frequency for different moments of time.

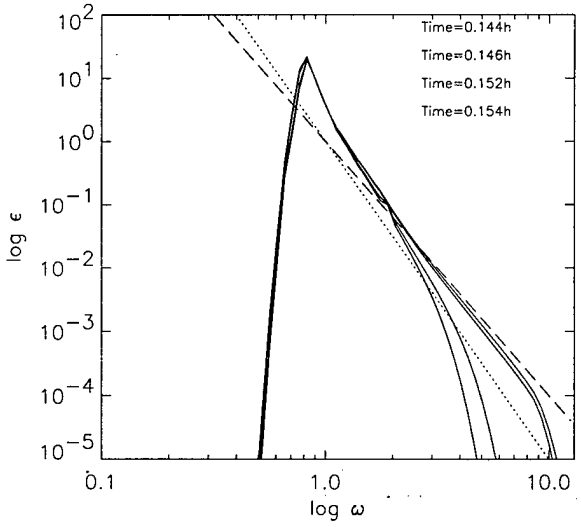

Figure 14: Dynamics of the "shock" propagation for different equidistant moments of time: logarithm of the wave energy at zero angle versus logarithm of ω. Dotted line - function proportional to ω^{-5}, dashed line - function proportional to ω^{-4}.

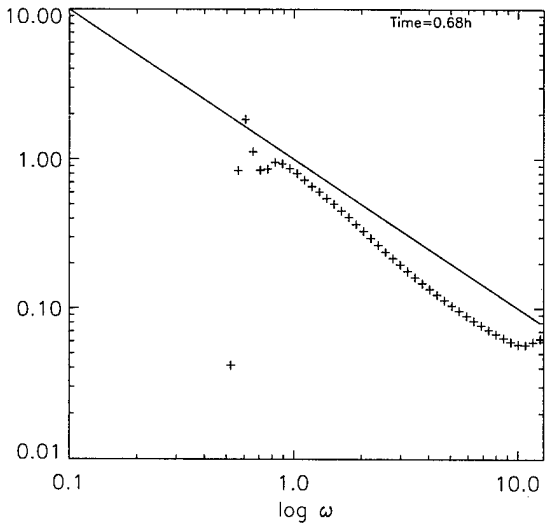

Figure 15: Logarithm of the function $\frac{\omega^4}{P^{1/3}} \int_0^{2\pi} \cos\theta d\theta$ as a function of the $\log\omega$

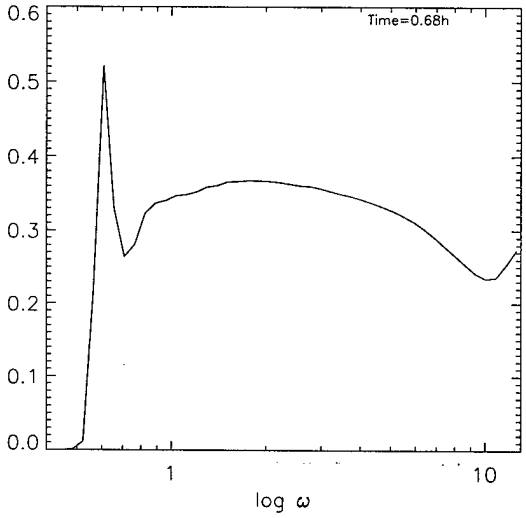

Figure 16: Function $\frac{\omega^4}{2\pi P^{1/3} g^{4/3}} \int_0^{2\pi} \varepsilon(\omega,\theta) d\theta$ as a function of $\log\omega$

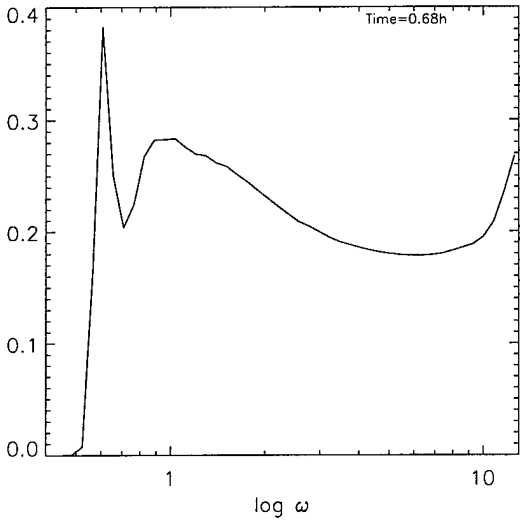

Figure 17: Function $\frac{P^{2/3}\omega^5}{\pi M g^{7/3}} \int_0^{2\pi} \varepsilon(\omega,\theta)\cos\theta d\theta$ as a function of $\log\omega$

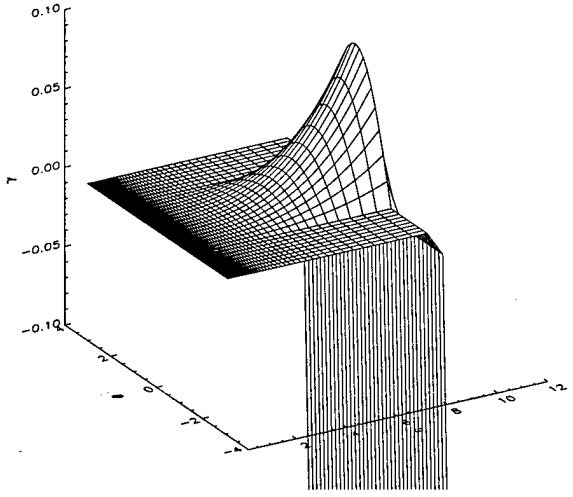

Figure 18: Linear growth rate as the function of frequency and angle.

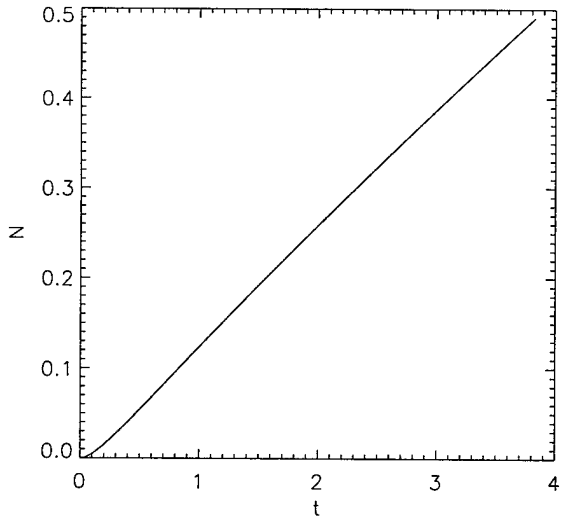

Figure 19: Total wave action as the function of time (hours)

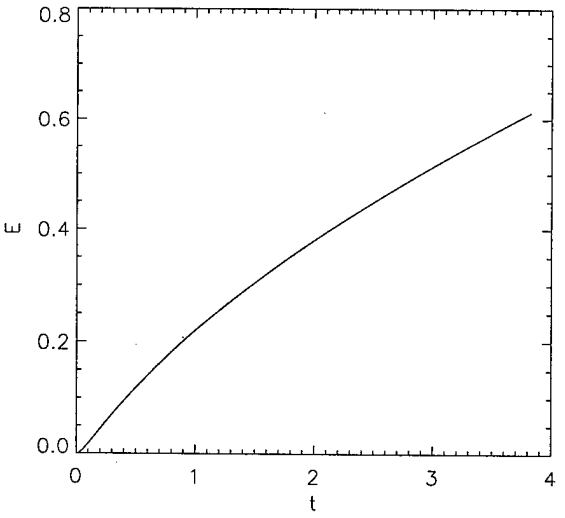

Figure 20: Total energy as the function of time (hours)

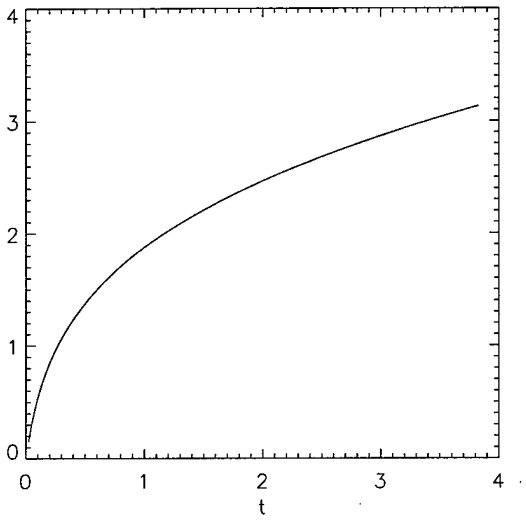

Figure 21: Significant wave height $< a_s >$ as the function of time (hours)

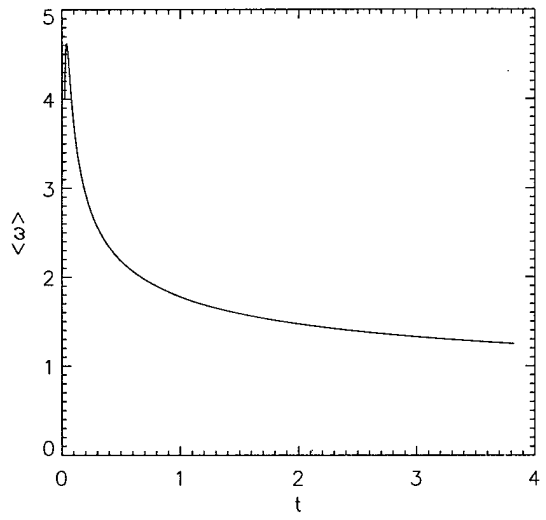

Figure 22: Average frequency $< \omega >$ as the function of time (hours)

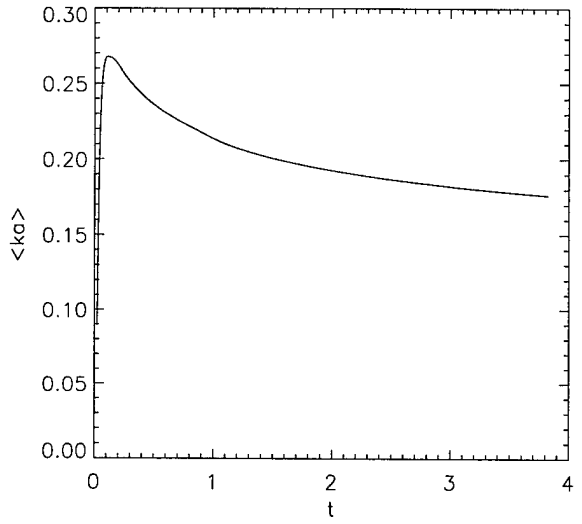

Figure 23: Average wave slope as the function of time (hours)

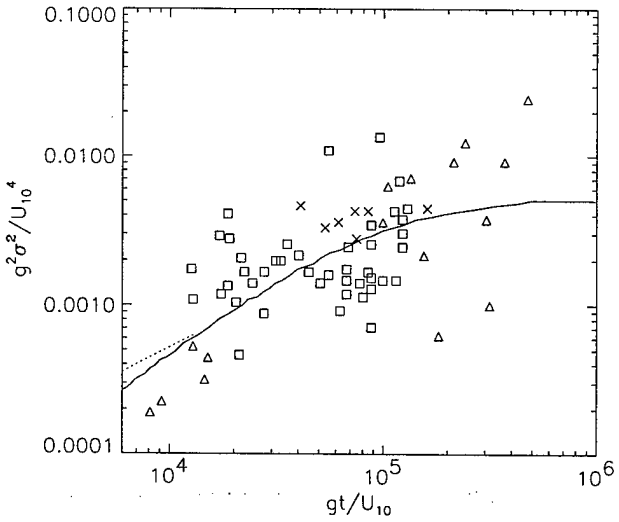

Figure 24: Data compiled by WIegel (1961) showing duration limited growth of nondimensional energy $g^2\sigma^2/U_{10}^4$ vs non-dimensional duration gt/U_{10}. The solid line is data fit by $CERC$. Data taken from [45]. Dotted line is data from current numerical experiment.

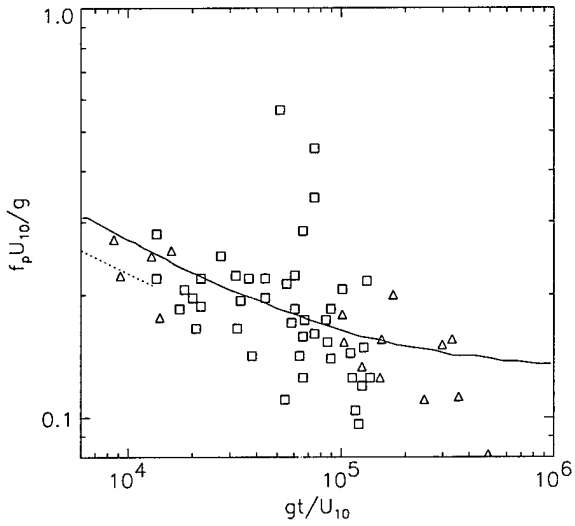

Figure 25: Data compiled by Wiegel (1961) showing duration limited growth of nondimensional frequency f_pU_{10}/g vs non-dimensional duration gt/U_{10}. The solid line is data fit by $CERC$. Data taken from [45]. Dotted line is data from current numerical experiment.

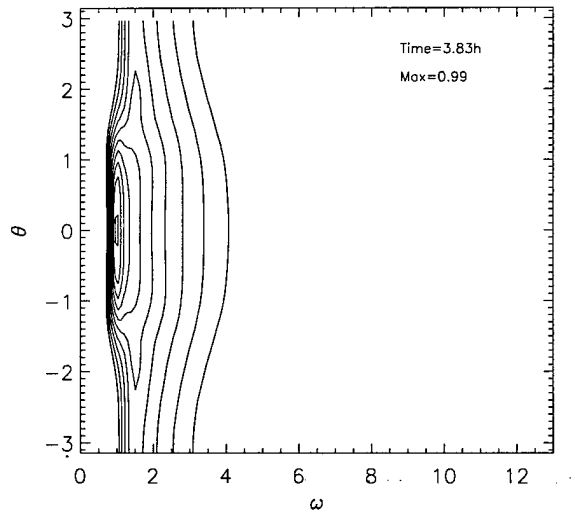

Figure 26: Levels of constant energy density as the function of frequency and angle. Levels positioned as $Max/2^{n-1}$, where Max is the maximum of the distribution and $n = 1, ...10$ are contour number starting from the highest contour.

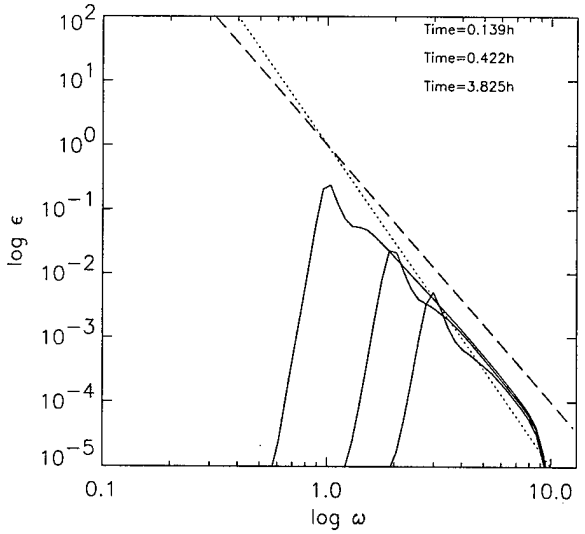

Figure 27: Logarithm of the wave energy averaged over the angle as the function of logarithm of frequency for different moments of time. Dotted line - function proportional to ω^{-5}, dashed line - function proportional to ω^{-4}.

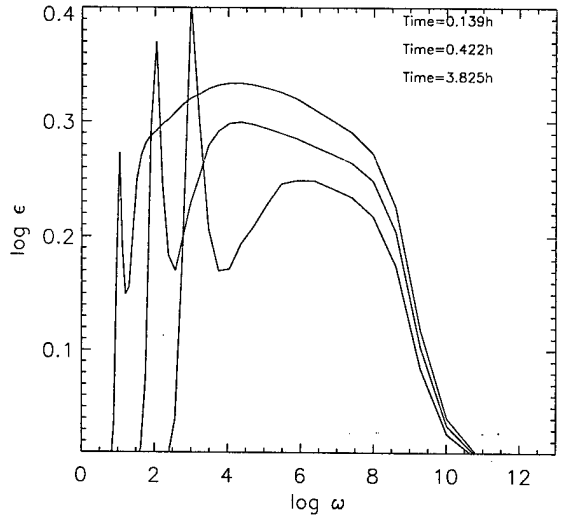

Figure 28: "Compensated" spectra $\omega^4 \varepsilon_\omega$ as a function of ω for different times.

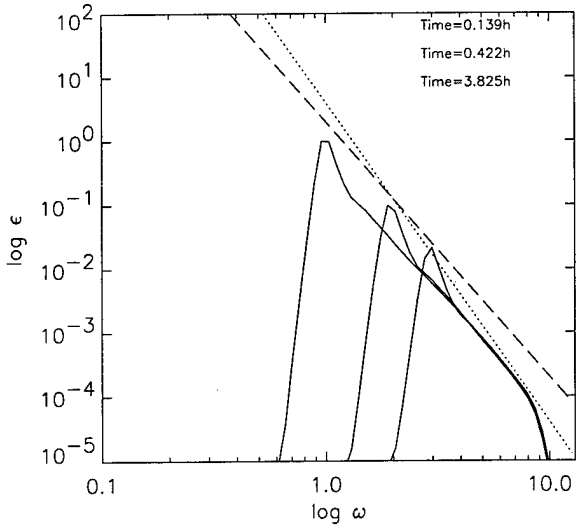

Figure 29: Logarithm of one-dimensional slices of wave energy at $\theta = 0$ as the function of logarithm of frequency for different moments of time. Dotted line - function proportional to ω^{-5}, dashed line - function proportional to ω^{-4}.

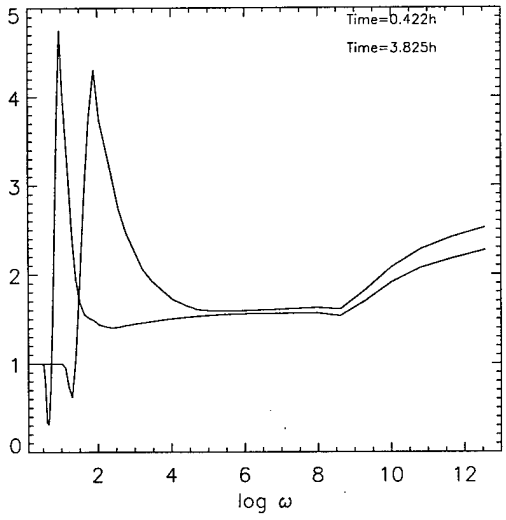

Figure 30: Ratio of one-dimensional slice of wave energy at $\theta = 0$ to angle averaged spectrum as the function of frequency for different moments of time.

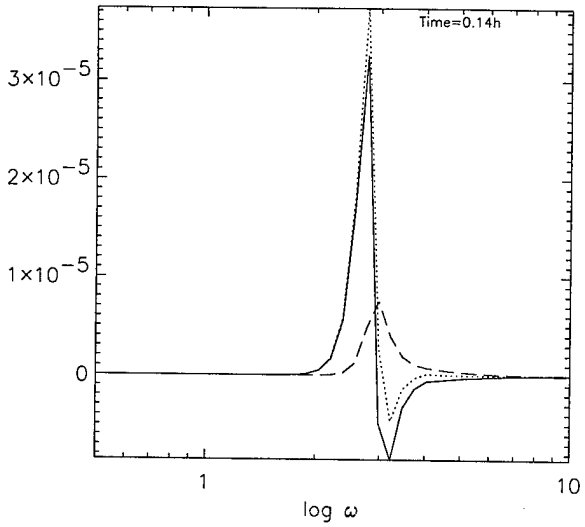

Figure 31: Angle averaged terms in the kinetic equation $\frac{\partial n}{\partial t} = S_{nl} + \gamma n$ as the function of $\log\omega$ at the moment of time $t = 0.14$. Term $\int_0^{2\pi} S_{nl} d\theta$ - solid line, term $\int_0^{2\pi} \gamma n d\theta$ - dashed line, term $\int_0^{2\pi} \frac{\partial n}{\partial t} d\theta$ - dotted line.

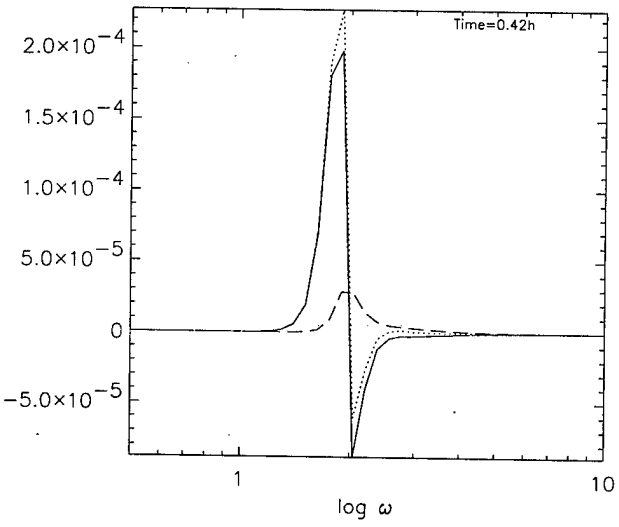

Figure 32: Same as 31, for $t = 0.42 hours$.

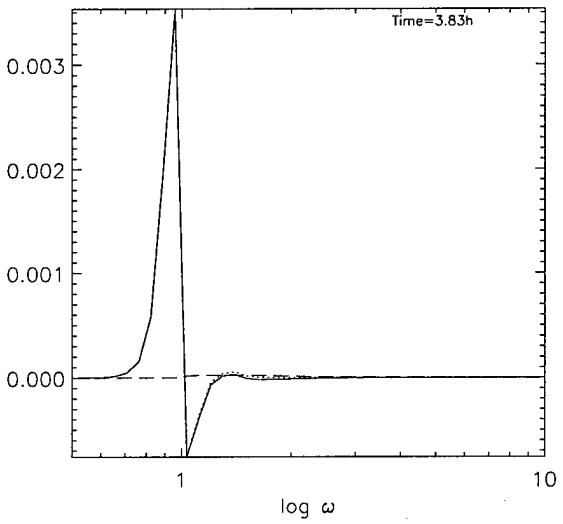

Figure 33: Same as 31, for $t = 3.83 hours$.

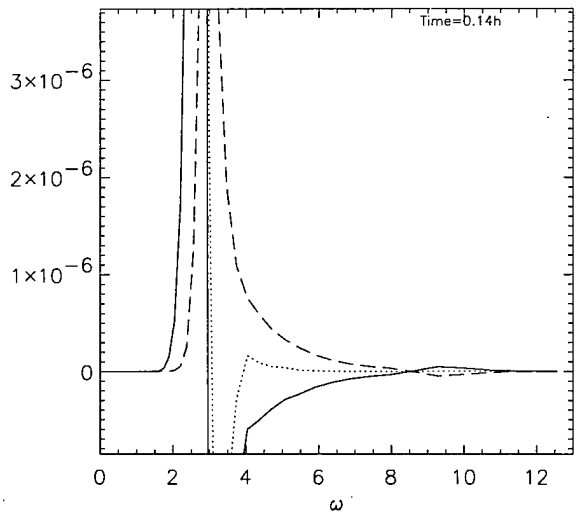

Figure 34: Angle averaged terms in the kinetic equation $\frac{\partial n}{\partial t} = S_{nl} + \gamma n$ as the function of ω. Term $\int_0^{2\pi} S_{nl} d\theta$ - solid line, term $\int_0^{2\pi} \gamma n d\theta$ - dashed line, term $\int_0^{2\pi} \frac{\partial n}{\partial t} d\theta$ - dotted line. Zoomed with respect to vertical axis.

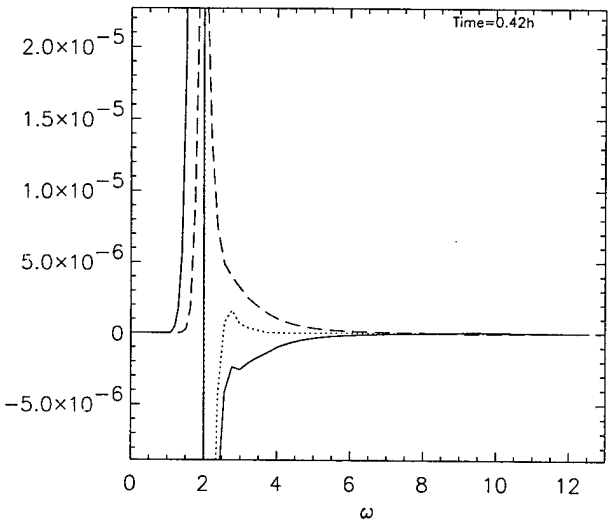

Figure 35: Same as 34, for $t = 0.42 hours$.

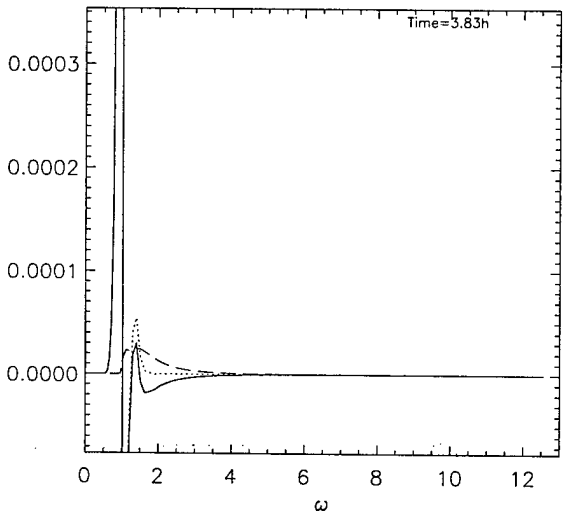

Figure 36: Same as 34, for $t = 3.83 hours$.

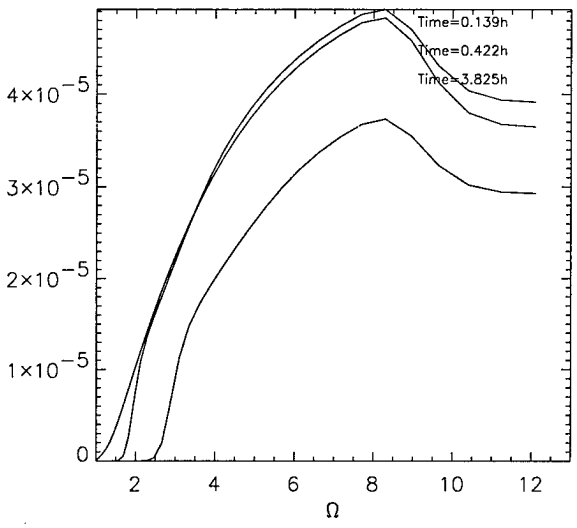

Figure 37: Integrated action input $\frac{2}{g^2}\int_0^{\Omega}\int_0^{2\pi}\gamma n\omega^3 d\omega d\theta$ as the function of Ω.

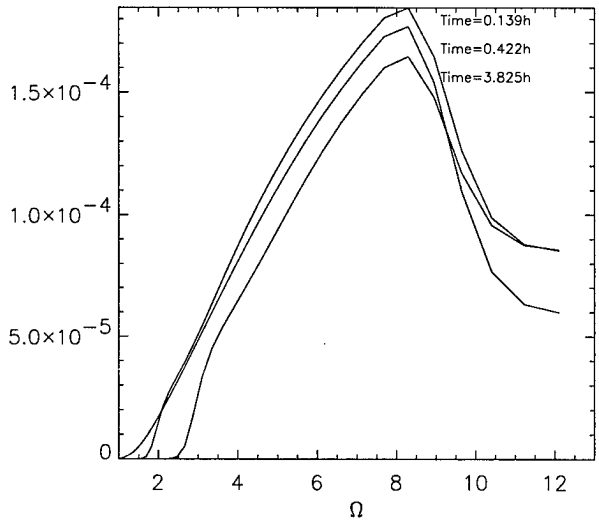

Figure 38: Integrated energy input $\frac{2}{g^2}\int_0^{\Omega}\int_0^{2\pi}\gamma n\omega^4 d\omega d\theta$ as the function of Ω.

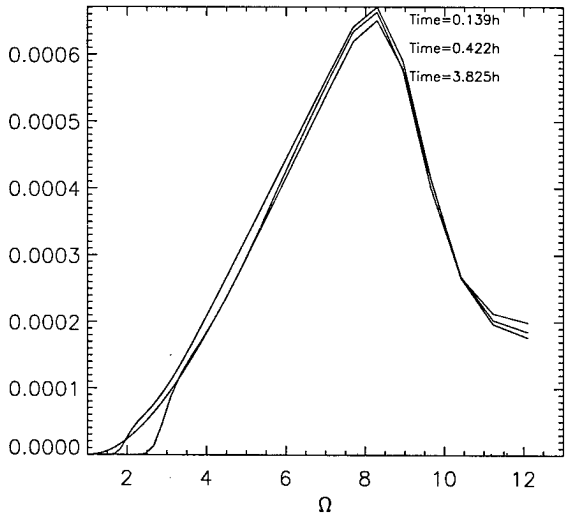

Figure 39: Integrated momentum input $\frac{2}{g^3}\int_0^{\Omega}\int_0^{2\pi}\gamma n\omega^5\cos\theta d\omega d\theta$ as the function of Ω.

ELSEVIER

3 December 2001

PHYSICS LETTERS A

Physics Letters A 291 (2001) 139–145

www.elsevier.com/locate/pla

Kolmogorov spectra of weak turbulence in media with two types of interacting waves

F. Dias [a,*], P. Guyenne [b], V.E. Zakharov [c]

[a] *Centre de Mathématiques et de Leurs Applications, Ecole Normale Supérieure de Cachan, 61 avenue du Président Wilson, 94235 Cachan cedex, France*

[b] *Department of Mathematics and Statistics, McMaster University, 1280 Main Street West, L8S 4K1 Hamilton, ON, Canada*

[c] *Landau Institute for Theoretical Physics, 2 Kosygin str., 117334 Moscow, Russia*

Received 2 July 2001; accepted 22 October 2001
Communicated by A.P. Fordy

Abstract

A system of one-dimensional equations describing media with two types of interacting waves is considered. This system can be viewed as an alternative to the model introduced by Majda, McLaughlin and Tabak in 1997 for assessing the validity of weak turbulence theory. The predicted Kolmogorov solutions are the same in both models. The main difference between both models is that coherent structures such as wave collapses and quasisolitons cannot develop in the present model. As shown recently these coherents structures can influence the weakly turbulent regime. It is shown here that in the absence of coherent structures weak turbulence spectra can be clearly observed numerically.

PACS: 05.20.Dd; 05.90.+m; 47.10.+g
Keywords: Kolmogorov spectra; Dispersive waves; Weak turbulence

1. Introduction

Weak turbulence theory is an efficient tool for describing turbulence in systems dominated by resonant interactions between small-amplitude waves. One of the key ingredients to the theory of weak wave turbulence is the so-called Kolmogorov spectrum [1]. Kolmogorov weak-turbulence spectra have been observed in several physical systems (for example, in a sea of wind-driven, weakly coupled, dispersive water waves). We believe that Kolmogorov weak-turbulence spectra are a useful theoretical tool for explaining various complex wave phenomena observed in nature.

Only a few attempts have been made to compare predictions of weak turbulence theory with numerical results. One can mention the results of Pushkarev and Zakharov [2] who numerically solved the three-dimensional equations for capillary water waves and observed a power-law spectrum close to that derived by Zakharov and Filonenko [3]. Majda, McLaughlin and Tabak [4] introduced a model, the so-called MMT model, for assessing numerically the validity of weak turbulence theory. Since their results indicated a failure of the predictions of weak turbulence theory, more computations have been carried out recently to get a better understanding of wave turbulence in the MMT model [5–7]. The present understanding is that co-

* Corresponding author.
E-mail address: dias@cmla.ens-cachan.fr (F. Dias).

0375-9601/01/$ – see front matter
PII: S0375-9601(01)00711-3

herent structures can strongly affect weak turbulence. These coherent structures essentially are wave collapses and quasisolitons. Wave collapses in the form of sporadic localized events represent a strongly nonlinear mechanism of energy transfer towards small scales. Quasisolitons or envelope solitons denote approximate solutions of the MMT model which tend to classical solitons in the limit of a narrowbanded spectrum. The presence of such quasisolitons may explain the deviation from weak turbulence leading to the appearance of a steeper spectrum (the so-called MMT spectrum) in some cases [6,7]. Recently, Biven et al. [8] addressed the problem of breakdown of wave turbulence by intermittent events associated with nonlinear coherent structures.

In the present Letter we consider a model which is quite similar to the MMT model. However, coherent structures cannot develop. Our model takes the form of a system of equations describing the interactions of two types of waves. This is a fairly widespread case which includes, for example, the interaction of electrons with photons or the interaction of electromagnetic waves with Langmuir waves [1,9]. The main conclusion of this Letter is that numerical results based on the present model are in agreement with the predictions of weak turbulence theory. Agreement between numerical simulations and weak turbulence theory was also recently obtained by Zakharov et al. [10], who examined a modified version of the MMT model that allows for "one to three" wave interactions.

Of course, it will be necessary in the future to perform numerical computations on the full equations describing the physical phenomena of interest. However, we believe that a lot of information can be obtained from the solution of simplified models. Since the theory of weak turbulence is quite general, its main statements can be tested with simple models, for which numerical simulations can be performed more easily.

2. Model equations and Kolmogorov spectra

We consider the system of equations proposed in [7],

$$i\frac{\partial a_k}{\partial t} = \omega_k a_k + \int T_{123k} a_1 b_2 b_3^* \times \delta(k_1 + k_2 - k_3 - k)\, dk_1\, dk_2\, dk_3,$$

$$i\frac{\partial b_k}{\partial t} = s\omega_k b_k + \int T_{123k} b_1 a_2 a_3^* \times \delta(k_1 + k_2 - k_3 - k)\, dk_1\, dk_2\, dk_3, \quad (1)$$

where a_k, b_k denote the Fourier components of two types of interacting wave fields and asterisk stands for complex conjugation. Like the MMT model, this model is determined by the linear dispersion relation $\omega_k = |k|^\alpha$ and the interaction coefficient $T_{123k} = |k_1 k_2 k_3 k|^{\beta/4}$. Thus ω_k, $s\omega_k$ and T_{123k} are homogeneous functions of their arguments. The three parameters s, α and β are real with the restriction $s, \alpha > 0$. If we set $\alpha = 2$ and $\beta = 0$, Eqs. (1) correspond to coupled nonlinear Schrödinger equations.

The system possesses two important conserved quantities, the positive definite Hamiltonian H, which we split into its linear part H_L and its nonlinear part H_{NL},

$$H = H_L + H_{NL} = \int \omega_k \left(|a_k|^2 + s|b_k|^2\right) dk + \int T_{123k} a_1 b_2 b_3^* a_k^* \delta(k_1 + k_2 - k_3 - k) \times dk_1\, dk_2\, dk_3\, dk,$$

and the total wave action (or number of particles)

$$N = \int \left(|a_k|^2 + |b_k|^2\right) dk.$$

Note that both individual wave actions $\int |a_k|^2\, dk$ and $\int |b_k|^2\, dk$ are conserved in the system.

Eqs. (1) describe four-wave resonant interactions satisfying

$$k_1 + k_2 = k_3 + k,$$
$$\omega_1 + s\omega_2 = s\omega_3 + \omega_k. \quad (2)$$

It is well known that when $s = 1$ conditions (2) have nontrivial solutions only if $\alpha < 1$. The case $s = 1$ and $\alpha = 1/2$, which mimics gravity waves in deep water, was treated in some recent studies [4–7]. In particular, Zakharov et al. [7] showed that the MMT model with $\alpha < 1$ exhibits coherent structures which strongly affect the weakly turbulent regime. Here accounting for $s \neq 1$ allows the resonance conditions (2) to be satisfied for any α. If $\alpha = 2$, we can solve explicitly Eqs. (2) to obtain

$$k_3 = k_1 - \frac{2(k_1 - sk_2)}{1 + s},$$

$$k = k_2 + \frac{2(k_1 - sk_2)}{1+s}. \tag{3}$$

It is clear that Eqs. (3) with $s = 1$ give the trivial solution $k_3 = k_2$, $k = k_1$. As a general rule, for a given α, nontrivial families of resonant quartets obeying Eqs. (2) can be found for all values of $s \neq 1$.

In the framework of weak turbulence theory, we are interested in the evolution of the two-point correlation functions

$$\langle a_k a^*_{k'} \rangle = n^a_k \delta(k - k') \quad \text{and} \quad \langle b_k b^*_{k'} \rangle = n^b_k \delta(k - k'),$$

where $\langle \cdot \rangle$ represents ensemble averaging. Under the assumptions of random phases and quasi-Gaussianity, it is then possible to write a system of kinetic equations for n^a_k and n^b_k as

$$\frac{\partial n^a_k}{\partial t} = 2\pi \int |T_{123k}|^2 U^{ab}_{123k} \delta(\omega_1 + s\omega_2 - s\omega_3 - \omega_k) \times \delta(k_1 + k_2 - k_3 - k)\, dk_1\, dk_2\, dk_3, \tag{4}$$

$$\frac{\partial n^b_k}{\partial t} = 2\pi \int |T_{123k}|^2 U^{ba}_{123k} \delta(s\omega_1 + \omega_2 - \omega_3 - s\omega_k) \times \delta(k_1 + k_2 - k_3 - k)\, dk_1\, dk_2\, dk_3, \tag{5}$$

with

$$U^{ab}_{123k} = n^a_1 n^b_2 n^b_3 + n^a_1 n^b_2 n^a_k - n^a_1 n^b_3 n^a_k - n^b_2 n^b_3 n^a_k.$$

The stationary power-law solutions of Eqs. (4), (5) can be found explicitly. To do so, let us examine Eq. (4) only since the problem is similar for Eq. (5) by permuting n^a_k and n^b_k as well as ω_k and $s\omega_k$. Looking for solutions of the form $n^a_k \propto \omega_k^{-\gamma}$, $n^b_k \propto (s\omega_k)^{-\gamma}$ and applying Zakharov's conformal transformations, the kinetic equation (4) becomes

$$\frac{\partial \mathcal{N}^a_\omega}{\partial t} \propto \omega_k^{-y-1} I^a_{s\alpha\beta\gamma}, \tag{6}$$

where $\mathcal{N}^a_\omega = n^a_k\, dk/d\omega_k$ and

$$I^a_{s\alpha\beta\gamma} = \int_\Delta S_{123}\left[1 + (s\xi_3)^\gamma - (s\xi_2)^\gamma - \xi_1^\gamma\right] \times \delta(1 + s\xi_3 - s\xi_2 - \xi_1) \times \delta\left(1 + \xi_3^{1/\alpha} - \xi_2^{1/\alpha} - \xi_1^{1/\alpha}\right) \times \left[1 + (s\xi_3)^y - (s\xi_2)^y - \xi_1^y\right] d\xi_1\, d\xi_2\, d\xi_3, \tag{7}$$

with

$$\Delta = \{0 < \xi_1 < 1,\ 0 < s\xi_2 < 1,\ \xi_1 + s\xi_2 > 1\},$$

$$S_{123} = \frac{2\pi}{\alpha^4 s^{2\gamma}} (\xi_1 \xi_2 \xi_3)^{(\beta/2+1)/\alpha - 1 - \gamma},$$

and

$$y = 3\gamma + 1 - \frac{2\beta + 3}{\alpha}.$$

The nondimensionalized integral $I^a_{s\alpha\beta\gamma}$ in Eq. (6) results from the change of variables $\omega_j \to \omega_k \xi_j$ $(j = 1, 2, 3)$.

Thermodynamic equilibrium solutions $(\gamma = 0, 1)$ given by

$$n^{a,b}_k = \text{const} \quad \text{and} \quad n^{a,b}_k \propto \omega_k^{-1} \tag{8}$$

are obvious. In addition, there exist Kolmogorov-type solutions $(y = 0, 1)$

$$n^{a,b}_k \propto \omega_k^{(-2\beta/3 - 1 + \alpha/3)/\alpha} \quad \text{and} \quad n^{a,b}_k \propto \omega_k^{-(2\beta/3+1)/\alpha}, \tag{9}$$

which correspond to a finite flux of wave action Q and energy P, respectively. We point out that Eqs. (8), (9) are also steady solutions of Eq. (5) and they are identical to those derived from the MMT model [4]. The fact that the kinetic equation depends on the parameter s implies that the fluxes and the Kolmogorov constants also depend on s (see below). However, there is no s-dependence on the Kolmogorov exponents because of the property of scale invariance. As found in [7], the criterion for appearance of the Kolmogorov spectra (9) is

$$\beta < -\frac{3}{2} \quad \text{or} \quad \beta > 2\alpha - \frac{3}{2}. \tag{10}$$

This means physically that a flux of wave action towards large scales (inverse cascade with $Q < 0$) and a flux of energy towards small scales (direct cascade with $P > 0$) should occur in the system. The full expressions of Eq. (9) can be obtained from dimensional analysis yielding

$$n^a_k = c^a_1 Q_a^{1/3} \omega_k^{(-2\beta/3 - 1 + \alpha/3)/\alpha},$$
$$n^b_k = c^b_1 Q_b^{1/3} (s\omega_k)^{(-2\beta/3 - 1 + \alpha/3)/\alpha}, \tag{11}$$

and

$$n^a_k = c^a_2 P_a^{1/3} \omega_k^{-(2\beta/3+1)/\alpha},$$
$$n^b_k = c^b_2 P_b^{1/3} (s\omega_k)^{-(2\beta/3+1)/\alpha}, \tag{12}$$

where

$$c_1^{a,b} = \left(-\frac{\partial I^{a,b}_{s\alpha\beta\gamma}}{\partial y}\bigg|_{y=0} \right)^{-1/3},$$

$$c_2^{a,b} = \left(\frac{\partial I^{a,b}_{s\alpha\beta\gamma}}{\partial y}\bigg|_{y=1} \right)^{-1/3} \tag{13}$$

denote the dimensionless Kolmogorov constants. These can be computed directly by using integral (7) and its analogue for $\partial \mathcal{N}^b_\omega / \partial t$.

In the numerical computations, we will fix $\alpha = 3/2 > 1$ in order to prevent the emergence of coherent structures such as wave collapses and quasisolitons revealed in [7]. Our goal is to check the validity of the Kolmogorov spectra which are relevant in several real wave media as already said in the introduction [1]. We will restrict our study to solutions (12) associated with the direct cascade.

3. Numerical results

Numerical experiments were carried out to integrate Eqs. (1) by use of a pseudospectral code with periodic boundary conditions. The method includes a fourth-order Runge–Kutta scheme in combination with an integrating factor technique which permits efficient computations over long times [4,7]. Resolution with up to 2048 de-aliased modes in a domain of length 2π is achieved here ($k_{\max} = 1024$). To generate weakly turbulent regimes, source terms of the form

$$i \begin{pmatrix} f_k^a \\ f_k^b \end{pmatrix} e^{i\theta_k} - i \left[\begin{pmatrix} \nu_-^a \\ \nu_-^b \end{pmatrix} (k - k_d^-)^2 + \begin{pmatrix} \nu_+^a \\ \nu_+^b \end{pmatrix} (k - k_d^+)^2 \right] \times \begin{pmatrix} a_k \\ b_k \end{pmatrix} \tag{14}$$

were added to both right-hand sides of Eqs. (1). The first term in Eq. (14) denotes a white-noise forcing where $0 \leqslant \theta_k < 2\pi$ is an uniformly distributed random number varying in time. The term in square brackets consists of a wave action sink at large scales and an energy sink at small scales. The random feature of the forcing makes it uncorrelated in time with the wave field. Consequently, it is easier to control the input energy with a random forcing than with a deterministic forcing. For the results presented below, the forcing region is located at small wave numbers, i.e.,

$$f_k^{a,b} = \begin{cases} 6,3 & \text{if } 8 \leqslant k \leqslant 12, \\ 0 & \text{otherwise.} \end{cases}$$

Parameters of the sinks are

$$\nu_-^{a,b} = \begin{cases} 16, 0.8 & \text{if } k \leqslant k_d^- \ (k_d^- = 5), \\ 0 & \text{otherwise,} \end{cases}$$

and

$$\nu_+^{a,b} = \begin{cases} 10^{-2}, 7 \times 10^{-4} & \text{if } k \geqslant k_d^+ \ (k_d^+ = 550), \\ 0 & \text{otherwise.} \end{cases}$$

Using this kind of selective dissipation ensures large enough inertial ranges at intermediate scales where solutions can develop under the negligible influence of damping. According to criterion (10), we focused on $\beta = 2$ and $s = 1/10$ as a typical case for testing weak turbulence predictions. Simulations are run from low-level initial data until a quasisteady state is reached and then averaging is performed over a sufficiently long time to compute the spectra. The time step, set equal to $\Delta t = 2 \times 10^{-5}$, has to resolve accurately the fastest harmonics $\tau \sim 1/\omega_{\max}$ of the medium or at least those from the inertial range. Time integration with such a small time step leads to a computationally time-consuming procedure despite the one-dimensionality of the problem. This explains why we chose $\alpha = 3/2$ rather than a greater integer value (e.g., $\alpha = 2$) as well as $s = 1/10$ rather than a value $s > 1$. Otherwise the constraint on Δt would be more severe. There is *a priori* no special requirement in the choice of the value of s, except $s \neq 1$.

Figs. 1 and 2 show the temporal evolution of the wave action N and the quadratic energy H_{L} over the window $80 \leqslant t \leqslant 100$. At this stage, the stationary regime is clearly established since the wave action and the quadratic energy fluctuate around some mean values $N \simeq 0.5$ and $H_{\mathrm{L}} \simeq 5.3$. Typically, the time interval for both the whole computation and the time averaging must exceed significantly the longest linear period. In order to monitor the level of turbulence, we define the average nonlinearity ϵ as the ratio of the nonlinear part to the linear part of the Hamiltonian, i.e.,

$$\epsilon = \frac{H_{\mathrm{NL}}}{H_{\mathrm{L}}}.$$

As in [2,7], this quantity provides a relatively good estimate of the level of nonlinearity once the system reaches the steady state. We can see in Fig. 3 that

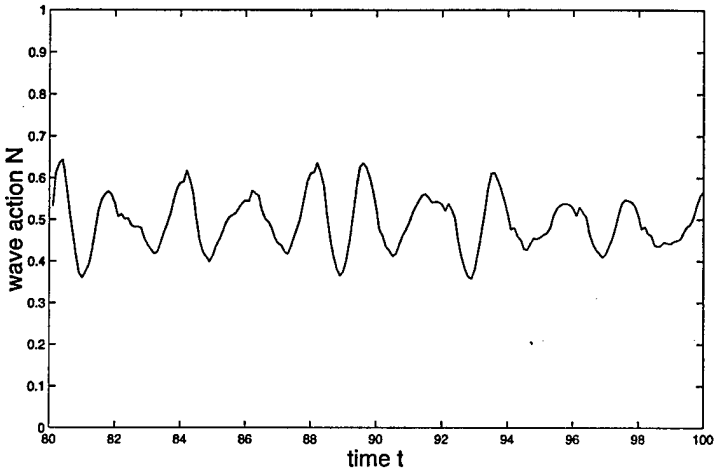

Fig. 1. $s = 1/10$, $\alpha = 3/2$, $\beta = 2$. Evolution of wave action N vs. time in the stationary state.

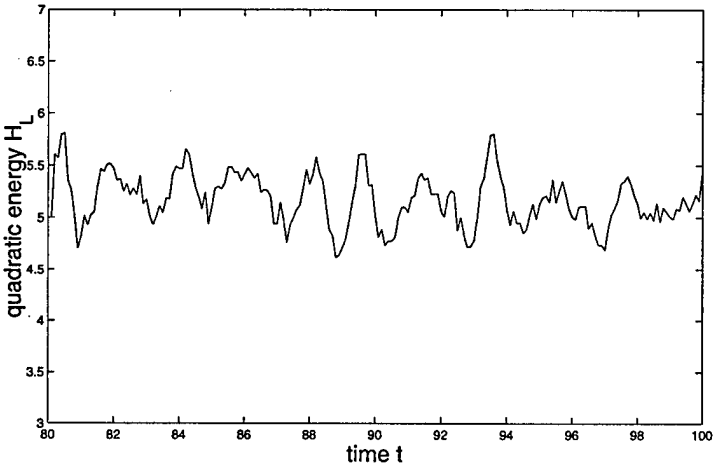

Fig. 2. $s = 1/10$, $\alpha = 3/2$, $\beta = 2$. Evolution of quadratic energy H_L vs. time in the stationary state.

the average nonlinearity fluctuates around some mean value $\epsilon \simeq 0.14$, which indicates that the condition of weak nonlinearity holds in our experiments. However, it should be emphasized that ϵ could not be imposed too small (by decreasing the forcing) otherwise the different modes would not be excited enough to generate an effective flux of energy. This problem is particularly important in numerics due to the discretization which restricts the possibilities for four-wave resonances. Since the effects of nonlinearity are assumed to be small in weak turbulence, it is sufficient to consider only the quantity H_L which contains the main part of the energy. We deduce the conservation of the total Hamiltonian from the conservation of H_L and ϵ, as illustrated in Figs. 2 and 3 because $H = H_L(1+\epsilon)$.

Fig. 4 displays the stationary isotropic spectra $n_k^{a,b}$ realized in the present situation. By comparison, we also plotted the predicted Kolmogorov solutions given by Eq. (12). For $\alpha = 3/2$ and $\beta = 2$, they read

$$n_k^a = c_2^a P_a^{1/3} \omega_k^{-14/9} = c_2^a P_a^{1/3} k^{-7/3}, \tag{15}$$

and

$$n_k^b = c_2^b P_b^{1/3} (s\omega_k)^{-14/9} = c_2^b P_b^{1/3} s^{-14/9} k^{-7/3}, \quad s = 1/10, \tag{16}$$

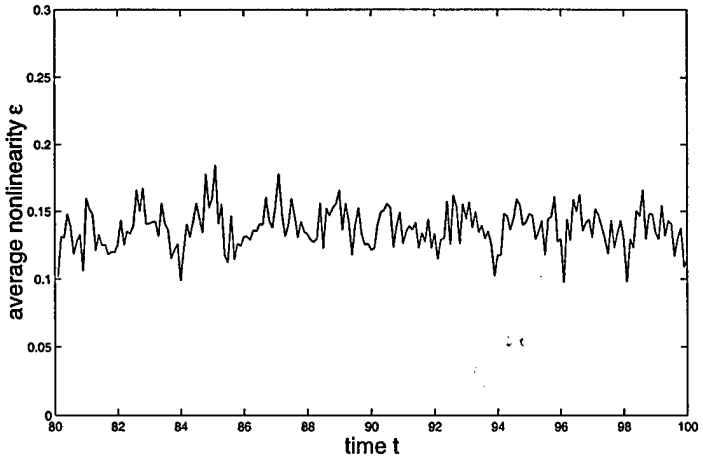

Fig. 3. $s = 1/10$, $\alpha = 3/2$, $\beta = 2$. Evolution of average nonlinearity ϵ vs. time in the stationary state.

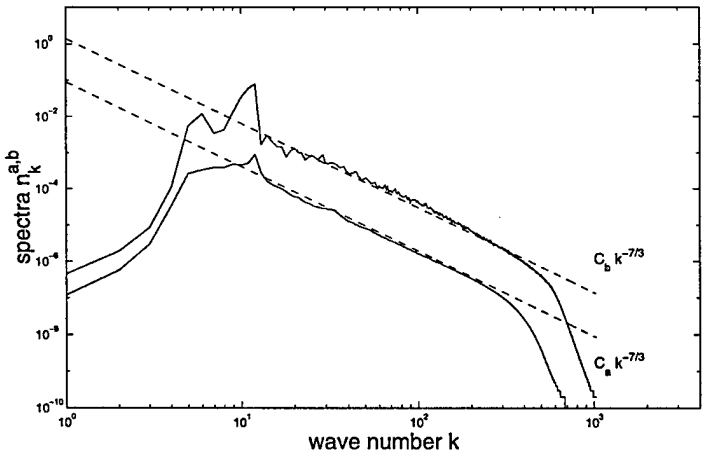

Fig. 4. $s = 1/10$, $\alpha = 3/2$, $\beta = 2$. Computed spectra (n_k^a for the lower one and n_k^b for the upper one) and predicted Kolmogorov spectra $C_{a,b}k^{-7/3}$ with $C_a = c_2^a P_a^{1/3}$ and $C_b = c_2^b P_b^{1/3} s^{-14/9}$ (dashed lines).

where $c_2^a = 0.094$ and $c_2^b = 0.047$ are numerically calculated from Eq. (13). The mean fluxes of energy $P_{a,b}$ in Eqs. (15) and (16) can be expressed as

$$P_a = 2 \int\limits_{k>k_d^+} v_+^a \left(k - k_d^+\right)^2 \omega_k n_k^a \, dk$$

and

$$P_b = 2 \int\limits_{k>k_d^+} v_+^b \left(k - k_d^+\right)^2 s\omega_k n_k^b \, dk,$$

with k_d^+ the cutoff of ultraviolet dissipation [1,7]. Then it is straightforward to get their values $P_a = 0.86$ and $P_b = 0.56$ from simulations. We can observe in Fig. 4 that for both wave fields the spectra are well approximated by the Kolmogorov power-laws over a wide range of scales (say $20 < k < 300$). Here the agreement between theory and numerics is found with respect to both the slope and the level of the spectra.

4. Conclusion

We have studied a simplified one-dimensional model describing media with two types of interacting waves. The regime of parameters has been chosen such

that weak turbulence theory can be applied correctly and coherent structures cannot develop. This way we avoid any interference between weak wave turbulence and coherent structures. Our numerical results show the appearance of a pure weak turbulence state with the formation of a complete Kolmogorov spectrum. This suggests the general relevance of weak turbulence even in one-dimensional systems. In the future it will be of interest to extend the present work to higher dimensions by still considering simplified models such as the present one, and to perform computations on the full equations describing the physical phenomena of interest. Recall that Pushkarev and Zakharov [2] successfully observed weak turbulence for capillary water waves in three dimensions. However, their numerical simulations based on the truncated basic equations were very time-consuming and the Kolmogorov spectrum that they measured extended only over a small range of scales.

Acknowledgements

This work was performed in the framework of the NATO Linkage Grant OUTR.LG 970583. V.E.Z. also acknowledges support of the US Army, under the grant DACA 42-00-C-0044, and of ONR, under the grant N00014-98-1-0070.

References

[1] V.E. Zakharov, V.S. Lvov, G. Falkovich, Kolmogorov Spectra of Turbulence, Springer, 1992.
[2] A.N. Pushkarev, V.E. Zakharov, Phys. Rev. Lett. 76 (1996) 3320.
[3] V.E. Zakharov, N.N. Filonenko, J. Appl. Mech. Tech. Phys. 4 (1967) 506.
[4] A.J. Majda, D.W. McLaughlin, E.G. Tabak, J. Nonlinear Sci. 6 (1997) 9.
[5] D. Cai, A.J. Majda, D.W. McLaughlin, E.G. Tabak, Proc. Natl. Acad. Sci. 96 (1999) 14216.
[6] P. Guyenne, V.E. Zakharov, A.N. Pushkarev, F. Dias, C. R. Acad. Sci. Paris IIb 328 (2000) 757.
[7] V.E. Zakharov, P. Guyenne, A.N. Pushkarev, F. Dias, Physica D 152–153 (2001) 573.
[8] L. Biven, S.V. Nazarenko, A.C. Newell, Phys. Lett. A 280 (2001) 28.
[9] M. Lyutikov, Phys. Lett. A 265 (2000) 83.
[10] V.E. Zakharov, O.A. Vasilyev, A.I. Dyachenko, JETP Lett. 73 (2001) 63.

ELSEVIER

Physica D 152–153 (2001) 573–619

PHYSICA D

www.elsevier.com/locate/physd

Wave turbulence in one-dimensional models

V.E. Zakharov [a,b], P. Guyenne [c], A.N. Pushkarev [d], F. Dias [e,*]

[a] *Landau Institute for Theoretical Physics, Moscow, Russia*
[b] *Department of Mathematics, University of Arizona, Tucson, AZ 85721, USA*
[c] *Institut Non-Linéaire de Nice, France*
[d] *Waves and Solitons LLC, 738 W. Sereno Dr., Gilbert, AZ, USA*
[e] *Centre de Mathematiques et de Leurs Applications, Ecole Normale Supérieure de Cachan, 61 Avenue du Président Wilson, 94235 Cachan Cedex, France*

Abstract

A two-parameter nonlinear dispersive wave equation proposed by Majda, McLaughlin and Tabak is studied analytically and numerically as a model for the study of wave turbulence in one-dimensional systems. Our ultimate goal is to test the validity of weak turbulence theory. Although weak turbulence theory is independent on the sign of the nonlinearity of the model, the numerical results show a strong dependence on the sign of the nonlinearity. A possible explanation for this discrepancy is the strong influence of coherent structures — wave collapses and quasisolitons — in wave turbulence. © 2001 Published by Elsevier Science B.V.

Keywords: Weak turbulence; Wave collapses; Quasisolitons; Kinetic wave equation; Kolmogorov spectra

1. Introduction

A wide variety of physical problems involve random nonlinear dispersive waves. The most common tool for the statistical description of these waves is a kinetic equation for squared wave amplitudes, the so-called kinetic wave equation. Sometimes this equation is also called Boltzmann's equation. This terminology is in fact misleading because the kinetic wave equation and Boltzmann's equation are the opposite limiting cases of a more general kinetic equation for particles which obey Bose–Einstein statistics like photons in stellar atmospheres or phonons in liquid helium. It was first derived by Peierls in 1929 [1]. In spite of the fact that both the kinetic wave equation and Boltzmann's equation can be derived from the quantum kinetic equation, the kinetic wave equation was derived independently and almost simultaneously in plasma physics and for surface waves on deep water. This was done in the early 1960s while Boltzmann's equation was derived in the 19th century! The derivation for surface waves is due to Hasselmann [2,3] (see also Zakharov [4]).

Once the kinetic wave equation has been derived, the shape of wave number spectra can be predicted by the so-called weak turbulence (WT) theory. It is called weak because it deals with resonant interactions between small-amplitude waves. Thus, contrary to fully developed turbulence, it leads to explicit analytical solutions provided some assumptions are made. So far, there have been only a few studies to check the results of WT the-

* Corresponding author.
E-mail address: dias@cmla.ens-cachan.fr (F. Dias).

0167-2789/01/$ – see front matter © 2001 Published by Elsevier Science B.V.
PII: S0167-2789(01)00194-4

ory. Recently, Pushkarev and Zakharov [5] numerically solved the three-dimensional dynamical equations for the free-surface elevation and the velocity potential in the case of capillary water waves. They obtained an isotropic spectrum close to the theoretical power-law found by Zakharov and Filonenko [6]. Majda, McLaughlin and Tabak [7] (hereafter referred to as MMT) considered four-wave interactions by introducing a one-dimensional model equation. This equation can be integrated numerically quite efficiently on large inertial intervals. They examined a family of Kolmogorov-type solutions depending on the parameters of the equation. The validity of several theoretical hypotheses was then assessed numerically. Namely, MMT confirmed the random phase and quasi-Gaussian approximations. They also showed the independence of the solutions on the nature of forces, initial conditions, and the size and level of discreteness of the computational domain. However, their simulations surprisingly displayed spectra steeper than the predicted ones. They explained the discrepancy by proposing a new inertial range scaling technique which seems to yield the appropriate exponents. More recently, Cai et al. [8–10] revisited their earlier results and found some results which agree with WT theory as well. [1] They considered two kinds of Hamiltonians: Hamiltonians which are the sum of a quadratic term and a quartic term (positive nonlinearity), as in [7], and Hamiltonians which are the difference between a quadratic and a quartic term (negative nonlinearity). For either sign of nonlinearity, they found agreement with MMT theory in some cases and agreement with WT theory in some other cases. Since their computations were performed with a dispersion relation in which the frequency varies like the square root of the wave number, one can see an analogy with deep water waves. Incidentally, the WT theory was recently developed for shallow water waves by Zakharov [11].

As in many other fields, numerical modeling leads to some difficulties, especially when one wants to compare with the theory. Most of these difficulties are related to finite-size effects, i.e. the domain is discretized into a grid of points in computations whereas one assumes an infinite medium in theory. We can mention the bottleneck phenomenon [12] which tends to flatten the slope of the inertial range at small scales. It is commonly observed in problems with a dissipative cutoff. In addition, Pushkarev [13] revealed the phenomenon of frozen turbulence at very low levels of nonlinearity. In this situation, the resonance conditions have very few solutions (or may not be fulfilled at all!) because of the discrete values of wave numbers. As a consequence, there is no energy flux due to the lack of resonating wave vectors. The power-law regime only takes place at moderate levels of nonlinearity where quasi-resonant interactions come into play. Pushkarev concluded that WT in bounded systems combines the features of both frozen and Kolmogorov-type turbulence. The beauty of the MMT model equation is that the above mentioned difficulties can be controlled completely.

After introducing the model equation, the paper is divided into two parts. In the first part (Sections 3–11), the MMT equation is studied analytically. A WT description of the equation is provided (see [7]). We find the Kolmogorov solutions of the kinetic equation and determine the set of parameters for which such solutions can be realized. Then we discuss the coherent structures which can compete with WT. The most simple coherent structures are solitons similar to the soliton solutions of the nonlinear Schrödinger equation (NLS).

Solitons for the MMT equation exist only if nonlinearity is negative. In the cases of interest, they are shown to be unstable (see Section 7) and cannot play an important role in the wave dynamics.

As an alternative to soliton coherent structures, there are wave collapses described by self-similar solutions of the MMT equation. These solutions can exist in a certain parameter regime for both signs of nonlinearity. Theoretically speaking, both solitons and collapses can coexist with WT.

Another type of coherent structures are quasisolitons, or envelope solitons. They were discussed recently by Zakharov and Kuznetsov [14]. In the MMT model quasisolitons exist at positive nonlinearity only. Their stability remains an open question.

[1] These three papers were kindly given to us when the present manuscript was essentially completed. Some of the results are similar to ours, but their interpretation is different.

The main new theoretical results of the first part are a careful tabulation of the signs of the fluxes for the MMT model equation, the existence and possible role of quasisolitons for positive nonlinearity, and an analogy with Phillips spectrum associated with the formation of collapses.

In the second part (Sections 12–14), we describe the results of the numerical study of the MMT equation. We find that the wave turbulence described by the MMT equation is different both quantitatively and qualitatively for both signs of nonlinearity. Since the predictions of WT theory are identical for both signs of nonlinearity, WT theory can be applied at best for one sign of nonlinearity. Our analysis of the results leads to somewhat contradictory results.

For positive nonlinearity the balance of energy and particle fluxes as well as the level of turbulence are in good agreement with WT theory. Meanwhile the slope of the spectrum in the window of transparency is steeper than predicted by WT theory.

In the case of negative nonlinearity the picture of turbulence is quite different from the WT predictions, both qualitatively and quantitatively. First of all, the turbulence is stabilized on a level which is one order of magnitude less than predicted by WT theory. Then the sign of the flux of particles is opposite to the one predicted by WT theory. Both these facts lead to a conjecture on the existence of a strong and essentially nonlinear mechanism which competes successfully with WT quartic resonances. In our opinion, this mechanism is the wave collapse, described by self-similar solutions of the MMT equations. At the same time, the high-frequency tail of the spectrum has a slope which coincides exactly with the slope predicted by WT theory. This leads to the conclusion that in spite of the presence of wave collapses, the high-frequency asymptotics of spectra is governed by the WT processes which are responsible for carrying only a small part of the energy. The coexistence of wave collapses and WT was already described in the context of the 2D NLS [15].

Wave collapse is an example of an essentially nonlinear coherent structure arising in wave turbulence under certain conditions. As said above, another important type of coherent structures are quasisolitons or envelope solitons living for a finite time. Such structures can arise in the MMT model in the case of positive nonlinearity. We believe that these structures are responsible for the deviation of the spectra from the ones predicted by WT theory.

2. Model equation

We investigate the family of dynamical equations

$$\mathrm{i}\frac{\partial\psi}{\partial t} = \left|\frac{\partial}{\partial x}\right|^{\alpha}\psi + \lambda\left|\frac{\partial}{\partial x}\right|^{\beta/4}\left(\left|\left|\frac{\partial}{\partial x}\right|^{\beta/4}\psi\right|^{2}\left|\frac{\partial}{\partial x}\right|^{\beta/4}\psi\right), \quad \lambda = \pm 1, \tag{2.1}$$

where $\psi(x,t)$ denotes a complex wave field and α, β are real parameters.

If $\lambda = +1$, one exactly recovers the MMT model which was treated in [7]. Note that our parameter β is the opposite of the parameter β in MMT. The extension $\lambda = \pm 1$ in Eq. (2.1), which was also treated in [8–10], raises an interesting problem because the balance between nonlinear and dispersive effects may change according to λ.

Besides the Hamiltonian

$$H = H_{\mathrm{L}} + H_{\mathrm{NL}} = \int\left(\left|\left|\frac{\partial}{\partial x}\right|^{\alpha/2}\psi\right|^{2} + \frac{\lambda}{2}\left|\left|\frac{\partial}{\partial x}\right|^{\beta/4}\psi\right|^{4}\right)\mathrm{d}x, \tag{2.2}$$

the system (2.1) preserves two other integrals of motion: wave action and momentum, respectively

$$N = \int|\psi|^{2}\,\mathrm{d}x \quad \text{and} \quad M = \frac{\mathrm{i}}{2}\int\left(\psi\frac{\partial\psi^{*}}{\partial x} - \frac{\partial\psi}{\partial x}\psi^{*}\right)\mathrm{d}x.$$

As usual, it is convenient to work in Fourier space. Let us write Eq. (2.1) as

$$\mathrm{i}\frac{\partial \hat{\psi}_k}{\partial t} = \omega(k)\hat{\psi}_k + \int T_{123k}\hat{\psi}_1\hat{\psi}_2\hat{\psi}_3^*\delta(k_1 + k_2 - k_3 - k)\,\mathrm{d}k_1\,\mathrm{d}k_2\,\mathrm{d}k_3, \tag{2.3}$$

where $\hat{\psi}_k = \hat{\psi}(k, t)$ denotes the kth component in the Fourier decomposition of $\psi(x, t)$ and $(*)$ stands for complex conjugation.

In this form, Eq. (2.3) looks like the so-called one-dimensional Zakharov's equation determined by the linear dispersion relation

$$\omega(k) = |k|^\alpha, \quad \alpha > 0, \tag{2.4}$$

and the simple interaction coefficient

$$T_{123k} = T(k_1, k_2, k_3, k) = \lambda|k_1k_2k_3k|^{\beta/4}. \tag{2.5}$$

One easily sees that the kernel T_{123k} possesses the symmetry required by the Hamiltonian property

$$T_{123k} = T_{213k} = T_{12k3} = T_{3k12}. \tag{2.6}$$

Moreover, the absolute values in Eqs. (2.4) and (2.5) ensure the basic assumptions of isotropy and scale invariance. In other words, $\omega(k)$ and T_{123k} are invariant with respect to rotations ($k \to -k$) and they are homogeneous functions of their arguments with degrees α and β, respectively, i.e.

$$T(\xi k_1, \xi k_2, \xi k_3, \xi k) = \xi^\beta T(k_1, k_2, k_3, k), \quad \xi > 0. \tag{2.7}$$

Following MMT, we fix $\alpha = \frac{1}{2}$ by analogy with gravity waves whose dispersion relation reads as $\omega(k) = (gk)^{1/2}$ (g being the acceleration due to gravity). The power β takes the value $+3$ if the analogy is extended to the nonlinear term but we will consider a wider range of values for β.

Eq. (2.3) describes four-wave interaction processes obeying the resonant conditions

$$k_1 + k_2 = k_3 + k, \tag{2.8}$$

$$\omega_1 + \omega_2 = \omega_3 + \omega. \tag{2.9}$$

For $\alpha > 1$ these equations only have the trivial solution $k_3 = k_1$, $k = k_2$ or $k_3 = k_2$, $k = k_1$. For $\alpha < 1$ there is also a non-trivial solution. Note that in this case the signs of k_i must be different. For instance, $k_1 < 0$ and $k_2, k_3, k > 0$. If $\alpha = \frac{1}{2}$, Eqs. (2.8) and (2.9) can be parameterized by two parameters A and ξ

$$k_1 = -A^2\xi^2, \qquad k_2 = A^2(1 + \xi + \xi^2)^2, \qquad k_3 = A^2(1 + \xi)^2, \qquad k = A^2\xi^2(1 + \xi)^2. \tag{2.10}$$

In the case $\alpha = 2$ and $\beta = 0$, Eq. (2.1) becomes the NLS equation

$$\mathrm{i}\frac{\partial \psi}{\partial t} = -\frac{\partial^2 \psi}{\partial x^2} + \lambda|\psi|^2\psi \tag{2.11}$$

(note here that $|\partial/\partial x|^2 = -\partial^2/\partial x^2$).

Positive nonlinearity $\lambda = +1$ corresponds to the *defocusing* NLS, while negative nonlinearity corresponds to the *focusing* NLS.

3. Weak turbulence description of the model equation

If one only considers small nonlinear effects, then the statistical behavior can be mainly described by the evolution of the two-point correlation function

$$\langle\hat{\psi}(k,t)\hat{\psi}^*(k',t)\rangle = n(k,t)\,\delta(k-k'),$$

where brackets denote ensemble averaging. We introduce also the four-wave correlation function

$$\langle\hat{\psi}(k_1,t)\hat{\psi}(k_2,t)\hat{\psi}^*(k_3,t)\hat{\psi}^*(k,t)\rangle = J_{123k}\delta(k_1+k_2-k_3-k). \tag{3.1}$$

On this basis, WT theory leads to the kinetic equation for $n(k,t)$ and provides tools for finding stationary power-law solutions (for details, see [7]). Here we explain the main steps of the procedure applied to our model.

The starting point is the original equation for $n(k,t)$. From Eq. (2.3), we have

$$\frac{\partial n_k}{\partial t} = 2\int \mathrm{Im}\, J_{123k}T_{123k}\delta(k_1+k_2-k_3-k)\,\mathrm{d}k_1\,\mathrm{d}k_2\,\mathrm{d}k_3. \tag{3.2}$$

Due to the quasi-Gaussian random phase approximation

$$\mathrm{Re}\, J_{123k} \simeq n_1n_2[\delta(k_1-k_3)+\delta(k_1-k)]. \tag{3.3}$$

The imaginary part of J_{123k} can be found through an approximate solution of the equation imposed on this correlator. The result is (see [16])

$$\mathrm{Im}\, J_{123k} \simeq 2\pi T^*_{123k}\delta(\omega_1+\omega_2-\omega_3-\omega)(n_1n_2n_3+n_1n_2n_k-n_1n_3n_k-n_2n_3n_k). \tag{3.4}$$

This gives

$$\begin{aligned}\frac{\partial n_k}{\partial t} = 4\pi\int |T_{123k}|^2(n_1n_2n_3+n_1n_2n_k-n_1n_3n_k-n_2n_3n_k)\delta(\omega_1+\omega_2-\omega_3-\omega)\\ \times\delta(k_1+k_2-k_3-k)\,\mathrm{d}k_1\,\mathrm{d}k_2\,\mathrm{d}k_3.\end{aligned} \tag{3.5}$$

Since the square norm cancels the sign of T_{123k}, it is clear that the WT approach is independent on λ. Here we point out that MMT mistakenly wrote a factor 12π instead of 4π in Eq. (3.5) and the right-hand side of Eq. (3.5) with the opposite sign. This fact is particularly important when determining the fluxes of wave action and energy.

Assuming that $n(-k) = n(k)$ (similarly to an angle averaging in higher dimensions), one gets

$$\begin{aligned}\frac{\partial\mathcal{N}(\omega)}{\partial t} = \frac{4\pi}{\alpha^4}\int(\omega_1\omega_2\omega_3\omega)^{(\beta/2-\alpha+1)/\alpha}(n_1n_2n_3+n_1n_2n_\omega-n_1n_3n_\omega-n_2n_3n_\omega)\delta(\omega_1+\omega_2-\omega_3-\omega)\\ \times[\delta(\omega_1^{1/\alpha}+\omega_2^{1/\alpha}-\omega_3^{1/\alpha}+\omega^{1/\alpha})+\delta(\omega_1^{1/\alpha}+\omega_2^{1/\alpha}+\omega_3^{1/\alpha}-\omega^{1/\alpha})\\ +\delta(\omega_1^{1/\alpha}-\omega_2^{1/\alpha}-\omega_3^{1/\alpha}-\omega^{1/\alpha})+\delta(-\omega_1^{1/\alpha}+\omega_2^{1/\alpha}-\omega_3^{1/\alpha}-\omega^{1/\alpha})]\,\mathrm{d}\omega_1\,\mathrm{d}\omega_2\,\mathrm{d}\omega_3,\end{aligned} \tag{3.6}$$

where $\mathcal{N}(\omega) = n(k(\omega))\,\mathrm{d}k/\mathrm{d}\omega$, n_ω stands for $n(k(\omega))$ and ω is given by Eq. (2.4).

The next step consists in inserting the power-law ansatz

$$n(\omega) \propto \omega^{-\gamma}, \tag{3.7}$$

and then performing the Zakharov's conformal transformations [7,15,16]. Finally, the kinetic equation becomes

$$\frac{\partial\mathcal{N}(\omega)}{\partial t} \propto \omega^{-\gamma-1}I(\alpha,\beta,\gamma), \tag{3.8}$$

where

$$I(\alpha,\beta,\gamma)=\frac{4\pi}{\alpha^4}\int_\Delta(\xi_1\xi_2\xi_3)^{((\beta/2+1)/\alpha)-1-\gamma}(1+\xi_3^\gamma-\xi_1^\gamma-\xi_2^\gamma)\delta(1+\xi_3-\xi_1-\xi_2)$$
$$\times\delta(\xi_1^{1/\alpha}+\xi_2^{1/\alpha}+\xi_3^{1/\alpha}-1)(1+\xi_3^y-\xi_1^y-\xi_2^y)\,d\xi_1\,d\xi_2\,d\xi_3 \tag{3.9}$$

with

$$\Delta=\{0<\xi_1<1,\ 0<\xi_2<1,\ \xi_1+\xi_2>1\}\quad\text{and}\quad y=3\gamma+1-\frac{2\beta+3}{\alpha}.$$

The non-dimensionalized integral $I(\alpha,\beta,\gamma)$ is obtained by using the change of variables $\omega_j\to\omega\xi_j$ $(j=1,2,3)$.

The ansatz (3.7) makes sense if the integral in (3.6) converges. It could diverge both at low and high frequencies. The condition of convergence at low frequencies coincides with the condition of convergence of the integral in (3.9) and can be easily found. It reads

$$2\gamma<-1+\frac{\beta+4}{\alpha}. \tag{3.10}$$

The condition of convergence at high frequencies can be found after substituting (3.7) into (3.6). Omitting the details, we get the result

$$\gamma>\frac{\beta+\alpha-1}{\alpha}. \tag{3.11}$$

In all the cases discussed in this paper, both conditions (3.10) and (3.11) are satisfied.

For the case $\alpha=\frac{1}{2}$, one can transform Eq. (3.6) into the form

$$\frac{\partial\mathcal{N}(\omega)}{\partial t}=64\pi\omega^{4(\beta+1)}[S_1+S_2+S_3+S_4],$$

where

$$S_1=2\int_0^1\frac{u^{2\beta+2}(u+1)^{2\beta+1}}{(1+u+u^2)^{3\beta+4}}\left[n\left(\frac{u}{1+u+u^2}\omega\right)n\left(\frac{u(u+1)}{1+u+u^2}\omega\right)n\left(\frac{u+1}{1+u+u^2}\omega\right)\right.$$
$$+n(\omega)n\left(\frac{u(u+1)}{1+u+u^2}\omega\right)n\left(\frac{u+1}{1+u+u^2}\omega\right)-n(\omega)n\left(\frac{u}{1+u+u^2}\omega\right)n\left(\frac{u+1}{1+u+u^2}\omega\right)$$
$$\left.-n(\omega)n\left(\frac{u}{1+u+u^2}\omega\right)n\left(\frac{u(u+1)}{1+u+u^2}\omega\right)\right]du,$$

$$S_2=\int_0^1\frac{(1+u+u^2)^{\beta+1}(u+1)^{2\beta+1}}{u^{2\beta+3}}\left[n\left(\frac{1+u+u^2}{u}\omega\right)n((u+1)\omega)n\left(\frac{u+1}{u}\omega\right)\right.$$
$$+n(\omega)n((u+1)\omega)n\left(\frac{u+1}{u}\omega\right)-n(\omega)n\left(\frac{1+u+u^2}{u}\omega\right)n\left(\frac{u+1}{u}\omega\right)$$
$$\left.-n(\omega)n\left(\frac{1+u+u^2}{u}\omega\right)n((u+1)\omega)\right]du,$$

$$S_3=\int_0^1\frac{u^{2\beta+2}(1+u+u^2)^{\beta+1}}{(1+u)^{2\beta+3}}\left[n(u\omega)n\left(\frac{1+u+u^2}{1+u}\omega\right)n\left(\frac{u}{1+u}\omega\right)\right.$$
$$\left.+n(\omega)n\left(\frac{1+u+u^2}{1+u}\omega\right)n\left(\frac{u}{1+u}\omega\right)-n(\omega)n(u\omega)n\left(\frac{1+u+u^2}{1+u}\omega\right)-n(\omega)n(u\omega)n\left(\frac{u}{1+u}\omega\right)\right]du,$$

$$S_4 = \int_0^1 \frac{(1+u+u^2)^{\beta+1}}{u^{2\beta+3}(1+u)^{2\beta+2}} \left[n\left(\frac{\omega}{u}\right) n\left(\frac{1+u+u^2}{u(1+u)}\omega\right) n\left(\frac{\omega}{1+u}\omega\right) + n(\omega) n\left(\frac{1+u+u^2}{u(1+u)}\omega\right) n\left(\frac{\omega}{u}\right) - n(\omega) n\left(\frac{\omega}{u}\right) n\left(\frac{\omega}{1+u}\right) - n(\omega) n\left(\frac{\omega}{u}\omega\right) n\left(\frac{1+u+u^2}{u(1+u)}\omega\right) \right] \mathrm{d}u.$$

This equation can be used for the numerical simulation of WT.

4. Kolmogorov solutions

The aim is to look for stationary solutions of the kinetic equation. From Eqs. (3.8) and (3.9) we easily find that the stationarity condition

$$\frac{\partial \mathcal{N}(\omega)}{\partial t} = 0 \Leftrightarrow I(\alpha, \beta, \gamma) = 0 \tag{4.1}$$

is satisfied only for $\gamma = 0, 1$ and $y = 0, 1$.

In terms borrowed from statistical mechanics, the cases $\gamma = 0, 1$ represent the thermodynamic equilibrium solutions

$$n(\omega) = c, \tag{4.2}$$

where c is an arbitrary constant and

$$n(\omega) \propto \omega^{-1} \propto |k|^{-\alpha}, \tag{4.3}$$

which stem from the more general Rayleigh–Jeans distribution

$$n_{\mathrm{RJ}}(\omega) = \frac{c_1}{c_2 + \omega}. \tag{4.4}$$

They correspond respectively to equipartition of particle number N and quadratic energy E

$$N = \int n(k)\,\mathrm{d}k = \int \mathcal{N}(\omega)\,\mathrm{d}\omega, \tag{4.5}$$

$$E = \int \omega(k) n(k)\,\mathrm{d}k = \int \omega \mathcal{N}(\omega)\,\mathrm{d}\omega. \tag{4.6}$$

The cases $y = 0, 1$ give the non-equilibrium Kolmogorov-type solutions, respectively

$$n(\omega) \propto \omega^{(-2\beta/3-1+\alpha/3)/\alpha} \propto |k|^{-2\beta/3-1+\alpha/3}, \tag{4.7}$$

and

$$n(\omega) \propto \omega^{-(2\beta/3+1)/\alpha} \propto |k|^{-2\beta/3-1}, \tag{4.8}$$

which exhibit typical dependence on the parameter β of the interaction coefficient. The latter solutions are more interesting since realistic sea spectra are of Kolmogorov-type by analogy.

For the case $\alpha = \frac{1}{2}$ and $\beta = 0$, the Kolmogorov-type solutions are

$$n(\omega) \propto \omega^{-5/3} \propto |k|^{-5/6}, \tag{4.9}$$

$$n(\omega) \propto \omega^{-2} \propto |k|^{-1}. \tag{4.10}$$

Both exponents satisfy the conditions of locality (3.10) and (3.11).

5. Nature and sign of the fluxes

The stationary non-equilibrium states are related to fluxes of integrals of motion, namely the quantities N and E in our four-wave interaction problem. We define the flux of particles (or wave action) and energy as, respectively

$$Q(\omega) = -\int_0^\omega \frac{\partial \mathcal{N}(\omega')}{\partial t}\,\mathrm{d}\omega', \tag{5.1}$$

$$P(\omega) = -\int_0^\omega \omega' \frac{\partial \mathcal{N}(\omega')}{\partial t}\,\mathrm{d}\omega'. \tag{5.2}$$

Here, Eq. (4.7), respectively Eq. (4.8), is associated with a constant mean flux Q_0, respectively P_0, of particles, respectively energy. Let us now mention a physical argument which plays a crucial role in deciding the realizability of the Kolmogorov-type spectra. A more detailed justification is provided in Section 11 (see also [7,16]). Suppose that pumping is performed at some frequencies around $\omega = \omega_f$ and damping at ω near zero and $\omega \gg \omega_f$. Weak turbulence theory then states that the energy is expected to flow from ω_f to higher ω's (direct cascade with $P_0 > 0$) while the particles mainly head for lower ω's (inverse cascade with $Q_0 < 0$). Accordingly, we need to evaluate the fluxes in order to select, among the rich family of power laws (4.7) and (4.8), those which are likely to result from numerical simulations of Eq. (2.1) with damping and forcing.

By inserting Eq. (3.8) into Eqs. (5.1) and (5.2), we obtain

$$Q_0 \propto \lim_{y\to 0} \frac{\omega^{-y}}{y} I, \qquad P_0 \propto \lim_{y\to 1} \frac{\omega^{-y+1}}{1-y} I \tag{5.3}$$

which become

$$Q_0 \propto \left.\frac{\partial I}{\partial y}\right|_{y=0}, \qquad P_0 \propto \left.\frac{\partial I}{\partial y}\right|_{y=1}. \tag{5.4}$$

Using Eq. (3.9), the derivatives in Eq. (5.4) can be expressed as

$$-\left.\frac{\partial I}{\partial y}\right|_{y=0} = \int_\Delta S(\xi_1,\xi_2,\xi_3)(1+\xi_3^\gamma - \xi_1^\gamma - \xi_2^\gamma)\delta(1+\xi_3-\xi_1-\xi_2) \times \ln\left(\frac{\xi_1\xi_2}{\xi_3}\right)\delta(\xi_1^{1/\alpha}+\xi_2^{1/\alpha}+\xi_3^{1/\alpha}-1)\,\mathrm{d}\xi_1\,\mathrm{d}\xi_2\,\mathrm{d}\xi_3,$$

$$\left.\frac{\partial I}{\partial y}\right|_{y=1} = \int_\Delta S(\xi_1,\xi_2,\xi_3)(1+\xi_3^\gamma - \xi_1^\gamma - \xi_2^\gamma)\delta(1+\xi_3-\xi_1-\xi_2) \times \left[\xi_1 \ln\left(\frac{1}{\xi_1}\right) + \xi_2 \ln\left(\frac{1}{\xi_2}\right) - \xi_3 \ln\left(\frac{1}{\xi_3}\right)\right]\delta(\xi_1^{1/\alpha}+\xi_2^{1/\alpha}+\xi_3^{1/\alpha}-1)\,\mathrm{d}\xi_1\,\mathrm{d}\xi_2\,\mathrm{d}\xi_3$$

with

$$S(\xi_1,\xi_2,\xi_3) = \frac{4\pi}{\alpha^4}(\xi_1\xi_2\xi_3)^{((\beta/2+1)/\alpha)-1-\gamma}.$$

The sign of each integral above is determined by the factor (see [15])

$$f(\gamma) = 1+\xi_3^\gamma - \xi_1^\gamma - \xi_2^\gamma.$$

It is found that $f(\gamma)$ is positive when

$$\gamma < 0 \quad \text{or} \quad \gamma > 1. \tag{5.5}$$

Table 1
Signs of the fluxes for the Kolmogorov-type solutions, $\alpha = \frac{1}{2}$

β	-1	$-\frac{3}{4}$	$-\frac{1}{2}$	$-\frac{1}{4}$	0	$+3$
γ_Q	$\frac{1}{3}$	$\frac{2}{3}$	1	$\frac{4}{3}$	$\frac{5}{3}$	$\frac{17}{3}$
Sign of Q_0	$+$	$+$	0	$-$	$-$	$-$
γ_P	$\frac{2}{3}$	1	$\frac{4}{3}$	$\frac{5}{3}$	2	6
Sign of P_0	$-$	0	$+$	$+$	$+$	$+$

For the same values of β as those considered by MMT and the additional value $\beta = +3$, Table 1 displays the corresponding frequency slopes from Eqs. (4.7) and (4.8) and the signs of Q_0, P_0 according to the criterion (5.5).

Our calculations show that WT theory should work most successfully for $\beta = 0$ (instead of $\beta = -1$ in [7]) at which they yield both $Q_0 < 0$ and $P_0 > 0$. Incidentally, MMT reported the smallest difference between numerics and theory for $\beta = 0$. The cases with spectral slopes less steep than the Rayleigh–Jeans distribution (i.e. $\gamma < 1$) are non-physical. At best, a thermodynamic equilibrium is expected in the conservative regime. Hence, we cannot strictly rely on the Kolmogorov-type exponents for $\beta = -1, -\frac{3}{4}$ to compare with the numerical results in forced regimes. Note that for $\beta = -\frac{1}{2}$, although we find $P_0 > 0$, a pure thermodynamic equilibrium state (i.e. $\gamma = 1$) is predicted instead of the inverse cascade. This is however not valid because of the necessity for a finite flux of particles towards $\omega = 0$. The direct cascade may then be influenced one way or another, possibly making the theory not applicable to the whole spectrum. Using both criteria (5.5), we deduce that the fluxes of particles and energy simultaneously have the correct signs in the region of parameter

$$\beta < -\tfrac{3}{2} \quad \text{and} \quad \beta > 2\alpha - \tfrac{3}{2}, \tag{5.6}$$

or

$$\beta < -\tfrac{3}{2} \quad \text{and} \quad \beta > -\tfrac{1}{2} \quad \text{if} \quad \alpha = \tfrac{1}{2}. \tag{5.7}$$

Since the strength of nonlinearity decreases with β, the case $\beta < -\frac{3}{2}$, which is close to a linear problem, is not interesting from a general viewpoint and may raise some difficulties in numerical studies.

Restricting again to $\alpha = \frac{1}{2}$ and $\beta = 0$, one has for the spectrum

$$n(\omega) = a P^{1/3} \omega^{-2}, \tag{5.8}$$

where P is the flux of energy towards high frequencies and

$$a = \left(\left. \frac{\partial I}{\partial y} \right|_{y=1} \right)^{-1/3} \tag{5.9}$$

is the Kolmogorov constant. Numerical calculations give for a

$$a = 0.376. \tag{5.10}$$

An important question is the stability of the stationary spectra. This question was studied by Balk and Zakharov in [17] from a general point of view. The particular situation discussed in the present paper requires an additional study based on the work [17]. However, one should note that instability of the present spectra is unlikely. The reason is that the stationary spectra are solutions of the kinetic equation, which is not sensitive to changing the sign of the nonlinearity in the dynamical equation. In other words, if the Kolmogorov solution was unstable, it would be unstable in both cases. Since, we observe the Kolmogorov spectrum in the numerical simulation for one of the signs of nonlinearity, instability is unlikely.

6. Solitons and quasisolitons

Besides random radiative waves, solitons are the most interesting features of nonlinear Hamiltonian models such as the focusing NLS. These localized coherent structures can naturally emerge and persist as the result of the stable competition between nonlinear and dispersive mechanisms. It is known that they act as statistical attractors to which the system relaxes and they can influence the dynamics in a substantial way.

Equally important coherent structures are *quasisolitons*. They could be defined as solitons having finite but long enough life time. Solitons and quasisolitons can be compared with stable and unstable elementary particles. Formally, both solitons and quasisolitons are defined as solutions of Eq. (2.3) of the form

$$\hat{\psi}_k(t) = \mathrm{e}^{\mathrm{i}(\Omega - kV)t}\hat{\phi}_k. \tag{6.1}$$

Here Ω and V are constants. In the x-space,

$$\psi(x,t) = \mathrm{e}^{\mathrm{i}\Omega t}\xi(x - Vt), \tag{6.2}$$

where $\xi(x)$ is the inverse Fourier transform of $\hat{\phi}_k$ and V is the soliton velocity. The amplitude $\hat{\phi}_k$ satisfies the integral equation

$$\hat{\phi}_k = -\frac{1}{\Omega - kV + \omega(k)} \int T_{123k}\,\hat{\phi}_1\hat{\phi}_2\hat{\phi}_3^*\delta(k_1 + k_2 - k_3 - k)\,\mathrm{d}k_1\,\mathrm{d}k_2\,\mathrm{d}k_3. \tag{6.3}$$

The "classical" or "true" soliton is a localized solution of Eq. (6.3). In this case,

$$|\xi(x)|^2 \to 0 \quad \text{as} \quad |x| \to \infty. \tag{6.4}$$

This implies that $\hat{\phi}_k$ is a continuous function which has no singularities for real k. Thus the denominator in Eq. (6.3) should not vanish on the real axis

$$\Omega - kV + \omega(k) \neq 0, \quad -\infty < k < +\infty. \tag{6.5}$$

For $\omega(k) = |k|^\alpha$ and $\alpha < 1$, the last condition is violated for any $V \neq 0$. So "true solitons" can exist only if $V = 0$.

Next, we show that "true" solitons can only exist for $\lambda = -1$. Eq. (6.3) can be rewritten in the variational form

$$\delta(H + \Omega N) = 0. \tag{6.6}$$

Obviously, $\Omega > 0$ should hold (otherwise, the denominator (6.5) has zeroes). Since

$$T_{123k} = \lambda|k_1k_2k_3k|^{\beta/4}, \quad \lambda = \pm 1, \tag{6.7}$$

the Hamiltonian is positive for $\lambda = +1$ and Eq. (6.6) can be satisfied only if $\hat{\phi}_k \equiv 0$. There are no solitons in this case. Meanwhile, solitons can exist for $\lambda = -1$. A rigorous proof of existence is beyond the frame of this paper.

Quasisolitons are a more sophisticated object. Let us allow the denominator (6.5) to have a zero at $k = k_0$ and suppose that $\hat{\phi}_k$ is a function which is sharply localized near the wave number $k = k_m$. Let the width of $\hat{\phi}_k$ near $k = k_m$ be κ. One can introduce

$$T(k) = \int T_{123k}\hat{\phi}_1\hat{\phi}_2\hat{\phi}_3^*\delta(k_1 + k_2 - k_3 - k)\,\mathrm{d}k_1\,\mathrm{d}k_2\,\mathrm{d}k_3. \tag{6.8}$$

We might expect that

$$T(k_0) \simeq \mathrm{e}^{-C(|k_0 - k_m|/\kappa)}|\hat{\phi}(k_m)|^2\hat{\phi}(k_m). \tag{6.9}$$

In other words, $\hat{\phi}_k$ has a pole at $k = k_0$ but the residue at this pole is exponentially small. It means that the soliton (6.2) is not exactly localized and goes to a very small-amplitude monochromatic wave with wave number $k = k_0$ as $x \to -\infty$.

If one eliminates the pole from $\hat{\phi}_k$, one gets a quasisoliton, which is a stationary solution of (2.3) only approximately. Such a quasisoliton lives for a finite time. If this time is long enough, the quasisoliton could become the basic unit of wave turbulence. This is what we believe may happen in the MMT model with positive nonlinearity.

7. Soliton stability and collapse

Coherent structures can play a role in wave turbulence only if they are stable. For $\lambda = -1$, a soliton satisfies the equation

$$(\Omega + |k|^{\alpha})\hat{\phi}_k = \int |k_1 k_2 k_3 k|^{\beta/4} \hat{\phi}_1 \hat{\phi}_2 \hat{\phi}_3^* \delta(k_1 + k_2 - k_3 - k)\, \mathrm{d}k_1\, \mathrm{d}k_2\, \mathrm{d}k_3. \tag{7.1}$$

The free parameter Ω can be eliminated by the scaling

$$\hat{\phi}_k = \Omega^{-(\beta-\alpha+2)/2\alpha} \chi(\Omega^{-1/\alpha} k), \tag{7.2}$$

where $\chi(\xi)$ satisfies the equation

$$(1 + |\xi|^{\alpha})\chi(\xi) = \int |\xi_1 \xi_2 \xi_3 \xi|^{\beta/4} \chi_1 \chi_2 \chi_3^* \delta(\xi_1 + \xi_2 - \xi_3 - \xi)\, \mathrm{d}\xi_1\, \mathrm{d}\xi_2\, \mathrm{d}\xi_3. \tag{7.3}$$

Let us calculate the total wave action in the soliton

$$N = \int |\hat{\phi}_k|^2\, \mathrm{d}k = \Omega^{-(\beta-\alpha+1)/\alpha} N_0, \tag{7.4}$$

where

$$N_0 = \int |\chi|^2\, \mathrm{d}\xi. \tag{7.5}$$

The stability question can be answered by computing $\partial N/\partial \Omega$. As is well-known (see [18]), a soliton is stable if $\partial N/\partial \Omega > 0$. In our case,

$$\frac{\partial N}{\partial \Omega} = -\left(\frac{\beta - \alpha + 1}{\alpha}\right) \frac{N}{\Omega}. \tag{7.6}$$

The soliton is stable if

$$\beta < \alpha - 1, \tag{7.7}$$

otherwise the soliton is unstable. For $\alpha = \frac{1}{2}$, the condition of soliton instability reads

$$\beta > -\tfrac{1}{2}. \tag{7.8}$$

This condition is satisfied in all the cases we studied.

The soliton instability leads us to guess that the typical coherent structure in the case of negative nonlinearity is a collapsing singularity. Typically, the formation of such singularities is described by self-similar solutions of the initial equations. Eq. (2.3) has the following family of self-similar solutions

$$\hat{\psi}(k, t) = (t_0 - t)^{p + \mathrm{i}\epsilon} \chi[k(t_0 - t)^{1/\alpha}], \tag{7.9}$$

where $p = (\beta - \alpha + 2)/2\alpha$ and ϵ is an arbitrary constant. $\chi(\xi)$ satisfies the equation

$$i(p + i\epsilon)\chi + \frac{i}{\alpha}\xi\chi' + |\xi|^\alpha\chi + \lambda\int |\xi_1\xi_2\xi_3\xi|^{\beta/4}\chi_1\chi_2\chi_3^*\delta(\xi_1 + \xi_2 - \xi_3 - \xi)\,d\xi_1\,d\xi_2\,d\xi_3 = 0. \tag{7.10}$$

The soliton (7.9) should stay finite when $t \to t_0$. This requirement imposes the following asymptotic behavior on $\chi(\xi)$

$$\chi(\xi) \to C\xi^{(-\beta+\alpha-2)/2}, \quad \xi \to 0. \tag{7.11}$$

At time $t = t_0$, Eq. (7.9) turns to the powerlike function

$$\hat{\psi}_k \to Ck^{-\nu}, \qquad \nu = \tfrac{1}{2}(\beta - \alpha + 2). \tag{7.12}$$

In reality, the self-similar solution is realized in x-space in a finite domain of order L. Hence, the solution (7.12) should be cut off at $k \simeq 1/L$. In k-space, Eq. (7.9) represents the formation of a powerlike "tail" (7.12). The wave action concentrated in this tail must be finite. Therefore the integral

$$\int_0^\infty |\hat{\psi}_k|^2\,dk \tag{7.13}$$

should converge as $k \to \infty$. It leads to the condition on parameters

$$\beta > \alpha - 1, \tag{7.14}$$

which coincides with the condition for soliton instability.

Let us plug (7.9) into the Hamiltonian in Fourier space

$$H = \int \omega(k)|\hat{\psi}_k|^2\,dk + \int T_{123k}\hat{\psi}_1\hat{\psi}_2\hat{\psi}_3^*\hat{\psi}_k^*\delta(k_1 + k_2 - k_3 - k)\,dk_1\,dk_2\,dk_3\,dk$$
$$= (t_0 - t)^{(\beta-2\alpha+1)/\alpha}H_0,$$

where

$$H_0 = \int |\xi|^\alpha|\chi|^2\,d\xi + \lambda\int |\xi_1\xi_2\xi_3\xi|^{\beta/4}\chi_1\chi_2\chi_3^*\chi^*\delta(\xi_1 + \xi_2 - \xi_3 - \xi)\,d\xi_1\,d\xi_2\,d\xi_3\,d\xi. \tag{7.15}$$

If $\alpha - 1 < \beta < 2\alpha - 1$, then $H \to \infty$ as $t \to t_0$, unless

$$H_0 = 0. \tag{7.16}$$

Apparently, this condition can be satisfied only for $\lambda = -1$ (negative nonlinearity). The condition (7.16) imposes implicitly a constraint on the constant ϵ. In fact, it can be realized only at one specific value of ϵ, which is an eigenvalue of the boundary problem (7.10) with the boundary conditions

$$\chi(\xi) \to C\xi^{(-\beta+\alpha-2)/2}, \quad \xi \to 0, \qquad |\chi(\xi)| \to \infty, \quad |\xi| \to \infty.$$

In the case $\beta > 2\alpha - 1$, $H \to 0$ as $t \to t_0$. There is no limitation on the value of H_0 and the singularity can take place for either sign of λ. If $\nu < 1$ in Eq. (7.12) or $\alpha - 1 < \beta < \alpha$, a collapse is the formation of an integrable singularity in x-space. If $\nu > 1$ or $\beta > \alpha$, the singularity is the formation of a discontinuity of the function $\psi(x)$ or its derivatives.

The formation of singularities leads to the formation in k-space of a powerlike spectrum

$$n_k \simeq |\hat{\psi}_k|^2 \simeq |k|^{-2\nu} \simeq |k|^{-\beta+\alpha-2}. \tag{7.17}$$

For $\alpha = \frac{1}{2}$ and $\beta = 0$, one obtains

$$n_k \simeq |k|^{-3/2} \simeq \omega^{-3}. \tag{7.18}$$

This spectrum can be called Phillips spectrum by analogy to the well-known "ω^{-5} spectrum" for deep water waves [19]. As $\omega \to \infty$, it decays faster than Kolmogorov spectra.

8. More on quasisolitons

Let us consider again the case of negative nonlinearity $\lambda = -1$ and denote

$$F = -\Omega + kV - \omega(k) = -\Omega + kV - |k|^{\alpha}. \tag{8.1}$$

If $V = 0$ and $\Omega > 0$, $|F|$ has a minimum at $k = 0$. The Fourier transform of the solution $\hat{\phi}_k$ is concentrated near this minimum in a domain of width

$$\kappa \simeq \Omega^{1/\alpha}. \tag{8.2}$$

Assuming that the soliton is smooth in x-space, $\hat{\phi}_k$ decays very fast outside of the domain (8.2). So far we assumed that $V = 0$. Let now V be positive but very small. Then the denominator F has a zero at $k = k_0 \simeq V^{1/(\alpha-1)}$. For small V, the wave number k_0 is much larger than κ and this zero occurs very far from the domain which supports the soliton. This means that $\hat{\phi}_k$ has a pole at $k = k_0$, but the residue at this pole is very small. The presence of this pole means that the stationary solution (6.3) looks in the x-space like a soliton, which is not completely localized. As $x \to +\infty$, it becomes a monochromatic wave with wave number k_0 and negligibly small amplitude.

If this "wave tail" is cut off in the initial data, one has a "quasisoliton" which slowly decays due to radiation of energy in the right direction. If V is small enough, the lifetime of the quasisoliton is very long and its shape is close to the shape of "real" solitons.

It is unlikely that quasisolitons play an important role in wave turbulence at negative nonlinearity. If V is not small, their lifetime is too short; if V is small, they are unstable like real solitons. Quasisolitons are more relevant in the case of positive nonlinearity $\lambda = +1$.

Let us choose an arbitrary $k = k_m > 0$ and plug in Eq. (6.3)

$$V = \alpha k_m^{\alpha-1}, \qquad \Omega = -(1-\alpha)k_m^{\alpha} - \tfrac{1}{2}\alpha(1-\alpha)k_m^{\alpha-2}q^2. \tag{8.3}$$

Then

$$F = k_m^{\alpha} - |k|^{\alpha} + \alpha k_m^{\alpha-1}(k - k_m) + \tfrac{1}{2}\alpha(1-\alpha)k_m^{\alpha-2}q^2. \tag{8.4}$$

Note that if $\alpha < 1$ then F has a zero at $k = k_0 < 0$ for any k_m. Hence, $1/F$ always has a pole on the negative real axis, and the soliton (6.3) cannot be a real soliton. But if $q^2 \ll k_m^2$, $1/F$ has a sharp maximum at $k \simeq k_m$. Introducing

$$\kappa = |k - k_m|, \tag{8.5}$$

one has approximately

$$F \simeq \tfrac{1}{2}\alpha(1-\alpha)k_m^{\alpha-2}[\kappa^2 + q^2], \tag{8.6}$$

and one gets for the width of the maximum of $1/F$

$$\kappa \simeq q. \tag{8.7}$$

If $\kappa \ll |k_0|$, one can construct a quasisoliton which is supported in k-space near k_m. In the general case, $|k_0| \simeq k_m$. If $\alpha = \frac{1}{2}$ and $q = 0$, one can easily find

$$k_0 = -(\sqrt{2}-1)^2 k_m. \tag{8.8}$$

The quasisoliton moves to the right direction with the velocity $V(k_m)$ and radiates backward monochromatic waves of wave number k_0. The shape of the quasisoliton can be found explicitly in the limit $q \to 0$. Now $\kappa \ll k_m$ and one has approximately

$$\int |k_1 k_2 k_3 k|^{\beta/4} \hat{\phi}_1 \hat{\phi}_2 \hat{\phi}_3^* \delta(k_1 + k_2 - k_3 - k)\, \mathrm{d}k_1\, \mathrm{d}k_2\, \mathrm{d}k_3 \simeq k_m^\beta \int \hat{\phi}_1 \hat{\phi}_2 \hat{\phi}_3^* \delta(\kappa_1 + \kappa_2 - \kappa_3 - \kappa)\, \mathrm{d}\kappa_1\, \mathrm{d}\kappa_2\, \mathrm{d}\kappa_3. \tag{8.9}$$

Taking into account Eq. (8.6), one can rewrite Eq. (6.3) as

$$\frac{1}{2}\alpha(1-\alpha)k_m^{\alpha-2}(\kappa^2+q^2)\hat{\phi}_\kappa = k_m^\beta \int \hat{\phi}_1 \hat{\phi}_2 \hat{\phi}_3^* \delta(\kappa_1 + \kappa_2 - \kappa_3 - \kappa)\, \mathrm{d}\kappa_1\, \mathrm{d}\kappa_2\, \mathrm{d}\kappa_3. \tag{8.10}$$

With the help of inverse Fourier transform, one can transform (8.10) into the stationary NLS

$$\frac{1}{2}\alpha(1-\alpha)k_m^{\alpha-2}\left[-\frac{\partial^2\phi}{\partial x^2} + q^2\phi\right] = k_m^\beta |\phi|^2 \phi \tag{8.11}$$

which has the soliton solution

$$\phi(x) = \sqrt{\frac{\alpha(1-\alpha)}{k_m^{\beta-\alpha+2}}}\frac{q}{\cosh qx}. \tag{8.12}$$

It gives the following approximate quasisoliton solution of Eq. (2.1) with $\lambda = +1$:

$$\psi(x,t) = \phi(x - Vt)\, \mathrm{e}^{\mathrm{i}\Omega t + \mathrm{i}k_m(x-Vt)}, \qquad \Omega = -(1-\alpha)k_m^\alpha - \tfrac{1}{2}\alpha(1-\alpha)k_m^{\alpha-2}q^2, \qquad V = \alpha k_m^{\alpha-1}. \tag{8.13}$$

The quasisoliton (8.13) is an "envelope soliton", which can be obtained directly from Eq. (2.1). Simply inject

$$\psi(x,t) = U(x,t)\, \mathrm{e}^{-\mathrm{i}(1-\alpha)k_m^\alpha t + \mathrm{i}k_m(x-Vt)}, \tag{8.14}$$

and use the binomial expansion

$$\left|\frac{\partial}{\partial x}\right|^a \mathrm{e}^{\mathrm{i}kx}U = \mathrm{e}^{\mathrm{i}kx}\left[|k|^a U + a|k|^{a-1}\left(-\mathrm{i}\frac{\partial}{\partial x}\right)U + \frac{1}{2}a(a-1)|k|^{a-2}\left(-\mathrm{i}\frac{\partial}{\partial x}\right)^2 U + \cdots\right]. \tag{8.15}$$

Plugging Eq. (8.15) into Eq. (2.1) with $\lambda = +1$, one obtains a differential equation of infinite order

$$\mathrm{i}\left(\frac{\partial U}{\partial t} + V\frac{\partial U}{\partial x}\right) = L_2 U + L_3 U + \cdots, \qquad V = \alpha k_m^{\alpha-1}. \tag{8.16}$$

Here

$$L_2 U = \frac{1}{2}\alpha(1-\alpha)k_m^{\alpha-2}\frac{\partial^2 U}{\partial x^2} + k_m^\beta |U|^2 U, \tag{8.17}$$

$$L_3 U = \mathrm{i}\left[\frac{1}{6}\alpha(\alpha-1)(\alpha-2)k_m^{\alpha-3}\frac{\partial^3 U}{\partial x^3} - \beta k_m^{\beta-1}|U|^2\frac{\partial U}{\partial x}\right]. \tag{8.18}$$

Taking into consideration only the first non-trivial term L_2U, one gets the non-stationary NLS

$$\mathrm{i}\left(\frac{\partial U}{\partial t}+V\frac{\partial U}{\partial x}\right)=\frac{1}{2}\alpha(1-\alpha)k_m^{\alpha-2}\frac{\partial^2 U}{\partial x^2}+k_m^{\beta}|U|^2U. \tag{8.19}$$

It has a soliton solution

$$U(x,t)=\phi(x-Vt)\,\mathrm{e}^{-(1/2)\mathrm{i}\alpha(1-\alpha)k_m^{\alpha-2}q^2t}. \tag{8.20}$$

To find the shape of the quasisoliton more accurately, one should keep in the right-hand side of Eq. (8.15) a finite (but necessary odd!) number of terms. The expansion in Eq. (8.16) runs in powers of the parameter q/k_m. Note that one cannot find the lifetime of the quasisoliton. The lifetime grows as $\mathrm{e}^{|k_0|/q}$ and its calculation is beyond the perturbation expansion.

As a matter of fact. the parameter

$$\epsilon=\frac{q}{k_m} \tag{8.21}$$

is crucial for quasisolitons. The smaller it is, the closer the quasisoliton is to a "real soliton". The amplitude of a quasisoliton is proportional to ϵ. Quasisolitons of small amplitude satisfy the integrable NLS and are stable. It is not obvious for quasisolitons of finite amplitude. One can guess that at least in the case $\beta > 0$, when collapse is not forbidden, there is a critical value of the amplitude of a quasisoliton ϵ_c such that for $\epsilon > \epsilon_c$ it is unstable and generates a singularity at a finite time. Our numerical experiments confirm this conjecture for $\beta = +3$.

Quasisolitons move with different velocities and collide. If the amplitudes of the quasisolitons are small and their velocities are close, they obey the NLS and their interaction is elastic. One can guess that the same holds for small-amplitude quasisolitons even if their velocities are quite different. This is not obvious for quasisolitons of moderate amplitude. One can think that their interaction is inelastic and leads to the merging and formation of a quasisoliton of larger amplitude.

9. Nonlinear frequency shift

Let us consider one more important nonlinear effect. In a linear system, the harmonic of wave number k oscillates with the frequency $\omega(k)$. In the presence of nonlinearity, the frequency changes due to the interaction with other harmonics. In a weakly nonlinear system, the frequency is modified by a functional depending linearly on the spectrum

$$\omega(k)\to\omega(k)+\int T_{1k}n_1\,\mathrm{d}k_1. \tag{9.1}$$

It is easy to show that T_{1k} can be expressed in terms of the coefficient T_{123k} in Eq. (2.3) as

$$T_{1k}=2T_{1k1k}. \tag{9.2}$$

For the MMT model,

$$T_{1k}=2\lambda(k_1k)^{\beta/2}. \tag{9.3}$$

For $\beta = 0$,

$$T_{1k}=2\lambda=\pm2, \tag{9.4}$$

and

$$\omega^{\pm}(k) = \omega(k) \pm 2N, \tag{9.5}$$

where $N = \int |\hat{\psi}_k|^2 \, dk$ is the total number of particles.

In the general case $\beta \neq 0$, renormalization of the frequency leads to modified resonance conditions (2.8) and (2.9). But in the particular case $\beta = 0$, renormalization terms in Eq. (2.9) cancel and the resonance conditions in the first nonlinear approximation remain unchanged. At the same time, the difference of frequencies for different signs of nonlinearity has the form

$$\omega^{+}(k) - \omega^{-}(k) = 4N. \tag{9.6}$$

In our case, it does not depend on the wave number.

10. On the MMT model spectrum

In [7], MMT found that in the case of positive nonlinearity the spectrum of wave turbulence is well described by the formula (MMT spectrum)

$$n_k \simeq |k|^{-1-(\beta+\alpha)/2}. \tag{10.1}$$

They checked this result for $\alpha = \frac{1}{2}$ and different values of β. Our experiments are in agreement with (10.1). In [8–10], it was found that the MMT spectrum can appear for either sign of nonlinearity. So far there is no proper theoretical derivation of the MMT spectrum. In this section, we offer some heuristic derivation of (10.1).

Assuming formula (3.2) to be exact, the problem of closure for the equation on particle number lies in the expression of Im J_{123k} in terms of n_k. This expression should a priori satisfy the conditions of symmetry

$$\text{Im } J_{123k} = \text{Im } J_{213k} = \text{Im } J_{12k3} = -\text{Im } J_{3k12}. \tag{10.2}$$

Moreover, one can assume that the nonlinearity is weak and that the wave energy is roughly

$$E \simeq \int \omega(k) n_k \, dk. \tag{10.3}$$

From conservation of energy, one obtains

$$\int T_{123k}(\omega_1 + \omega_2 - \omega_3 - \omega) \, \text{Im } J_{123k} \, dk_1 \, dk_2 \, dk_3 \, dk = 0. \tag{10.4}$$

Hence, one must have

$$\text{Im } J_{123k} \simeq \delta(\omega_1 + \omega_2 - \omega_3 - \omega). \tag{10.5}$$

For Gaussian wave turbulence, the real part of J_{123k} is given by Eq. (3.3) and dimensional analysis gives

$$\text{Re } J_{123k} \simeq \frac{n_k^2}{k}. \tag{10.6}$$

Up to this point, our consideration was more or less rigorous. Now, we present a heuristic conjecture. We suppose that the imaginary part of the four-wave correlator has the same scaling as the real part. In other words, it is quadratic in n_k.

If one takes into account the necessary conditions (10.2) and (10.4) and the scaling (10.6) for Im J_{123k}, there are only a few possibilities for the construction of Im J_{123k}. We offer the following closure:

$$\operatorname{Im} J_{123k} = a\left(\frac{\partial\omega_1}{\partial k_1} + \frac{\partial\omega_2}{\partial k_2} + \frac{\partial\omega_3}{\partial k_3} + \frac{\partial\omega}{\partial k}\right)\delta(\omega_1+\omega_2-\omega_3-\omega)(n_1n_2 - n_3n_k), \tag{10.7}$$

where $a \ll 1$ is a dimensionless constant. The closure leads to the kinetic equation

$$\frac{\partial n_k}{\partial t} = 2a\int T_{123k}(n_1n_2 - n_3n_k)\left(\frac{\partial\omega_1}{\partial k_1} + \frac{\partial\omega_2}{\partial k_2} + \frac{\partial\omega_3}{\partial k_3} + \frac{\partial\omega}{\partial k}\right)\delta(\omega_1+\omega_2-\omega_3-\omega) \times\delta(k_1+k_2-k_3-k)\,\mathrm{d}k_1\,\mathrm{d}k_2\,\mathrm{d}k_3. \tag{10.8}$$

It is easy to check that the Kolmogorov solution of Eq. (10.8) leads to the MMT spectrum. Eq. (10.8) resembles the Boltzmann's equation for interacting particles. Apparently, it can make sense only if $aT_{123k} > 0$. Otherwise, the $\mathcal{H}$-theorem and the second law of thermodynamics will be violated. We must stress that the formula (10.7) is heuristic and has no rigorous justification.

11. Particle and energy balance

In the presence of damping and linear instability, Eq. (2.3) can be written in the form

$$\mathrm{i}\frac{\partial\hat\psi_k}{\partial t} = \frac{\delta H}{\delta\hat\psi_k^*} + \mathrm{i}D(k)\hat\psi_k, \tag{11.1}$$

where

$$H = \int\omega(k)|\hat\psi_k|^2\,\mathrm{d}k + \frac{1}{2}\int T_{123k}\hat\psi_1\hat\psi_2\hat\psi_3^*\hat\psi_k^*\delta(k_1+k_2-k_3-k)\,\mathrm{d}k_1\,\mathrm{d}k_2\,\mathrm{d}k_3\,\mathrm{d}k, \tag{11.2}$$

is the Hamiltonian, $D(k)$ is the damping or the growth rate of instability depending on its sign.

Let $N = \int|\hat\psi_k|^2\,\mathrm{d}k$ be the total number of particles in the system. From (11.1), one can obtain the exact equation for the particle balance

$$\frac{\mathrm{d}N}{\mathrm{d}t} = Q = 2\int D(k)|\hat\psi_k|^2\,\mathrm{d}k. \tag{11.3}$$

After averaging, one has

$$\frac{\mathrm{d}\langle N\rangle}{\mathrm{d}t} = 2\int D(k)n_k\,\mathrm{d}k = \langle Q\rangle. \tag{11.4}$$

The total mean flux of particles $\langle Q\rangle$ is a linear functional of n_k at any level of nonlinearity.

For the total flux of energy, one has the exact identity

$$P = \frac{\mathrm{d}H}{\mathrm{d}t} = 2\int\omega(k)D(k)|\hat\psi_k|^2\,\mathrm{d}k + \frac{1}{2}\int[D(k_1)+D(k_2)+D(k_3)+D(k)]T_{123k}\hat\psi_1\hat\psi_2\hat\psi_3^*\hat\psi_k^* \times\delta(k_1+k_2-k_3-k)\,\mathrm{d}k_1\,\mathrm{d}k_2\,\mathrm{d}k_3\,\mathrm{d}k. \tag{11.5}$$

For the averaged density of energy, one has

$$\langle P\rangle = 2\int\omega(k)D(k)n_k\,\mathrm{d}k + \frac{1}{2}\int[D(k_1)+D(k_2)+D(k_3)+D(k)]T_{123k}\operatorname{Re}J_{123k} \times\delta(k_1+k_2-k_3-k)\,\mathrm{d}k_1\,\mathrm{d}k_2\,\mathrm{d}k_3\,\mathrm{d}k. \tag{11.6}$$

Assuming that Gaussian statistics holds, one can write

$$\mathrm{Re}\, J_{123k} \simeq n_1 n_2[\delta(k_1 - k_3) + \delta(k_1 - k)], \tag{11.7}$$

and one obtains after simple calculations

$$\langle P\rangle = 2\int \tilde{\omega}(k) D(k) n_k \,\mathrm{d}k, \tag{11.8}$$

where $\tilde{\omega}(k) = \omega(k) + \int T_{1k} n_1 \,\mathrm{d}k_1$ is the renormalized frequency.

In the case $\beta = 0$ and $T_{1k} = \pm 2$,

$$\langle P\rangle = 2\int \omega(k) D(k) n_k \,\mathrm{d}k + 2\lambda N\langle Q\rangle. \tag{11.9}$$

In the stationary state, $\langle Q\rangle = 0$, $\langle P\rangle = 0$ and the balance equations are

$$\int D(k) n_k \,\mathrm{d}k = 0, \tag{11.10}$$

$$\int \omega(k) D(k) n_k \,\mathrm{d}k = 0. \tag{11.11}$$

In this particular case, renormalization of the frequency does not influence the balance equations.

The balance equations (11.10) and (11.11) can be rewritten as

$$Q_0 = Q^+ + Q^-, \tag{11.12}$$

$$P_0 = P^+ + P^-, \tag{11.13}$$

where Q_0 and P_0 are the input of particles and energy in the area of instability $\omega \simeq \omega_0$. Q^+ and P^+ are the sinks of particles and energy in the high frequency region $\omega \sim \omega^+$. Q^- and P^- are the sinks in the low frequency region $\omega \sim \omega^-$.

Roughly speaking,

$$P_0 \simeq \omega_0 Q_0, \tag{11.14}$$

$$P^+ \simeq \omega^+ Q^+, \tag{11.15}$$

$$P^- \simeq \omega^- Q^-, \tag{11.16}$$

and the balance equations can be written as

$$Q_0 = Q^+ + Q^-, \tag{11.17}$$

$$\omega_0 Q_0 \simeq \omega^+ Q^+ + \omega^- Q^-. \tag{11.18}$$

Hence

$$\frac{Q^+}{Q^-} \simeq \frac{\omega_0 - \omega^-}{\omega^+ - \omega_0}, \qquad \frac{P^+}{P^-} \simeq \frac{\omega^+}{\omega^-}\frac{\omega_0 - \omega^-}{\omega^+ - \omega_0}. \tag{11.19}$$

For $\omega^- \sim \omega_0 \ll \omega^+$, one has

$$\frac{Q^+}{Q^-} \simeq \frac{\omega_0 - \omega^-}{\omega^+}, \qquad \frac{P^+}{P^-} \simeq \frac{\omega_0 - \omega^-}{\omega^-}. \tag{11.20}$$

In other words, if $\omega_0 \ll \omega^+$, almost all particles are absorbed at low frequencies. The amounts of energy absorbed in both ranges have the same order of magnitude. These conclusions are valid only under the hypothesis of approximate Gaussianity of wave turbulence.

12. Numerical integration scheme

The direct method employed to simulate the model is similar to that in [7]. With the aim of observing direct and inverse cascades, the complete equation to be integrated reads

$$\mathrm{i}\frac{\partial \hat{\psi}_k}{\partial t} = \omega(k)\hat{\psi}_k + \int T_{123k}\hat{\psi}_1\hat{\psi}_2\hat{\psi}_3^*\delta(k_1+k_2-k_3-k)\,\mathrm{d}k_1\,\mathrm{d}k_2\,\mathrm{d}k_3 + \mathrm{i}[F(k)+D(k)]\hat{\psi}_k \tag{12.1}$$

with

$$F(k) = \sum_j f_j\delta(k-k_j) \quad \text{and} \quad D(k) = -\nu^-|k|^{-d^-} - \nu^+|k|^{d^+}.$$

The forcing term $F(k)$ denotes an instability localized in a narrow spectral band. The damping part $D(k)$ contains a wave action sink at large scales and an energy sink at small scales. The presence of these two sinks is necessary to reach a stationary regime if two different fluxes are assumed to flow in opposite k-directions from the stirred zone. In our experiments, we set $d^- = 8$ and $d^+ = 16$ unless other values are specified. The purpose of using high-order viscosity (also referred to as hyperviscosity), which separates sharply the inertial and dissipative ranges, is to minimize the effects of dissipation at intermediate scales of the simulated spectrum.

A pseudospectral code solves Eq. (12.1) in a periodic interval of Fourier modes. We define the discrete direct Fourier transform (FT) as

$$\hat{\psi}(k_n) = \hat{\psi}_n = \mathrm{FT}(\psi_j) = \frac{1}{N_d}\sum_{j=0}^{N_d-1}\psi_j\,\mathrm{e}^{-\mathrm{i}k_n x_j}, \tag{12.2}$$

and the discrete inverse Fourier transform (FT^{-1}) as

$$\psi(x_j) = \psi_j = \mathrm{FT}^{-1}(\hat{\psi}_n) = \sum_{n=-(N_d/2)+1}^{N_d/2}\hat{\psi}_n\,\mathrm{e}^{\mathrm{i}k_n x_j}, \tag{12.3}$$

where N_d is the number of grid points, $k_n = 2\pi n/L$ the nth wave number, $x_j = jL/N_d$ the location of the jth grid point and L the size of the computational domain $0 < x < L$. We usually choose $L = 2\pi$ so that the k_ns are integers and the spacing in Fourier space is $\Delta k = 1$. In our experiments, quantities defined as integrals along the spectral interval are computed in their discrete forms without any renormalization. For instance, we use for the number of particles the formula

$$N = \sum_{n=-(N_d/2)+1}^{N_d/2}|\hat{\psi}_n|^2, \tag{12.4}$$

and for the quadratic part of energy

$$E = H_{\mathrm{L}} = \sum_{n=-(N_d/2)+1}^{N_d/2}\omega(k_n)|\hat{\psi}_n|^2. \tag{12.5}$$

The linear frequency term is treated exactly by an integrating factor technique, removing it from the timestepping procedure. As emphasized by MMT, we thus avoid the natural stiffness of the problem as well as possible numerical instabilities. Consequently, we do not need to shorten the inertial interval by downshifting the cutoff of ultraviolet absorption (as in [5]). The nonlinear term is calculated through the Fast Fourier Transform by first transforming to real space where a multiplication is computed and then transforming back to spectral space. For the multiplication operation, twice the effective number of grid points are required in order to avoid aliasing errors. A fourth-order Runge–Kutta scheme integrates the conservative model in time, giving a solution to which the diagonal factor $e^{[F(k)+D(k)]\Delta t}$ is applied at each time step Δt.

13. Numerical results for $\beta = 0, \lambda = \pm 1$

A series of numerical simulations of Eq. (12.1) with resolution up to $N_d = 2048$ de-aliased modes has been performed. We choose the case $\beta = 0$ as the candidate for testing WT in our experiments. Both cases $\lambda = \pm 1$ are examined, providing an additional test of the theory, and the study is focused on the direct cascade. Forcing is located at large scales and the inertial interval is defined by the right transparency window $k_f \ll k \ll k_d$ (where k_f and k_d are the characteristic wave numbers of forcing and ultraviolet damping, respectively). As displayed in Table 1, the theoretical spectrum which can be realized in this window is

$$n_k \propto k^{-1}. \tag{13.1}$$

Typically, initial conditions are given by the random noise in the spectral space. Simulations are run until a quasi-steady regime is established which is characterized by small fluctuations of the energy and the number of particles around some mean value. Then time averaging begins and continues for a length of time which significantly exceeds the characteristic time scale of the slowest harmonic from the inertial range (free of the source and the sink). In turn, the time-step of the integration has to provide, at least, accurate enough resolution of the fastest harmonic in the system. As our experiments show, one has to use an even smaller time-step than defined by the last condition: the presence of fast nonlinear events in the system requires the use of a time-step $\Delta t = 0.005$, which is 40 times smaller than the smallest linear frequency period. Time averaging with such a small time step leads to a computationally time consuming procedure despite the one-dimensionality of the problem.

From now on, we will present numerical results in the specific situations $\nu^- = 196.61(\lambda = \pm 1)$, $\nu^+ = 5.39 \times 10^{-48}(\lambda = +1)$ or $\nu^+ = 2.1 \times 10^{-47}(\lambda = -1)$, and $f_j = 0.2$, non-zero only for $k_j \in [6, 9](\lambda = \pm 1)$.

The numerical simulations clearly display the development of dynamical chaos and statistically uniform turbulence. Both the amplitude and the phase of each harmonic fluctuate independently of each other. Figs. 1–4 show the behavior of the seventh and eighth harmonics.

Figs. 5–8 show the behavior of the real and imaginary parts of the amplitude of the harmonic $k = 200$. One sees amplitude-modulated oscillations with carrying frequency close to the corresponding linear frequency of the harmonic $\omega \simeq 14$.

Figs. 9–12 represent FTs in time of the evolution of the harmonic $k = 200$ from the previous pictures. One can see that the maximum of the spectra corresponds to the linear frequency shifted in accordance with the nonlinearity sign $\lambda = \pm 1$.

Figs. 13 and 14 demonstrate the behavior of the fourth- and sixth-order moments as functions of the second-order moment. They fit the Gaussian laws very well. They provide a justification of the initial conjecture that the statistics of the turbulence is close to Gaussian.

Fig. 15 represents the time evolution of the quadratic energy E for $\lambda = \pm 1$ with the same amplitude of forcing. The curves are plotted over the interval $t \in [5000, 10\,000]$ where the time averaging actually takes place. One

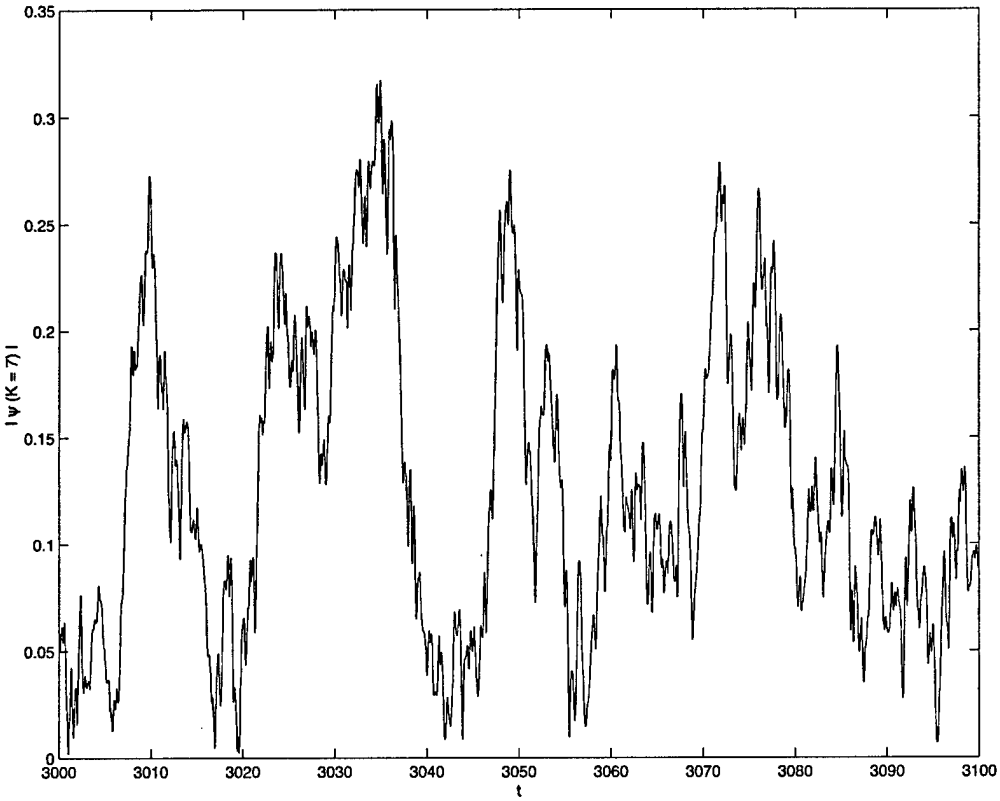

Fig. 1. $\beta = 0, \lambda = -1$. Amplitude of the mode $k = 7$ vs. time.

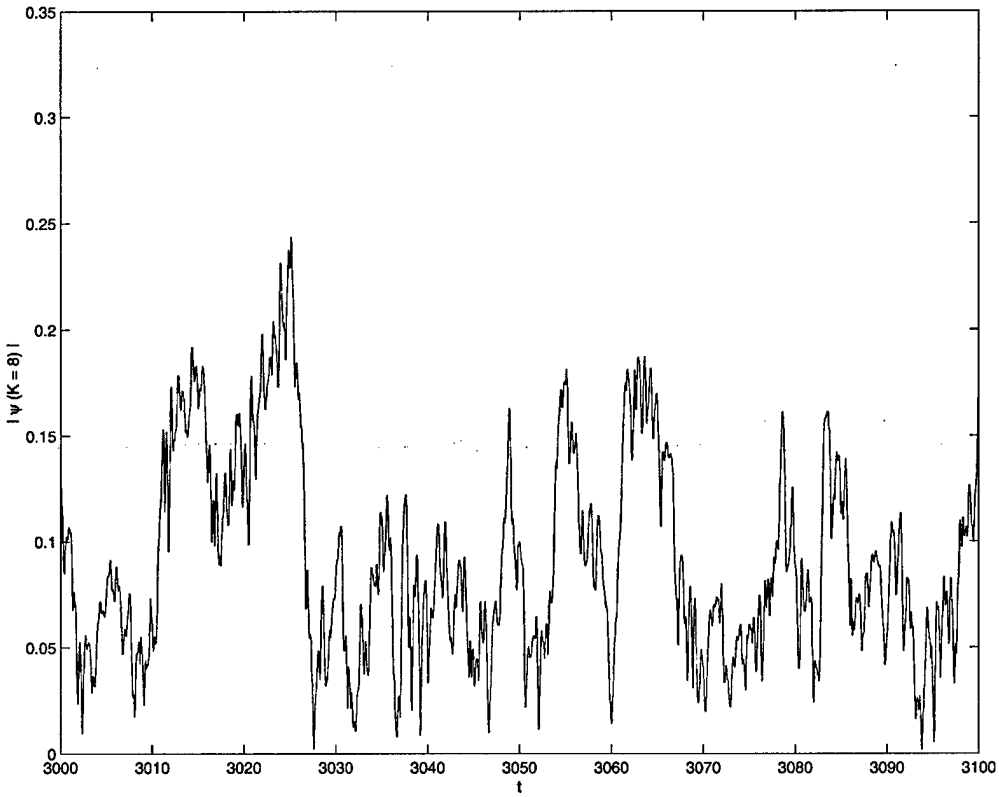

Fig. 2. $\beta = 0, \lambda = -1$. Amplitude of the mode $k = 8$ vs. time.

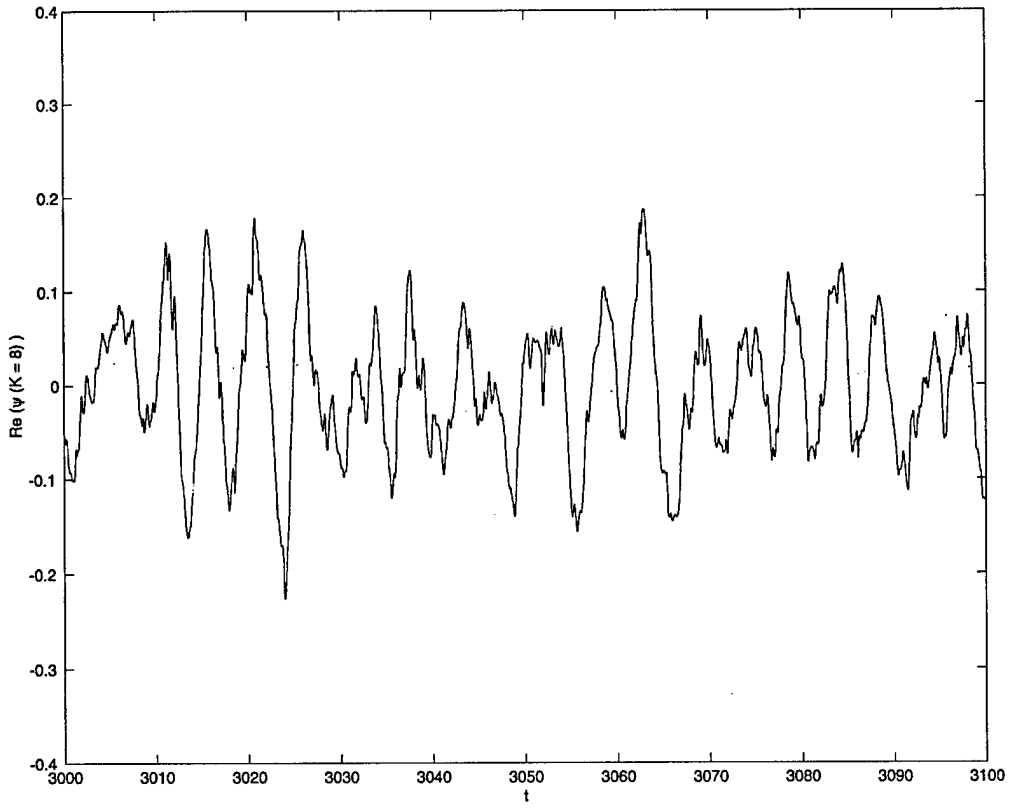

Fig. 3. $\beta = 0, \lambda = -1$. Time evolution of the real part of the amplitude for the mode $k = 8$.

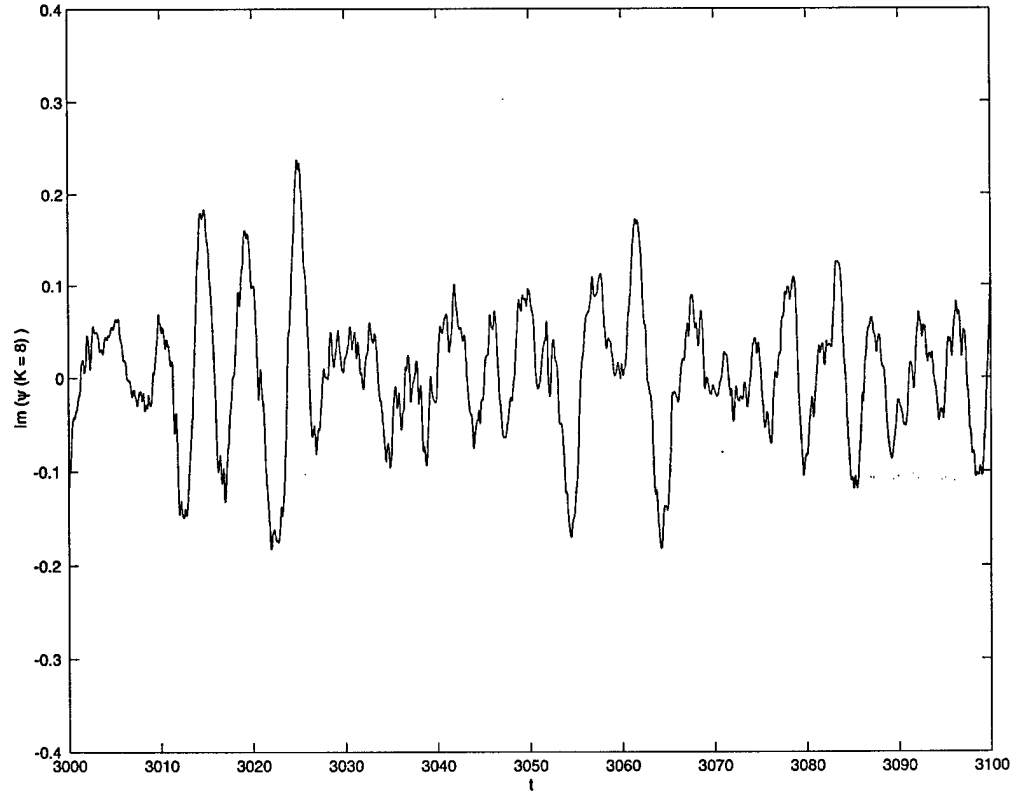

Fig. 4. $\beta = 0, \lambda = -1$. Time evolution of the imaginary part of the amplitude for the mode $k = 8$.

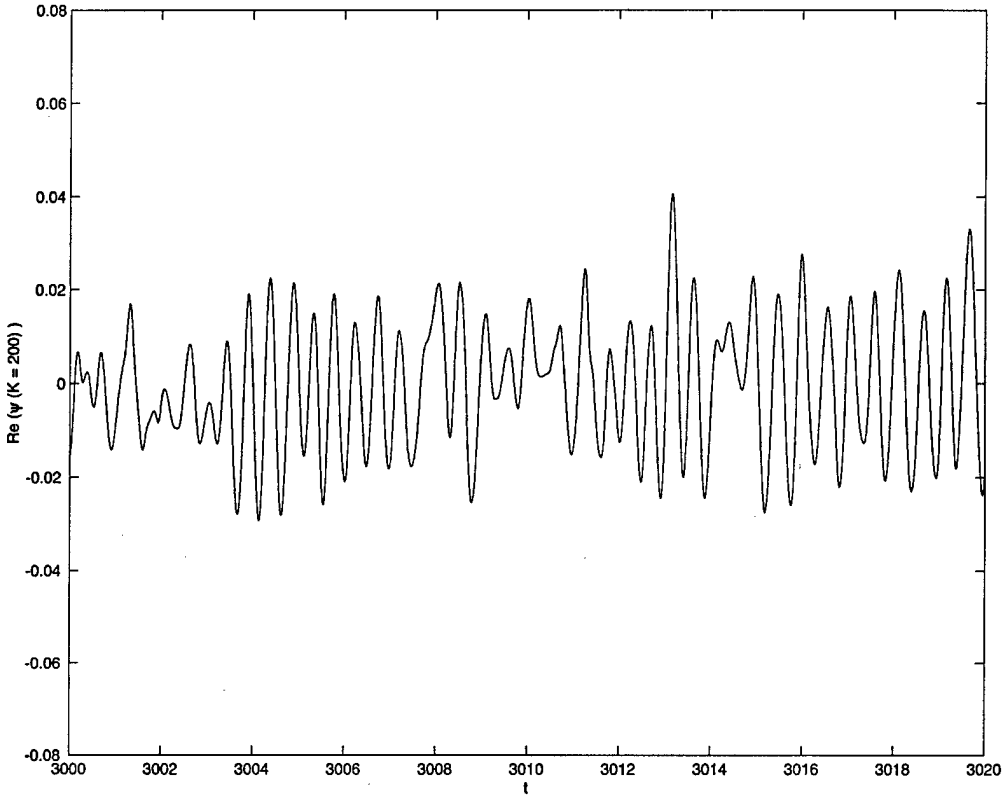

Fig. 5. $\beta = 0$, $\lambda = -1$. Time evolution of the real part of the amplitude for the mode $k = 200$ (time resolution $\tau = 0.015$).

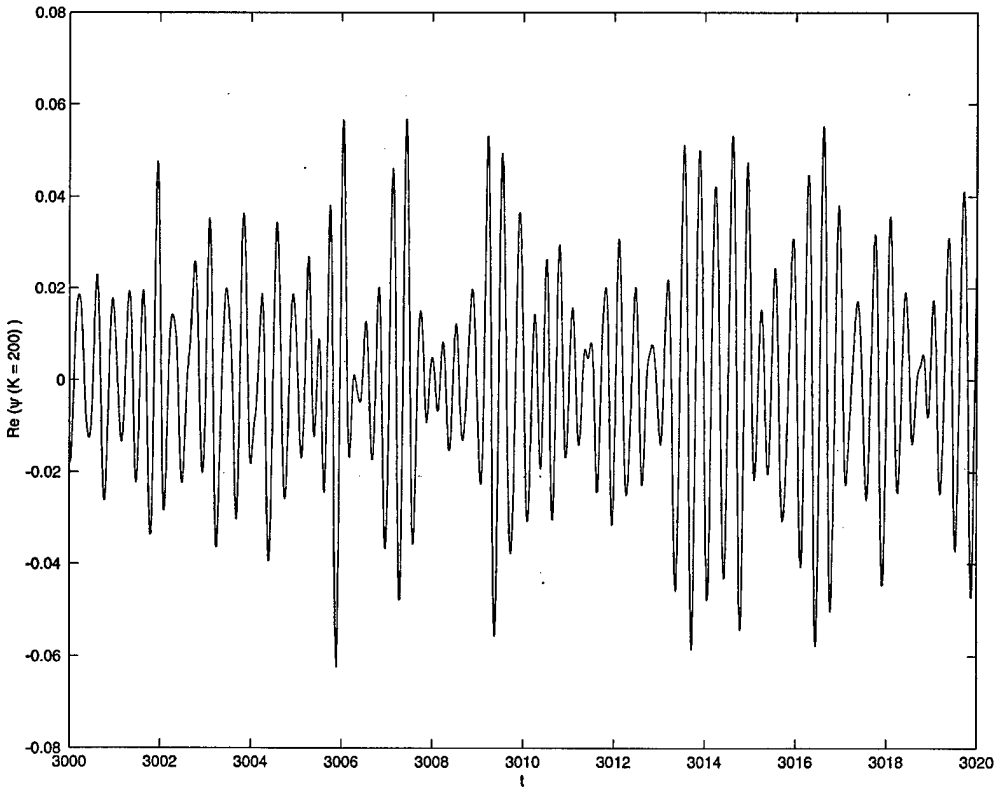

Fig. 6. $\beta = 0$, $\lambda = +1$. Time evolution of the real part of the amplitude for the mode $k = 200$ (time resolution $\tau = 0.015$).

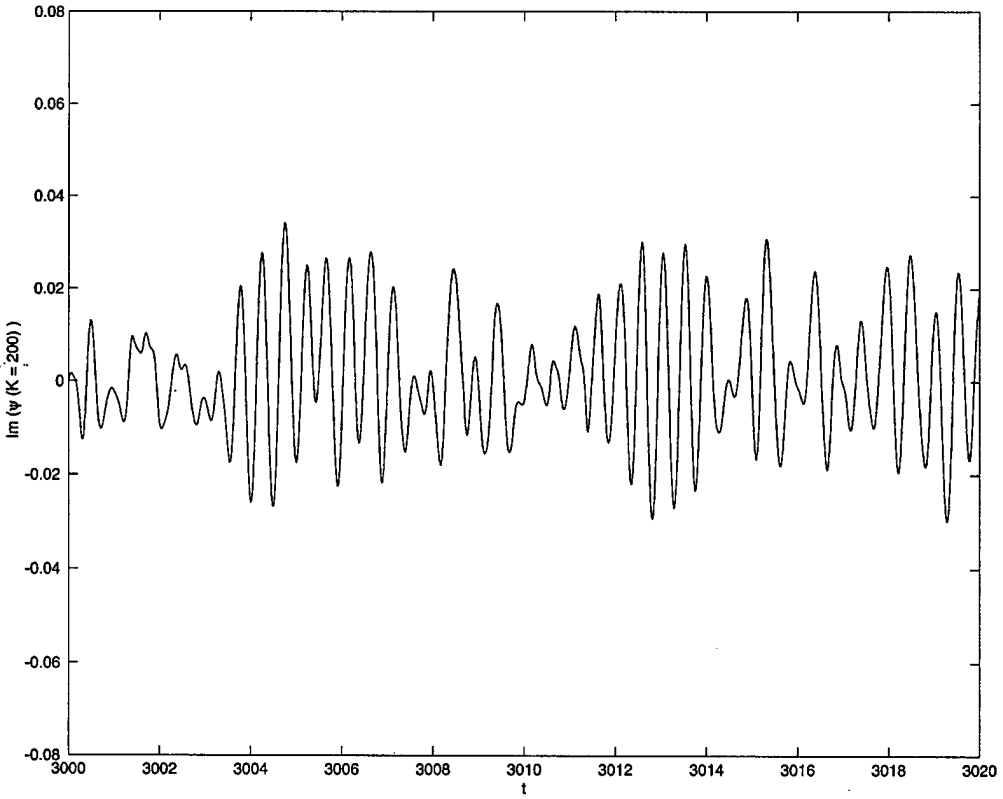

Fig. 7. $\beta = 0, \lambda = -1$. Time evolution of the imaginary part of the amplitude for the mode $k = 200$ (time resolution $\tau = 0.015$).

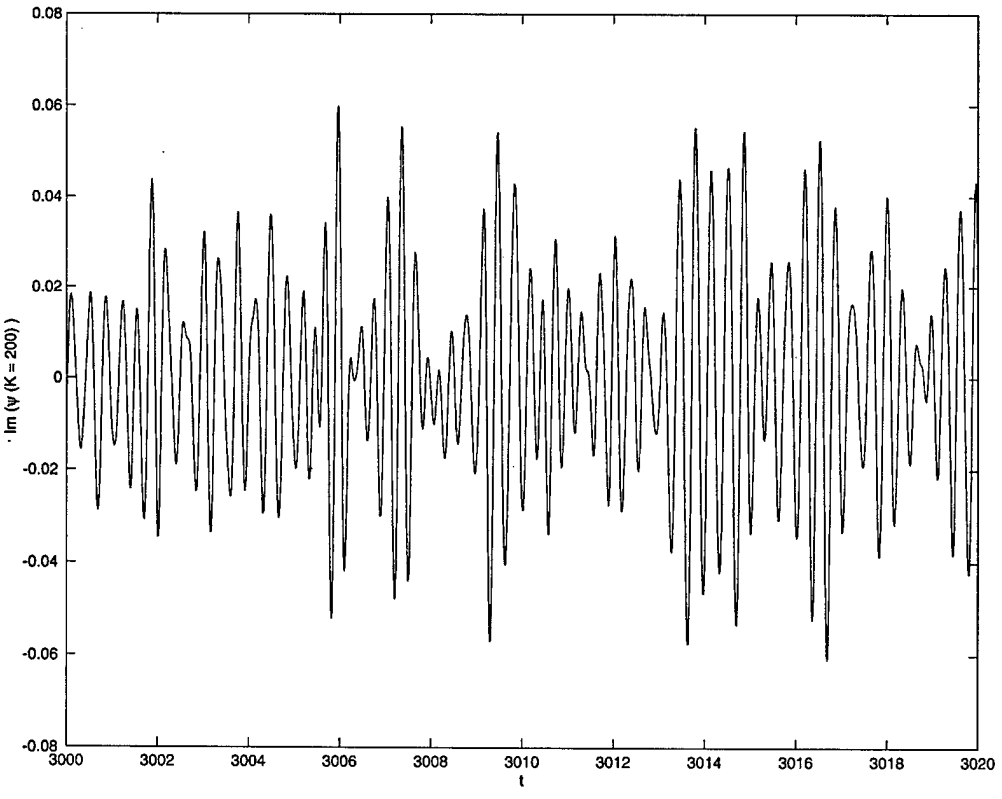

Fig. 8. $\beta = 0, \lambda = +1$. Time evolution of the imaginary part of the amplitude for the mode $k = 200$ (time resolution $\tau = 0.015$).

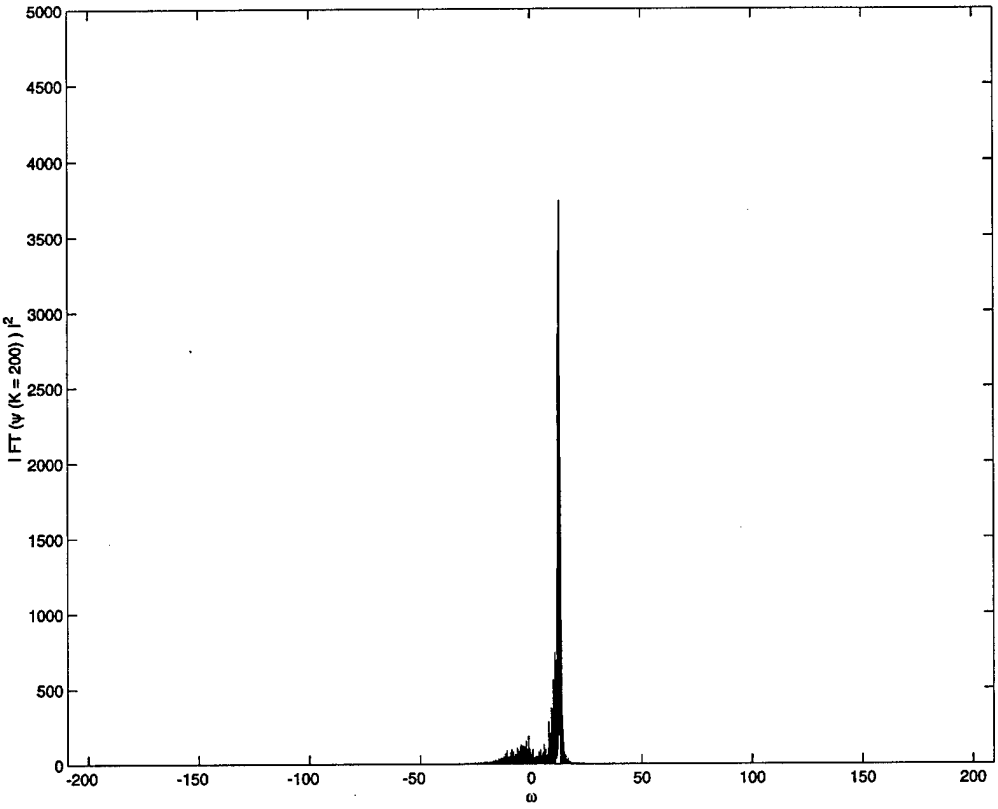

Fig. 9. $\beta = 0, \lambda = -1$. Square amplitude of the FT for the mode $k = 200$ vs. frequency (time resolution $\tau = 0.015$).

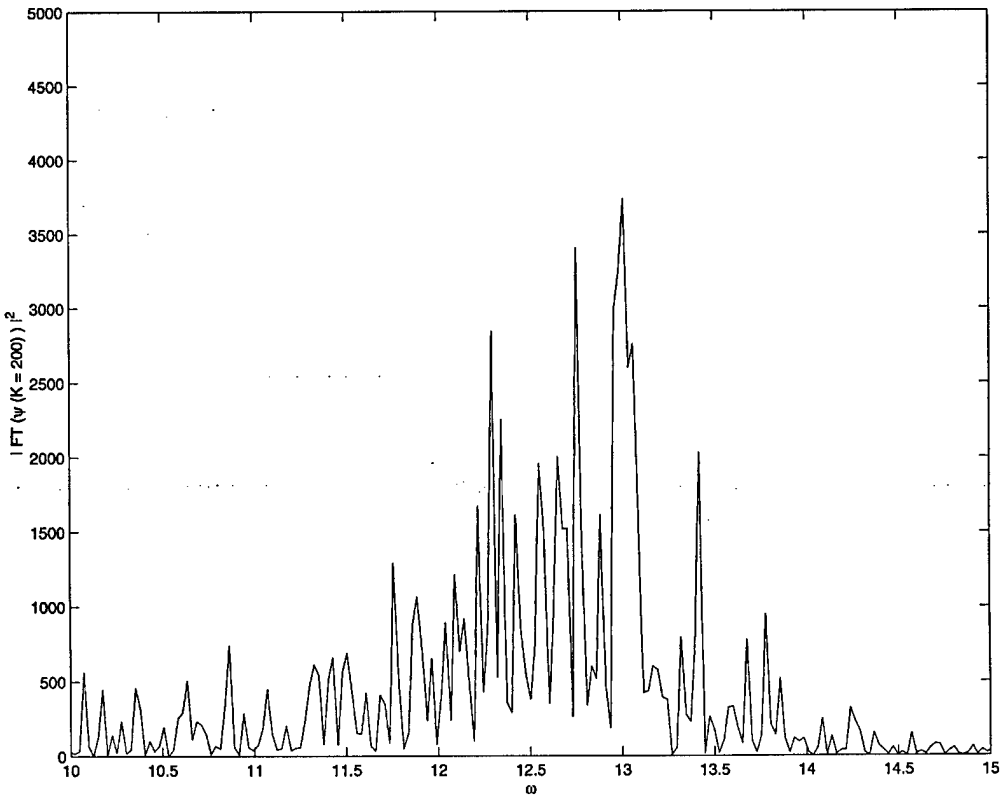

Fig. 10. $\beta = 0, \lambda = -1$. Same as before but with a zoom on a smaller frequency window.

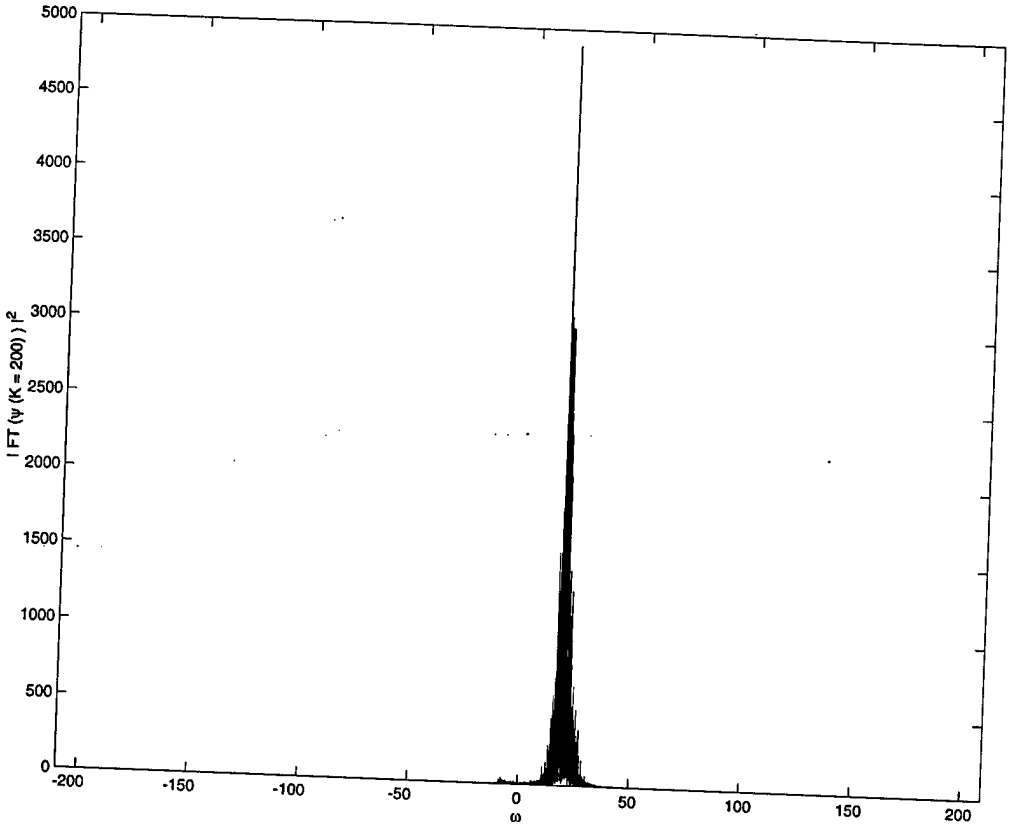

Fig. 11. $\beta = 0, \lambda = +1$. Square amplitude of the FT for the mode $k = 200$ vs. frequency (time resolution $\tau = 0.015$).

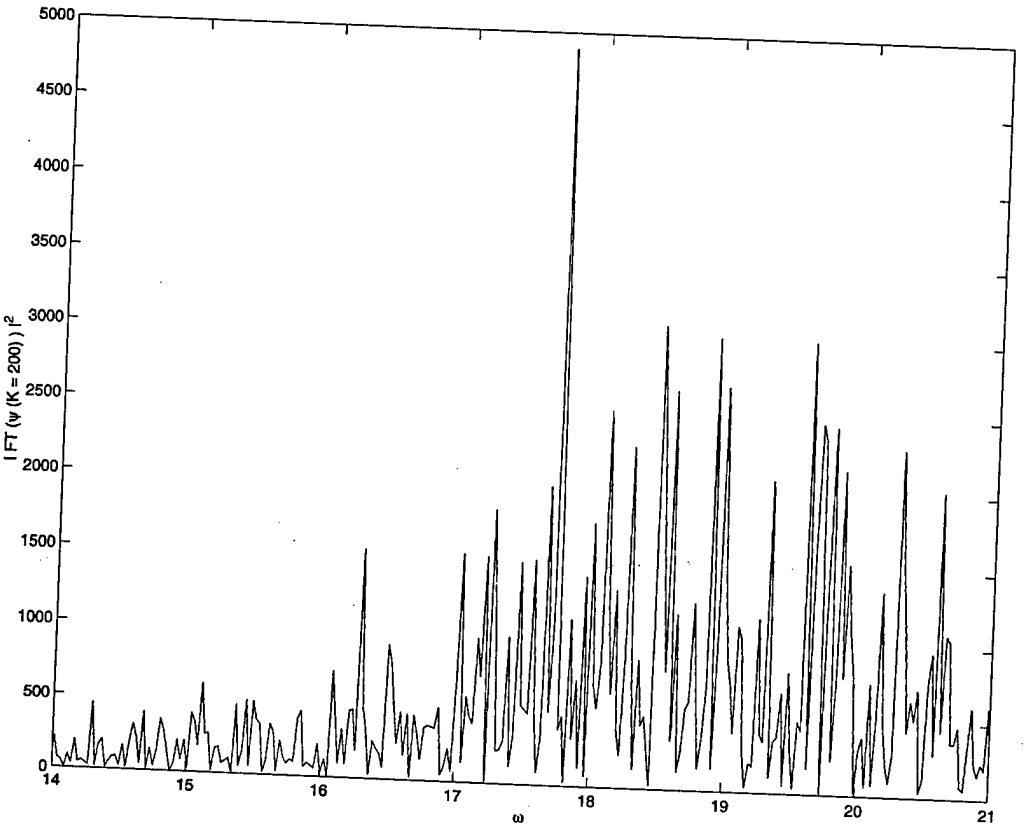

Fig. 12. $\beta = 0, \lambda = +1$. Same as before but with a zoom on a smaller frequency window.

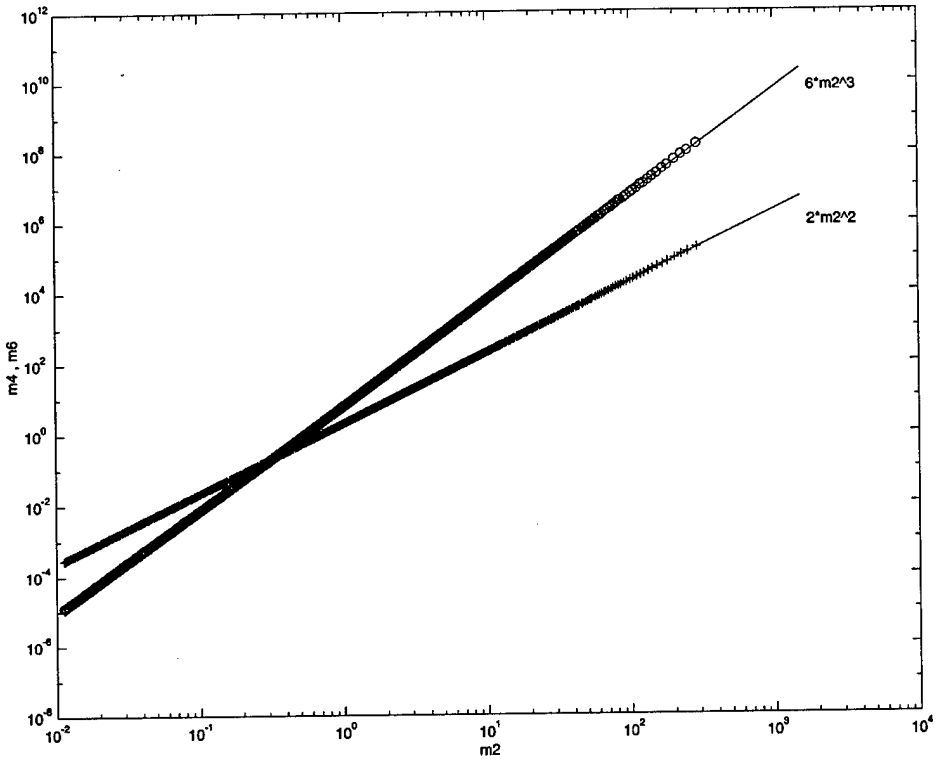

Fig. 13. $\beta = 0, \lambda = +1$. Fourth-order (crosses) and sixth-order (circles) moments as functions of the second-order moments. The straight lines are the fitted Gaussian laws.

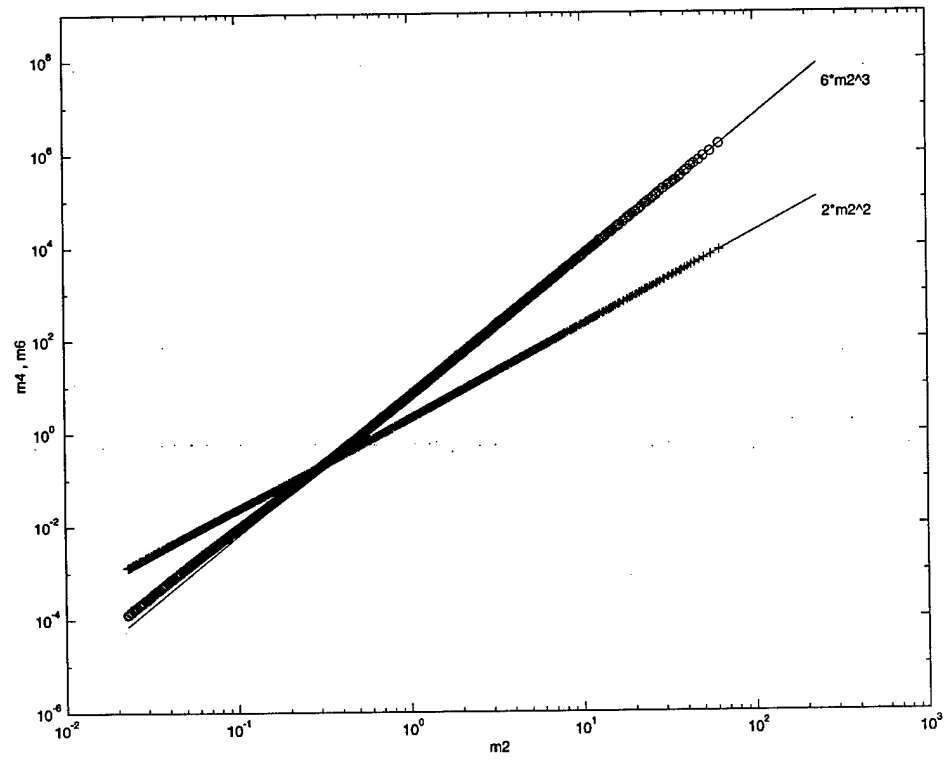

Fig. 14. $\beta = 0, \lambda = -1$. Fourth-order (crosses) and sixth-order (circles) moments as functions of the second-order moments. The straight lines are the fitted Gaussian laws.

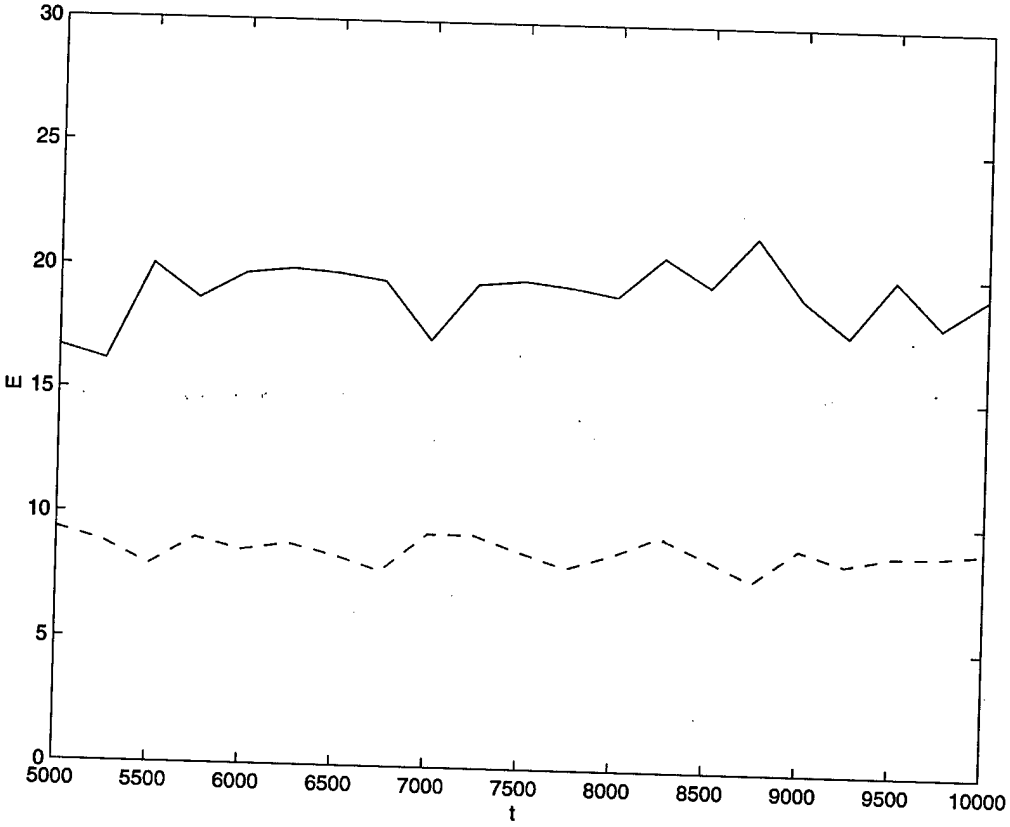

Fig. 15. $\beta = 0$. Quadratic energy vs. time. $\lambda = +1$ (solid line), $\lambda = -1$ (dashed line).

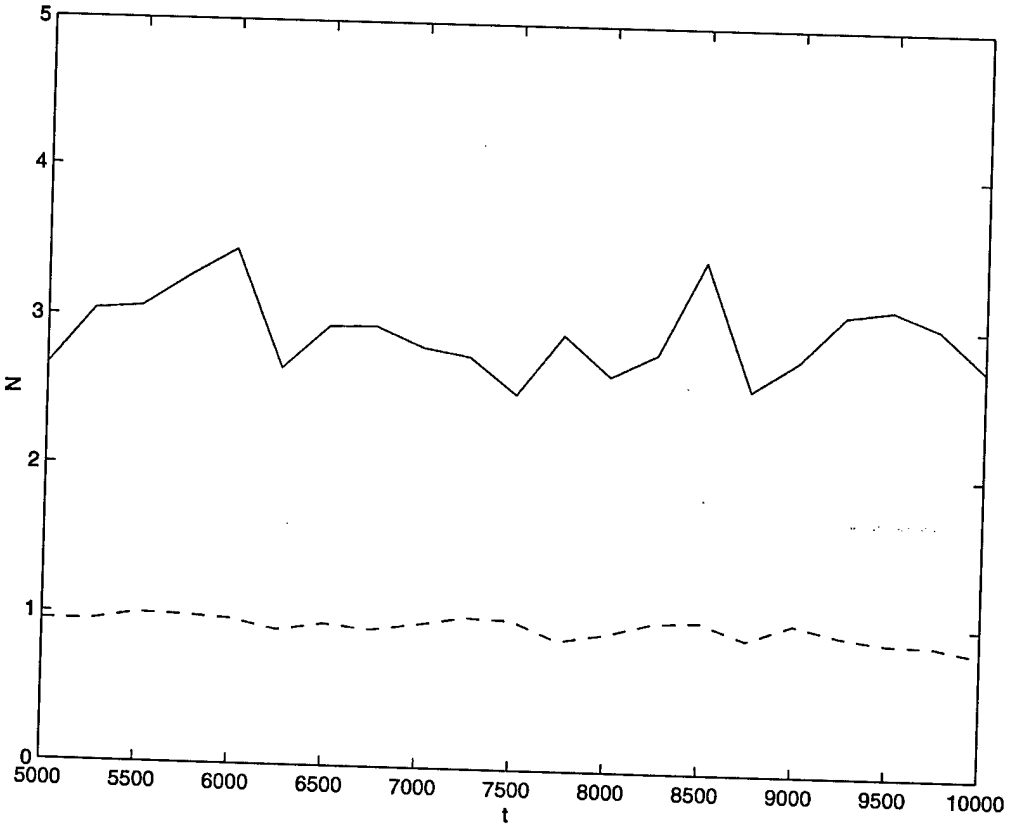

Fig. 16. $\beta = 0$. Number of particles vs. time. $\lambda = +1$ (solid line), $\lambda = -1$ (dashed line).

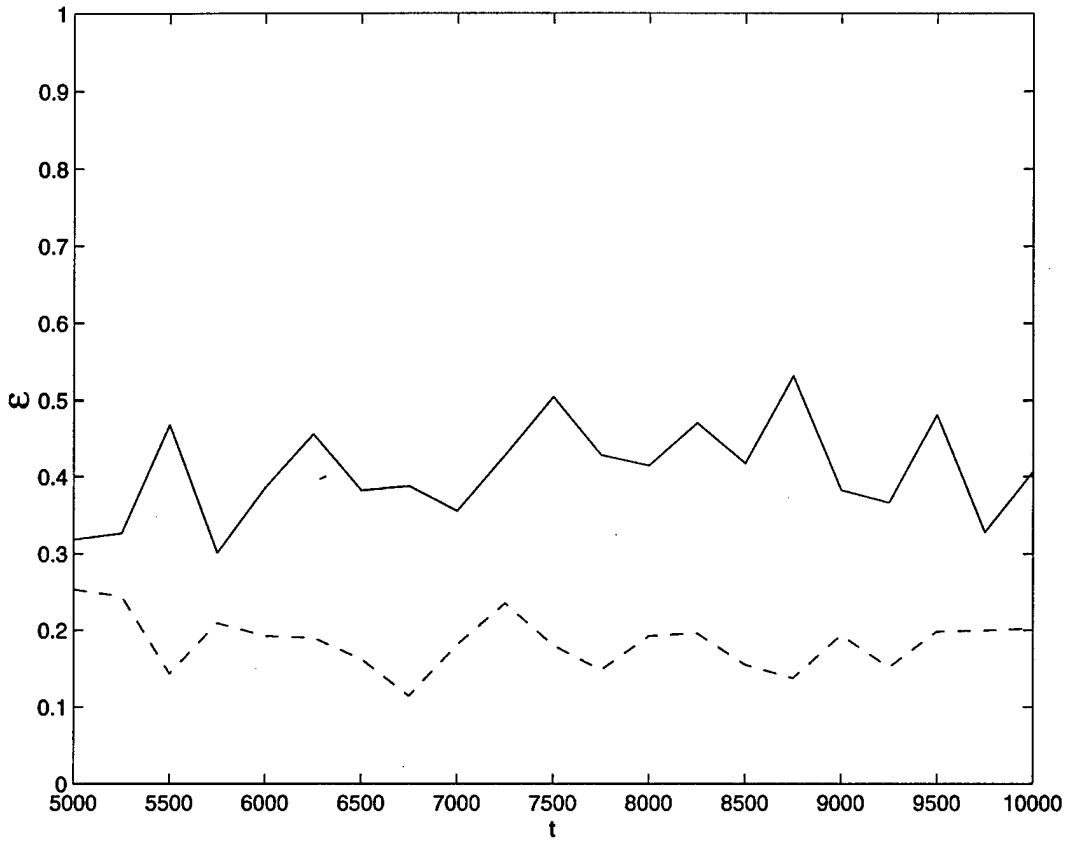

Fig. 17. $\beta = 0$. Average nonlinearity $\epsilon = |H_{NL}/H_L|$ vs. time. $\lambda = +1$ (solid line), $\lambda = -1$ (dashed line).

obviously sees that the systems have already reached the steady state. Their energies moderately fluctuate about mean values which are $E \simeq 19\,(\lambda = +1)$ and $E \simeq 9\,(\lambda = -1)$. This significant difference with respect to the sign of λ is quite unexpected from the viewpoint of the WT theory since the same rate of forcing is imposed in both systems. We can make the same remarks about the evolution of the number of particles N. In Fig. 16, the mean values stay near $N \simeq 3\,(\lambda = +1)$ and $N \simeq 1\,(\lambda = -1)$ so that their relative difference is even bigger than for E. Fluctuations also spread much more in the case $\lambda = +1$.

In Fig. 17, the stationarity as well as the gap between both signs of λ are verified again in the time evolution of the average nonlinearity ϵ. We define the average nonlinearity in the system as the ratio of the nonlinear part to the linear part of the Hamiltonian $\epsilon = |H_{NL}/H_L|$, each part being calculated over the whole field. Of course, this definition does not really make sense when external forces are applied but it provides a relatively good estimation of the level of nonlinearity once the systems reach the steady state. Note here that the mean values $\epsilon \simeq 0.4(\lambda = +1)$ and $\epsilon \simeq 0.2(\lambda = -1)$ are relatively small. Thus, the condition of small nonlinearity required by the theory holds for both systems. This conclusion is also supported by comparing Figs. 10 and 12. It is seen that the difference of frequencies caused by nonlinearity is relatively small. We point out that in our numerical

Table 2
Time-averaged values of the wave action, quadratic energy and corresponding fluxes in the stationary state, $\alpha = \frac{1}{2}$, $\beta = 0$

λ	N	E	Q^-	Q^+	P^-	P^+
+1	3	19	0.1957	0.0090	0.276	0.258
−1	1	9	0.0098	0.0478	0.014	1.430

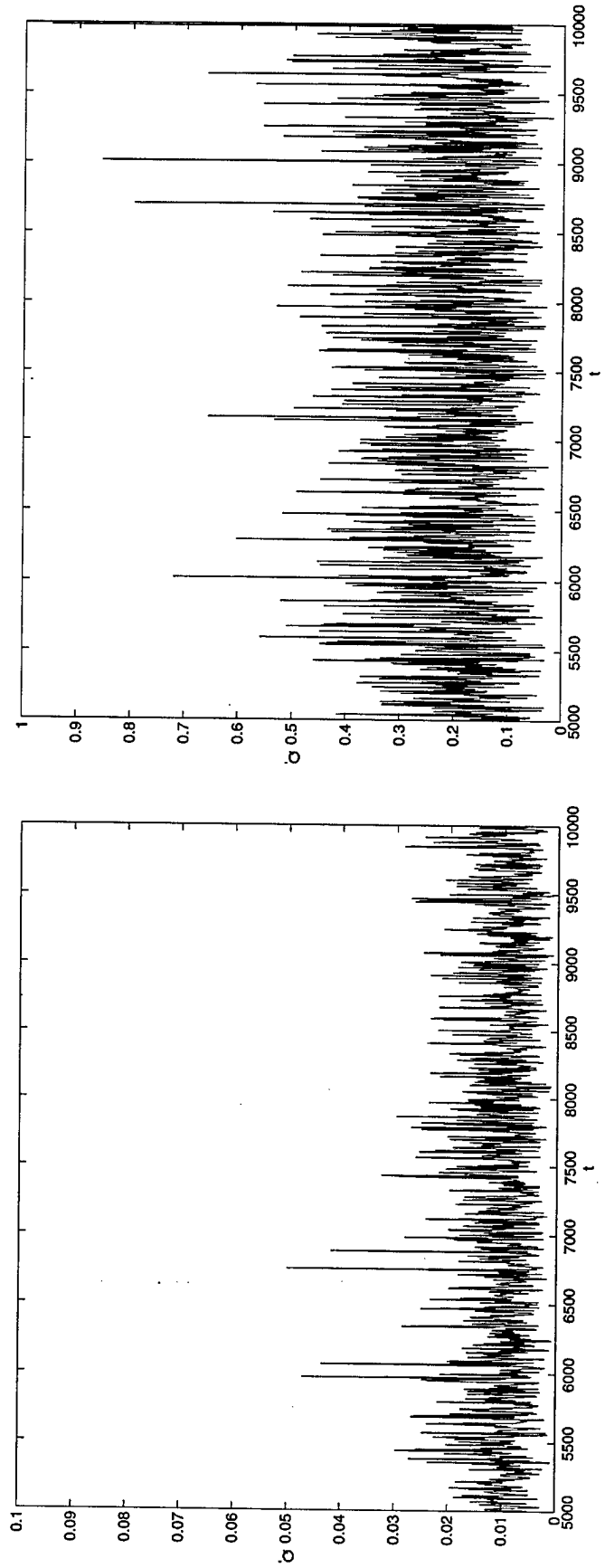

Fig. 18. $\beta = 0, \lambda = -1$ (left), $\lambda = +1$ (right). Dissipation rate of particles at low wave numbers vs. time.

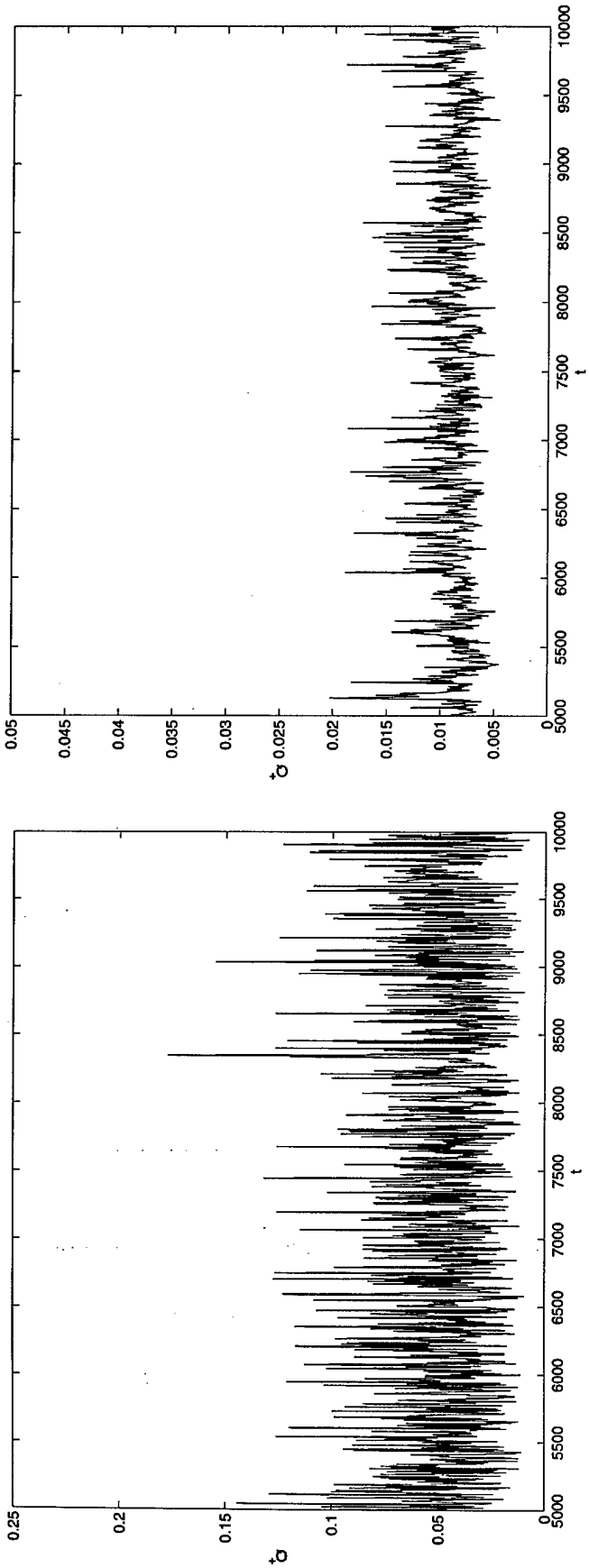

Fig. 19. $\beta = 0$, $\lambda = -1$ (left), $\lambda = +1$ (right). Dissipation rate of particles at high wave numbers vs. time.

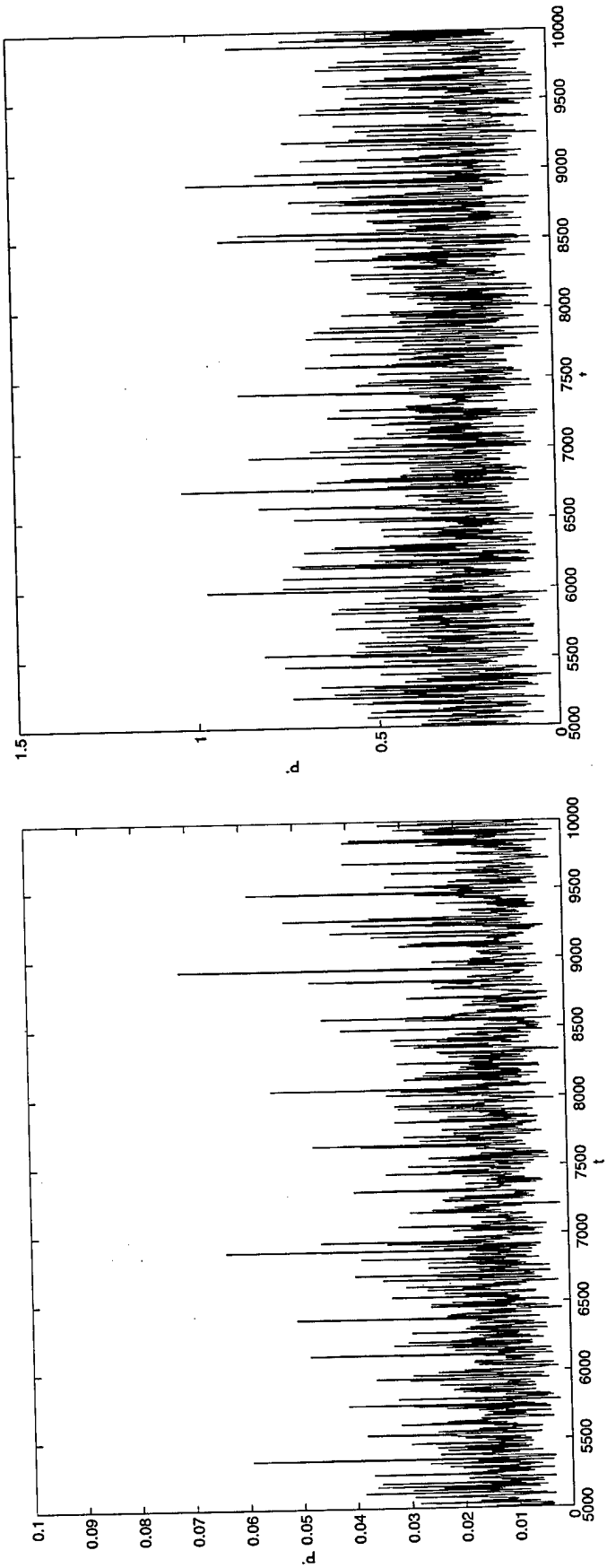

Fig. 20. $\beta = 0, \lambda = -1$ (left), $\lambda = +1$ (right). Dissipation rate of energy at low wave numbers vs. time.

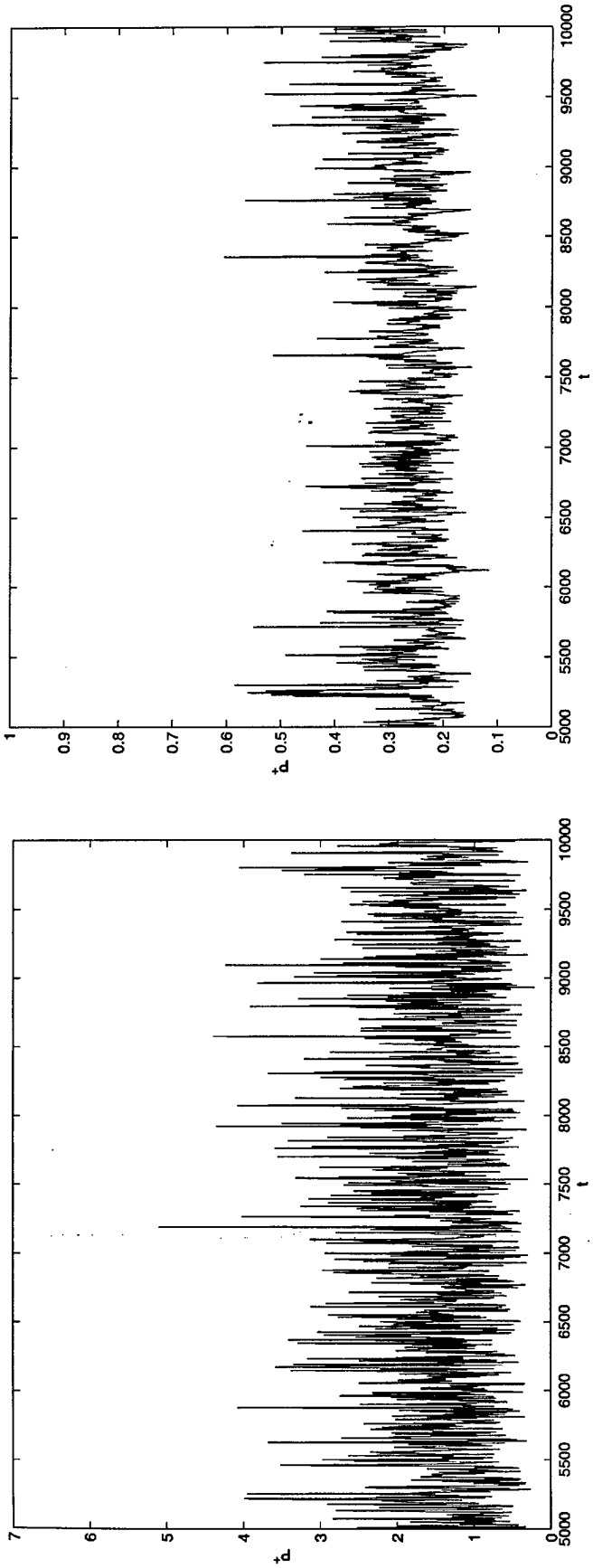

Fig. 21. $\beta = 0$, $\lambda = -1$ (left), $\lambda = +1$ (right). Dissipation rate of energy at high wave numbers vs. time.

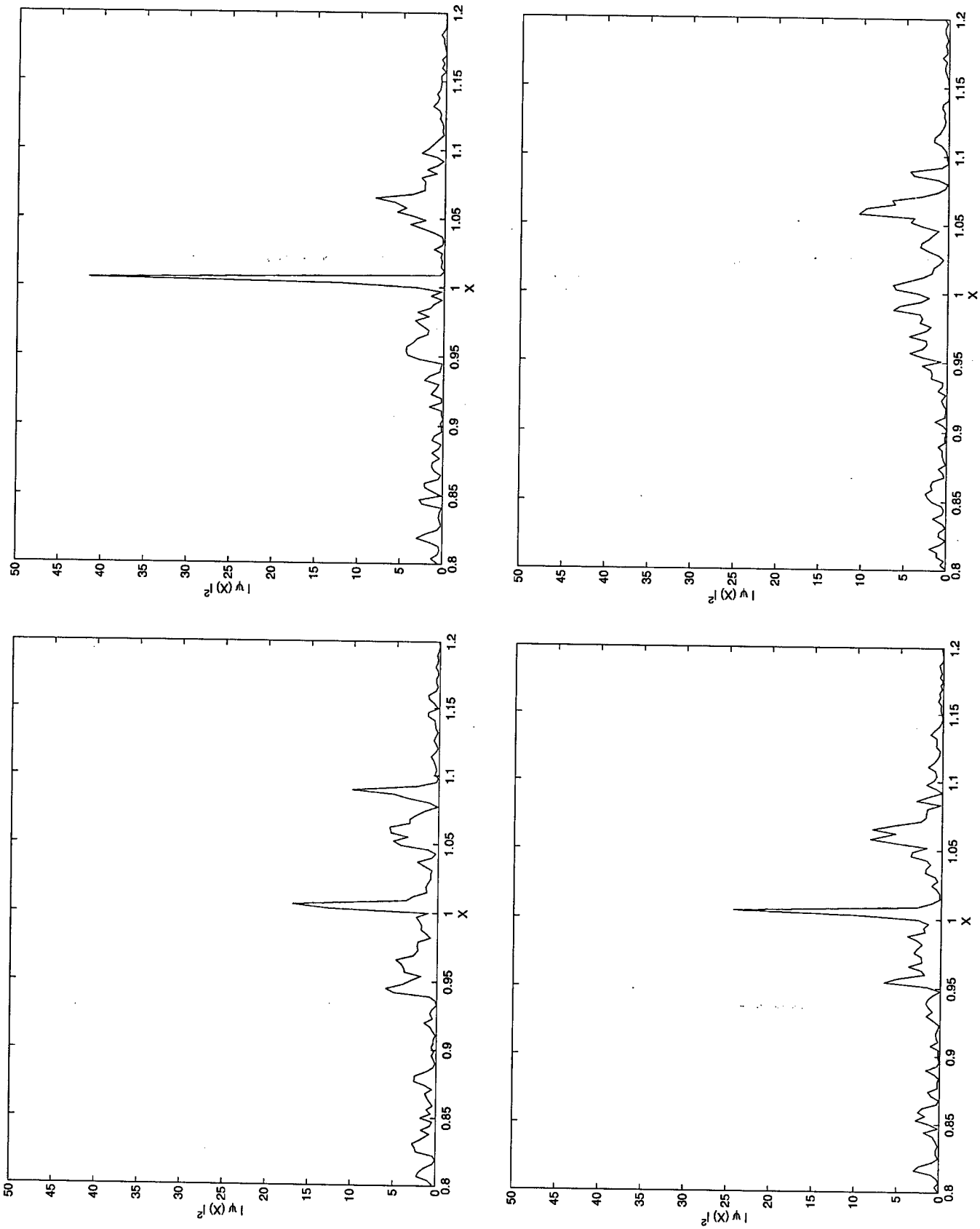

Fig. 22. $\beta = 0, \lambda = -1$. Evolution of a single collapsing peak at $x \simeq 1.006$ at $t = 4999.98, 5000.19, 5000.295$ and $t = 5000.4$ from left to right and from top to bottom.

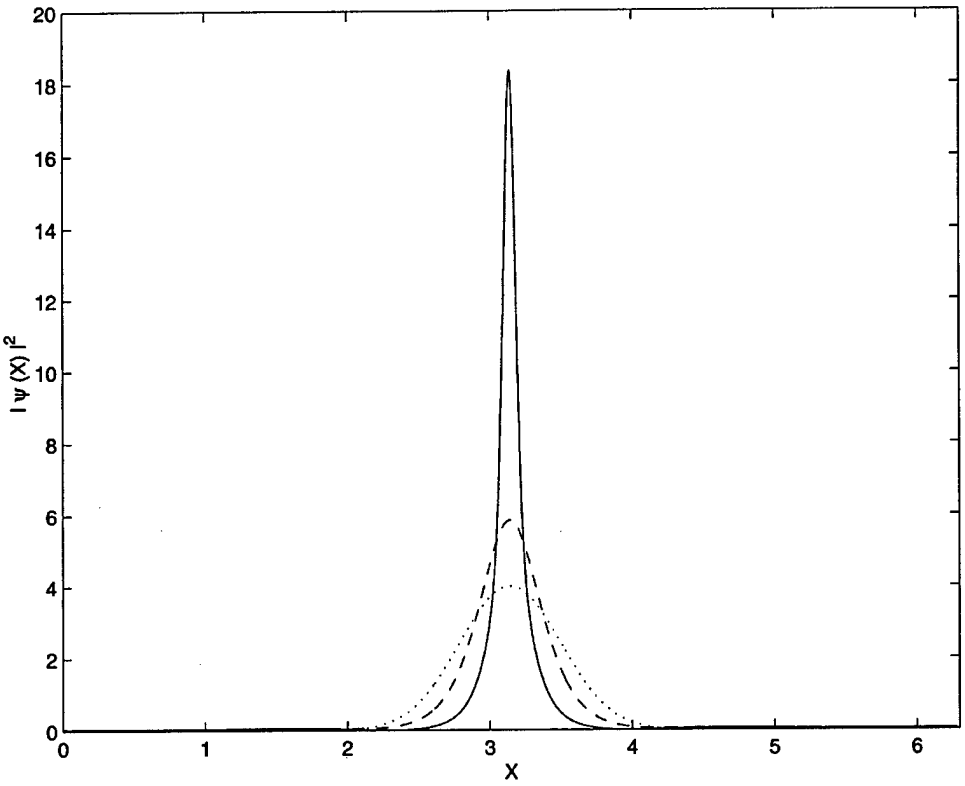

Fig. 23. $\beta = 0, \lambda = -1$. Evolution towards a collapsing peak of the isolated solution for the initial amplitude $\psi_0 = 2$. Dotted line $t = 0$, dashed line $t = 0.55$, solid line $t = 1.1$.

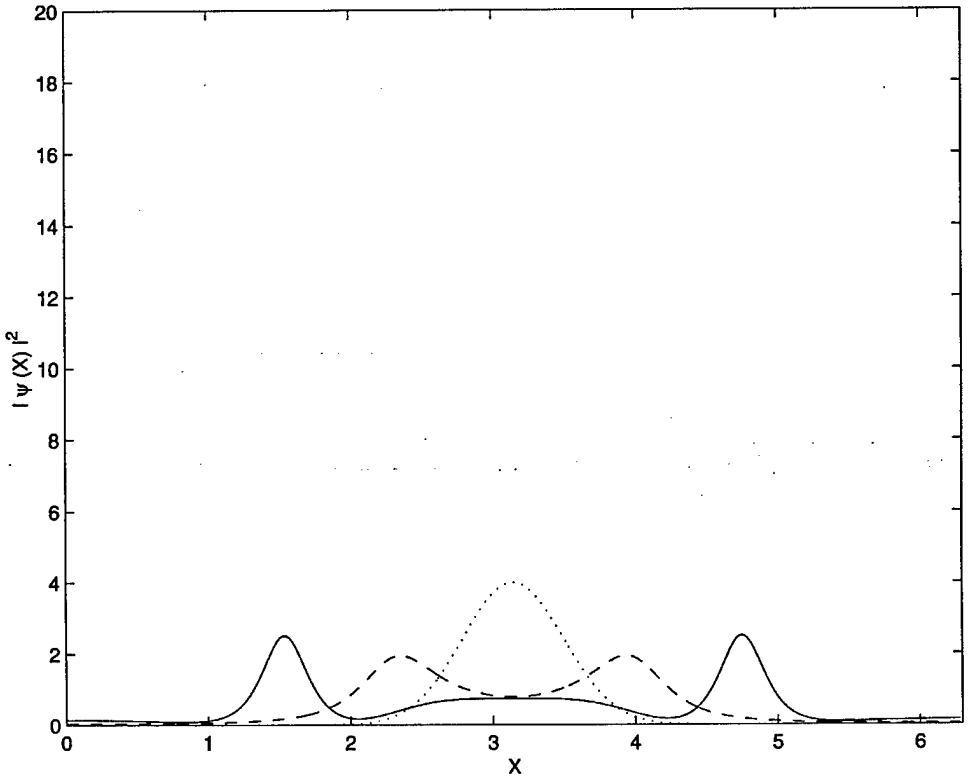

Fig. 24. $\beta = 0, \lambda = +1$. Evolution towards decay of the isolated solution for the initial amplitude $\psi_0 = 2$. Dotted line $t = 0$, dashed line $t = 1.65$, solid line $t = 3.85$.

Fig. 22. $\beta = 0, \lambda = -1$. Evolution of a single collapsing peak at $x \simeq 1.006$ at $t = 4999.98, 5000.19, 5000.295$ and $t = 5000.4$ from left to right and from top to bottom.

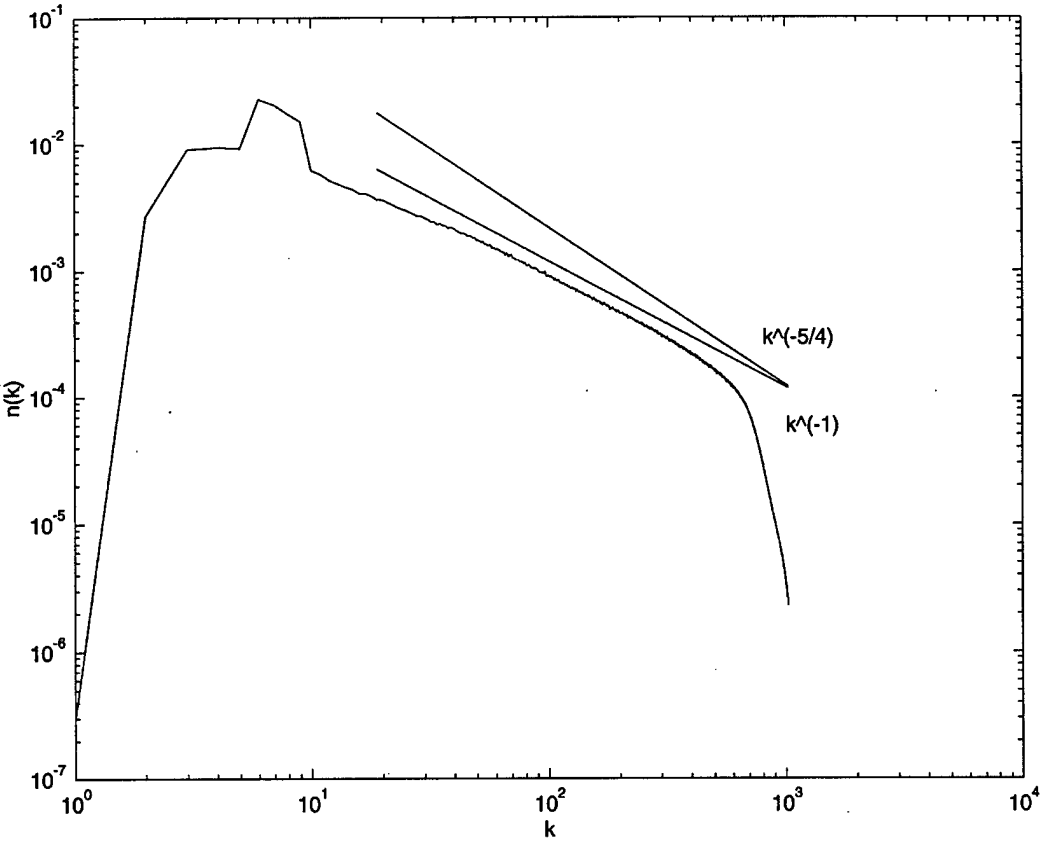

Fig. 25. $\beta = 0, \lambda = -1$. Computed spectrum vs. wave number. The theoretical slopes are shown as well (k^{-1} for WT and $k^{-5/4}$ for MMT).

experiments ϵ could not be taken too small (i.e. $\epsilon \leq 10^{-3}$) for two reasons. First, the nonlinear turnover time grows longer and the energy flux is too weak to act effectively. Second, one may catch the undesirable frozen turbulence [13] due to the disappearance of quasi-resonances. One should note that, in general, frozen turbulence arises more easily in one-dimensional problems due to fewer degrees of freedom than in higher-dimensional problems.

The difference between the cases $\lambda = \pm 1$ is especially conspicuous if one considers the dissipation rates of particles and quadratic energy for small wave numbers

$$Q^- = 2\int_{k<k_f} \nu^- |k|^{-d^-} |\hat{\psi}_k|^2 \, dk, \qquad P^- = 2\int_{k<k_f} \nu^- |k|^{-d^-} \omega(k) |\hat{\psi}_k|^2 \, dk,$$

and for large wave numbers

$$Q^+ = 2\int_{k>k_f} \nu^+ |k|^{d^+} |\hat{\psi}_k|^2 \, dk, \qquad P^+ = 2\int_{k>k_f} \nu^+ |k|^{d^+} \omega(k) |\hat{\psi}_k|^2 \, dk,$$

where k_f is the characteristic wave number of forcing. Figs. 18–21 represent the time evolution of these quantities and their time-averaged values are collected in Table 2.

One can see that the case $\lambda = +1$ quantitatively fits WT theory. Indeed, in this case $Q^+/Q^- \simeq 0.046 \ll 1$ and $P^+/P^- \simeq 0.94$. But in the case of negative nonlinearity $\lambda = -1$ the situation is opposite. In this case $Q^+/Q^- \simeq 4.9$ and $P^+/P^- \simeq 102$ which means that most of both quadratic energy and particles are transported to high frequencies.

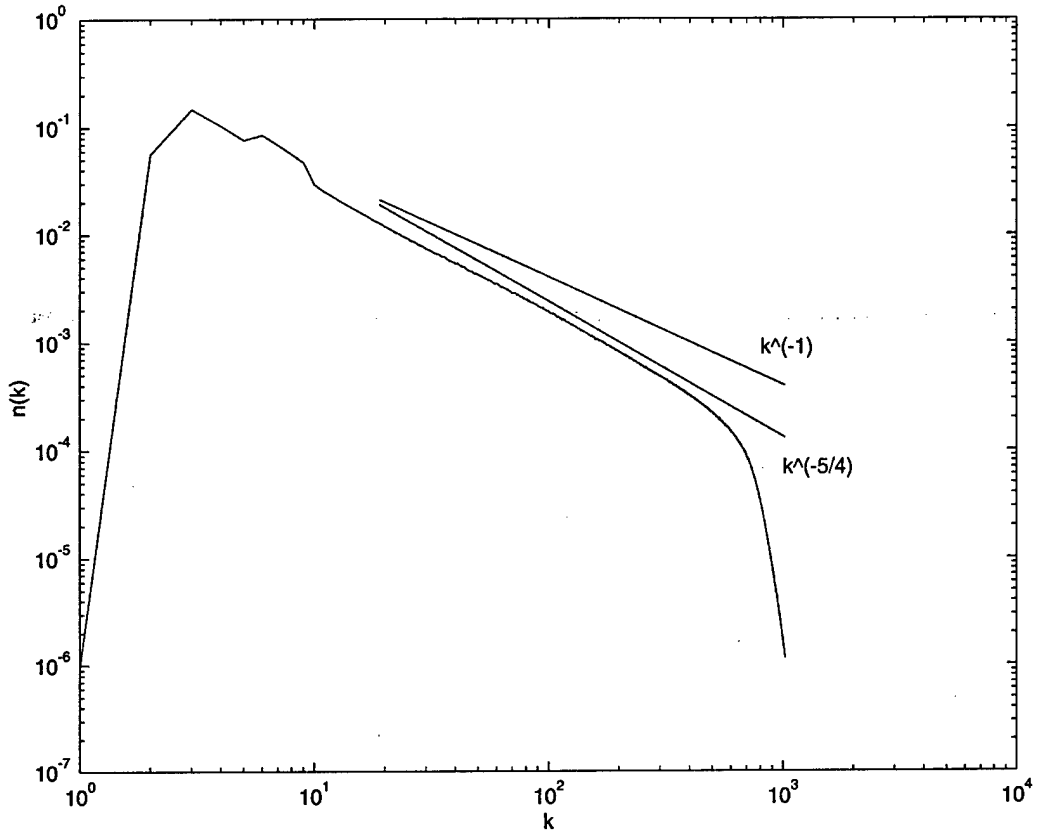

Fig. 26. $\beta = 0$, $\lambda = +1$. Computed spectrum vs. wave number. The theoretical slopes are shown as well (k^{-1} for WT and $k^{-5/4}$ for MMT).

Comparison of the turbulence levels and fluxes of particles Q^+ for both signs of nonlinearity leads to a paradoxal result. At $\lambda = -1$ the total number of particles is three times less than at $\lambda = +1$, while the dissipation rate of particles is higher by one order of magnitude. It can be explained only by the presence in this case of a much more powerful mechanism of nonlinear interactions, which provides very fast wave particles transport to high frequencies. In our opinion, this mechanism is wave collapse, studied theoretically in Section 7. Sporadic collapsing events developing on top of the WT background could send most of particles to high wave numbers without violation of energy conservation, because in each self-similar collapse structure the amount of total energy is zero.

We observed such collapsing events in our numerical experiments. Fig. 22 displays the collapse event taking place at the point $x = 1.006$ at time $t = 5000.19$. One can conjecture that the collapses are described by self-similar solutions. For such solutions $H \equiv 0$. It means that the collapse can carry particles to high frequencies, *without carrying any energy at that time*! As far as the Hamiltonian is the difference of quadratic and quartic terms and both of them go to infinity, it becomes possible to explain the apparent contradictions of the dissipation rates.

The hypothesis related to the prevailing role of collapses at $\lambda = -1$ is corroborated by the following facts:

1. Intermittency in dissipation rates of quadratic energy and particles for $\lambda = -1$ is much higher than for $\lambda = +1$ in the region of large wave numbers. This intermittency can be explained by outbursts of dissipation when wave collapses occur.
2. The analysis of time FTs of separate harmonics (we take $k = 200$) shows the presence of two components, see Fig. 9. The peak at $\omega \simeq 13$ corresponds to a linear wave with a moderate nonlinear shift of frequency. This is the "WT" component of the wave field. Another component is roughly symmetrical with respect to the

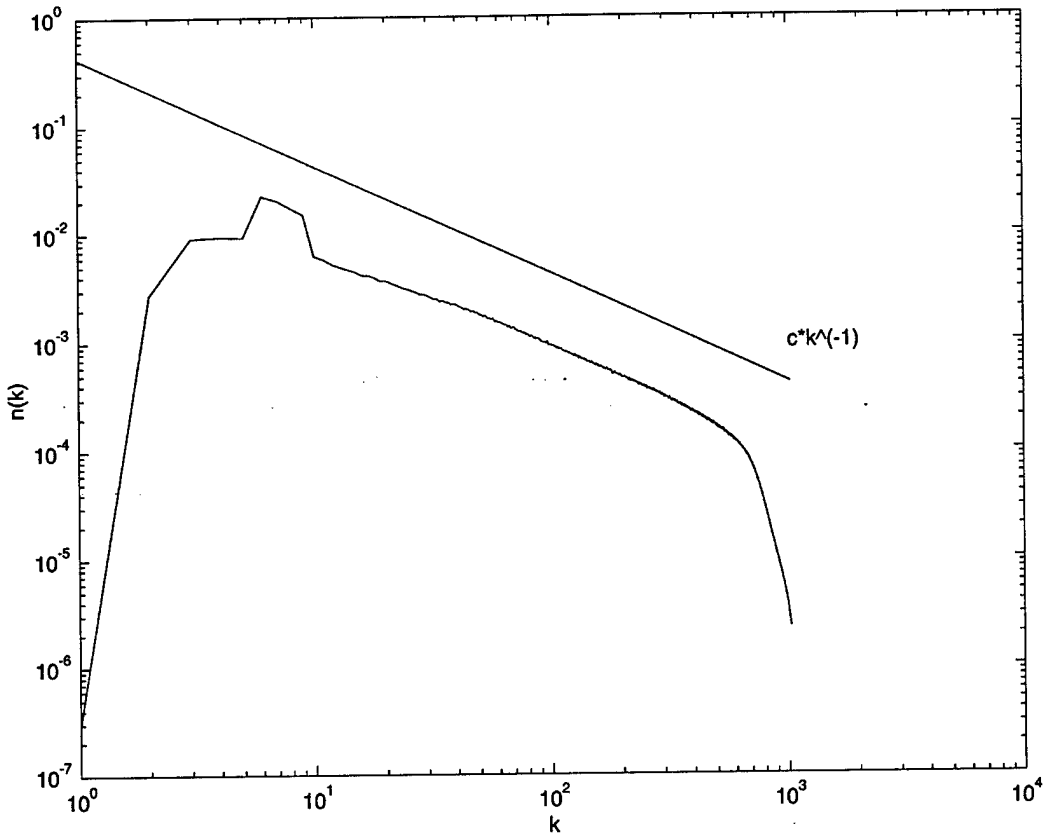

Fig. 27. $\beta = 0$, $\lambda = -1$. Computed spectrum and WT spectrum vs. wave number. The WT spectrum (straight line) is given by $n(k) = ck^{-1}$ with $c = aP^{1/3} \simeq 0.42$.

reflection $\omega \to -\omega$ with the maximum at $\omega = 0$. This is certainly a strongly nonlinear component which could be associated with wave collapses.

Another indication of the difference of the wave dynamics in the cases $\lambda = +1$ and $\lambda = -1$ follows from the following experiment. Figs. 23 and 24 show the early stages in the conservative evolution of the same isolated initial condition

$$\psi(x) = \psi_0 \, \mathrm{e}^{-(x-\pi)^2/2\sigma^2}, \quad \sigma = 0.5.$$

In the case $\lambda = -1$, a sufficiently large initial condition collapses into a sharp spike, while in the case $\lambda = +1$ it decays. This experiment could serve as an evidence of the finite-time singularity formation for the case $\lambda = -1$.

Now, we discuss the stationary isotropic spectra of turbulence which are displayed in Figs. 25–28. We plotted on the same pictures the Kolmogorov spectra calculated by putting either $P = P^+ = 1.430$ ($\lambda = -1$) or $P = P^+ = 0.258$ ($\lambda = +1$) and $a = 0.376$ in Eq. (5.8). In Figs. 27 and 28, one can see that for both cases this spectrum provides a higher level of turbulence than the observed one. For $\lambda = -1$ this difference is almost of one order of magnitude. For $\lambda = +1$, the observed spectrum almost coincides with the WT one at low frequencies and then decays faster at higher wave numbers (approximately as MMT spectrum in Fig. 26).

It is interesting that for $\lambda = -1$ the high frequency asymptotics is fairly close to the one predicted by WT theory (Fig. 25). One can explain this fact as follows. In this case, the turbulence is the coexistence of collapsing events and WT. Collapses carry most of the fluxes of particles and quadratic energy to high frequencies. But their contribution

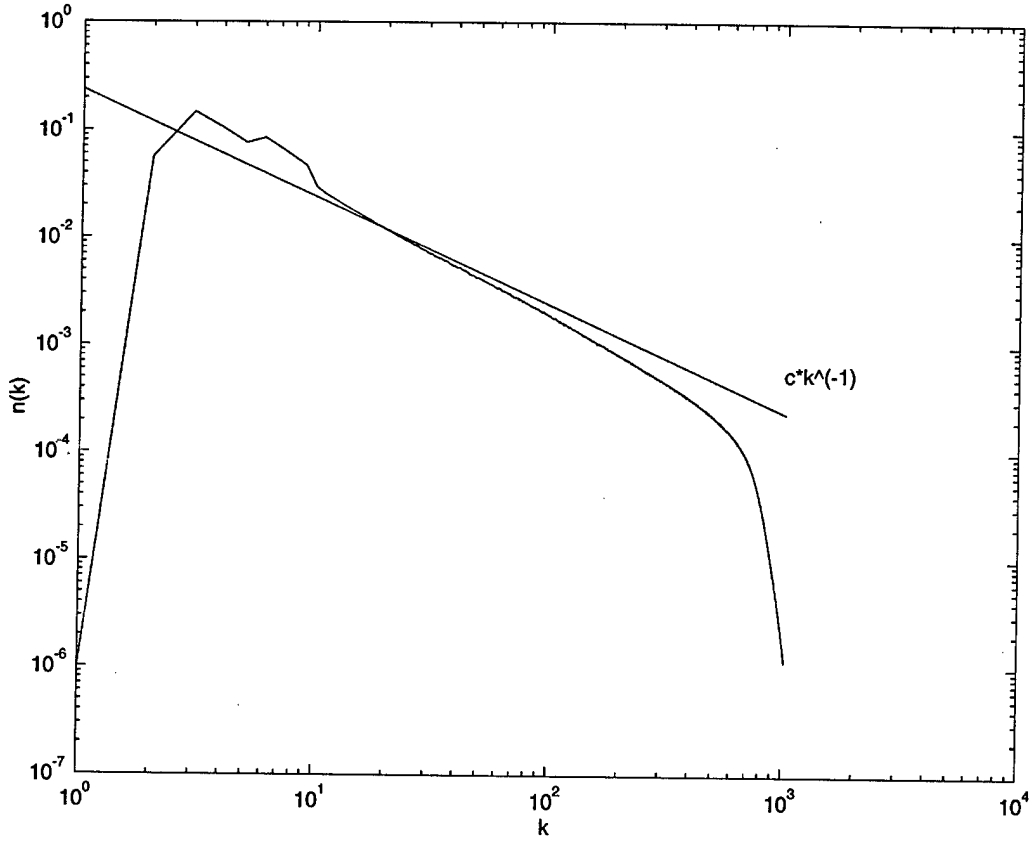

Fig. 28. $\beta = 0$, $\lambda = +1$. Computed spectrum and WT spectrum vs. wave number. The WT spectrum (straight line) is given by $n(k) = ck^{-1}$ with $c = aP^{1/3} \simeq 0.24$.

to the high-frequency part of the spectrum is weak, because they produce Phillips-type spectra, decaying very fast as $k \to \infty$. In our case, this spectrum is

$$n_k \simeq k^{-3/2}. \tag{13.2}$$

Hence as $k \to \infty$, only the WT component survives. Even $P \simeq 10^{-2}P^+$ is enough to provide an observable tail in the WT Kolmogorov spectrum.

We should stress out again that at $\lambda = +1$ the picture of turbulence matches the WT prediction both quantitatively and qualitatively. Meanwhile, the spectrum at high ks is steeper and closer to the MMT formula. So far we cannot give a consistent explanation of this fact. We can just guess that it is somehow connected with quasisolitons. As an illustration, Fig. 29 shows the conservative evolution of the initial quasisoliton (8.13) with parameter $q/k_m = 0.1$, which is small enough to justify the Taylor expansion used in its derivation. As expected, we observe that the solution propagates and persists over a relatively long time. This similarity between quasisolitons and real solitons is verified even better in Figs. 30–33 where two initial quasisolitons with $q/k_m = 0.2$ for the smaller one and $q/k_m = 0.25$ for the bigger one collide almost elastically. Note here that the solution with smaller amplitude moves with a greater velocity.

14. Numerical results for $\beta = +3$ and $\lambda = +1$

Another series of experiments has been performed for the case $\beta = +3$ and $\lambda = +1$. This case is especially attractive due to the fact that the intensity of interaction grows with characteristic wave number in Fourier space

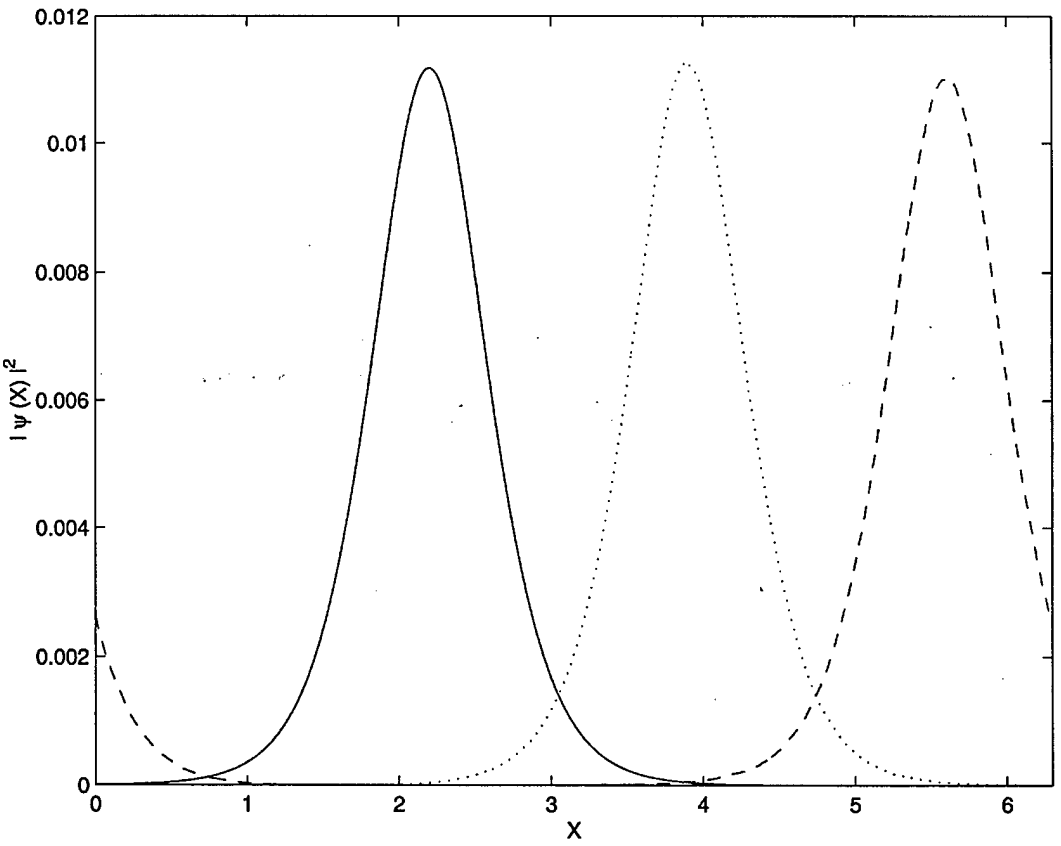

Fig. 29. $\beta = 0$, $\lambda = +1$. Evolution of the initial quasisoliton for $q/k_m = 0.1$. Solid line $t = 0$, dotted line $t = 1250$, dashed line $t = 2500$.

and one can expect reduced "frozen" turbulence effects compared to the case $\beta = 0$. Another motivation is the fact that the scaling of the interaction kernel reproduces the kernel for gravity water waves. Therefore, Eq. (12.1) with $\alpha = \frac{1}{2}$, $\beta = +3$ can be considered as a model of turbulence of the ocean surface.

The numerical simulation of Eq. (12.1) was performed on a grid of 2048 points in the real space domain of length 2π. Parameters of the forcing are defined by

$$F(k) = \begin{cases} 0.001 & \text{if } 30 < k < 42, \\ 0 & \text{otherwise,} \end{cases}$$

and parameters of damping in the "hyperviscosity" form by

$$D(k) = \begin{cases} -0.05(k-4)^8 & \text{if } 0 < k < 4, \\ -0.1(k-824)^2 & \text{if } 824 < k < 1024, \\ 0 & \text{otherwise.} \end{cases}$$

Aliasing effects were not of concern due to the run-time control of the fastness of the spectrum decay toward high wave numbers.

The time-step of integration was equal to $\frac{1}{50}$ of the inverse fastest linear frequency in the problem. Such a small value was chosen due to the fact that the time dependence of the individual Fourier harmonics corresponding to intermediate range wave numbers showed the presence of processes of time scale smaller than the smallest linear

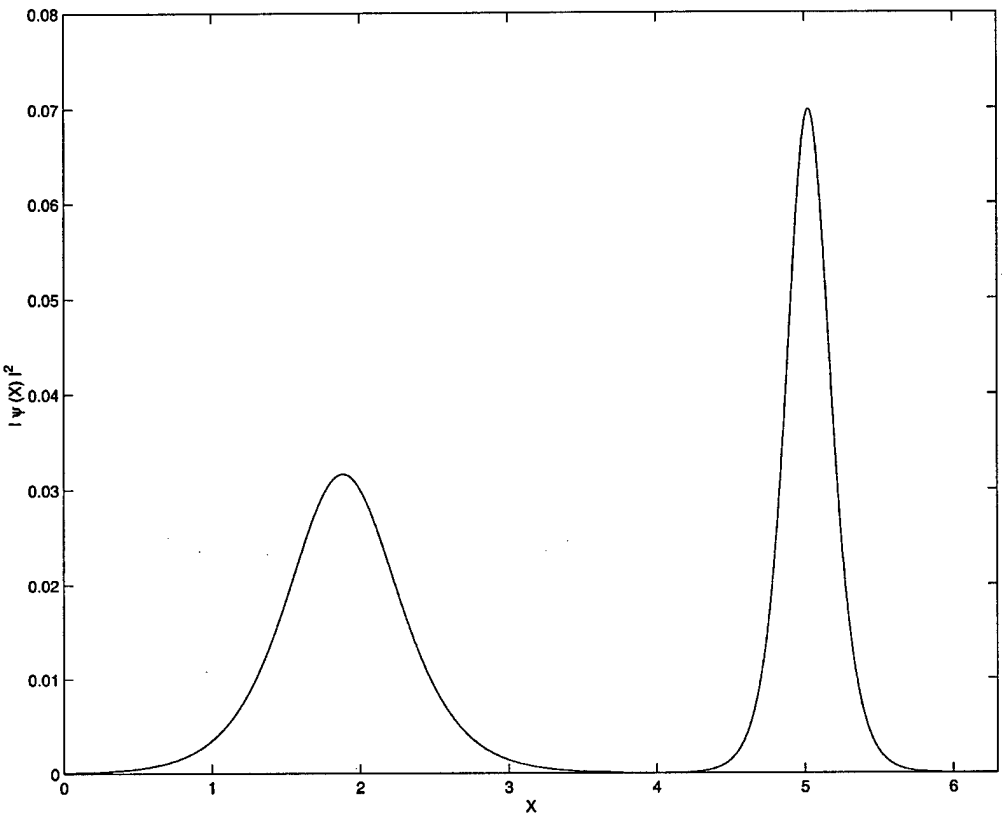

Fig. 30. $\beta = 0$, $\lambda = +1$. Interaction of two initial quasisolitons at $t = 0$. The smaller and bigger ones correspond to $q/k_m = 0.2$ and 0.25, respectively.

time in the system. This observation was an initial indication of the significant role of nonlinearity in the problem under consideration.

Eq. (12.1) was integrated numerically over long times for different kinds of initial conditions: low level random noise and single harmonic excitation ($k = 30$) initial conditions. While initial stages of computations were quantitatively different, the later stages of evolution were strikingly similar. Starting from big enough times, the wave system was separated into several soliton-like moving structures and low-amplitude quasi-linear waves. Processes of interaction of solitons and waves slowly redistributed the number of waves in a way leading to the growth of initially bigger solitons and the collapse of initially smaller solitons. Finally, the system was clearly separated into a state with one moving soliton and quasi-linear waves.

We interpret the observed phenomenon as similar to the "droplet" effect observed earlier in non-integrable NLS equation [20]. The soliton solution turns out to be the statistical attractor for nonlinear non-integrable wave systems: long time evolution leads to the condensation of the integral of total number of waves into the single soliton which minimizes the Hamiltonian.

Figs. 34 and 35 show snapshots of the final state of the system: the single soliton is moving with constant speed on the background of quasi-linear waves. A quantitative comparison shows that the parameters of the observed object are close to the parameters of the quasisoliton solution (8.13).

One should emphasize that there is a difference between the situation observed in the present work and former observations of "droplet" effects in non-integrable NLS equations. Solitons observed in [20] were exact stable solutions of the corresponding NLS equation. Solitary solutions observed in the present work are "quasisolitons" which are unstable at least in a certain range of parameters.

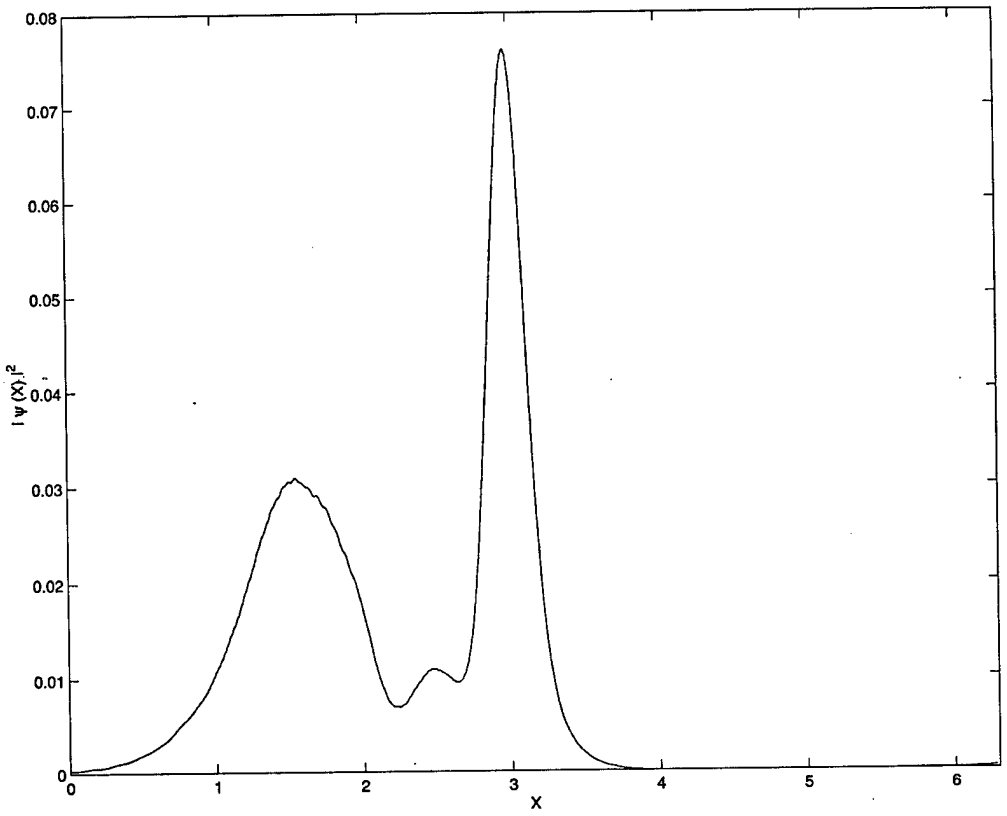

Fig. 31. $\beta = 0$, $\lambda = +1$. Interaction of two initial quasisolitons at $t = 37.5$.

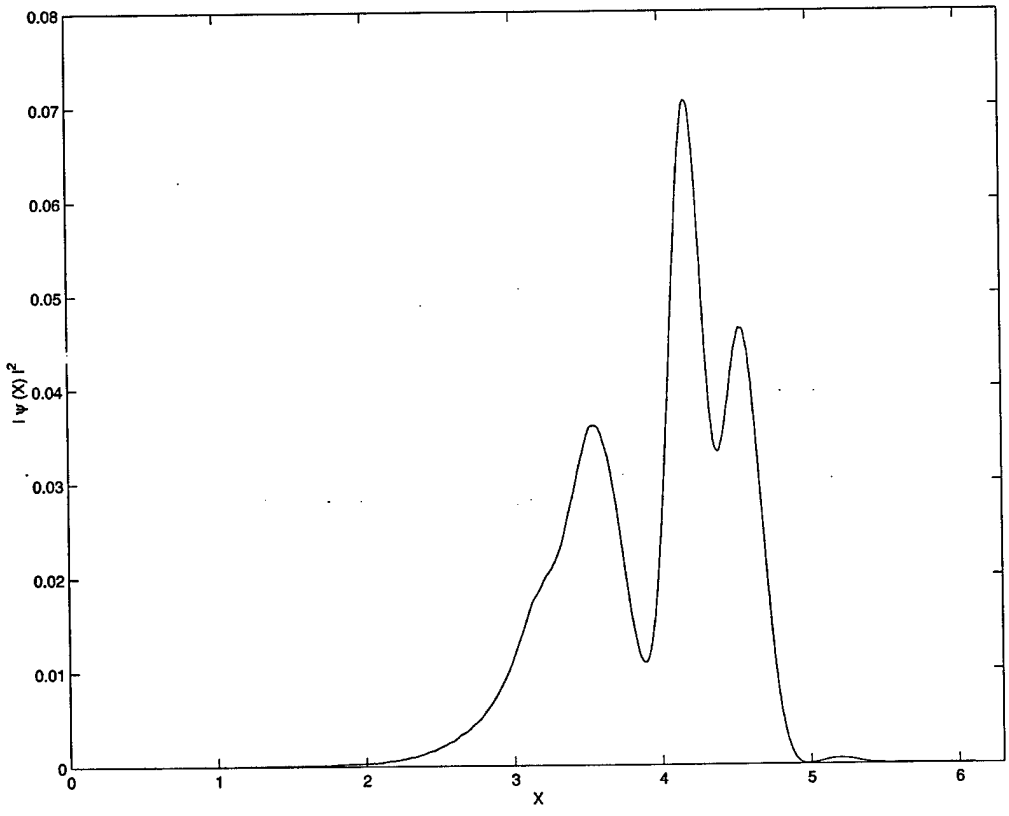

Fig. 32. $\beta = 0$, $\lambda = +1$. Interaction of two initial quasisolitons at $t = 50$.

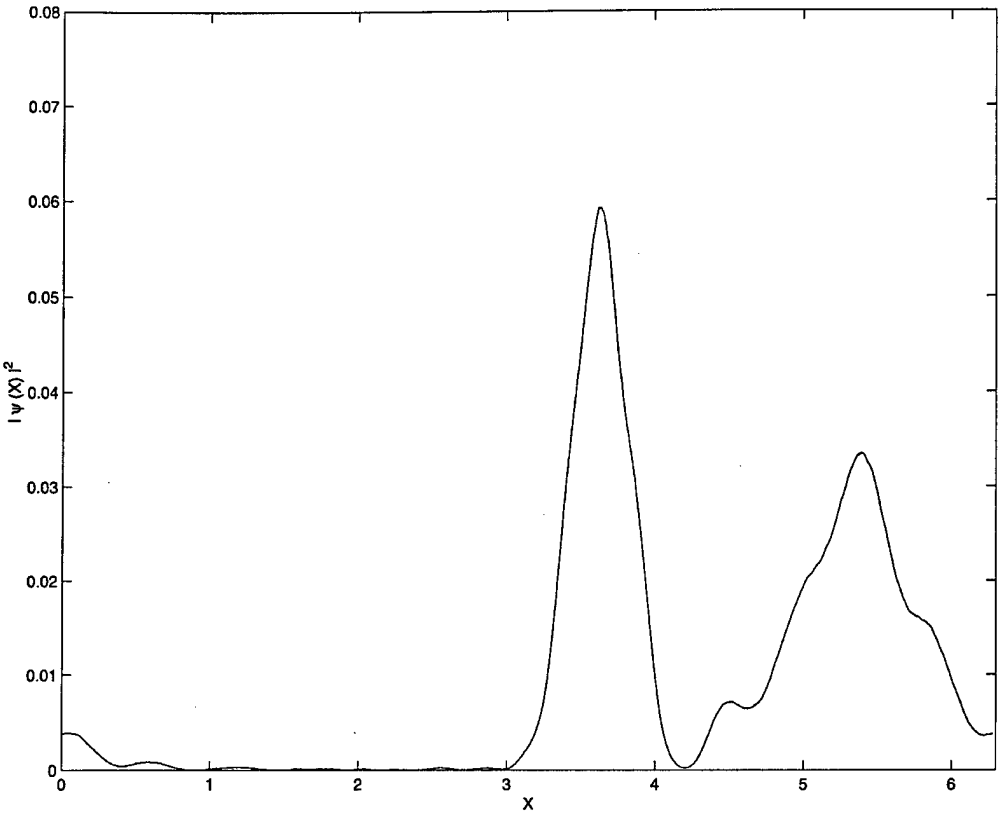

Fig. 33. $\beta = 0$, $\lambda = +1$. Interaction of two initial quasisolitons at $t = 100$.

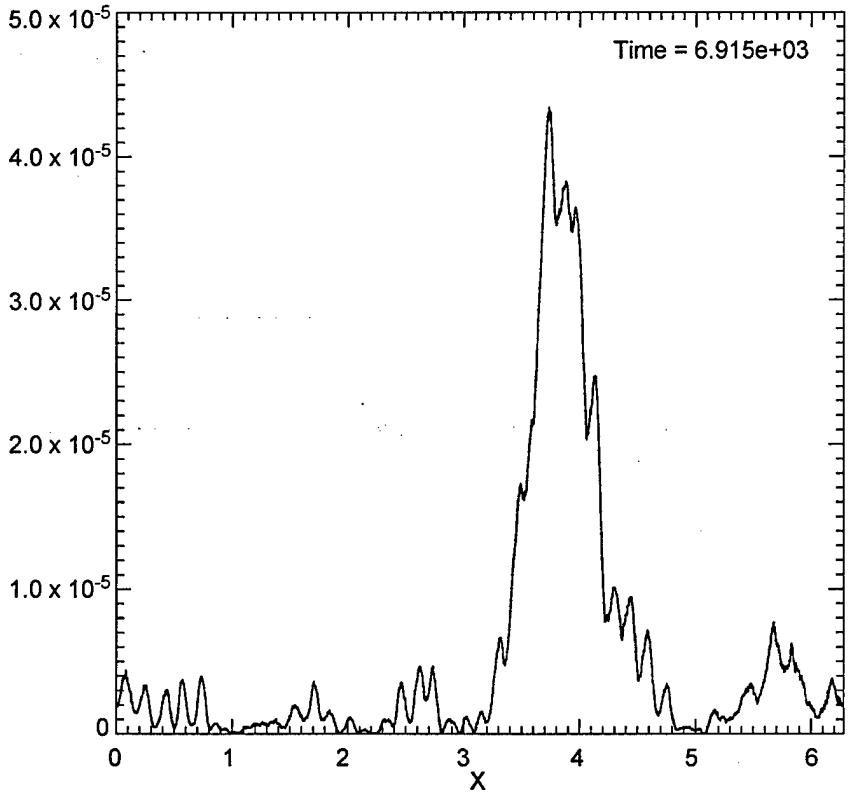

Fig. 34. $\beta = 3$, $\lambda = +1$. Single moving soliton, $t = 6915$.

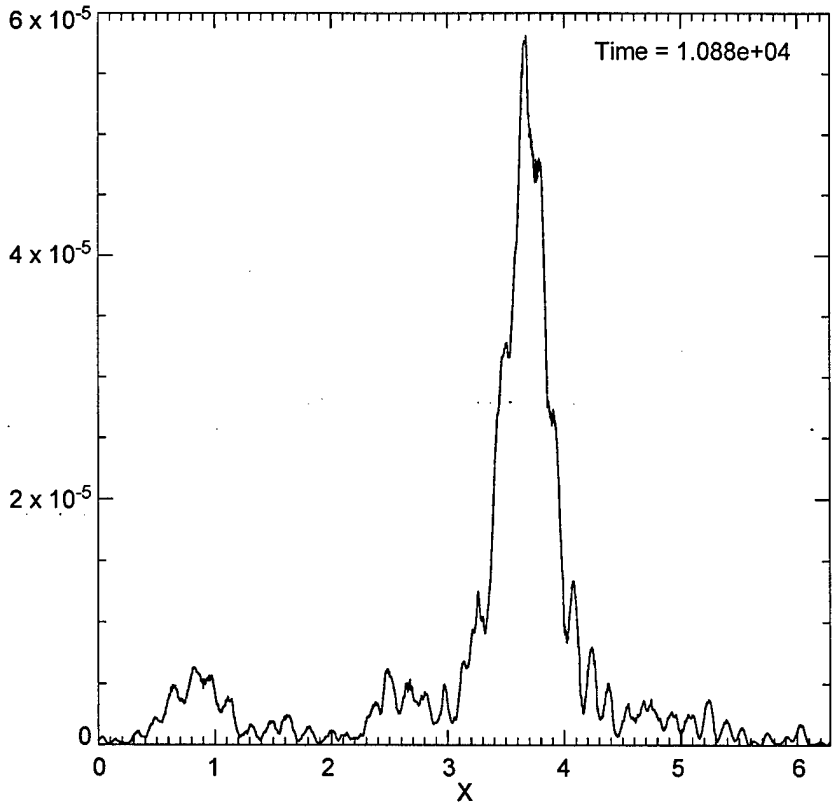

Fig. 35. $\beta = 3$, $\lambda = +1$. Single moving soliton, $t = 10\,880$.

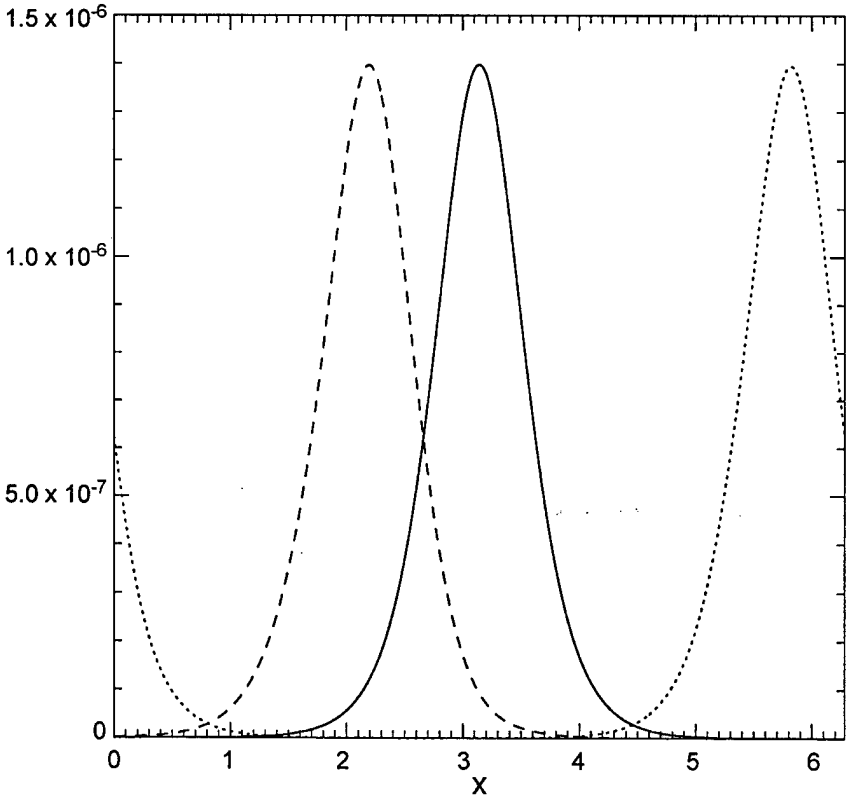

Fig. 36. $\beta = 3$, $\lambda = +1$. Evolution of the initial quasisoliton for $q/k_m = 0.1$. Solid line $t = 0$, dotted line $t = 23.6$, dashed line $t = 47.1$.

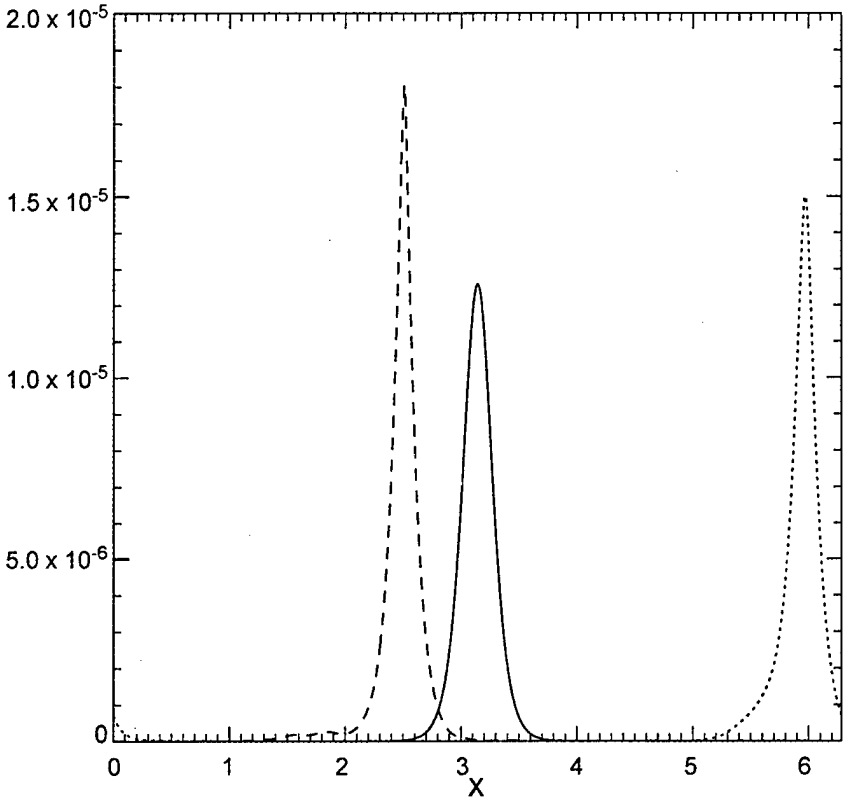

Fig. 37. $\beta = 3, \lambda = +1$. Evolution of the initial quasisoliton for $q/k_m = 0.3$. Solid line $t = 0$, dotted line $t = 23.6$, dashed line $t = 47.1$.

In Fig. 36 the initial condition is the quasisoliton (8.13) with parameter $q/k_m = 0.1$. Here again, it behaves as the soliton should: it moves without any detectable change of shape. Fig. 37 shows the evolution for $q/k_m = 0.3$. One can interpret such initial condition as a "deformed" quasisoliton. This initial condition rapidly develops moving singularity collapsing, presumably, in finite time.

15. Conclusion

The MMT model with $\alpha < 1$ and either sign of nonlinearity exhibits coherent structures. In the case of negative nonlinearity these structures are weak collapses. These collapses are a powerful mechanism of energy dissipation, which dominates in all our numerical experiments. Weak turbulence coexists with collapses, and is responsible for the formation of Kolmogorov-type tails of wave spectra. But it carries to high wave numbers just a small part of the energy (less than 5%).

One may hope to get "pure" WT by decreasing the level of nonlinearity. But to achieve an adequate modeling of the continuous medium, one should take a very fine mesh (at least 10^4 harmonics) and apply forcing in a broad range (say $10 < k < 100$). Otherwise effects of "frozen turbulence" will blur the picture. Such experiments would be very time consuming.

The case of positive nonlinearity is less clear. In this case the picture of turbulence is qualitatively similar to WT, but the slope of the spectrum fits better the MMT spectrum. So far we do not have a satisfactory explanation of this phenomenon. Probably it could be explained by the presence of interacting quasisolitons. In this case again, experiments with a larger number of harmonics could give a result closer to WT predictions.

The relative "suppression" of WT in the MMT model can be explained by a peculiarity of the resonant conditions. In the one-dimensional case with $\alpha = \frac{1}{2}$, only well-separated waves interact. Indeed, one can see from (2.10) that

$$\left|\frac{k_2}{k_1}\right| = \left(\frac{1}{\xi} + 1 + \xi\right)^2, \quad \xi > 0, \tag{15.1}$$

and therefore $\min|k_2/k_1| = 9$ is reached at $\xi = 1$. This phenomenon can be called "sparsity of resonances". Due to this sparsity, four-wave resonances easily lose the competition with coherent structures — collapses and quasisolitons. In this sense the MMT model is not an optimal object for checking the validity of WT theory. We can offer the following model, which includes the interaction of two types of waves

$$H = \int |k|^\alpha (|a_k|^2 + s|b_k|^2)\,\mathrm{d}k + \int |kk_1k_2k_3|^{\beta/4}(a_k^* a_1^* a_2 a_3 + 2p_1 a_k^* b_1^* a_2 b_3 + p_2 b_k^* b_1^* b_2 b_3) \times \delta(k + k_1 - k_2 - k_3)\,\mathrm{d}k\,\mathrm{d}k_1\,\mathrm{d}k_2\,\mathrm{d}k_3. \tag{15.2}$$

If $\alpha > 1$ and $\beta < 2\alpha - 1$, the corresponding dynamical system does not describe any coherent structures which could compete with four-wave resonances. Meanwhile, for $s \neq 1$, it describes non-trivial resonant interactions for different waves propagating in the same direction. The system (15.2) looks like a possible object for the simulation of wave turbulence. In the special case $\alpha = 2$ and $\beta = 0$, it describes coupled NLS equations.

Acknowledgements

The authors are grateful to D. McLaughlin, A. Majda, D. Cai and E. Tabak for useful discussions and for providing their results before publication. This work was performed in the framework of the NATO Linkage Grant OUTR.LG 970583. V. Zakharov and A. Pushkarev also acknowledge support of the US Army, under the grant DACA 39-99-C-0018, and of ONR, under the grant N00014-98-1-0439. F. Dias and P. Guyenne acknowledge support of DGA, under the contract ERS 981135. A. Pushkarev wishes to thank F. Dias for his hospitality during a visit to Nice in the fall of 1998.

References

[1] R.E. Peierls, Zur kinetischen Theorie der Wärmeleitungen in Kristallen, Ann. Phys. 3 (1929) 1055–1101.
[2] K. Hasselmann, On the non-linear energy transfer in a gravity-wave spectrum. Part 1. General theory, J. Fluid Mech. 12 (1962) 481–500.
[3] K. Hasselmann, On the non-linear energy transfer in a gravity-wave spectrum. Part 2. Conservative theorems, wave-particle analogy, irreversibility, J. Fluid Mech. 15 (1963) 273–281.
[4] V.E. Zakharov, Stability of periodic waves of finite amplitude on a surface of deep fluid, J. Appl. Mech. Tech. Phys. 9 (1968) 190–194.
[5] A.N. Pushkarev, V.E. Zakharov, Turbulence of capillary waves, Phys. Rev. Lett. 76 (1996) 3320–3323.
[6] V.E. Zakharov, N.N. Filonenko, Weak turbulence of capillary waves, J. Appl. Mech. Tech. Phys. 4 (1967) 506–515.
[7] A.J. Majda, D.W. McLaughlin, E.G. Tabak, A one-dimensional model for dispersive wave turbulence, J. Nonlinear Sci. 6 (1997) 9–44.
[8] D. Cai, A.J. Majda, D.W. McLaughlin, E.G. Tabak, Spectral bifurcations in dispersive wave turbulence, Proc. Natl. Acad. Sci. 96 (1999) 14216-14221.
[9] D. Cai, D. McLaughlin, A. Majda, E. Tabak, Dispersive wave turbulence in one dimension, Physica D 152–153 (2001) 551–572.
[10] D. Cai, D. McLaughlin, Chaotic and turbulent behavior of unstable one-dimensional nonlinear dispersive waves, J. Math. Phys. 41 (2000) 4125–4153.
[11] V.E. Zakharov, Statistical theory of gravity and capillary waves on the surface of a finite-depth fluid, Eur. J. Mech. B 18 (1999) 327–344.
[12] G. Falkovich, Bottleneck phenomenon in developed turbulence, Phys. Fluids 6 (1994) 1411–1414.
[13] A.N. Pushkarev, On the Kolmogorov and frozen turbulence in numerical simulation of capillary waves, Eur. J. Mech. B 18 (1999) 345–352.
[14] V.E. Zakharov, E.A. Kuznetsov, Optical solitons and quasisolitons, ZhETF (JETP) 113 (1998) 1892–1913.

[15] S. Dyachenko, A.C. Newell, A.N. Pushkarev, V.E. Zakharov, Optical turbulence: weak turbulence, condensates and collapsing filaments in the nonlinear Schrödinger equation, Physica D 57 (1992) 96–160.
[16] V.E. Zakharov, V. Lvov, G. Falkovich, Kolmogorov Spectra of Turbulence, Vol. I, Springer, Berlin, 1992.
[17] A.M. Balk, V.E. Zakharov, Stability of weak turbulence Kolmogorov spectra, Am. Math. Soc. Transl. Ser. 2 182 (1998) 31–81.
[18] E.A. Kuznetsov, A.M. Rubenchik, V.E. Zakharov, Soliton stability in plasmas and hydrodynamics, Phys. Rep. 142 (1986) 103–165.
[19] O.M. Phillips, The Dynamics of the Upper Ocean, Cambridge University Press, Cambridge, 1977.
[20] V.E. Zakharov, A.N. Pushkarev, V.F. Shvets, V.V. Yan'kov, Soliton turbulence, JETP Lett. 48 (1988) 83–87.

Nonlinear Processes in Geophysics (1999) 6: 1–10

Nonlinear Processes in Geophysics

Diffusion model of interacting gravity waves on the surface of deep fluid

V. E. Zakharov and A. N. Pushkarev

Arizona Center of Mathematical Science, Department of Mathematics, University of Arizona, Tucson, AZ 85721, USA
L. D. Landau Institute for Theoretical Physics, Russian Academy of Sciences, 117940 GSP-1 Moscow V-334, ul.Kosygina 2, Russia

Received: 11 March 1999 – Accepted: 20 May 1999

Abstract. A simple phenomenological model for nonlinear interactions of gravity waves on the surface of deep water is developed. The S_{nl} nonlinear interaction term in the kinetic equation for wave action is replaced by the nonlinear second-order diffusion-type operator.

Analytical and numerical studies show that the new model gives a reasonably good description of a real situation, consuming three order of magnitude less computer time.

1 Introduction

The leading nonlinear interaction of gravity waves on the surface of deep liquid is four-wave interaction (Phillips, 1966) satisfying the resonant conditions

$$\vec{k_1} + \vec{k_2} = \vec{k_3} + \vec{k_4} \tag{1}$$

$$\omega_k + \omega_{k_1} = \omega_{k_2} + \omega_{k_3} \tag{2}$$

where $\omega = \sqrt{gk}$ is the dispersion law.

The four-wave interactions play a very important role in the surface dynamics. They arrest the growth of wave amplitudes, caused by instability of the flat surface in the presence of the wind, redistribute wave energy along the K-plane and form the basic cascades, governing the wave kinetics: direct cascade of the energy to large k and inverse cascade of the wave-action to small k (see Zakharov and Zaslavskii (1982), Zakharov (1992)).

The four-wave interactions are described by the kinetic equation for squared wave amplitudes derived first by Hasselmann (1962). This equation is a natural base for practical models of wave-prediction. Due to this reason many people during last two decades endeavored to develop efficient numerical solvers for this equation (Hasselmann and Hasselmann (1985) , Hasselmann at al. (1985) , Masuda (1980) , Komatsu and Masuda (1996) , Resio and Perrie (1991) , Polnikov (1989) , Lavrenov (1991)).

Due to complexity of the kinetic equation, existing codes are still time-consuming and hardly can be used for practical purposes. The development of a simplified model of four-wave interaction describing in an adequate way the main feature of this process is, therefore, an urgent problem.

There is another reason for development of such a model. The stationary kinetic equation has remarkable exact solution: weak-turbulent Kolmogorov spectra (Zakharov and Filonenko (1966), Zakharov and Zaslavskii (1982)). For energy spectrum they are

$$E_\omega = C_1 \epsilon \frac{gu}{\omega^4}, \quad \epsilon = \frac{\rho_{atm}}{\rho_{water}} \tag{3}$$

$$E_\omega = C_2 \epsilon \frac{g^{\frac{2}{3}} u^{\frac{4}{3}}}{\omega^{\frac{11}{3}}} \tag{4}$$

where u is the wind velocity.

The spectrum (3) describes the transport of energy to small scales, while (4) describes the transport of wave action to large scales. Both spectra are obtained in a very idealistic assumption of isotropy in angles. Real wave spectra both in the ocean and in the laboratory are strongly anisotropic. Meanwhile, there are a lot of evidences, that at least the spectrum (4) fits very well the real situation.

Asymptotic ω^{-4} was observed by many experimentalists since Toba (e.g. Toba (1973), Donelan et al. (1985), Phillips (1966)). This asymptotic appears systematically in numerical experiments (Resio and Perrie (1991), Komatsu and Masuda (1996), Polnikov (1989)). But the complexity of the real kinetic equation does not allow to construct analytical angle – dependent anisotropic spectra. A properly simplified model would serve better this purpose.

In this article we suggest a very simple model of four-wave interaction of the gravity waves. We replace the

complex nonlinear integral interaction term by simple nonlinear elliptic differential operator of the second order.

The whole kinetic equation becomes the nonlinear diffusion equation. Its stationary solution can be easily found analytically. They describe not only isotropic Kolmogrov spectra (3) and (4), but also anisotropic spectra corresponding to momentum transport to small scales. We developed the code for numerical solution of new model equation in the presence of a wind and received quite reasonable results. Due to simplicity of the model, it consumes three order of magnitude less computer time than the model using exact kinetic equation. We hope that the new model can be efficiently used in practical programs of wave prediction.

2 General background

Let $\eta(k)$ be a Fourier Transform of the surface elevation and

$$I_k\delta(k+k') = \langle\eta(k)\eta(k')\rangle \tag{5}$$

where I_k is the spatial spectrum of the surface. It contains important, but incomplete information about the surface and cannot satisfy any self-consistent evolutionary equation. More complete information is contained in the distribution of wave action

$$n_k\delta(k-k') = \langle a(k)a(k')\rangle \tag{6}$$

where a_k is the complex normal amplitude (see Zakharov (1968)) , $n_{-k} \neq n_k$ and

$$I_k = \frac{1}{2g}\omega_k(n_k + n_{-k}) \tag{7}$$

Hasselmann showed that n_k satisfies the kinetic equation (Hasselmann, 1962)

$$\frac{\partial n}{\partial t} = S_{nl}(n,n,n) - \beta_k n_k \tag{8}$$

where β_k is the coefficient describing interaction with the wind and wave-breaking and

$$S_{nl}(n,n,n) = 4\pi\int |T_{kk_1k_2k_3}|^2\delta_{k+k_1-k_2-k_3}$$
$$\delta_{\omega_k+\omega_{k_1}-\omega_{k_2}-\omega_{k_3}}(n_{k_1}n_{k_2}n_k + n_kn_{k_2}n_{k_3}$$
$$-n_kn_{k_1}n_{k_2} - n_kn_{k_1}n_{k_3})dk_1dk_2dk_3 \tag{9}$$

where $T_{kk_1k_2k_3}$ is the coefficient, describing four-wave interaction. It is a homogeneous function of the third degree

$$T(\epsilon k, \epsilon k_1, \epsilon k_2, \epsilon k_3) = \epsilon^3 T(k, k_1, k_2, k_3) \tag{10}$$

A relatively compact explicit expression for $T_{kk_1k_2k_3}$ can be found in the article of Webb (1978). This function has the following symmetry properties

$$T_{kk_1k_2k_3} = T_{k_1kk_2k_3} = T_{kk_1k_3k_2} = T_{k_2k_3kk_1} \tag{11}$$

Due to these properties, equation (8) formally preserves the following quantities of wave action N, wave energy E and momentum P if $\beta_k = 0$:

$$\begin{aligned} N &= \int n_k dk \\ E &= \int \omega_k n_k dk \\ P &= \int \vec{k} n_k dk \end{aligned} \tag{12}$$

Conservation of these quantities is "formal" because one have to change the order of the integration in four-dimensional integrals to prove it. According to Fubini theorem, this change is permitted if n_k vanishes fast enough at $|k| \to \infty$.

For conservation of the wave action N one has to satisfy the condition

$$n_k < Ck^{-(\frac{23}{6}+\epsilon)} \tag{13}$$

Conservation of the wave energy E is guaranteed if

$$n_k < Ck^{-(4+\epsilon)} \tag{14}$$

and conservation of the momentum P takes place if

$$n_k < Ck^{(-\frac{25}{6}+\epsilon)} \tag{15}$$

where $\epsilon > 0$.

Corresponding critical behavior of the energy spectral density

$$\varepsilon_\omega d\omega = \omega_k n_k k dk d\phi \tag{16}$$

is $\varepsilon_\omega < \omega^{-\frac{11}{3}}$ for wave action, $\varepsilon_\omega < \omega^{-4}$ for energy and $\varepsilon_\omega < \omega^{-\frac{15}{3}}$ for momentum.

In reality, typical asymptotic for ε_ω is $\varepsilon_\omega \simeq \omega^{-4}$, and conditions (14) and (15) are not satisfied while the condition (13) is fulfilled. Thus, in the typical situation only wave action N is a real constant of motion. Energy and momentum "leak" to the small-scale region.

Let us consider the equation

$$S_{nl}(n,n,n) = 0 \tag{17}$$

It has obvious thermodynamic solutions

$$n_k = \frac{T}{\mu + \omega_k} \tag{18}$$

where T and μ are the constant temperature and chemical potential. Special cases of this solution are

$$\begin{aligned} n_k^{(1)} &= \frac{T}{\omega_k}, \quad (\mu = 0) \\ n_k^{(2)} &= n_0, \quad (T \to \infty, \mu \to \infty, \frac{T}{\mu} = n_0) \end{aligned} \tag{19}$$

All motion constants on thermodynamic solutions diverge on thermodynamic solutions at $k \to \infty$. This fact makes thermodynamic solutions useless for applications.

Equation (17) has also non-thermodynamic solutions. Looking for the solutions in the form

$$n_k = C|k|^{-x} \tag{20}$$

one can find (Zakharov and Filonenko (1966), Zakharov and Zaslavskii (1982), Zakharov at al. (1992)) that x can take four values

$$x_1 = 0, \quad x_2 = \frac{1}{2}, \quad x_3 = \frac{23}{6}, \quad x_4 = 4 \tag{21}$$

Exponents $x_1 = 0$ and $x_2 = \frac{1}{2}$ correspond to thermodynamic solutions (19). Exponents $x_3 = \frac{23}{6}$ and $x_4 = 4$ give the spectra

$$n_k = C_3|k|^{-\frac{23}{6}}, \quad E_\omega = C_3\omega^{-\frac{11}{3}} \tag{22}$$

$$n_k = C_4|k|^{-4}, \quad E_\omega = C_4\omega^{-4} \tag{23}$$

These solutions are Kolmogorov spectra (3), (4).

Since the equation (17) preserves the momentum, it must have Kolmogorov solution, carrying the momentum to small scales. From dimensional consideration it has a form

$$n_k = f(\phi)k^{-\frac{25}{6}} \tag{24}$$

where $f(\phi)$ is some unknown function of the angle , which cannot be found analytically so far. Solution (24) is realized in the case when there is the source of the momentum, but no source of the energy in the region of small k. This situation is non-physical and therefore one can't get much use from the solution (24). The generic Kolmogorov solution, corresponding to given fluxes of both the energy and the momentum, is much more important. This solution is anisotropic and non-power-like. It has the form

$$n_k = Ck^{-4}F(\phi, k) \tag{25}$$

where $F(\phi, k)$ is so far unknown function of ϕ and k. One can guess that its dependence on k is "slow". In the limit of large k this function should has the form (Kats and Kontorovich, 1971) :

$$F(\phi, k) = 1 + a\frac{S}{P}\cos\phi\sqrt{\frac{g}{k}} \tag{26}$$

where S is the momentum flux, P is the energy flux and a is a constant.

Complexity of the equation (9) is the compelling factor for construction of the simplified models of four-wave interaction. The most popular model is the WAM model. In this model, five-dimensional variety of resonances satisfying conditions (1)-(2) is contracted to 2-dimensional manifold describing the resonance of a single type

$$\vec{k_1} = \vec{k}, \quad \vec{k_2} = (1 + \hat{s})\vec{k}, \quad \vec{k_3} = (1 - \hat{s})\vec{k} \tag{27}$$

where $\hat{s}$ is certain linear operator on the k-plane.

In WAM model, integral equation (9) transforms into nonlinear difference equation. The most basic properties of this equation stay the same. In particular, the stationary WAM equation has the same Kolmogorov solutions (22), (23).

The most weak point of the WAM approximation is an ambiguity in the choice of the basic resonance. Actually, there is no particular reasons for preferring of the resonance (27) over others. Some sort of the optimization of the choice of the basic resonance could essentially improve this "difference" model.

3 Differential approximation

In this article we replace the integral equation (9) by nonlinear diffusive equation of the second order. In the contrary to the difference models, the differential model can be constructed in the unique way. Our model is quite convenient for numerical simulation and gives quite reasonable description of the four-wave interaction. Differential approximation in the theory of the four -wave interaction was offered independently in the papers of Iroshnikov (1985) and Hasselmann at al. (1985). More simple derivation of this equation was done in the article of Balk and Zakharov (1988). Later, the differential equation was used in the work of Dyachenko at al. (1992).

Rigorously speaking, the integral operator in (9) can be replaced by the differential operator only when $T_{kk_1k_2k_3} \neq 0$ and the wave vectors k_1, k_2, k_3 are close to k. In this case, the differential approximation can be obtained using the expansion of $n_{k_1}, n_{k_2}, n_{k_3}$ into the Taylor series in the vicinity of the points $k_i = k$. This cumbersome procedure was done by Hasselmann and

Hasselmann (1985) who obtained nonlinear differential equation of the fourth order.

We, following the work of Balk and Zakharov (1988), offer the more simple way of derivation of this equation. First, we put $g = 1$ and introduce the polar coordinates $(\phi, k = \omega^2)$ on K-plane. In these coordinates, eq. (8) reads

$$\frac{\partial n(\phi,t)}{\partial t} = 32 \int |T(\omega,\omega_1,\omega_2,\omega_3,\phi,\phi_1,\phi_2,\phi_3)|^2 \cdot\delta(\omega+\omega_1-\omega_2-\omega_3)\delta(\omega^2\cos\phi+\omega_1^2\cos\phi_1 -\omega_2^2\cos\phi_2-\omega_3^2\cos\phi_3)\delta(\omega^2\sin\phi+\omega_1^2\sin\phi_1 -\omega_2^2\sin\phi_2-\omega_3^2\sin\phi_3)(n_1n_2n_3+nn_2n_3 -nn_1n_2-nn_1n_3)d\omega_1 d\omega_2 d\omega_3 \quad (28)$$

This equation preserves the following quantities

$$N = \int \omega^3 n(\omega,\phi)d\phi d\omega \quad (29)$$

$$E = \int \omega^4 n(\omega,\phi)d\phi d\omega \quad (30)$$

$$R_1 = \int \omega^5 \cos\phi\, n(\omega,\phi)d\phi d\omega \quad (31)$$

$$R_2 = \int \omega^5 \sin\phi\, n(\omega,\phi)d\phi d\omega \quad (32)$$

It has the following stationary thermodynamic solutions

$$n = \frac{1}{C_1 + C_2\omega + C_3\omega^2\cos\phi + C_4\omega^2\sin\phi} \quad (33)$$

where C_1, C_2, C_3, C_4 are the arbitrary constants. Let us introduce the differential operator

$$L = \frac{1}{2}\frac{\partial^2}{\partial\omega^2} + \frac{1}{\omega^2}\frac{\partial^2}{\partial\phi^2} \quad (34)$$

One can see that the equation

$$\frac{\partial n}{\partial t} = \frac{1}{\omega^3}Lu \quad (35)$$

preserves all four quantities (29)-(32) if u is periodic function bounded at $\omega = 0$, satisfying the condition $u \to 0$ at $\omega \to \infty$.

From the other hand, one can check that

$$L\frac{1}{n} = 0 \quad (36)$$

if n is given by (33).

Since $T_{kk_1k_2k_3} \sim k^3$, equation (28) can be roughly estimated as

$$\frac{\partial n}{\partial t} \simeq \omega^{12-1-2-2+9}n^3 = \omega^{19}n^3 \quad (37)$$

Let us consider the fours-order differential equation

$$\frac{\partial n}{\partial t} = \frac{C}{\omega^3}Ln^4\omega^{26}L\frac{1}{n} \quad (38)$$

This equation can be treated as a differential model for kinetic equation (28). Indeed, it preserves the same constants of motion, has the same thermodynamic solutions and the same dimensional estimate (37) as the exact equation (8). It is uniquely constructed up to the constant C.

We have to stress that the equation (38) is heuristic. It cannot be derived from the exact kinetic equation (8)-(9) for any realistic $T_{kk_1k_2k_3}$. Therefore, if the differential model (38) (or more simple one) is applied for description of the real situation, there is absolutely no way to find the constant C analytically. It has to be found from the comparison of the physical and numerical experiment. This fact was first mentioned by Hasselmann and Hasselmann (1985).

The equation (38) satisfies the H-theorem. Let us define the entropy as

$$H = \int \ln n_k d\vec{k} = 2\int \omega \ln n d\phi d\omega$$

From (38) one gets

$$\frac{dH}{dt} = 2C\int n^4\omega^{26}\left(L\frac{1}{n}\right)^2 d\omega d\phi > 0$$

This is an additional argument in favor of this equation.

The stationary equation (17) in the simplest axially-symmetric case takes a form

$$\frac{1}{\omega^2}\frac{\partial^2}{\partial\omega^2}n^4\omega^{26}\frac{\partial^2}{\partial\omega^2}\frac{1}{n} = 0 \quad (39)$$

Looking for power-like solutions of the equation (39), one obtains

$$n = \omega^{-y} \qquad y = y_1, y_2, y_3, y_4 \quad (40)$$

$$y_1 = 0, \quad y_2 = 1, \quad y_3 = \frac{23}{2} \quad y_4 = 8 \quad (41)$$

Equation (39) has four power-like solutions

$$n_1 = const, \quad n_2 = \frac{1}{\omega}, \quad n_3 = \omega^{-\frac{23}{3}}, \quad n_4 = \omega^{-8} \quad (42)$$

First two solutions are thermodynamic, the other two are Kolmogorov spectra (22),(23).

Differential equation (38) coincides with the equations obtained earlier by Iroshnikov (1985) and Hasselmann and Hasselmann (1985).

4 Diffusion approximation

Equation (38) is good for the description of both thermodynamic and Kolmogorov solutions. It can be essentially simplified if we are interested only in turbulent solutions of Kolmogorov type. In accordance with (25)

$$n_\omega = \omega^{-8} F(\phi,\omega) \tag{43}$$

Since $F(\phi,\omega)$ is a slow function of ω, one gets approximately

$$L\frac{1}{n} = \left(\frac{1}{2}\frac{\partial^2}{\partial\omega^2} + \frac{1}{\omega^2}\frac{\partial^2}{\partial\phi^2}\right)\frac{\omega^8}{F(\phi,\omega)} \simeq \frac{28}{F}\omega^6 \simeq \frac{28}{n\omega^2} \tag{44}$$

This calculation prompts us to replace (38) by more simple equation

$$\frac{\partial n}{\partial t} = \frac{a}{\omega^3} L n^3 \omega^{24} = \frac{a}{\omega^3}\left[\frac{1}{2}\frac{\partial^2}{\partial\omega^2} + \frac{1}{\omega^2}\frac{\partial^2}{\partial\phi^2}\right] n^3\omega^{24} \tag{45}$$

where a is new indefinite constant. This is a nonlinear diffusion equation. It preserves the integrals (29)-(32) and has the correct dimensional estimate (37). One can easily find its stationary solutions. They are given by the equation

$$LU = \left(\frac{1}{2}\frac{\partial^2}{\partial\omega^2} + \frac{1}{\omega^2}\frac{\partial^2}{\partial\omega^2}\right) U = 0, \quad U = a n_1^3 \omega^{24} \tag{46}$$

A general periodic solution of this equation can be presented in the form

$$\begin{aligned} u &= q_0 + q_1\omega + (\frac{a_1}{\omega} + b_1\omega^2)\cos(\phi-\phi_0) \\ &+ \omega^{\frac{1}{2}}\sum_{n=2}^{\infty}(a_n\omega^{-\lambda_n} + b_n\omega^{\lambda_n})\cos n(\phi-\phi_n), \\ \lambda &= \sqrt{\frac{1}{4}+2n^2} \end{aligned} \tag{47}$$

To find a physical interpretation of this solution, one should calculate fluxes of the conservative quantities (29)-(32). Let us denote

$$\begin{aligned} Q &= \int_0^\omega d\omega\int_0^{2\pi} d\phi\,\omega^3\dot{n}(\omega,\phi) = \int_0^\omega d\omega\int_0^{2\pi} d\phi Lu \\ &= \frac{1}{2}\frac{\partial}{\partial\omega}\langle u\rangle|_0^\infty \\ \langle u\rangle &= \int_0^{2\pi} u d\phi \end{aligned} \tag{48}$$

From the physical consideration, one has to assume that $u \to 0$ at $\omega \to 0$ together with all its derivatives. Hence

$$Q = \frac{\partial}{\partial\omega}\langle u(\omega,\phi)\rangle = \pi q_1 \tag{49}$$

Thus q_1 is the flux of the wave action coming from infinity.

In the same way one can find

$$P = -\int_0^\omega d\omega\int_0^{2\pi} d\phi\ \omega^4\dot{n}(\omega,\phi) = \pi q_0 \tag{50}$$

where P is the flux of the energy to infinity.

A little bit more complicated calculation gives

$$S = -\int_0^\omega d\omega\int_0^{2\pi} d\phi\ \omega^5 cos\phi\ \dot{n}(\omega,\phi) = 3\pi a_1 \tag{51}$$

where S is the flux of the longitudinal momentum to infinity.

Thus the special stationary solution

$$U = \frac{1}{\pi}(P + Q\omega + \frac{1}{3}\frac{S}{\omega}\cos\phi) \tag{52}$$

can be easily interpreted. It is the Kolmogorov spectrum, corresponding to constant flux of the wave action from infinity Q and constant fluxes of energy P and momentum S from $\omega = 0$.

A general Kolmogorov solution has a form

$$n_\omega = \frac{1}{(\pi a)^{\frac{1}{3}}\omega^8}\left(P + Q\omega + \frac{1}{3}\frac{S}{\omega}\cos\phi\right)^{\frac{1}{3}} \tag{53}$$

If the flux of wave action from infinity is absent, equation (53) gives the expression for $F(\phi,\omega)$:

$$F(\phi,\omega) = \frac{1}{\pi^{\frac{1}{3}}}\left(P + \frac{1}{3}\frac{S}{\omega}\cos\phi\right)^{\frac{1}{3}} \tag{54}$$

It is the "slow function" in comparison to ω^{-8}.

If $S \neq 0$, Kolmogorov solution (53) becomes negative for small enough ω. It can not be applied in this range of frequencies. Asymptotically, at $\omega \gg \frac{1}{3}\frac{S}{P}$, this solution becomes isotropic. At infinity

$$F(\phi,\omega) \simeq \left(\frac{P}{a\pi}\right)^{\frac{1}{3}}\left(1 + \frac{S}{g\omega}\cos\phi\right) \tag{55}$$

Referring to the formula (26) one can find that in this model $a = \frac{1}{9}$.

The other stationary solutions have no simple physical interpretation.

5 Numeral simulation

We solved the equation

$$\frac{\partial n}{\partial t} = \frac{a}{\omega^3} L n^3 \omega^{24} + \Gamma_\omega n \tag{56}$$

numerically, assuming that the dumping coefficient Γ_ω is the sum of two parts

$$\Gamma_\omega = \Gamma_1 + \Gamma_2 \tag{57}$$

Coefficient Γ_1 was nonzero in all experiments. It consists of high-frequency hyper-viscosity Γ_h and strong damping Γ_l in low frequency region:

$$\Gamma_l(\omega) = -C_l(\omega - \omega_0)^2, \quad \omega_0 = 4, \quad \omega \le \omega_0 \tag{58}$$

$$\Gamma_h(\omega) = -C_h(\frac{\omega}{\omega_1} - 1)^2, \quad \omega_1 = 98, \quad \omega \ge \omega_1 \tag{59}$$

where C_l and C_h are the positive constants. Presence of the low-frequency damping is necessary for the numerical reasons.

Coefficient Γ_2 includes forcing due to external physical mechanisms, and the damping due to the wave-breaking.

We studied the following variants of the forcing:

Case A. Symmetric forcing

$$\Gamma_2(\omega) = C_p \delta(\omega - 8), \ C_p > 0$$

Case B. Point forcing

$$\Gamma_2(\omega) = C_p \delta(\omega - 8)\delta(\phi), \ C_p > 0$$

Case C. "Realistic" forcing

This point should be explained. There is no universal agreement in the wave-modeling community about the form of the source of the energy transmitted from wind to the surface waves. One of the commonly used expression for Γ_f is

$$\Gamma_f(\omega) = \begin{cases} \alpha \frac{\rho_{atm}}{\rho_{water}} \omega (\frac{v}{c} - 1)\cos\phi, & c > v \\ 0, & c < v \end{cases} \tag{60}$$

Here v is wind velocity, $c = \frac{\omega}{k} = \frac{g}{\omega}$ is phase velocity, α is dimensionless constant.

Therefore we used the following parameters of forcing corresponding to "realistic" situation:

$$\Gamma_2(\omega, \phi) = \Gamma_f - C_b \omega^2$$

$$\Gamma_f(\omega) = \begin{cases} C_1^f(\omega - 10)\omega\cos\phi, & 10 < \omega < 94 \\ C_2^f e^{-(\frac{\omega - 94}{2.5})^2}\cos\phi, & 94 < \omega < 98 \end{cases}$$

where C_b, C_1^f and C_2^f are positive constants.

This means that in the region $10 < \omega < 94$ $\Gamma_f(\omega)$ is chosen to get the accordance with (60), while in the interval $94 < \omega < 98$ $\Gamma_f(\omega)$ is chosen to provide a smooth transition from region of forcing to the region of high-frequency viscosity.

Equation (56) is not convenient for direct numerical simulation due to the presence of the numerical instabilities appearing from "simple-minded" discretizations. It can be regularized and effectively solved by introducing a new variable $y = (\omega^8 n)^3$:

$$\frac{\partial y}{\partial t} = P(\omega, y)\frac{\partial^2 y}{\partial \omega^2} + Q(\omega, y)\frac{\partial^2 y}{\partial \phi^2} + 3\Gamma_\omega y \tag{61}$$

where

$$P(\omega, y) = \frac{3}{2} a \omega^5 y^{\frac{2}{3}}, \quad Q(\omega, y) = 3a\omega^3 y^{\frac{2}{3}}$$

are nonlinear diffusion coefficients.

This "classical" diffusion equation is solved economically with the help of implicit numerical scheme by simple recursion in the direction of ω and cyclical recursion in the direction of ϕ. The efficiency of the algorithm is illustrated by the fact that it takes just a few dozen of minutes to calculate the development of the turbulence from the random noise initial conditions to stationary state using Pentium 133 MHz CPU on the grid of 128×32 nodes of (ω, ϕ) domain.

We started with the "free" case ($\Gamma_\omega = 0$) putting as an initial data the JONSWAP spectrum:

$$n(\omega, \phi) = -\omega^5 e^{-\frac{5}{4}(\frac{\omega}{\omega_p})^{-4}} \gamma^{e^{-\frac{(\omega - \omega_p)^2}{2\sigma^2\omega_p^2}}} cos^4\phi$$

where $\omega_p = 2\pi f_m$, $f_m = 0.144Hz$, $\gamma = 3.3$, $-\frac{\pi}{2} < \phi < \frac{\pi}{2}$, $\sigma = 0.07$ for $\omega < \omega_p$ and $\sigma = 0.09$ for $\omega > \omega_p$

Fig.1 presents $\frac{\partial n}{\partial t}|_{t=0}$ plotted together with the results of Resio and Perrie (RP), Masuda (RIAM) and WAM method. It is seen that the diffusion approximation results are close to the results of first two groups and essentially differ from the DIA WAM results.

In the symmetric *Case A* (see Fig.2, 3) there was an ample range of frequency with $\Gamma = 0$ (transparency window). Stationary isotropic solution in this case is

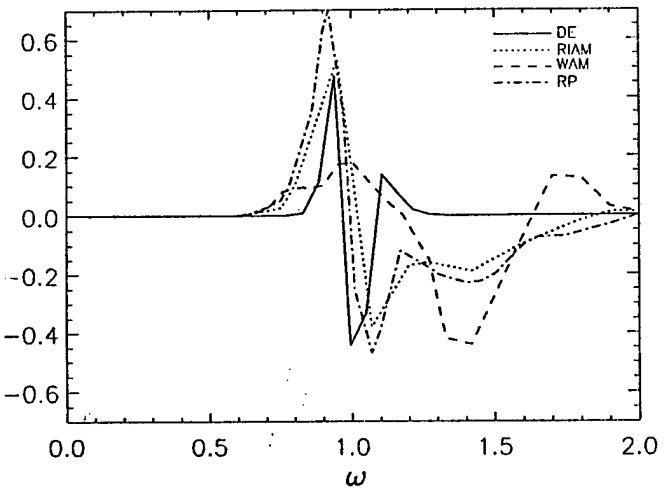

Fig. 1. Comparison of the collision terms for diffusion approximation with RIAM, WAM and RP data taken from Komatsu and Masuda (1996).

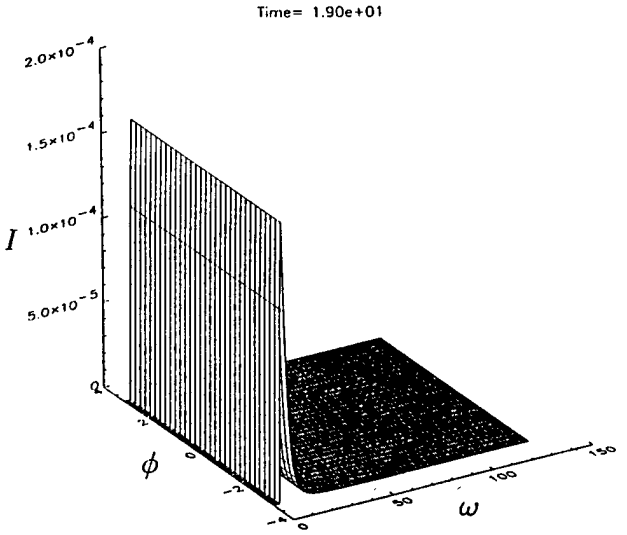

Fig. 2. Energy density $I = \omega^4 n(\omega, \phi)$ for symmetrical forcing at $\omega = 8$

$$y = A\omega + B \tag{62}$$

where $A < 0$ is the flux of the wave action to large frequencies. The stationary spectrum was established rather soon.

In the case of "point forcing" (see Fig.4, Fig.5 and Fig.6; $\langle\rangle$ means angle averaging), the stationary spectrum is essentially anisotropic. It was reached very soon as well.

An essential anisotropy also exists in the case of "realistic" forcing (see Fig.7, Fig.8).

It is important to note that in all three abovementioned cases the angle-averaged spectrum exhibits ω^{-4} Kolmogorov law despite angular dependence in the last two cases. Temporal evolution of the "realistic" spectrum in the form of the wave propagating toward low ω is presented on Fig.9.

Fig.10, Fig.11 and Fig.12 show temporal behavior of the integrals N,E and average frequency $\omega = \frac{E}{N}$ in the "realistic" case.

Fig.13, Fig.14, Fig.15 show temporal behavior of the same functions for the case $\Gamma_2 = 0$. We used as an initial condition the stationary spectrum obtained for $\Gamma_2 \neq 0$ case.

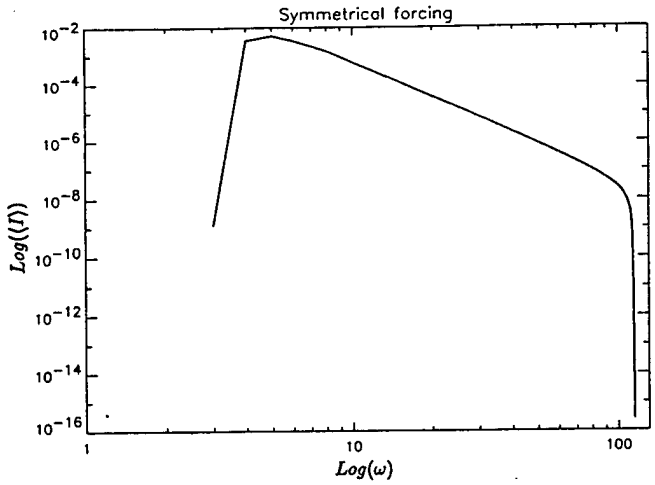

Fig. 3. $Log(\langle I(\log(\omega))\rangle)$ for symmetrical forcing at $\omega = 8$

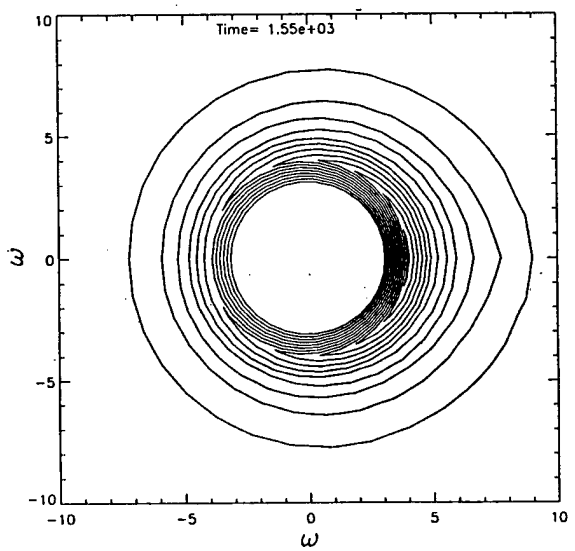

Fig. 4. Line levels for $I(\omega, \phi)$ - point forcing at $\omega = 8$, $\phi = 0$

6 Conclusion

The diffusion model of four-wave interaction is the most simple model presenting the major feature of the physical phenomenon under investigation – conservation of the constants of motion and righteous scaling. It is very convenient and effective for numerical simulation. The numerical experiments show that this model describes

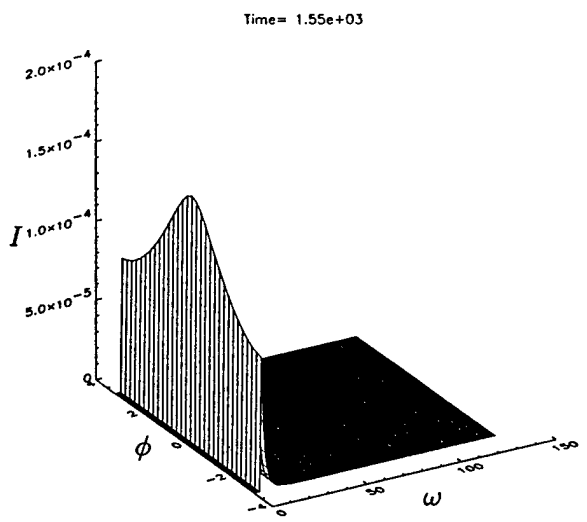

Fig. 5. Energy density $I = \omega^4 n(\omega, \phi)$ for point forcing at $\omega = 8$, $\phi = 0$

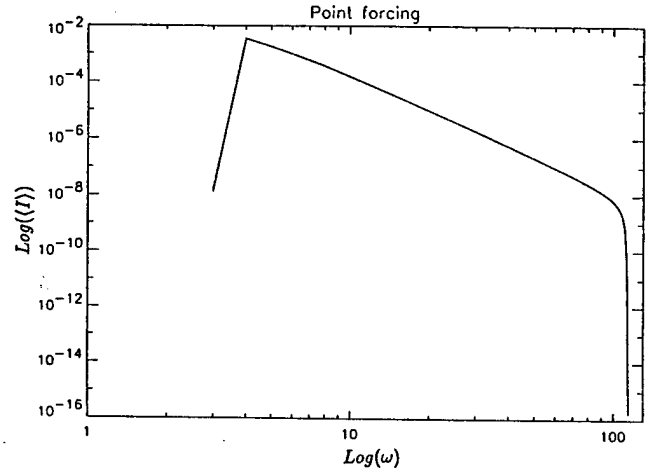

Fig. 6. $\log(\langle I(\log(\omega))\rangle)$ for point forcing at $\omega = 8$, $\phi = 0$

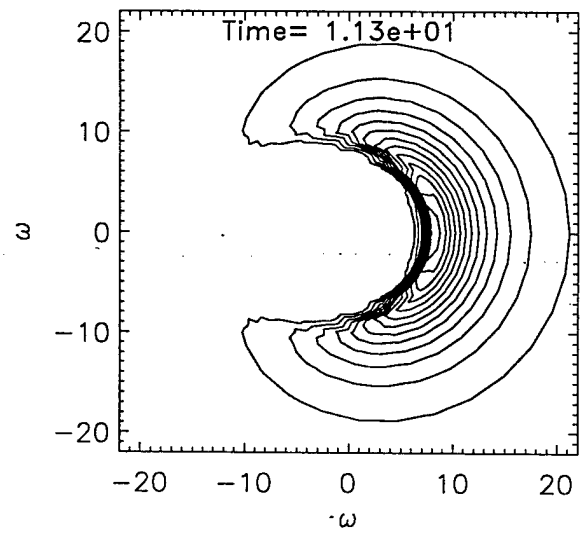

Fig. 7. Same as Fig.4 for "realistic" case

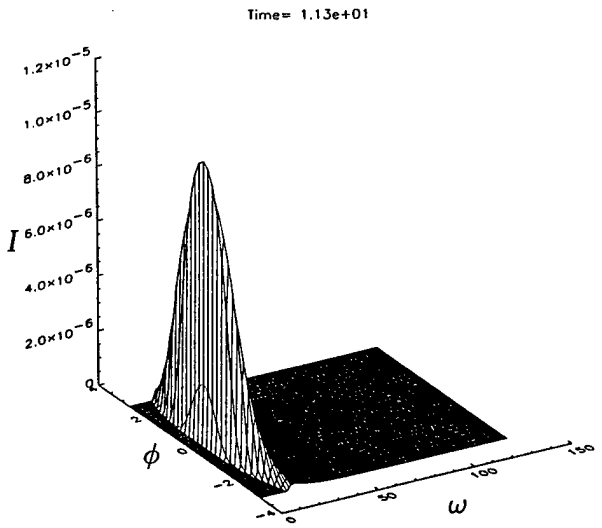

Fig. 8. Same as Fig.5 for "realistic" case

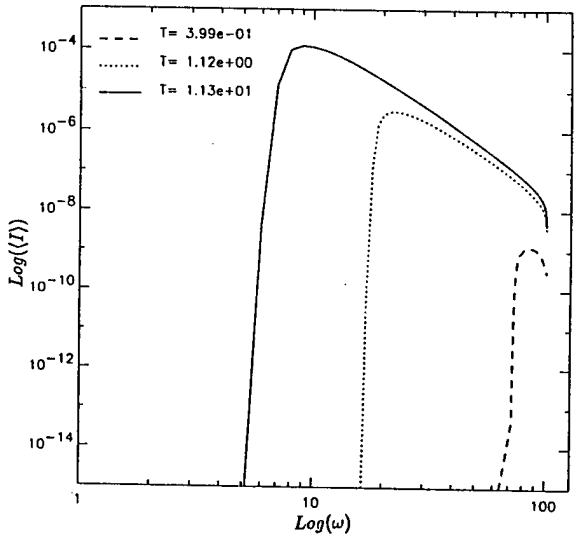

Fig. 9. $\log(\langle I(\log(\omega))\rangle)$ for "realistic" forcing for three different time moments

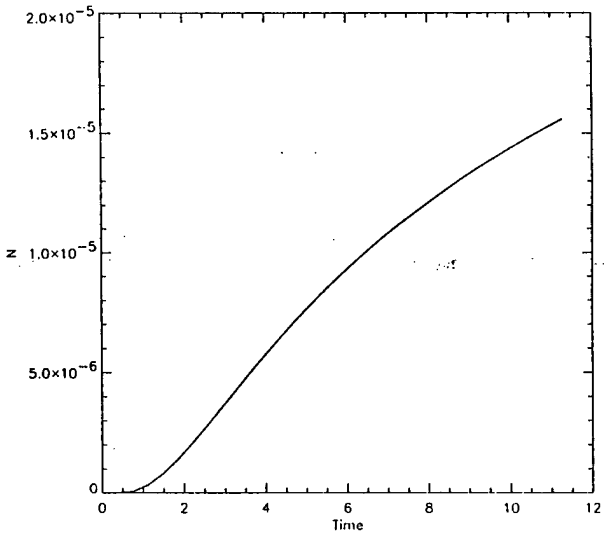

Fig. 10. Temporal behavior of integral N in the "realistic case"

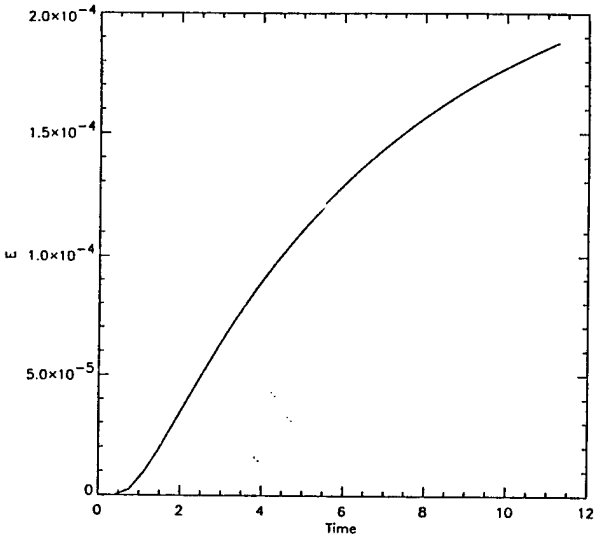

Fig. 11. Temporal behavior of integral E in the "realistic case"

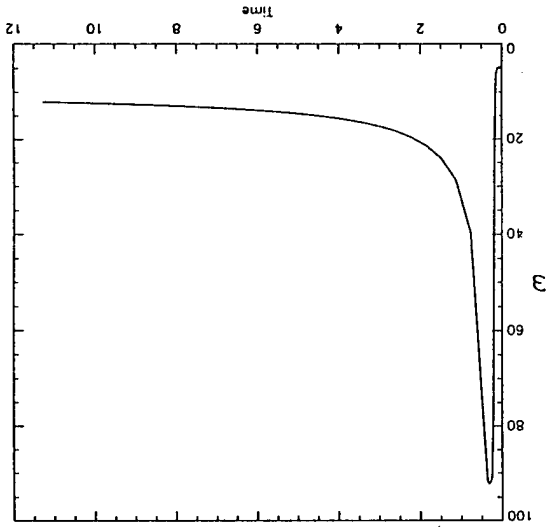

Fig. 12. Temporal behavior of the averaged frequency in the "realistic case"

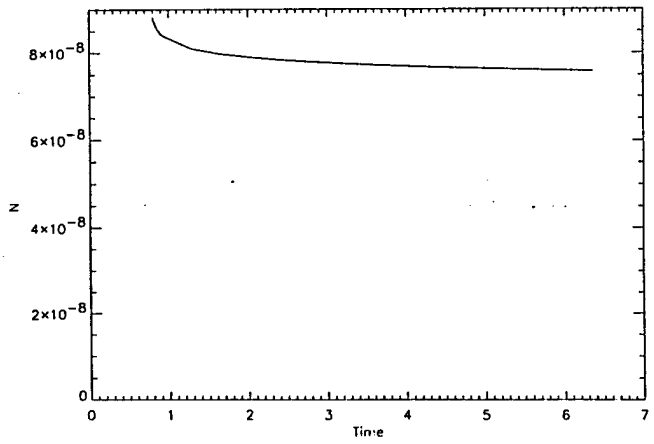

Fig. 13. Temporal behavior of integral N in the $\Gamma_2 \neq 0$ case

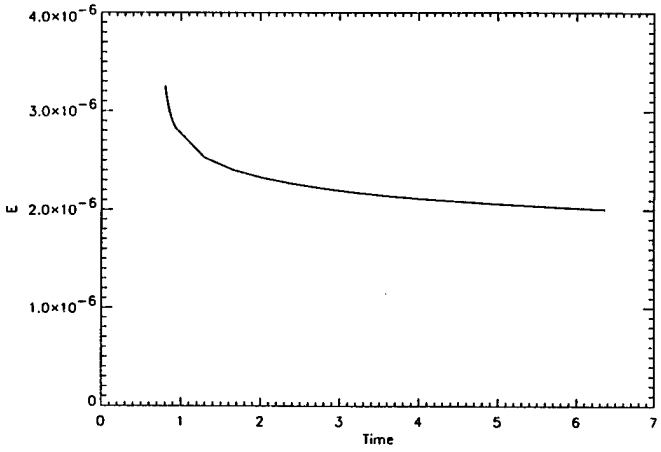

Fig. 14. Temporal behavior of integral E in the $\Gamma_2 \neq 0$ case

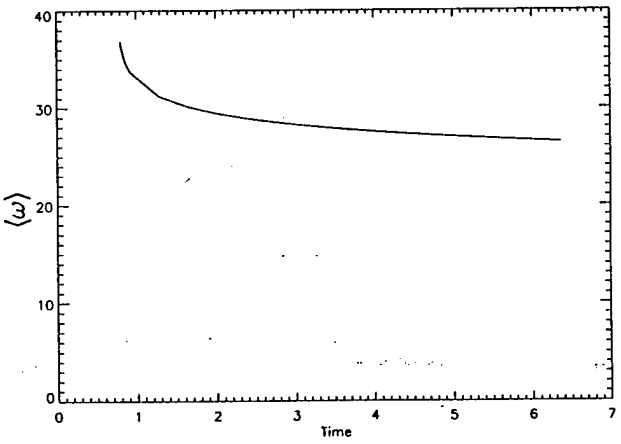

Fig. 15. Temporal behavior of the averaged frequency in the $\Gamma_2 \neq 0$ case

evolution of the wave spectra reasonably well and can be used for development of the new generation of wave-prediction models. It would be desirable to compare the new model with numerous accumulated data of the field observations and laboratory experiments. To do this we should include in the equation (35) the dependence on the spatial coordinate x (the fetch). The new equation is

$$\frac{\partial n}{\partial t} + \frac{\cos\phi}{2\omega}\frac{\partial n}{\partial x} = \frac{1}{\omega^3}Lu + \Gamma(\omega,\phi)n \qquad (63)$$

The numerical simulation of the equation (63) is separate and nontrivial problem. We hope to present the results of the simulation of this equation in the next article.

Acknowledgements. We would like to thank the referee who has made valuable remark about the H-theorem in the differential model.

This work was supported by the Office of Naval Research (ONR grant N 00014-98-1-0070). We are using this opportunity to acknowledge this foundation.

References

Balk A. M., Zakharov V. E., Stability of weak turbulent Kolmogorov spectra. Plasma theory and nonlinear and turbulent processes in physics, *Proc. Inter. Workshop*, Kiev, April 1987, World Scientific, Singapore, 359–376, 1988.

Donelan M. , Hamilton and W. H. Hui, Directional spectra of wind-generated waves, *Phil. Trans. Roy. Soc.*, London, *A 315*, 509–562, 1985.

Dyachenko S., Newell A., Pushkarev A. and Zakharov V., Optical turbulence, weak turbulence condensates and collapsing filaments in the Nonlinear Schroedinger Equation, *Physica D*, *57*, 96–100, 1992.

Hasselmann, K., On the nonlinear energy transfer in gravity-wave spectrum. Part 1. General theory. *Journ. of Fl. Mech.*, *12*, 481–500, 1962.

Hasselmann B. and Hasselmann K., Computations and parameterizations of the nonlinear energy transfer in gravity wave spectrum. Part 1. *J. Phys. Oceanogr.*, *15*, 1369–1377, 1985.

Hasselmann S., Hasselmann K., Allender J. H. and Bernett T.P, Computations and parameterizations of the nonlinear energy transfer in gravity-wave spectrum. Part II, *J. Phys. Oceanography*, *15*, 1378–1391, 1985.

Iroshnikov R. S., Possibility of a non-isotropic spectrum of wind waves by their weak nonlinear interaction, *Dokl.Acad.Nauk SSSR*, *280*, 6, 1331–1325, 1985. (English transl. *Soviet Phys. Dokl.*, *30*, 126 – 128, 1985)

Kats A. V., Kontorovich V. M. Drifting stationary solutions in the weak turbulence theory, *Pis'ma Zh.Eksper.Teoret. Fiz.. 14*, N 6, 392 – 395, 1971.

Komatsu K., Masuda A, A new scheme of nonlinear energy transfer among the wind waves: RIAM method - Algorithm and Performance, *J. of Oceanography*, *52*, 509–537, 1996.

Lavrenov, I. V., Nonlinear interaction of waves rips, *Izv. USSR AS J. fizika atmosfery i okeana*, *27*, N 4, 438–447,1991.

Masuda A., Nonlinear energy transfer between wind waves, *J. of Physical Oceanography*, *23*, 1249–1258, 1980

Resio D., Perrie W., A numerical study of nonlinear energy fluxes due to wave-wave interactions, *J.Fl.Mech.*, *223*, 603–629, 1991.

Polnikov, V. G. Calculation of nonlinear energy transfer by surface gravitational waves spectrum, *Izv. USSR AS J.fizika atmosfery i okeana*, *25*, 1214 – 1225, 1989.

Phillips O. M., Spectral and statistical properties of the equilibrium range in wind-generated gravity waves, *J.Fluid Mech.*, 505–531, 1985.

Phillips, O. M. *The dynamic of the upper ocean.* Cambridge University Press, Cambridge.(2nd ed., 1977, 336 pp.).

Toba Y., Local balance in the air-sea boundary processes. III. On the spectrum of wind waves, *J. Oceanogr. Soc. Japan*, *29*, 209–220, 1973.

Zakharov V. E. Stability of periodic waves of finite amplitudes on a surface of deep fluid, *J. Appl. Mech. Tech. Phys.*, *2*, 190 – 198, 1968.

Zakharov V. E., Inverse and direct cascades in the wind-driven surface turbulence and wave-breaking. Breaking waves (Banner M. and Grimshaw eds). IUTAM symposium. Sydney, Australia, Springer-Verlag, Heidelberg, Berlin, 69–91, 1992.

Zakharov V. E., Filonenko N. N, The energy spectrum for stochastical oscillation of fluid surface, *Doklady Acad.Nauk SSSR*, *170*, 1292–1295, 1966 (in Russian)

Zakharov V. E., Zaslavskii M. M., The kinetic equation and Kolmogorov spectra in the weak-turbulence theory of wind waves, *Izv.Atm.Ocean.Phys.*, *18*, 747–753, 1982.

Zakharov V. E., Falkovich, G., Lvov, V., *Kolmogorov spectra of wave turbulence*, Springer-Verlag, Berlin, 1992.

Webb D.J. Nonlinear transfer between sea waves, *Deep-sea Res.*, *25*, 279 – 298, 1978.

ISSN : 0997-7546
EJBFEV

EUROPEAN JOURNAL OF MECHANICS

B/FLUIDS

1999 VOL. 18 □ N° 3
May - June

Special Issue
Three-Dimensional Aspects of Air-Sea Interaction

ELSEVIER

EUROPEAN JOURNAL OF MECHANICS
B/FLUIDS

An official medium of publication for EUROMECH – 'European Mechanics Society'

The manuscripts should be sent to one of the Editors-in-Chief

The European Journal of Mechanics is abstracted and/or indexed in:

Applied Mechanics Reviews, Current Contents (PC & ES), Mechanics Contents, Mathematical Reviews, Inspec Science Abstracts, Pascal Database, Current Mathematical Publications, Math Sci., Current Contents (EC & T), Science Citation Index, Sci Search, Research Alert, Materials Science Citation Index, Zentralblatt Für Mathemathik.

ÉDITIONS ELSEVIER
23, rue Linois
75724 Paris cedex 15, France
http://www.elsevier.fr
A member of Elsevier Science
Éditions scientifiques et médicales Elsevier
SAS au capital de 80 250 000 F - 399 113 877 RCS Paris

HARD SCIENCES DEPARTMENT
Tel.: 33 1 45 58 90 67 Fax: 33 1 45 58 94 21
Desk editor: Christine Gray Tel.: +33 1 45 58 98 63, c.gray@elsevier.fr
http://www.elsevier.fr

SUBSCRIPTIONS Tel.: +33 1 45 58 90 67 Fax: +33 1 45 58 94 24. abt2@elsevier.fr
Subscription information 1999 – ***EJM-B/Fluids*** – Vol 18 – 6 issues – ISSN 0997-7546

	France	EU*	North, Central and South America	Rest of the world
EJM-B	❑ FF 2 551	❑ FF 2 605	❑ US$ 530	❑ FF 3 139
EJM-A	❑ FF 2 944	❑ FF 3 005	❑ US$ 592	❑ FF 3 506
EJM-A + EJM-B	❑ FF 4 946	❑ FF 5 048	❑ US$ 1 010	❑ FF 5 981

** Customers resident in the EU (European Union) are liable for VAT (2.1%). For tax exemption, VAT registration number must be indicated. Special rates apply for Euromech members, please contact your society. All prices include air delivery*

Address order and payment to: Éditions scientifiques et médicales Elsevier, 23, rue Linois, 75724 Paris cedex 15, Fra
• by cheque or credit card (CB, EuroCard, MasterCard or Visa) indicate number and expiration date
• by transfer: CCP Paris n° 30041 00001 1904540 H 020/70

Subscriptions begin 4 weeks after receipt of payment and start with the first issue of the calendar year. Back issues and volumes are available fr the publisher. Claims for missing issues should be made within 6 months of publication.

Imprimé en France par STEDI
1, bd Ney, F-75018 Paris
Dépôt légal : 5795 – À parution

Président-directeur général et directeur de la publication : Catherine L
Commission paritaire n° 0603 T 7
Périodicité : 6 nos

Eur. J. Mech. B/Fluids

STATISTICAL THEORY OF GRAVITY AND CAPILLARY WAVES ON THE SURFACE OF A FINITE-DEPTH FLUID

V. Zakharov[1]

[1]: *L. D. Landau Institute for Theoretical Physics, Moscow 117334, Russia, e-mail:* zakharov@itp.ac.ru

(Received 1 December 1998, accepted 2 February 1999)

1. Introduction

In many physical situations, the oscillations of the free surface of a fluid is are a random process in space and time. This is equally correct for ripples in a tea cup as well as for large ocean waves. In both cases the situation must be described by the averaged equations imposed on a certain set of correlation functions. The derivation of such equations is not a simple problem even on a "physical" level of rigor. It is especially important to determine correctly the conditions of applicability for a given statistical description. For some physical reasons they might happen to be narrow. In this article we discuss the statistical description of potential surface waves on the surface of an ideal fluid of finite depth. We will show that this problem becomes nontrivial in the limit of long waves, i.e. in the case of "shallow water".

The most common tool for the statistical description of nonlinear waves is a kinetic equation for squared wave amplitudes. We will call it the "wave kinetic equation". Sometimes it is called "Boltzmann's equation". This is not exactly accurate. In fact, a wave kinetic equation and Boltzmann's equation are the opposite limiting cases of a more general kinetic equation for particles obeying Bose-Einstein statistics like photons in stellar atmospheres or phonons in liquid helium. It was derived by Peierls in 1929 and can be found now in any textbook on the physics of condensed matter. Both Boltzmann's equation and the wave kinetic equation can be simply derived from the quantum kinetic equation. In spite of this fact, the wave kinetic equation was derived independently and almost simultaneously by Patric, Petchek and others (see Kadomtsev, 1965) in plasma physics and by K. Hasselmann (1962) for surface waves on deep water. It was done in the early sixties. Recall that Boltzmann derived his equation in the last century. Some authors call this equation after Hasselmann. We will use a more general term – "kinetic wave equation".

The pioneers starting from Boltzmann did not care about rigorously justifying the kinetic equation and finding the exact limits of its applicability. This work was done later. Boltzmann's equation was derived in a systematic and self-consisted way by Bogoliubov in 1949. The quantum kinetic equation was studied systematically by the use of diagram technique in fifties.

The wave kinetic equation can be derived and justified in a similar way. It is a lengthy procedure, thus in this short article we will give the final results of the diagram procedure - the kinetic equation and the limits of its validity. We will see that in the case of shallow water the limits are very restrictive.

2. Hamiltonian formalism

We will study weakly-nonlinear waves on the surface of an ideal fluid in an infinite basin of constant depth h. The vertical coordinate is

$$-h < z < \eta(\vec{r}), \qquad \vec{r} = (x, y). \tag{2.1}$$

The fluid is incompressible,

$$\operatorname{div} V = 0 \tag{2.2}$$

and the velocity V is a potential field,

$$V = \nabla\Phi, \tag{2.3}$$

where the potential Φ satisfies the Laplace equation

$$\Delta\Phi = 0 \tag{2.4}$$

under the boundary conditions

$$\Phi|_{z=\eta} = \Psi(\vec{r}, t), \qquad \Phi_z|_{z=-h} = 0. \tag{2.5}$$

Let us assume that the total energy of the fluid, $H = T + U$, has the following expressions for kinetic and potential energies:

$$T = \frac{1}{2}\int dr \int_{-h}^{\eta} (\nabla\Phi)^2 dz, \tag{2.6}$$

$$U = \frac{1}{2} g \int \eta^2 dr + \sigma \int (\sqrt{1 + (\nabla\eta)^2} - 1)\, dr. \tag{2.7}$$

Here g is the acceleration of gravity, and σ is the surface tension coefficient.

The Dirichlet-Neumann boundary problem (2.4)–(2.5) is uniquely solvable, thus the flow is defined by fixing η and Ψ. This pair of variables is canonical, so the equation of motion for η and Ψ takes the form (Zakharov, 1968):

$$\frac{\partial\eta}{\partial t} = \frac{\delta H}{\delta\Psi}, \quad \frac{\partial\Psi}{\partial t} = -\frac{\delta H}{\delta\eta}. \tag{2.8}$$

Taking their Fourier transform yields

$$\frac{\partial\eta}{\partial t} = \frac{\delta H}{\delta\Psi(\vec{k})^*}, \quad \frac{\partial\Psi(\vec{k})}{\partial t} = -\frac{\delta H}{\delta\eta(\vec{k})^*}. \tag{2.9}$$

Here $\Psi(\vec{k})$ is the Fourier transform of $\Psi(\vec{r})$:

$$\Psi(\vec{k}) = \frac{1}{2\pi}\int \Psi(\vec{r}) e^{-i\vec{k}\cdot\vec{r}} dr. \tag{2.10}$$

The Hamiltonian H can be expanded in Taylor series in powers of η:

$$H = H_0 + H_1 + H_2 + \cdots \tag{2.11}$$

Omitting the procedure of calculating H_i we present the final expressions for the first three terms in this expansion:

$$H_0 = \frac{1}{2}\int \{A_k|\Psi_k|^2 + B_k|\eta_k|^2\}dk, \qquad A_k = k\,\tanh(kh),\ B_k = g + \sigma\,k^2 \tag{2.12}$$

$$H_1 = \frac{1}{2(2\pi)}\int L^{(1)}(\vec{k}_1,\vec{k}_2)\,\Psi_{k_1}\,\Psi_{k_2}\,\eta_{k_3}\,\delta(\vec{k}_1+\vec{k}_2+\vec{k}_3)dk_1\,dk_2\,dk_3, \tag{2.13}$$

$$\begin{aligned} H_2 = {} & \frac{1}{2(2\pi)^2}\int L^{(2)}(\vec{k}_1,\vec{k}_2,\vec{k}_3,\vec{k}_4)\,\Psi_{k_1}\,\Psi_{k_2}\eta_{k_3}\,\eta_{k_4}\,\delta(\vec{k}_1+\vec{k}_2+\vec{k}_3+\vec{k}_4)\,dk_1\,dk_2\,dk_3\,dk_4 \\ & -\frac{\sigma^2}{8(2\pi)^2}\int (\vec{k}_1\vec{k}_2)(\vec{k}_3\vec{k}_4)\,\eta_{k_1}\,\eta_{k_2}\,\eta_{k_3}\,\eta_{k_4}\,\delta(\vec{k}_1+\vec{k}_2+\vec{k}_3+\vec{k}_4)\,dk_1\,dk_2\,dk_3\,dk_4\,. \end{aligned} \tag{2.14}$$

The formulas for $L^{(1)}$ and $L^{(2)}$ were found in 1970 by Zakharov and Kharitonov (see also Craig and Sulem 1992, Zakharov 1998). Here are their expressions:

$$L^{(1)}(\vec{k}_1,\vec{k}_2) = -(\vec{k}_1\vec{k}_2) - |k_1||k_2|\,\tanh k_1h\,\tanh k_2h, \tag{2.15}$$

and

$$\begin{aligned} L^{(2)}(\vec{k}_1,\vec{k}_2,\vec{k}_3,\vec{k}_4) = {} & \frac{1}{4}|k_1||k_2|\,\tanh k_1h\,\tanh k_2h \\ & \times \left\{-\frac{2|k_1|}{\tanh k_1h} - \frac{2|k_2|}{\tanh k_2h} + |\vec{k}_1+\vec{k}_3|\tanh|\vec{k}_1+\vec{k}_3|h\right. \\ & + \left.|\vec{k}_2+\vec{k}_3|\,\tanh|\vec{k}_2+\vec{k}_3|h + |\vec{k}_1+\vec{k}_4|\tanh|\vec{k}_1+\vec{k}_4|h + |\vec{k}_2+\vec{k}_4|\,\tanh|\vec{k}_2+\vec{k}_4|h\right\} \\ = {} & \frac{1}{4}A_1A_2\left\{-\frac{2k_1^2}{A_1} - \frac{2k_2^2}{A_2} + A_{1+3} + A_{2+3} + A_{1+4} + A_{2+4}\right\} \end{aligned} \tag{2.16}$$

One can introduce the normal variables a_k, a_k^*. They can be expressed as follows:

$$\begin{aligned} \eta_k &= \frac{1}{\sqrt{2}}\left(\frac{A_k}{B_k}\right)^{1/4}(a_k + a_{-k}^*) \\ \Psi_k &= \frac{i}{\sqrt{2}}\left(\frac{B_k}{A_k}\right)^{1/4}(a_k - a_{-k}^*) \\ a_k &= \frac{1}{\sqrt{2}}\left\{\left(\frac{B_k}{A_k}\right)^{1/4}\eta_k - i\left(\frac{A_k}{B_k}\right)^{1/4}\Psi_k\right\} \end{aligned} \tag{2.17}$$

The transformation $\Psi_k\,,\eta_k \to a_k$ is canonical. One can check that

$$\frac{\partial a_k}{\partial t} + i\,\frac{\delta H}{\delta a_k^*} = 0, \tag{2.18}$$

where the Hamiltonian H can be represented as the sum of two terms

$$H = H_0 + H_{int}. \tag{2.19}$$

For the first term we have

$$H_0 = \int \omega_k\,a_k\,a_k^*\,dk, \tag{2.20}$$

where $\omega_k > 0$ is defined by the formula

$$\omega_k = \sqrt{A_k B_k} = \sqrt{k \tanh(kh)\,(g + \sigma k^2)}. \tag{2.21}$$

The second term, H_{int}, is represented by the infinite series

$$H_{int} = \frac{1}{n!m!} \sum_{n+m\geq 3} \int V^{(n,m)}(\vec{k}_1, \dots, \vec{k}_n, \vec{k}_{n+1}, \dots, \vec{k}_{n+m}) a^*_{k_1} \cdots a^*_{k_n} a_{k_{n+1}} \cdots a_{k_{n+m}}$$

$$\times \delta(\vec{k}_1 + \cdots + \vec{k}_n - \vec{k}_{n+1} - \cdots - \vec{k}_{n+m})\, dk_1 \dots dk_{n+m} \tag{2.22}$$

In the case under consideration we have

$$V^{(n,m)}(P, Q) = V^{(m,n)}(Q, P), \tag{2.23}$$

where $P = (\vec{k}_1, \dots, \vec{k}_n)$ and $Q = (\vec{k}_{n+1}, \dots, \vec{k}_{n+m})$ are multi-indices.

For more general Hamiltonian systems (in the presence of wind, for instance), the coefficients $V^{(n,m)}(P, Q)$ are complex, and

$$V^{(n,m)}(P, Q) = V^{*(m,n)}(Q, P). \tag{2.24}$$

The condition (2.24) guarantees that the Hamiltonian H_{int} is real.

For surface waves the coefficients can be written as

$$\begin{aligned} V^{(1,2)}(\vec{k}, \vec{k}_1, \vec{k}_2) &= \frac{1}{4\pi\sqrt{2}} \left\{ \left(\frac{A_k\, B_{k_1}\, B_{k_2}}{B_k\, A_{k_1}\, A_{k_2}} \right)^{1/4} L^{(1)}(\vec{k}_1, \vec{k}_2) - \right. \\ &\left. - \left(\frac{B_k\, A_{k_1}\, B_{k_2}}{A_k\, B_{k_1}\, A_{k_2}} \right)^{1/4} L^{(1)}(-\vec{k}, \vec{k}_1) - \left(\frac{B_k\, B_{k_1}\, A_{k_2}}{A_k\, A_{k_1}\, B_{k_2}} \right)^{1/4} L^{(1)}(-\vec{k}, \vec{k}_2) \right\} \end{aligned} \tag{2.25}$$

$$\begin{aligned} V^{(0,3)}(\vec{k}, \vec{k}_1, \vec{k}_2) &= \frac{1}{4\pi\sqrt{2}} \left\{ \left(\frac{A_k\, B_{k_1}\, B_{k_2}}{B_k\, A_{k_1}\, A_{k_2}} \right)^{1/4} L^{(1)}(\vec{k}_1, \vec{k}_2) + \right. \\ &\left. + \left(\frac{B_k\, A_{k_1}\, B_{k_2}}{A_k\, B_{k_1}\, A_{k_2}} \right)^{1/4} L^{(1)}(\vec{k}, \vec{k}_1) + \left(\frac{B_k\, B_{k_1}\, A_{k_2}}{A_k\, A_{k_1}\, B_{k_2}} \right)^{1/4} L^{(1)}(\vec{k}, \vec{k}_2) \right\} \end{aligned} \tag{2.26}$$

In this paper we will use only one coefficient of fourth order $V^{(2,2)}(P, Q)$. After a simple calculation we can obtain the following expression for this coefficient:

$$\begin{aligned} V^{(2,2)}(\vec{k}_1, \vec{k}_2, \vec{k}_3, \vec{k}_4) &= -\frac{1}{2\pi^2} \left\{ \tilde{L}^{(2)}(-\vec{k}_1, -\vec{k}_2, \vec{k}_3, \vec{k}_4) + \tilde{L}^{(2)}(\vec{k}_3, \vec{k}_4, -\vec{k}_1, -\vec{k}_2) - \tilde{L}^{(2)}(-\vec{k}_1, \vec{k}_3, -\vec{k}_2, \vec{k}_4) \right. \\ &\left. - \tilde{L}^{(2)}(-\vec{k}_1, \vec{k}_4, -\vec{k}_2, \vec{k}_3) - \tilde{L}^{(2)}(-\vec{k}_2, \vec{k}_3, -\vec{k}_1, \vec{k}_4) - \tilde{L}^{(2)}(-\vec{k}_2, \vec{k}_4, -\vec{k}_1, \vec{k}_3) \right\} \\ &- \frac{\sigma^2}{16\pi^2} \left\{ (\vec{k}_1, \vec{k}_2)(\vec{k}_3, \vec{k}_4) + (\vec{k}_1, \vec{k}_3)(\vec{k}_2, \vec{k}_4) + (\vec{k}_1, \vec{k}_4)(\vec{k}_2, \vec{k}_3) \right\} \left(\frac{A_{k_1}\, A_{k_2}\, A_{k_3}\, A_{k_4}}{B_{k_1}\, B_{k_2}\, B_{k_3}\, B_{k_4}} \right)^{1/4}, \end{aligned} \tag{2.27}$$

where

$$\tilde{L}^{(2)}(\vec{k}_1, \vec{k}_2, \vec{k}_3, \vec{k}_4) = \frac{1}{4} \left(\frac{B_{k_1}\, B_{k_2}\, A_{k_3}\, A_{k_4}}{A_{k_1}\, A_{k_2}\, B_{k_3}\, B_{k_4}} \right)^{1/4} L^{(2)}(\vec{k}_1, \vec{k}_2, \vec{k}_3, \vec{k}_4). \tag{2.28}$$

We will not discuss the five-wave processes systematically. This makes it possible to use the following approximation for the Hamiltonian:

$$\begin{aligned} H &= \int \omega_k |a_k|^2 dk + \frac{1}{2}\int V^{(1,2)}(\vec{k},\vec{k}_1,\vec{k}_2)(a_k\, a^*_{k_1}\, a^*_{k_2} + a^*_k\, a_{k_1}\, a_{k_2})\,\delta(\vec{k}-\vec{k}_1-\vec{k}_2)\,dk\,dk_1\,dk_2 + \\ &+\frac{1}{6}\int V^{(0,3)}(\vec{k},\vec{k}_1,\vec{k}_2)(a_k\, a_{k_1}\, a_{k_2} + a^*_k\, a^*_{k_1}\, a^*_{k_2})\,\delta(\vec{k}+\vec{k}_1+\vec{k}_2)\,dk\,dk_1\,dk_2 + \\ &+\frac{1}{4}\int V^{(2,2)}(\vec{k},\vec{k}_1,\vec{k}_2,\vec{k}_3)\, a^*_k\, a^*_{k_1}\, a_{k_2}\, a_{k_3}\,\delta(\vec{k}+\vec{k}_1-\vec{k}_2-\vec{k}_3)\,dk\,dk_1\,dk_2\,dk_3 \end{aligned} \tag{2.29}$$

3. Canonical Transformation

In this chapter we will study only gravity waves and put $\sigma = 0$, so that

$$\omega_k = \sqrt{gk\,\tanh(kh)}\,. \tag{3.1}$$

The dispersion relation (3.1) is of the "non-decay type" and the equations

$$\omega_k = \omega_{k_1} + \omega_{k_2} \qquad \vec{k} = \vec{k}_1 + \vec{k}_2 \tag{3.2}$$

have no real solution. This means that in the limit of small nonlinearity, the cubic terms in the Hamiltonian (2.11) can be excluded by a proper canonical transformation. The transformation

$$a(k,t) \to b(k,t) \tag{3.3}$$

must transform equation (2.18) into the same equation:

$$\frac{\partial b_k}{\partial t} + i\frac{\delta H}{\delta b^*_k} = 0. \tag{3.4}$$

This requirement imposes the following conditions on Poisson's brackets between a_k and b_k:

$$\{a_k, a_{k'}\} = \int \left\{ \frac{\delta a_k}{\delta b_{k''}}\frac{\delta a_{k'}}{\delta b^*_{k''}} - \frac{\delta a_k}{\delta b^*_{k''}}\frac{\delta a_{k'}}{\delta b_{k''}} \right\} dk'' = 0 \tag{3.5}$$

$$\{a_k, a^*_{k'}\} = \int \left\{ \frac{\delta a_k}{\delta b_{k''}}\frac{\delta a^*_{k'}}{\delta b^*_{k''}} - \frac{\delta a_k}{\delta b^*_{k''}}\frac{\delta a^*_{k'}}{\delta b_{k''}} \right\} dk'' = \delta(k-k') \tag{3.6}$$

$$\{b_k, b_{k'}\} = \int \left\{ \frac{\delta b_k}{\delta a_{k''}}\frac{\delta b_{k''}}{\delta a^*_{k'}} - \frac{\delta b_k}{\delta a^*_{k''}}\frac{\delta b_{k''}}{\delta a_{k'}} \right\} dk'' = 0 \tag{3.7}$$

$$\{b_k, b^*_{k'}\} = \int \left\{ \frac{\delta b_k}{\delta a_{k''}}\frac{\delta b^*_{k''}}{\delta a^*_{k'}} - \frac{\delta b_k}{\delta a^*_{k''}}\frac{\delta b^*_{k''}}{\delta a_{k'}} \right\} dk'' = \delta(k-k') \tag{3.8}$$

The canonical transformation excluding cubic terms is given by the infinite series:

$$a_k = a^{(0)}_k + a^{(1)}_k + a^{(2)}_k + \cdots \tag{3.9}$$

where

$$
\begin{aligned}
a_k^{(0)} &= b_k \\
a_k^{(1)} &= \int \Gamma^{(1)}(\vec{k},\vec{k}_1,\vec{k}_2)\, b_{k_1}\, b_{k_2}\, \delta(\vec{k}-\vec{k}_1-\vec{k}_2)\, dk_1\, dk_2 - 2\int \Gamma^{(1)}(\vec{k}_2,\vec{k},\vec{k}_1)\, b^*_{k_1}\, b_{k_2}\, \delta(\vec{k}+\vec{k}_1-\vec{k}_2)\, dk_1\, dk_2 \\
&+ \int \Gamma^{(2)}(\vec{k},\vec{k}_1,\vec{k}_2)\, b^*_{k_1}\, b^*_{k_2}\, \delta(\vec{k}+\vec{k}_1+\vec{k}_2)\, dk_1\, dk_2 \\
a_k^{(2)} &= \int B(\vec{k},\vec{k}_1,\vec{k}_2,\vec{k}_3)\, b^*_{k_1}\, b_{k_2}\, b_{k_3}\, \delta(\vec{k}+\vec{k}_1-\vec{k}_2-\vec{k}_3)\, dk_1\, dk_2\, dk_3 + \cdots
\end{aligned}
\tag{3.10}
$$

Plugging (3.9) into (3.5)–(3.8), we obtain infinite series in powers of b, b^*, which must identically cancel out at all orders except zero.

Let us assume that

$$
\Gamma^{(2)}(\vec{k},\vec{k}_1,\vec{k}_2) = \Gamma^{(2)}(\vec{k}_1,\vec{k},\vec{k}_2) = \Gamma^{(2)}(\vec{k}_2,\vec{k},\vec{k}_1). \tag{3.11}
$$

This condition guarantees that (3.11), (3.5)–(3.8) are satisfied at first order in b, b^*. Substituting (3.9) into H we observe that the cubic terms cancel out:

$$
\Gamma^{(1)}(\vec{k},\vec{k}_1,\vec{k}_2) = -\frac{1}{2}\,\frac{V^{(1,2)}(\vec{k},\vec{k}_1,\vec{k}_2)}{(\omega_k-\omega_{k_1}-\omega_{k_2})} \tag{3.12}
$$

$$
\Gamma^{(2)}(\vec{k},\vec{k}_1,\vec{k}_2) = -\frac{1}{2}\,\frac{V^{(0,3)}(\vec{k},\vec{k}_1,\vec{k}_2)}{(\omega_k+\omega_{k_1}+\omega_{k_2})} \tag{3.13}
$$

A simple method for the recurrent calculation of $B(\vec{k},\vec{k}_1,\vec{k}_2,\vec{k}_3)$ and higher terms in the expansion (3.9) was found by the author in the article (Zakharov, 1998). By the use of this method one can find

$$
\begin{aligned}
B(\vec{k},\vec{k}_1,\vec{k}_2,\vec{k}_3) &= \Gamma^{(1)}(\vec{k}_1,\vec{k}_2,\vec{k}_1-\vec{k}_2)\,\Gamma^{(1)}(\vec{k}_3,\vec{k},\vec{k}_3-\vec{k}) + \Gamma^{(1)}(\vec{k}_1,\vec{k}_3,\vec{k}_1-\vec{k}_3)\,\Gamma^{(1)}(\vec{k}_2,\vec{k},\vec{k}_2-\vec{k}) \\
&-\Gamma^{(1)}(\vec{k},\vec{k}_2,\vec{k}-\vec{k}_2)\,\Gamma^{(1)}(\vec{k}_3,\vec{k}_1,\vec{k}_3-\vec{k}_1) - \Gamma^{(1)}(\vec{k}_1,\vec{k}_3,\vec{k}_1-\vec{k}_3)\,\Gamma^{(1)}(\vec{k}_2,\vec{k}_1,\vec{k}_2-\vec{k}_1) \\
&-\Gamma^{(1)}(\vec{k}+\vec{k}_1,\vec{k},\vec{k}_1)\,\Gamma^{(1)}(\vec{k}_2+\vec{k}_3,\vec{k}_2,\vec{k}_3) + \Gamma^{(2)}(-\vec{k}-\vec{k}_1,\vec{k},\vec{k}_1)\,\Gamma^{(2)}(-\vec{k}_2-\vec{k}_3,\vec{k}_2,\vec{k}_3)
\end{aligned}
\tag{3.14}
$$

The series (3.10) should be at least asymptotic. Hence we require

$$
|a_k^{(1)}| \ll |b_k| \tag{3.15}
$$

Let us consider the limit of shallow water as $kh \to 0$. We will assume also that the wave packet is narrow in angle: $k_y \ll k_x$. In this limit

$$
\omega_k \to s|k|\left(1-\frac{1}{3}(kh)^2+\cdots\right), \qquad s=\sqrt{gh}, \tag{3.16}
$$

and

$$
L^{(1)}(\vec{k}_1,\vec{k}_2) \simeq -k_1k_2\,, \quad A_k \simeq h|k|^2\,, \quad B_k \simeq g\,, \quad V^{(1,2)}(\vec{k},\vec{k}_1,\vec{k}_2) \simeq \frac{3}{4\pi\sqrt{2}}(kk_1k_2)^{1/2}\left(\frac{g}{h}\right)^{1/4}.
$$

Denoting $k_y = q$, $k_x = p$ and $|p| \gg |q|$, one obtains:

$$
\omega(p,q) \simeq s\left(p+\frac{1}{2}\,\frac{q^2}{p}-\frac{1}{3}\,h^2p^3\right), \quad V^{(1,2)} \simeq \frac{3}{4\pi\sqrt{2}}\left(\frac{g}{h}\right)^{1/4}(pp_1p_2)^{1/2}. \tag{3.17}
$$

We will study two opposite cases - wave packets narrow in angle and broad in angle. In both cases we will look only for the leading order terms in $1/kh$. For a packet which is very narrow in angle:

$$\begin{aligned} a^{(0)}(p,q) &\simeq b(p)\,\delta(q),\ \ a^{(1)}(p,q) = b^{(1)}(p)\,\delta(q) \\ b^{(1)}(p) &\simeq \frac{3}{8\pi\sqrt{2}}\left(\frac{g}{h}\right)^{1/4}\frac{1}{sh^2}\left\{\int_0^p \frac{b(p_1)b(p-p_1)}{pp_1(p-p_1))^{1/2}}\,dp_1 + 2\int_0^\infty \frac{b^*(p_1)b(p+p_1)}{pp_1(p+p_1))^{1/2}}\,dp_1\right\} + \cdots \end{aligned} \tag{3.18}$$

The condition (3.15) now reads now

$$\frac{|b|}{p^{1/2}}\left(\frac{g}{h}\right)^{1/4}\frac{1}{sh^2} \ll 1 \tag{3.19}$$

Let a be a characteristic elevation of the free surface, $\mu = (ka)^2$, $\delta = kh$. The condition (3.19) is equivalent to

$$\mu \ll \delta^6\,, \quad \text{or} \quad N = \frac{\mu^{1/2}}{\delta^3} \ll 1\,. \tag{3.20}$$

N is known as "Stokes number".

For wave packets which are broad in angle the condition (3.15) is less restrictive. In this case the denominator of $\Gamma^{(1)}(\vec{k},\vec{k}_1,\vec{k}_2)$ is small if all three vectors $\vec{k},\vec{k}_1,\vec{k}_2$ are parallel. Let us put $\vec{k} = (p,q)$, $\vec{k}_1 = (p_1,q_1)$, $\vec{k}_2 = (p_2,-q_2)$. Then $\Gamma^{(1)}(p,p_1,p_2,q)$ has a sharp maximum at $q=0$. Performing integration over q yields

$$\begin{aligned} b^{(1)}(p,0) = \frac{3}{8\sqrt{2}}\left(\frac{g}{h}\right)^{1/4}\frac{1}{shp^{1/2}}\Bigg\{&\int_0^p p^{1/2}(p-p_1)^{1/2}\,b(p_1,0)\,b(p-p_1,0)dp_1 \\ &+ 2\int_0^\infty p_1^{1/2}\,(p+p_1)^{1/2}\,b^*(p_1,0)\,b(p+p_1,0)dp_1\Bigg\} + \cdots \end{aligned} \tag{3.21}$$

The condition

$$|b^{(1)}\,(p,0)| \ll |b^{(0)}\,(p,0)| \tag{3.22}$$

now reads

$$\mu \ll \delta^4. \tag{3.23}$$

4. Effective Hamiltonian

After performing the canonical transformation the cubic terms in the Hamiltonian cancel out. In new variables b_k we have

$$H = H_0 + H_2 + H_3 + \cdots\,, \tag{4.1}$$

$$H_0 = \int \omega_k\,|b_k|^2\,dk\,, \tag{4.2}$$

$$H_2 = \frac{1}{4}\int T(\vec{k},\vec{k}_1,\vec{k}_2,\vec{k}_3)\,b_k^*\,b_{k_1}^*\,b_{k_2}\,b_{k_3}\,\delta(\vec{k}+\vec{k}_1-\vec{k}_2-\vec{k}_3)\,dk\,dk_1\,dk_2\,dk_3\,, \tag{4.3}$$

$$H_3 = \ldots$$

where

$$T(\vec{k},\vec{k}_1,\vec{k}_2,\vec{k}_3) = \frac{1}{4}\left(\tilde{T}(\vec{k},\vec{k}_1,\vec{k}_2,\vec{k}_3)+\tilde{T}(\vec{k}_1,\vec{k},\vec{k}_2,\vec{k}_3)+\tilde{T}(\vec{k}_2,\vec{k}_3,\vec{k},\vec{k}_1)+\tilde{T}(\vec{k}_3,\vec{k}_2,\vec{k},\vec{k}_1)\right)$$
$$\tilde{T}(\vec{k},\vec{k}_1,\vec{k}_2,\vec{k}_3) = V^{(2,2)}(\vec{k},\vec{k}_1,\vec{k}_2,\vec{k}_3)+R^{(1)}(\vec{k},\vec{k}_1,\vec{k}_2,\vec{k}_3)+R^{(2)}(\vec{k},\vec{k}_1,\vec{k}_2,\vec{k}_3) \tag{4.4}$$

and

$$R^{(1)}(\vec{k},\vec{k}_1,\vec{k}_2,\vec{k}_3) = -\frac{V^{(0,3)}(-\vec{k}-\vec{k}_1,\vec{k},\vec{k}_1)\,V^{(0,3)}(-\vec{k}_2-\vec{k}_3,\vec{k}_2,\vec{k}_3)}{\omega(-k-k_1)+\omega(k)+\omega(k_2)}, \tag{4.5}$$

$$R^{(2)}(\vec{k},\vec{k}_1,\vec{k}_2,\vec{k}_3) = -\frac{V^{(1,2)}(\vec{k}+\vec{k}_1,\vec{k},\vec{k}_1)\,V^{(1,2)}(\vec{k}_2+\vec{k}_3,\vec{k}_2,\vec{k}_3)}{\omega_{k+k_1}-\omega_k-\omega_{k_1}} -$$
$$-\frac{V^{(1,2)}(\vec{k},\vec{k}_2,\vec{k}-\vec{k}_2)\,V^{(1,2)}(\vec{k}_3,\vec{k}_3-\vec{k}_1,\vec{k}_1)}{\omega_{k-k_2}-\omega_k+\omega_{k_2}} - \frac{V^{(1,2)}(\vec{k},\vec{k}_3,\vec{k}-\vec{k}_3)\,V^{(1,2)}(\vec{k}_2,\vec{k}_2-\vec{k}_1,\vec{k}_1)}{\omega_{k-k_3}-\omega_k+\omega_{k_3}} -$$
$$-\frac{V^{(1,2)}(\vec{k}_2,\vec{k},\vec{k}_2-\vec{k})\,V^{(1,2)}(\vec{k}_1,\vec{k}_1-\vec{k}_3,\vec{k}_3)}{\omega_{k_2-k}+\omega_k-\omega_{k_2}} - \frac{V^{(1,2)}(\vec{k}_3,\vec{k},\vec{k}_3-\vec{k})\,V^{(1,2)}(\vec{k}_2,\vec{k}_2-\vec{k}_1,\vec{k}_1)}{\omega_{k_3-k}+\omega_k-\omega_{k_3}} \tag{4.6}$$

In the presence of capillarity, the expression (4.6) makes sense everywhere except in the vicinity of the zeros of the denominators. The width of these vicinities depends on the level of nonlinearity.

The equation of motion (3.4) in new variables takes the form

$$\frac{\partial b_k}{\partial t}+i\,\omega_k\,b_k = -\frac{i}{2}\int T(\vec{k},\vec{k}_1,\vec{k}_2,\vec{k}_3)\,b^*_{k_1}\,b_{k_2}\,b_{k_3}\,\delta(\vec{k}+\vec{k_1}-\vec{k_2}-\vec{k_3})\,dk_1\,dk_2\,dk_3 \tag{4.7}$$

The term $T(\vec{k},\vec{k}_1,\vec{k}_2,\vec{k}_3)$ is defined on the resonance manifold

$$\omega_k+\omega_{k_1}=\omega_{k_2}+\omega_{k_3},\quad \vec{k}+\vec{k_1}=\vec{k_2}+\vec{k_3}\,. \tag{4.8}$$

Further we will omit the wave numbers k and keep only their labels. After a series of transformations the four-wave interaction coefficient T can be simplified into the form

$$T_{1234} = \frac{1}{2}(\tilde{T}_{1234}+\tilde{T}_{2134}),$$
$$\tilde{T}_{1234} = -\frac{1}{16\pi^2}\left(\frac{A_1A_2A_3A_4}{B_1B_2B_3B_4}\right)^{1/4}$$
$$\times\left[k_1^2\,B_1+k_2^2\,B_2+k_3^2\,B_3+k_4^2\,B_4-(\omega_1-\omega_3)^2\,A_{1-3}-(\omega_1-\omega_4)^2\,A_{1-4}-(\omega_1+\omega_2)^2\,A_{1+2}\right]$$
$$-\frac{1}{16\pi^2}\left(\frac{B_1B_2B_3B_4}{A_1A_2A_3A_4}\right)^{1/4}\times\left\{\frac{1}{B_{1+2}}\left[L_{1,2}\,L_{3,4}+\frac{u_{1,2}\,u_{3,4}}{\omega_{1+2}^2-(\omega_1+\omega_2)^2}\right]\right.$$
$$\left.+\frac{1}{B_{1-3}}\left[L_{-1,3}\,L_{-2,4}+\frac{u_{-1,3}\,u_{-2,4}}{\omega_{1-3}^2-(\omega_1-\omega_3)^2}\right]+\frac{1}{B_{1-4}}\left[L_{-1,4}\,L_{-2,3}+\frac{u_{-1,4}\,u_{-2,3}}{\omega_{1-4}^2-(\omega_1-\omega_4)^2}\right]\right\} \tag{4.9}$$

Here

$$A_k = k\tanh kh,\quad B_k = g+\sigma k^2,\quad L_{1,2}=-(\vec{k}_1\cdot\vec{k}_2)-A_1A_2,\quad \omega_k=\sqrt{A_kB_k}. \tag{4.10}$$

The expression for $u_{1,2}$ is

$$\begin{aligned} u_{1,2} &= (\vec{k}_1\cdot\vec{k}_2)\left[\omega_1\Big(1+\frac{B_{1+2}}{B_1}\Big)+\omega_2\Big(1+\frac{B_{1+2}}{B_2}\Big)\right] \\ &+\frac{B_{1+2}}{B_2}\,\omega_2\,k_1^2+\frac{B_{1+2}}{B_1}\,\omega_1\,k_2^2+\Big(\frac{A_1A_2}{B_1B_2}\Big)^{1/2}(\omega_1\,\omega_2-\omega_{1+2}^2)(\omega_1+\omega_2) \\ u_{-1,3} &= -(\vec{k}_1\cdot\vec{k}_3)\left[\omega_1\Big(1+\frac{B_{1-3}}{B_1}\Big)-\omega_3\Big(1+\frac{B_{1-3}}{B_3}\Big)\right] \\ &-\frac{B_{1-3}}{B_3}\,\omega_3^2\,k_1^2+\frac{B_{1-3}}{B_1}\,\omega_1 k_3^2+(\omega_1-\omega_3)(\omega_1\omega_3+\omega_{1-3}^2)\Big(\frac{A_1A_3}{B_1B_3}\Big)^{1/2} \end{aligned} \tag{4.11}$$

The above expression is the most general form of four-wave interaction coefficient and is applicable for gravity as well as for capillary waves on an arbitrary depth. It can be simplified in different limiting cases.

In the absence of capillarity $\sigma = 0$, $B_k = g$ and

$$\begin{aligned} u_{1,2} &= (\omega_1+\omega_2)\left\{2(\vec{k}_1\cdot\vec{k}_2)+\frac{1}{g}\omega_1\omega_2(\omega_1^2+\omega_2^2-\omega_{1+2}^2)\right\} \\ u_{-1,3} &= (\omega_1-\omega_3)\left\{-2(\vec{k}_1\cdot\vec{k}_3)+\frac{1}{g}\omega_1\omega_3(\omega_{1-3}^2-\omega_1^2+\omega_3^2)\right\} \end{aligned} \tag{4.12}$$

5. Deep water limit

The coefficient of four-wave interaction for pure gravity waves on deep water was calculated by many authors since Hasselmann (1962). We present here a relatively compact expression for this coefficient.

$$\begin{aligned} T_{1234} &= -\frac{1}{16\pi^2}\,\frac{1}{(k_1k_2k_3k_4)^{1/4}}\Bigg\{-12k_1k_2k_3k_4- \\ &-2(\omega_1+\omega_2)^2\Big[\omega_3\omega_4\Big((\vec{k}_1\cdot\vec{k}_2)-k_1k_2\Big)+\omega_1\omega_2\Big((\vec{k}_3\cdot\vec{k}_4)-k_3k_4\Big)\Big]\,\frac{1}{g^2} \\ &-2(\omega_1-\omega_3)^2\Big[\omega_2\omega_4\Big((\vec{k}_1\cdot\vec{k}_3)+k_1k_3\Big)+\omega_1\omega_3\Big((\vec{k}_2\cdot\vec{k}_4)+k_2k_4\Big)\Big]\,\frac{1}{g^2} \\ &-2(\omega_1-\omega_4)^2\Big[\omega_2\omega_3\Big((\vec{k}_1\cdot\vec{k}_4)+k_1k_4\Big)+\omega_1\omega_4\Big((\vec{k}_2\cdot\vec{k}_3)+k_2k_3\Big)\Big]\,\frac{1}{g^2} \\ &+[(\vec{k}_1\cdot\vec{k}_2)+k_1k_2][(\vec{k}_3\cdot\vec{k}_4)+k_3k_4]+[-(\vec{k}_1\cdot\vec{k}_3)+k_1k_3][-(\vec{k}_2\cdot\vec{k}_4)+k_2k_4] \\ &+[-(\vec{k}_1\cdot\vec{k}_4)+k_1k_4][-(\vec{k}_2\cdot\vec{k}_3)+k_2k_3] \\ &+4(\omega_1+\omega_2)^2\,\frac{[(\vec{k}_1\cdot\vec{k}_2)-k_1k_2][-(\vec{k}_2\cdot\vec{k}_4)+k_2k_4]}{\omega_{1+2}^2-(\omega_1+\omega_2)^2}+4(\omega_1-\omega_3)^2\,\frac{[(\vec{k}_1\cdot\vec{k}_3)+k_1k_3][(\vec{k}_2\cdot\vec{k}_4)+k_2k_4]}{\omega_{1-3}^2-(\omega_1-\omega_3)^2} \\ &+4(\omega_1-\omega_4)^2\,\frac{[(\vec{k}_1\cdot\vec{k}_4)+k_1k_4][(\vec{k}_2\cdot\vec{k}_3)+k_2k_3]}{\omega_{1-4}^2-(\omega_1-\omega_4)^2}\Bigg\} \end{aligned} \tag{5.1}$$

Here $\omega_i = \sqrt{g\,|k_i|}$.

In spite of its complexity the expression (5.1) has an inner symmetry and beauty. It was mentioned that in the one dimensional case the coefficient T_{1234} cancels out (Dyachenko and Zakharov, 1994). This result was obtained earlier by computer. We will obtain it below "by hand". Another compact expression for T_{1234} was

found by Webb (1978). Both expressions coincide on the resonant surface (5.2), but a proof of cancellation of T_{1234} in a one dimensional geometry is more difficult with the Webb formula.

In the one-dimensional case the resonant conditions

$$\begin{aligned} \omega_2 + \omega_2 &= \omega_3 + \omega_3 \\ k_1 + k_2 &= k_3 + k_4 \end{aligned} \tag{5.2}$$

have trivial solutions $k_3 = k_1, k_4 = k_2; k_3 = k_2, k_4 = k_1$ describing wave scattering without momentum exchange, and nontrivial solutions providing the momentum exchange. For these solutions the sign of one of the wave vectors is opposite to others. For instance, we can put

$$k_1 > 0, \;\; k_2 < 0, \;\; k_3 > 0, \;\; k_4 > 0.$$

In the one-dimensional case most of the terms in (5.1) cancel out, and the expression is simplified down to the form

$$T_{1234} = -\frac{1}{8\pi^2}\omega_1(\omega_1\omega_2\omega_3\omega_4)^{1/2}\Big\{-3\omega_2\omega_3\omega_4 + \omega_2(\omega_1+\omega_2)^2 - \omega_3(\omega_1-\omega_3)^2 - \omega_4(\omega_1-\omega_4)^2\Big\} \tag{5.3}$$

The resonant conditions (5.2) can be solved by the parametrization

$$\begin{aligned} \omega_1 = A(1+\xi+\xi^2),\; \omega_2 = A\xi,\; \omega_3 = A(1+\xi),\; \omega_4 = A\xi(1+\xi) \\ k_1 = A^2(1+\xi+\xi^2)^2,\; k_2 = -A^2\xi^2,\; k_3 = A^2(1+\xi)^2,\; k_4 = A^2\xi^2(1+\xi)^2 \end{aligned} \tag{5.4}$$

By plugging the parametrization (5.4) into (5.3) we get

$$T_{1234} = -\frac{1}{4\pi^2}\omega_1(\omega_1\omega_2\omega_3\omega_4)^2\, A^3\xi(1+\xi)\left(-3\xi(1+\xi) + (1+\xi)^3 - 1 - \xi^3\right) \equiv 0 \tag{5.5}$$

6. Shallow water limit

The shallow water limit takes place if $kh \to 0$. In this limit

$$A_k \to k^2 h \quad \omega_k \to sk, \quad s^2 = gh, \quad L_{12} \to -(\vec{k}_1\cdot\vec{k}_2), \quad u_{1,2} \to s(k_1+k_2)(\vec{k}_1\cdot\vec{k}_2), \quad u_{-1,3} \to -s(k_1-k_3)(\vec{k}_1\cdot\vec{k}_3). \tag{6.1}$$

The coefficient (4.9) can be simplified into the form

$$\begin{aligned} T_{1234} = -\frac{1}{16\pi^2 h}\frac{1}{(k_1k_2k_3k_4)^{1/2}}\Bigg\{&(\vec{k}_1\cdot\vec{k}_2)(\vec{k}_3\cdot\vec{k}_4) + (\vec{k}_1\cdot\vec{k}_3)(\vec{k}_2\cdot\vec{k}_4) + (\vec{k}_1\cdot\vec{k}_4)(\vec{k}_2\cdot\vec{k}_3) \\ &+2\left[\frac{(\vec{k}_1\cdot\vec{k}_2)(\vec{k}_3\cdot\vec{k}_4)(k_1-k_2)^2}{(\vec{k}_1\cdot\vec{k}_2)-k_1k_2} - \frac{(\vec{k}_1\cdot\vec{k}_3)(\vec{k}_2\cdot\vec{k}_4)(k_1-k_3)^2}{(\vec{k}_1\cdot\vec{k}_3)-k_1k_3} - \frac{(\vec{k}_1\cdot\vec{k}_4)(\vec{k}_2\cdot\vec{k}_3)(k_1-k_4)^2}{(\vec{k}_1\cdot\vec{k}_4)-k_1k_4}\right]\Bigg\} \end{aligned} \tag{6.2}$$

The three terms in (6.2) are singular if the vectors k_i are parallel. But there is a remarkable fact: these singularities cancel and the whole expression (6.2) is a regular continuous function. The cancellation of singularities is a quite nontrivial circumstance. It could be checked by a straightforward calculation.

The singular part of $\tilde{T}_{1234}$ can be written as follows:

$$\tilde{T}_{1234} = -\frac{1}{4\pi^2 h}\frac{k_2k_3k_4}{(k_1k_2k_3k_4)^{1/2}}\left[\frac{(k_1+k_2)^2}{k_2(\cos\phi_2-1)} - \frac{(k_1-k_3)^2}{k_3(\cos\phi_3-1)} - \frac{(k_1-k_4)^2}{k_4(\cos\phi_4-1)}\right] \tag{6.3}$$

Here $\cos\phi_i = (\vec{k}_1 \cdot \vec{k}_i)/k_1 k_i$.

The resonant conditions are:

$$\begin{aligned} k_1 + k_2 &= k_3 + k_4, \\ k_1 + k_2\cos\phi_2 &= k_3\cos\phi_3 + k_4\cos\phi_4, \\ k_2\sin\phi_2 &= k_3\sin\phi_3 + k_4\sin\phi_4. \end{aligned} \tag{6.4}$$

For small angles $|\phi_i| \ll 1$, we can put approximately

$$\cos\phi_i - 1 \simeq -\frac{\phi_i^2}{2}, \quad \sin\phi_i \simeq \phi_i.$$

The resonant conditions now become now

$$k_2\phi_2^2 = k_3\phi_3^2 + k_4\phi_4^2, \quad k_2\phi_2 = k_3\phi_3 + k_4\phi_4 \tag{6.5}$$

The most singular part of $\tilde{T}_{1234}$ is

$$\tilde{T}_{sing} \simeq -\frac{1}{2\pi^2 h}\frac{(k_3k_3k_4)^{1/2}}{k_1^{1/2}}\left\{-\frac{(k_1+k_2)^2}{k_2\phi_2^2} + \frac{(k_1-k_3)^2}{k_3\phi_3^3} + \frac{(k_1-k_4)^2}{k_4\phi_4^2}\right\} \tag{6.6}$$

But one can check by a direct calculation that

$$\frac{(k_1+k_2)^2}{k_2\phi_2^2} - \frac{(k_1-k_3)^2}{k_3\phi_3^2} - \frac{(k_1-k_4)^2}{k_4\phi_4^2} \equiv 0 \tag{6.7}$$

in virtue of (6.5). Hence the singularities cancel and (6.2) is a regular function.

We can calculate $\tilde{T}_{1234}$ more accurately by putting

$$\begin{aligned} \tilde{T}_{1234} = -\frac{1}{16\pi^2 h}\frac{1}{(k_1k_2k_3k_4)^{1/2}}\Bigg\{&(\vec{k_1}\vec{k_2})(\vec{k_3}\vec{k_4}) + (\vec{k_1}\vec{k_3})(\vec{k_2}\vec{k_4}) + (\vec{k_1}\vec{k_4})(\vec{k_2}\vec{k_3}) \\ &+ 4s^2\left[\frac{(\vec{k_1}\vec{k_2})(\vec{k_3}\vec{k_4})(k_1+k_2)^2}{\omega_{1+2}^2 - (\omega_1+\omega_2)^2} - \frac{(\vec{k_1}\vec{k_3})(\vec{k_2}\vec{k_4})(k_1-k_3)^2}{\omega_{1-3}^2 - (\omega_1-\omega_3)^2} - \frac{(\vec{k_1}\vec{k_4})(\vec{k_2}\vec{k_4})(k_1-k_4)^2}{\omega_{1-4}^2 - (\omega_1-\omega_4)^2}\right]\Bigg\} \end{aligned} \tag{6.8}$$

Here we put

$$\omega(k) = sk\Big(1 - \frac{1}{3}(kh)^2\Big) \tag{6.9}$$

Now denominators in (6.8) cannot reach zero, but for almost parallel k_i they are of order $(kh)^2$ and small if $kh \to 0$. As a result, some terms in (6.8) are large, of order $1/h^3$, but in fact they cancel each other. The major terms in (6.8) are

$$\tilde{T}_{sing} \simeq \frac{1}{2\pi^2 h}\frac{(k_2k_3k_4)^{1/2}}{k_1^{1/2}}\left\{\frac{(k_1+k_2)^2}{k_2[\phi_2^2 + h^2(k_1+k_2)^2]} - \frac{(k_1-k_3)^2}{k_3[\phi_3^2 + h^2(k_1-k_3)^2]} - \frac{(k_1-k_4)^2}{k_4[\phi_4^2 + h^2(k_1-k_4)^2]}\right\} = 0 \tag{6.10}$$

The expression (6.10) is identically zero in virtue of (6.5). As $h \to 0$ (6.10) goes to (6.7).

Cancellations (6.7), (6.10) have a very deep hidden reason - they are consequencies of the integrability of the KP-2 equations (see Zakharov 1998).

7. Statistical description

The statistical description of nonlinear wave fields is realized by the correlation function

$$< a^*_{k_1} \cdots a^*_{k_n} a_{k_{n+1}} \cdots a_{k_{n+m}} >= J^{n,m}(\vec{k}_1 \cdots \vec{k}_n, \vec{k}_{n+1} \cdots \vec{k}_{n+m}) \delta(\vec{k}_1 + \cdots + \vec{k}_n - \vec{k}_{n+1} \cdots - \vec{k}_{n+m}) \tag{7.1}$$

The presence of δ-functions in (7.1) is a result of spatial uniformity of the wave field.

In the same way we can introduce correlation functions for the transformed variables b_k:

$$< b^*_{k_1} \cdots b^*_{k_n} b_{k_{n+1}} \cdots b_{k_{n+m}} >= I^{n,m}(\vec{k}_1 \cdots \vec{k}_n, \vec{k}_{n+1} \cdots \vec{k}_{n+m}) \delta(\vec{k}_1 + \cdots + \vec{k}_n - \vec{k}_{n+1} \cdots - \vec{k}_{n+m}) \tag{7.2}$$

To find the connection between $J^{n,m}$ and $I^{n,m}$ one has to substitute (3.9) into (7.1) and perform the averaging. The following pair of correlation functions is the most important:

$$\begin{aligned} < a_k a^*_{k'} > &= n_k \, \delta(k - k') \\ < b_k b^*_{k'} > &= N_k \, \delta(k - k') \end{aligned} \tag{7.3}$$

Here n_k and N_k are different functions. n_k is a measurable quantity, connected directly with observable correlation functions. For instance, from (2.17) we get

$$I_k =< |\eta_k|^2 >= \frac{1}{2} \left(\frac{A_k}{B_k} \right)^{1/2} (n_k + n_{-k}) = \frac{1}{2} \frac{\omega_k}{B_k} (n_k + n_{-k}) \tag{7.4}$$

The function N_k cannot be measured directly. It is an important auxiliary tool used in analytical constructions. In most articles on physical oceanography the authors make no difference between n_k and N_k. This is a source of persistent and systematic mistakes. We will see that the difference between n_k and N_k is especially important on shallow water.

Plugging (3.9) into (7.3) we get:

$$n_k = N_k + < a^{(0)}_k a^{(1)*}_k > + < a^{(0)*}_k a^{(1)}_k > + < a^{(1)}_k a^{(1)*}_k > + < a^{(0)}_k a^{(2)*}_k > + < a^{(0)*}_k a^{(2)}_k > + \cdots \tag{7.5}$$

Terms $< a^{(0)}_k a^{(1)*}_k >$, $< a^{(0)*}_k a^{(1)}_k >$ are expressed through triple correlation functions $< b^* b b >$ and $< b b b >$. As far as the cubic terms in the effective Hamiltonian are cancelled, triple correlation is defined by the fifth-order correlation functions and is small and can be neglected. In fact, $I^{(1,2)} \simeq n^5$.

The next terms in (7.5) are expressed through quartic correlation. Only one quartic correlation function is really important

$$< b^*_k b^*_{k_1} b_{k_2} b_{k_3} >= I^{(2,2)}(\vec{k}, \vec{k}_1, \vec{k}_2, \vec{k}_3) \, \delta(\vec{k} + \vec{k}_1 - \vec{k}_2 - \vec{k}_3) \tag{7.6}$$

We study only weakly nonlinear waves and can assume that the stochastic process of surface oscillations is close to Gaussian. Thus we can put approximately

$$I^{(2,2)}(\vec{k}, \vec{k}_1, \vec{k}_2, \vec{k}_3) = N_k N_{k_2} \, \delta(\vec{k} - \vec{k}_3) + N_k N_{k_3} \, \delta(\vec{k} - \vec{k}_2) \tag{7.7}$$

By the use of (7.7) we obtain the following expression:

$$\begin{aligned} n_k &= N_k + 2\int |\Gamma^{(1)}(\vec{k},\vec{k}_1,\vec{k}_2)|^2\, N_{k_1}\, N_{k_2}\, \delta(\vec{k}-\vec{k}_1-\vec{k}_2)dk_1dk_2 \\ &+2\int |\Gamma^{(1)}(\vec{k}_2,\vec{k},\vec{k}_1)|^2\, N_{k_1}\, N_{k_2}\, \delta(\vec{k}+\vec{k}_1-\vec{k}_2)\, dk_1dk_2 + \\ &+2\int |\Gamma^{(1)}(\vec{k}_1,\vec{k},\vec{k}_2)|^2\, N_{k_1}\, N_{k_2}\, \delta(\vec{k}-\vec{k}_1+\vec{k}_2)\, dk_1dk_2 + \\ &+2\int |\Gamma^{(2)}(\vec{k},\vec{k}_1,\vec{k}_2)|^2\, N_{k_1}\, N_{k_2}\, \delta(\vec{k}+\vec{k}_1+\vec{k}_2)\, dk_1dk_2 - 4N_k\int B(\vec{k},\vec{k}_1,\vec{k},\vec{k}_1)\, N_{k_1}\, dk_1 \end{aligned} \tag{7.8}$$

Using the expression (3.14) for B and formulae (3.12), (3.13) we get the final result:

$$\begin{aligned} n_k &= N_k + \frac{1}{2}\int \frac{|V^{(1,2)}(\vec{k},\vec{k}_1,\vec{k}_2)|^2}{(\omega_k-\omega_{k_1}-\omega_{k_2})^2}\,(N_{k_1}N_{k_2}-N_kN_{k_1}-N_kN_{k_2})\,\delta(\vec{k}-\vec{k}_1-\vec{k}_2)\,dk_1dk_2 + \\ &+\frac{1}{2}\int \frac{|V^{(1,2)}(\vec{k},\vec{k}_1,\vec{k}_2)|^2}{(\omega_{k_1}-\omega_k-\omega_{k_2})^2}\,(N_{k_1}N_{k_2}+N_kN_{k_1}-N_kN_{k_2})\,\delta(\vec{k}_1-\vec{k}-\vec{k}_2)\,dk_1dk_2 + \\ &+\frac{1}{2}\int \frac{|V^{(1,2)}(\vec{k}_2,\vec{k},\vec{k}_1)|^2}{(\omega_{k_2}-\omega_k-\omega_{k_1})^2}\,(N_{k_1}N_{k_2}+N_kN_{k_2}-N_kN_{k_1})\,\delta(\vec{k}_2-\vec{k}-\vec{k}_1)\,dk_1dk_2 + \\ &+\frac{1}{2}\int \frac{|V^{(0,3)}(\vec{k},\vec{k}_1,\vec{k}_2)|^2}{(\omega_k+\omega_{k_1}+\omega_{k_2})^2}\,(N_{k_1}N_{k_2}+N_kN_{k_1}+N_kN_{k_2})\,\delta(\vec{k}+\vec{k}_1+\vec{k}_2)\,dk_1dk_2 \end{aligned} \tag{7.9}$$

On deep water all the terms in (7.9) are of the same order, and the difference between n_k and N_k is small:

$$\frac{n_k-N_k}{n_k} \simeq \mu \tag{7.10}$$

However, in shallow water, denominators in (7.9) are small, and this difference can be dangerously big. The integration in (7.9) for a wave distribution which is broad in angle in the perpendicular direction can be performed explicitly. The last, nonresonant, term in (7.9) must be neglected. It is suitable to present the result in polar coordinates in the k-plane. The final formula is astonishingly simple:

$$n(k,\theta) = N(k,\theta) + \frac{9}{64}\left(\frac{h}{g}\right)^{1/2}\frac{1}{h^5k}\left\{\int_0^k N(k_1,\theta)\,N(k-k_1,\theta)dk_1 + 2\int_0^\infty N(k_1,\theta)\,N(k+k_1,\theta)dk_1\right\} \tag{7.11}$$

Comparing the leading term with the next terms in (7.11) we obtain

$$\frac{n_k-N_k}{n_k} \simeq \mu/\delta^5 \quad \delta \sim (kh) \tag{7.12}$$

Then the condition of applicability for a weakly-nonlinear statistical theory of waves on shallow water becomes

$$\mu \ll \delta^5 \tag{7.13}$$

For a very shallow water, $kh \simeq 0.1$, this condition can practically never be satisfied. But for a moderately shallow water, $kh \simeq 0.3$, it could be satisfied for small amplitude waves, $\mu \simeq 10^{-4}$. In many real situations the corrections in (7.11) are important and cannot be neglected. Generally speaking, the weakly-nonlinear theory has narrow frames of applicability in shallow water.

8. Kinetic equation

The function n_k is usually named "wave action distribution". There is no standard name for the function N_k so far. We will call it "renormalized wave action". It is very important that the kinetic equation is imposed, not on the wave action n_k but on the renormalized wave action N_k.

To derive this equation we can begin from the equation (4.7). It imposes an infinite set of relations on correlation functions. The statistical description means a loss of time reversibility and needs an introduction of negligibly small damping. It can be done by replacing in (4.7)

$$\omega_k \to \omega_k + i\gamma_k$$

Directly from (4.7) we obtain

$$\frac{\partial N_k}{\partial t} + 2\gamma_k N_k = \int T(\vec{k},\vec{k}_1,\vec{k}_2,\vec{k}_3)\, J_m\, I(\vec{k},\vec{k}_1,\vec{k}_2,\vec{k}_3)\, \delta(\vec{k}+\vec{k}_1-\vec{k}_2-\vec{k}_3) dk_1 dk_2 dk_3 \tag{8.1}$$

We will shorten the notation further.

$$\frac{\partial}{\partial t} I_{1234} + (i\Delta + \Gamma)\, I_{1234} = -\frac{i}{2}\int \Big\{ T_{1567}\, \delta_{1+5-6-7}\, I_{267345} +$$

$$+ T_{2567}\, \delta_{2+5-6-7}\, I_{167345} - T_{3567}\, I_{125467}\, \delta_{3+5-6-7} - T_{4567}\, I_{125367}\, \delta_{4+5-6-7} \Big\} dk_5 dk_6 dk_7 \tag{8.2}$$

Here

$$\Delta = \Delta_{1234} = -\omega_1 - \omega_2 + \omega_3 + \omega_4$$
$$\Gamma = \gamma_1 + \gamma_2 + \gamma_3 + \gamma_4 \tag{8.3}$$

To make a closure in the system we perform the canonical expansion of the correlation function

$$I_{1234} = N_1 N_2 (\delta_{13} + \delta_{14}) + \tilde{I}_{1234} \tag{8.4}$$

into

$$I_{123456} = N_1 N_2 N_3 (\delta_{14}\delta_{25} + \delta_{14}\delta_{26} + \delta_{15}\delta_{24} + \delta_{15}\delta_{26} + \delta_{16}\delta_{24} + \delta_{16}\delta_{25}) +$$
$$+ N_4 ((\tilde{I}_{2356}\delta_{14} + \tilde{I}_{1356}\delta_{24} + \tilde{I}_{1256}\delta_{34}) +$$
$$+ N_5 (\tilde{I}_{2346}\delta_{15} + \tilde{I}_{1346}\delta_{25} + \tilde{I}_{1246}\delta_{35}) +$$
$$+ N_6 (\tilde{I}_{2345}\delta_{16} + \tilde{I}_{1345}\delta_{26} + \tilde{I}_{1245}\delta_{36}) + \tilde{I}_{123456} \tag{8.5}$$

The formulae (8.1)–(8.4) are exact. There $\tilde{I}_{1234}$ and $\tilde{I}_{123456}$ are the cumulants, irreducible parts of the correlators.

Substituting (8.5) into (8.3) and using (8.1) we obtain

$$\frac{\partial}{\partial t}\tilde{I}_{1234} + (i\tilde{\Delta} + T)\tilde{I}_{1234} = T_{1234}(N_2 N_3 N_4 + N_1 N_3 N_4 - N_1 N_2 N_3 - N_1 N_2 N_4) + \hat{L}\, I + Q \tag{8.6}$$

Here Q is the right part of the equation (8.2) where the six-point correlator is replaced by a corresponding cumulant, for instance, $I_{256347} \to \tilde{I}_{256347}$.

$$\tilde{\Delta} = -\tilde{\omega} - \tilde{\omega_2} + \tilde{\omega_3} + \tilde{\omega_4}, \tag{8.7}$$

where $\tilde{\omega}(k)$ is a renormalized dispersion relation

$$\tilde{\omega}(k) = \omega(k) + \int T(\vec{k},\vec{k}_1) N_{k_1}\, dk_1\,, \quad T(\vec{k},\vec{k}_1) = T(\vec{k},\vec{k}_1,\vec{k},\vec{k}_1) \tag{8.8}$$

$\hat{L}I$ is a linear operator:

$$(\hat{L}I)_{1234} = M_{1234} + M_{2134} - M_{3412} - M_{4312} \tag{8.9}$$

$$M_{1234} = -\frac{i}{2} N_2 \int T_{1256}\, I_{5634}\, \delta(1+2-5-6)\, dk_5 dk_6 \tag{8.10}$$
$$-iN_3 \int T_{1546}\, I_{2645}\, \delta(1+5-4-6)\, dk_5 dk_6 - iN_4 \int T_{1536}\, I_{2635}\, \delta(1+5-3-6) dk_5 dk_6$$

The system (8.1),(8.6) becomes closed by putting $\tilde{I}_{123456} = 0$. It is still very complicated. For further simplification one has to neglect $\hat{L}I$. Sending $\Gamma \to 0$, we finally get

$$I_m\, \tilde{I}_{1234} = \pi\, T_{1234}(N_2N_3N_4 + N_1N_3N_4 - N_1N_2N_3 - N_1N_2N_4)\, \delta(\tilde{\Delta}) \tag{8.11}$$

Substituting (8.9) into (8.1) leads to the final result

$$\frac{\partial N_k}{\partial t} + 2\gamma_k N_k = st(N,N,N)$$
$$st(N,N,N) = \pi \int |T_{1234}|^2\, (N_2N_3N_4 + N_1N_3N_4 - N_1N_2N_3 - N_1N_2N_4) \times$$
$$\times \delta_{1+2-3-4}\, \delta(\tilde{\omega_1} + \tilde{\omega_2} - \tilde{\omega_3} - \tilde{\omega_4})\, dk_2 dk_3 dk_4 \tag{8.12}$$

Due to the inclusion of the frequency normalization, the equation (8.12) is more exact than the "common" wave kinetic equation.

To get the quantum kinetic equation we can use the same procedure, assuming that a_k, a_k^+ are noncommutative operators of annihilation and creation of quasiparticles.

9. Renormalized dispersion relation

Frequency renormalization is described by the diagonal part of the four-wave interaction coefficient

$$T(\vec{k}_1,\vec{k}_2) = T(\vec{k}_1,\vec{k}_2,\vec{k}_1,\vec{k}_2) = T_{12} \tag{9.1}$$

This "naive" formula presumes the existence of the limit:

$$T(\vec{k}_1,\vec{k}_2) = \lim_{|\vec{q}|\to 0} T(\vec{k}_1,\vec{k}_2,\vec{k}_1+\vec{q},\vec{k}_2-\vec{q}) \tag{9.2}$$

This limit exists and does not depend on the direction of the vector $\vec{q}$ only in deep water. In the general case, we can obtain from (4.9)

$$T_{12} = -\frac{1}{16\pi^2}\left(\frac{A_1A_2}{B_1B_2}\right)^{1/2} \left[2k_1^2B_1 + 2k_2^2B_2 - (\omega_1+\omega_2)^2\, A_{1+2} - (\omega_1-\omega_2)^2\, A_{1-2}\right] \tag{9.3}$$
$$-\frac{1}{32\pi^2}\left(\frac{B_1B_2}{A_1A_2}\right)^{1/2} \left\{\frac{1}{B_{1+2}}\left[L_{12}^2 + \frac{u_{12}^2}{\omega_{1+2}^2 - (\omega_1+\omega+2)^2}\right] + \frac{1}{B_{1+2}}\left[L_{-1,2}^2 + \frac{u_{-1,2}^2}{\omega_{1-2}^2 - (\omega_1-\omega_2)^2}\right]\right\}$$

In the absence of capillarity in deep water the expression (9.3) becomes

$$T_{12} = -\frac{1}{8\pi^2}\frac{1}{(k_1k_2)^{1/2}}\left\{3k_1^2k_2^2+(\vec{k}_1\cdot\vec{k}_2)^2-4\omega_1\omega_2(\vec{k}.\vec{k}_2)(k_1+k_2)+\right.$$
$$\left.+2\frac{(\omega_1+\omega_2)^2\left[(\vec{k}_1\cdot\vec{k}_2)^2-k_1^2k_2^2\right]}{\omega_{1+2}^2-(\omega_1+\omega_2)^2}+2\frac{(\omega_1-\omega_2)^2\left[(\vec{k}_1\cdot\vec{k}_2)^2+k_1^2k_2^2\right]}{\omega_{1-2}^2-(\omega_1-\omega_2)^2}\right\} \tag{9.4}$$

In the one-dimensional case the formula (9.4) becomes remarkably simple

$$T_{12}=\frac{1}{2\pi^2}\begin{cases}k_1^2k_2 & k_1<k_2\\ k_1k_2^2 & k_1>k_2\end{cases} \tag{9.5}$$

The function T_{12} is continuous at $k=k_1$, but its first derivative has a jump. This result was published by the author in 1992 (Zakharov, 1992). At $k_2=k_1$

$$T_{12}\to T_{11},\quad T_{11}=\frac{1}{2\pi^2}k^3. \tag{9.6}$$

In the presence of capillarity

$$T_{11}=\frac{k^3}{4\pi^2}\frac{2-\sigma k^2}{1-2\sigma k^2}. \tag{9.7}$$

For monochromatic waves we have:

$$b=F\,\delta(k-k_0),\quad \delta\omega=\frac{1}{2}T_{11}\,|F|^2 \tag{9.8}$$

In natural variables

$$\eta=a\cos(k_0x-\omega t-\phi),\quad a^2=\frac{1}{2\pi^2}\frac{k_0}{\omega_{k_0}}|F|^2$$

and

$$\frac{\delta\omega}{\omega}=\frac{1}{4}\frac{2-\sigma k^2}{1-2\sigma k^2}(ka)^2 \tag{9.9}$$

It is in agreement with the classical results of Stokes and other authors. In shallow water the limiting procedure (9.2) needs some accuracy and falls beyond the framework of this article.

10. Kolmogorov spectra

Let us look now for stationary solutions of the kinetic wave equation (8.12). They satisfy the equation

$$st(N,N,N)=0 \tag{10.1}$$

This equation has an ample array of solutions describing direct and inverse cascades of energy, momentum, and wave action. A full description of these solutions has not been done so far. Only very special, isotropic solutions could be found analytically in the case when ω_k is a power function

$$\omega_k=a|k|^\alpha, \tag{10.2}$$

and $T(\vec{k}_1, \vec{k}_2, \vec{k}_3, \vec{k}_4)$ is a homogeneous function:

$$T(\epsilon\vec{k}_1, \epsilon\vec{k}_2, \epsilon\vec{k}_3, \epsilon\vec{k}_4) = \epsilon^\beta T(\vec{k}_1, \vec{k}_2, \vec{k}_3, \vec{k}_4) \tag{10.3}$$

It is assumed that the function $T(\vec{k}_1, \vec{k}_2, \vec{k}_3, \vec{k}_4)$ is invariant with respect to rotation in $\vec{k}$-space.

In the general case of water of finite depth ω_k is *not* a homogeneous function. As a result, all known analytical methods are unable to construct any nontrivial (non-thermodynamic) solution of equation (10.1). But in two limiting cases, deep water and very shallow water, some solutions can be found. On deep water

$$\omega_k = \sqrt{gk}, \quad \alpha = 1/2, \tag{10.4}$$

and $T(\vec{k}_1, \vec{k}_2, \vec{k}_3, \vec{k}_4)$ is given by the expression (5.1). Apparently, $\beta = 3$. On very shallow water

$$\omega_k = s|k|, \quad \alpha = 1, \tag{10.5}$$

and $T(\vec{k}_1, \vec{k}_2, \vec{k}_3, \vec{k}_4)$ is given by formula (6.2). As far as singularities in (6.2) are cancelled, it is a regular continuous function on the resonant manifold (6.4). Now $\beta = 2$. On a flat bottom the isotropy with respect to rotation is satisfied.

It is well known (see, for instance, Zakharov, Falkovich and Lvov, 1992) that under conditions (10.2), (10.3) the equation (10.1) has powerlike Kolmogorov solutions

$$\begin{aligned} n_k^{(1)} &= a_1 P^{1/3} k^{-\frac{2\beta}{3}-d} \\ n_k^{(2)} &= a_2 Q^{1/3} k^{-\frac{2\beta-\alpha}{3}-d} \end{aligned} \tag{10.6}$$

Here d is a spatial dimension ($d = 2$ in our case).

The first one is a Kolmogorov spectrum, corresponding to a constant flux of energy P to the region of small scales (direct cascade of energy). The second one is a Kolmogorov spectrum, describing inverse cascade of wave action to large scales, and Q is the flux of action. In both cases a_1 and a_2 are dimensionless "Kolmogorov's constants". They depend on the detailed structure of $T(k, k_1, k_2, k_3)$ and are represented by some three-dimensional integrals.

It is known since 1966 (Zakharov and Filonenko, 1966) that on deep water

$$n_k^{(1)} = a_1 P^{1/3} k^{-4}. \tag{10.7}$$

For the energy spectrum

$$I_\omega d\omega = \omega_k n_{\vec{k}} d\vec{k} \tag{10.8}$$

one obtains

$$I_\omega \simeq P^{1/3} \omega^{-4}. \tag{10.9}$$

This result is supported now by many observational data as well as numerical simulations.

In the same way on deep water (Zakharov and Zaslavsky, 1982):

$$n_k^{(2)} = a_2 Q^{1/3} k^{-23/6}, \quad I_\omega \simeq Q^{1/3} \omega^{-11/3}. \tag{10.10}$$

On a very shallow water $\alpha = 1$, $\beta = 2$, and we obtain:

$$n_k^{(1)} = \tilde{a}_1 P^{1/3} k^{-10/3} h^{2/3}, \quad I_\omega^{(1)} \simeq P^{1/3} \omega^{-4/3} \tag{10.11}$$

$$n_k^{(2)} = \tilde{a}_2 Q^{1/3} k^{-3} h^{2/3}, \quad I_\omega^{(2)} \simeq Q^{1/3} \omega^{-1} \tag{10.12}$$

Formulae (10.11), (10.12) are new. We must keep in mind that they are applicable only if the condition $\mu \ll \delta^5$ is satisfied.

11. Conclusions

The weakly nonlinear theory of gravity waves has some window of applicability on shallow water. But this window shrinks dramatically when the parameter $\delta = kh$ tends to zero. For $\delta \simeq 0.5$ the window is relatively wide, $\mu \leq 10^{-2}$, but for $\delta \simeq 0.2$ it barely exists, $\mu \ll 10^{-4}$.

On deep water we can neglect the difference between the observed, n_k, and renormalized, N_k, wave action. On shallow water the difference could be very important for correct interpretation of observed data. We have to remember that the kinetic equation is written not for real, but for "renormalized" wave action.

Many problems pertaining to the statistical theory of gravity waves on shallow water are still unresolved. The most important problem is finding a Kolmogorov spectra for a fluid of arbitrary depth. From dimensional consideration we can conclude that it has the form

$$N_k^{(1)} = P^{1/3}\, k^{-4}\, F(kh), \quad F \to a_1, \quad kh \to \infty, \quad F \to \tilde{a_1}\, (kh)^{2/3} \quad kh \to 0 \tag{11.1}$$

The function $F(\xi)$ is unknown and should be found numerically.

Acknowledgement

This work is supported by the ONR grant N 00014-98-1-0070.

References

[1] W.Craig, C.Sulem and P.L.Sulem, Nonlinear modulation of gravity waves - a rigorous approach, Nonlinearity, vol. 5 (1992), 497-522.

[2] A.Dyachenko, V.Zakharov, Is free-surface hydrodynamics an integrable system? Physics Letters A 190 (1994), 144-148.

[3] K.Hasselmann, On the nonlinear energy transfer in gravity-wave spectrum. Part 1. General theory. J. Fluid Mech. 12 (1962), 481-500.

[4] B.B.Kadomtsev, Plasma Turbulence, Academic Press, London, 1965.

[5] D.J.Webb, Nonlinear transfer between sea waves, Deep-Sea Res. 25 (1978), 279-298.

[6] V.E.Zakharov, Stability of periodic waves of finite amplitude on a surface of deep fluid, J. Appl. Mech. Tech. Phys. 2 (1968), 190-198.

[7] V.E.Zakharov, Inverse and direct cascade in a wind-driven surface wave turbulence and wave-breaking, IUTAM symposium, Sydney, Australia, Springer-Verlag, (1992), pp.69-91.

[8] V.E.Zakharov, Weakly-nonlinear waves on the surface of an ideal finite depth fluid, Amer. Math. Soc. Transl. (2), vol. 182 (1998), 167-197.

[9] V.E.Zakharov and N.Filonenko, The energy spectrum for stochastic oscillation of a fluid's surface, Doklady Akad.Nauk, vol.170 (1966), 1292-1295.

[10] V.E.Zakharov and V.Kharitonov, Instability of monochromatic waves on the surface of an arbitrary depth fluid, Prikl. Mekh. Tekh. Fiz. (1970), 45-50 (Russian).

[11] V.E.Zakharov and M.M.Zaslavsky, The kinetic equation and Kolmogorov spectra in the weak-turbulence theory of wind waves, Izv. Atm. Ocean. Phys. 18 (1982), 747-753.

EUROPEAN JOURNAL OF MECHANICS
B/FLUIDS

INSTRUCTIONS TO AUTHORS

AIMS AND SCOPE

Papers submitted for publication must contain original research results, be clearly written and meet a high scientific standard. The manuscript must not have been published before (except in the form of an abstract or as part of a lecture, review or thesis). **The text must be written in good English.**
The authors must secure the rights of reproduction of any material that has previously been published elsewhere.
Although investigations in well established areas are within the scope of the journal, recent developments and innovative ideas are particularly welcome.
The 'EJM/B–Fluids' publishes papers in all fields of fluid mechanics. Theoretical, computational and experimental papers are equally welcome. Mathematical methods, be they deterministic or stochastic, analytical or numerical, will be accepted provided they serve to clearly solve identifiable problems in fluid mechanics, and provided the significance of the results is explained. Similarly, experimental papers must add physical insight to the understanding of fluid mechanics.
Manuscripts should be sent to one of the Editors-in-Chief (address on the inside front cover).

GENERAL PRESENTATION

Four complete copies of the manuscript should be submitted. The manuscript should be double-spaced, with margins of at least 3.5 cm at the top, bottom and sides for editor's comments. The pages should be numbered.
The layout should be presented as follows: title page, abstract, introduction, main text, results, conclusion, acknowledgements, references, figure captions, tables, figures.
The total length of the manuscript should not exceed the equivalent of 20 pages when printed.
Section headings should be numbered following the international numbering system (1.; 1.1.; 1.1.1., etc.).
Tables and figures, with their captions, should not appear in the text, but be placed together on separate sheets at the end of the manuscript.
Abbreviations should be punctuated.
Uppercase letters should be accented; small capitals should not be used.
After the article has been accepted for publication, the authors are encouraged to forward the **revised version on disk** to the editor (RTF or TEX format for the text, and, if possible, TIFF format–300 dpi–for the figures).
The publication of the text and black and white figures is free of charge. The publisher will be pleased to send you a quote for colour reproduction.

Title page

The title page should include the following: the title of the article, which should be concise but explicit, the surname and forenames (in full) of each author, the department and institution where the study was carried out, telephone and fax numbers and e-mail address of the corresponding author (this author being identified by an asterisk), a short title (running head) of no more than 45 characters, including spaces.

Abstracts

The abstracts (not more than 200 words each) should be in a suitable form for abstracting services. Paragraphs, footnotes, references, cross-references to figures or tables and undefined abbreviations should be avoided.

Keywords

Up to five key words should be provided to assist the reader and facilitate information retrieval. Keywords may be taken from the title, abstract or text. The plural form and uppercase letters should be avoided. Keywords should be written in bold lowercase letters, separated by slashes.

Parameters and units

Only ISO symbols, always written in italic, should be used for the various parameters. SI units should be used throughout, and should always be written in roman and separated from the numerical value by a space (whatever the language). The μ in μg or μm is always in roman. The symbol for litre is L and that for minute is min. For temperatures, please note the use of °C and °F but K. As the Ångström (1 Å = 10^{-10} m) is not an SI unit, it should be replaced by the nanometre (1 nm = 10^{-9} m) or by the picometre (1 pm = 10^{-12} m): 1 Å = 0.1 nm = 100 pm. Multiple units should be written with negative superscripts (for example, 25 $mg \cdot L^{-1} \cdot s^{-1}$).
The list of notations should appear just before the first paragraph of full text.

Equations and numbers

Equations should be carefully typed with attention paid to exponents and subscripts. Those that are referred to in the text [in the form: equation (1), for example] should be numbered using Arabic numerals, in brackets, on the right-hand margin. Punctuation should not be used at the end of an equation. Particular care should be taken to distinguish between the number zero (0) and the letter O; the number one (1) and the letter l, the Roman letter v and the Greek letter nu (ν). The decimal logarithm should be written 'log' and the natural log 'ln'. The abbreviation of the exponential function is a roman e (for example, e^x) or exp (for example, exp ($u^2 + v$)). In expressions of the type d*x*d*t*, the letter d (derivative function) is always written in roman, whereas the physical parameter (*x* or *t*) is always in italics. Numbers are written in numerals when they are followed by units, these being represented by their SI symbols (10 % but a few percent). In numerals, each group of three letters should be separated by a space (except for dates and postal codes).

References

The references are cited in the text followed by an Arabic numeral enclosed in square brackets. They are numbered in **order of their citation in the text**.
In the reference list, the references appear in numerical order, preceded by the appropriate number enclosed in square brackets.
Wherever possible the authors' names should be mentioned in the text too.
All entries in the reference list must correspond to references in the text and vice versa. When authors are cited, the spelling of the authors' names must be exactly the same as in the reference list.
The titles of journals should be abbreviated according to the standardised rules (cf. 'ISI', 'Current Contents', 'Physical Abstracts', for instance). Titles for which no abbreviation is given should be written in full.
Examples are given below of the layout and punctuation to be used in the references.
• Article (all authors must be mentioned)
[1] Nagara M., Nonlinear solutions of modified plane Couette flow in the presence of a transverse magnetic field, J. Fluid Mech. 307 (1996) 231–243.
[2] Gaster M., On the effects of boundary-layer growth on flow stability, J. Fluid Mech. 66 (1974) 465–480.
• Book
[3] Proctor M.R.E., Gilbert A.D., Lectures on Solar and Planetary Dynamos, Cambridge University Press, Cambridge, 1994.
• Chapter in a book
[4] d'Almeida A., Gatignol R., Boundary conditions for discrete models of gases and application to Couette flows, in: Leutloff D., Srivastava R.C. (Eds.), Computational Fluid Dynamics, Springer-Verlag, Berlin, 1995, pp. 115–130.
A list of all the other possibilities (journal supplements, proceedings of a congress, accepted articles, edited books, translations, theses, patents, standards, etc.) is available on request from the Editorial Board.

Illustrations (figures and tables)

Illustrations (one original and two good copies) should be numbered in Arabic numerals for figures and Roman numerals for tables, and should be referred to in the text by their number (*figure 1, table I*). Lettering (symbols, numbers, etc.) should not differ from figure to figure and should be of sufficient size to remain legible after reduction (letters 1–2 mm high after reduction to either one or two column format). Figures should be presented in the form of drawings on drawing or tracing paper or as sharp glossy prints. Half-tones should contain good contrast and should be originals (i.e. not already reproduced); line drawings should have a white background. Photographs should be presented in the form of plates to be reproduced without reduction (maximum size 12 × 19 cm^2 or 16.5 × 24 cm^2 for 'full page' illustrations. The lettering (height 1–2 mm) should not be placed any closer to the edges than 1 cm. Graphs should include only the co-ordinate axes with unit divisions or the major mesh lines. The figure captions should be explicit so that the illustrations are comprehensible without reference to the text, and should be presented together on a separate sheet at the end of the paper. As many details as possible should be included in the captions rather than in the figures themselves. Authors are responsible for the cost of reproduction of colour figures. Tables should not exceed 84 characters per line (140 if in landscape format). The title of each table should be written above the corresponding table. Figures and tables published elsewhere cannot be accepted without the prior consent of the publisher and the author(s).
The Editorial Board retains the right of returning, before evaluation, manuscripts to authors who do not comply with these recommendations. The author is advised to keep one manuscript and a set of figures.

PROOFS AND REPRINTS

Proofs will be sent to the author indicated on the title page. They should be carefully corrected and returned to the publisher within 48 hours of reception. If this period is exceeded, the galleys may be printed with the editor's corrections only. Should substantial changes in the original manuscript be requested (other than typographical errors), they will be made at the author's expense. Twenty-five reprints per contribution are available free of charge. An order form for additional reprints will accompany the proofs.

COPYRIGHT

EUROPEAN JOURNAL OF MECHANICS

B/FLUIDS

An official medium of publication for EUROMECH "European Mechanics Society"

Eur. J. Mech. B/Fluids, **18**, n° 3, 1999